National Library of Canada
Bibliothèque nationale du Canada

Acquisitions and Bibliographic Services Branch
Direction des acquisitions et des services bibliographiques

395 Wellington Street
Ottawa, Ontario
K1A 0N4

395, rue Wellington
Ottawa (Ontario)
K1A 0N4

Your file Votre référence

Our file Notre référence

## NOTICE

The quality of this microform is heavily dependent upon the quality of the original thesis submitted for microfilming. Every effort has been made to ensure the highest quality of reproduction possible.

If pages are missing, contact the university which granted the degree.

Some pages may have indistinct print especially if the original pages were typed with a poor typewriter ribbon or if the university sent us an inferior photocopy.

Reproduction in full or in part of this microform is governed by the Canadian Copyright Act, R.S.C. 1970, c. C-30, and subsequent amendments.

## AVIS

La qualité de cette microforme dépend grandement de la qualité de la thèse soumise au microfilmage. Nous avons tout fait pour assurer une qualité supérieure de reproduction.

S'il manque des pages, veuillez communiquer avec l'université qui a conféré le grade.

La qualité d'impression de certaines pages peut laisser à désirer, surtout si les pages originales ont été dactylographiées à l'aide d'un ruban usé ou si l'université nous a fait parvenir une photocopie de qualité inférieure.

La reproduction, même partielle, de cette microforme est soumise à la Loi canadienne sur le droit d'auteur, SRC 1970, c. C-30, et ses amendements subséquents.

Canada

# Development of Efficient Techniques using Substructuring and Extended Transfer-Matrix Approach for Analysis of Large Scale Vehicular Structures

Krishnamurthi Ganapathi

A thesis

in

The Department

of

Mechanical Engineering

Presented in Partial Fulfillment of the Requirements
for the Degree of Doctor of Philosophy at
Concordia University
Montreal, Quebec, Canada

December 1995

© Krishnamurthi Ganapathi, 1995

National Library of Canada
Acquisitions and Bibliographic Services Branch
395 Wellington Street
Ottawa, Ontario
K1A 0N4

Bibliothèque nationale du Canada
Direction des acquisitions et des services bibliographiques
395, rue Wellington
Ottawa (Ontario)
K1A 0N4

Your file Votre référence

Our file Notre référence

**The author has granted an irrevocable non-exclusive licence allowing the National Library of Canada to reproduce, loan, distribute or sell copies of his/her thesis by any means and in any form or format, making this thesis available to interested persons.**

**L'auteur a accordé une licence irrévocable et non exclusive permettant à la Bibliothèque nationale du Canada de reproduire, prêter, distribuer ou vendre des copies de sa thèse de quelque manière et sous quelque forme que ce soit pour mettre des exemplaires de cette thèse à la disposition des personnes intéressées.**

**The author retains ownership of the copyright in his/her thesis. Neither the thesis nor substantial extracts from it may be printed or otherwise reproduced without his/her permission.**

**L'auteur conserve la propriété du droit d'auteur qui protège sa thèse. Ni la thèse ni des extraits substantiels de celle-ci ne doivent être imprimés ou autrement reproduits sans son autorisation.**

ISBN 0-612-10852-X

Canada

# ABSTRACT

**Development of Efficient Reanalysis Techniques using Substructuring and Extended Transfer-Matrix Approach for Analysis of Large Scale Vehicular Structures**

Krishnamurthi Ganapathi, Ph. D.
Concordia University, 1995

In this dissertation, analytical methods for design reanalysis of large scale structures are developed using substructuring techniques. The computational efficiency of the methods is specifically emphasized to perform analyses in a personal computer environment, and the reanalysis based design methodologies are applied to investigate large scale trailer structures in view of their integrity and light weight design. Two reanalysis methods are developed using substructuring in conjunction with Potters' method of matrix solution, and extended finite element-transfer matrix method (EFETM) comprising the design sensitivity vectors. The Potters' method of analysis is developed upon decomposing the stiffness matrices at the substructure level resulting in reduced size of the overall stiffness matrix. The EFETM method is also developed using substructuring, which combines the compactness of the transfer matrix technique and numerical efficiency of the finite element method. In both techniques, the reanalysis solution of a structure is obtained upon deriving and integrating the change in stiffness matrix of the substructure affected by a design modification into the overall matrix. The accuracy and numerical efficiency of both the reanalysis techniques are investigated through analysis of various bench mark structures. The solutions

are compared with those reported in the published studies to demonstrate the validity and superior computational efficiency of both the techniques.

The reanalysis methods are then employed to analyze large scale trailer structures. Two candidate trailer structures are identified: (i) a smaller span two-axle trailer employed in highway freight transportation; and (ii) a long-span tridem trailer employed in log-hauling operations. Although the design characteristics of two trailers are considerably different, both the structures utilize a ladder-type configuration, which is ideally suited for design reanalysis methods developed in this study. Analytical models of the candidate structures are developed using the proposed analysis methods. A modal analysis of the trailer structure was performed and the results were compared with those derived from the experimental modal analysis. The analytical methods were further validated upon comparing the solutions with those derived from a commercial FEM software. A performance criteria based upon the torsional and flexural deformations and stresses is formulated to assess the potential benefits of various design modifications. A comprehensive parametric study is performed to study the role of primary design parameters on the performance criteria using the reanalysis methods based upon the specified local design modification. A methodology is proposed to assess the performance of the trailer structure under torsional loads caused by severe directional maneuvers. From the investigation it is concluded that the methods yield accurate analysis of large scale structures with extremely high numerical efficiency. The execution time required by the reanalysis methods is 70% less than that required for the direct analysis performed using a 486 DX 33 personal computer.

## ACKNOWLEDGEMENTS

The author wishes to express his sincere appreciation to Dr. S. Sankar, for initiating the study topic and providing guidance and support during the course of the investigation. The author sincerely thanks and appreciates the support and guidance provided by his thesis supervisors, Dr. S. Rakheja and Dr. A. K. W. Ahmed during the rest of the course of this investigation.

Thanks are due to the colleagues, at the CONCAVE Research Centre for their contribution and cooperation during the study. Grateful acknowledgements are given to Dr. D. Taddeo and Dr. S. V. Hoa for providing the financial support during the final stages of this study.

Finally, the author would like to express his special thanks to his wife and son, and members of his family, for their support and encouragement.

## TABLE OF CONTENTS

# LIST OF FIGURES

## List of Figures(continued)

## List of Figures (continued)

## List of Figures (continued)

## List of Figures (continued)

## List of Figures (continued)

# LIST OF TABLES

## List of Tables (continued)

## List of Tables (continued)

## NOMENCLATURE

| | |
|---|---|
| $A_i$ | submatrix of assembled stiffness matrix of a substructure 'i' |
| B | width of the cross-section of a structural member |
| $B_i$ | submatrix of assembled stiffness matrix of a substructure 'i' |
| $C_i$ | submatrix of assembled stiffness matrix of a substructure 'i' |
| $d_i$ | design variable of a design vector of size (r x 1) |
| $d_{i0}$ | design variable of a design vector of size (r x 1) of the base line design |
| $f_i$ | force vector defined in a substructure 'i |
| F | force vector of the total structure' |
| $g_i$ | force vector defined in a substructure 'i' |
| H | height of the web of the cross-section of a structural member |
| i | any partition in the substructure analysis |
| K | stiffness matrix of the total structure |
| $K_k$ | linear rate of king-pin reaction spring |
| $K_{k_{dyn}}$ | linear rate of king-pin reaction under dynamic condition |
| $K_s$ | linear rate of suspension spring |
| $K_{s_{dyn}}$ | linear rate of suspension spring under dunamic condition |
| L | decomposed matrix of K |
| M | mass matrix of the total structure |
| $M_x$ | moment about catesian X-axis |
| $M_y$ | moment about cartesian Y-axis |
| n | number of partition in a structure |
| P | product matrix used in substructure solution |

## NOMENCLATURE (continued)

| | |
|---|---|
| $q_i$ | intermediate force vector defined for substructure solution method |
| r | number of design variables in a design space |
| $T_i$ | transfer matrix of a substructure 'i' |
| Tf | flange thickness of the cross-section of a structural member |
| Tw | web thickness of the cross-section of a structural member |
| U | displacement vector of the total structure |
| V | trial vector used in simultaneous iteration method |
| $W_{axle}$ | rated axle load |
| $W_k$ | reaction force due to king-pin spring |
| $W_{sus}$ | suspension reaction force |
| $W_u$ | unsprung weight due to axle, wheel and tire assembly |
| X | cartesian coordinate |
| Y | cartesian coordinate |
| $Y_i$ | response vector of the structure for the ith normal mode |
| $z_i$ | displacement vector for a substructure 'i' |
| Z | cartesian coordinate |
| $\Phi_i$ | modal displacement vector of a partical mode ' i ' |
| $\theta_x$ | rotation about X cartesian coordinate |
| $\theta_y$ | rotation about Ycatrtesian coordinate |
| $\omega$ | natural frequency (rad/s) |
| $\varsigma$ | modal damping |

# CHAPTER 1

# INTRODUCTION AND LITERATURE REVIEW

## 1.1 Problem Background

Structural reliability and longevity in service, have been the principal criteria in the design of commercial vehicles used in cargo transportation applications. Although vehicle design considerations include ride comfort, safety, crash worthiness, handling, directional stability, etc., the structural integrity and the tare weight form the most important considerations to achieve economical freight transportation. The global competition consideration further plays an important role in the way new vehicle components are designed and built. Cargo trailers are traditionally fabricated using rugged designs resulting in high material costs and reduced payload capacity. The cost of freight transportation is directly related to the payload capacity of the trailers as governed by the road laws. In view of the vehicle weights and dimension regulations on maximum allowable gross vehicle weight and axle loads, the freight transportation industry has identified the need to develop light weight trailers in order to maximize the payload, without compromising the structural reliability. Modern manufacturing requirements of vehicles for transportation of cargo thus demand energy-efficient trailer design with a reasonable life time for commercial viability. A study presented at the CPPA Annual meeting has estimated that a trailer owner can expect a payback of between CAN$ 4.50 and CAN$ 7.0 per year per extra kg of payload [1].

With the need to design large scale trailers, effective design and reanalysis tools with limited number of field evaluations has also been identified in view of the growing global competition. Development of such design and reanalysis tools necessitates an efficient study of the role of different design parameters on the weight, structural integrity and fatigue life in order to derive cost effective design alternatives or optimal designs. The design and analysis tools based upon Finite Element Methods (FEM) are being increasingly applied to design and evaluate structures including those of vehicles. Over the past two decades, many general purpose FEM packages have been developed, such as, NASTRAN, ANSYS, ALGOR, etc., [2,3,4]. The computer-aided design and drafting software, such as, I-DEAS, AUTOCAD, CADKEY, etc. [5,6,7] are frequently used to model the structure components, which is then interfaced with the FEM software to perform analyses. While such methodologies yield reliable design and analyses, the lack of flexibility and their structured nature often pose certain complexities, specifically with the analysis of large scale structures. Furthermore, design of complex structures with several design variables frequently involves numerous modifications and repetitive analyses in an iterative or trial and error based manner, the use of general purpose FEM packages in such an iterative design methodology poses unreasonable demands on computing as well as human resources and expertise.

Alternatively, a number of reanalysis techniques have been developed to analyze the intermediate design stages in an efficient manner using finite element techniques [8]. Reanalysis methods in general utilize the analysis results derived from the previous analysis in order to efficiently analyze the modified structure. Analysis of large structures using personal computers (PC), however, poses further constraints on the size of the matrices due to limitations of the memory.

Considerable attention has therefore, been directed towards the use of Transfer Matrix and "substructuring" techniques to minimize the computing and memory requirements [9]. These methods can provide highly efficient design, analysis and reanalysis tools for large scale structures specifically, when the structure comprises various repetitive or symmetrical components, through refined meshing and analysis of limited substructures reflecting local design modifications.

The Finite Element-Transfer Matrix (FETM) methods, which combine the efficiency of FEM and compactness of transfer matrix, have been used to perform efficient analysis of some large structures [10,11]. The transfer matrices relating the behavior vectors (displacement, forces, moments, etc.)of adjacent elements. A method based upon transfer matrices relating the state vectors comprising displacement and forces together with their respective derivatives, has been proposed to further enhance the efficiency of the analyses [10]. The method referred to as 'extended transfer matrix method' provides a highly efficient approach that combines the FETM and sensitivity vector in seeking reanalysis solutions using first order Taylor series approximation. The extended finite element transfer matrix (EFETM) formulation has been applied for solving a plate vibration problem while attempting to improve the convergence of eigenroots using the Newton-Raphson method.

In this study, two reanalysis techniques based upon substructuring in conjunction with the sensitivity vectors are formulated. The extended sensitivity vectors, comprising derivatives of the behavior vector with respect to design variables, are computed simultaneously, while seeking the first solution. The advantages of the proposed technique are demonstrated through their applications to large structure with certain symmetric and repetitive features incorporating

beam elements with predominant flexural and torsional characteristics. The results obtained from the study are validated using the results derived from the experimental modal analysis of a candidate trailer. The validated model is further used to assess the structure in view of the dynamic response and stresses caused by dynamic loads imposed by random road profiles.

## 1.2 Review of Literature

Numerous studies on design and analysis of structures using different methods of varying complexities have been reported in the literature. The relevant published studies on design of vehicle structures, and methods of analysis, reanalysis and substructuring are thoroughly reviewed and presented in the following subsections in order to formulate the scope of the present investigation.

### 1.2.1 Design and Analysis of Vehicle Structures

Although design and analysis of various large scale structures have been extensively reported in the literature [12-21], only limited number of studies have reported the static and dynamic analysis of heavy vehicle structures. Although the economy and competitiveness associated with freight transportation is directly related to the weight and fatigue life of the trailer structure; only limited efforts have been mounted to develop effective design and analysis tools for trailer structures. The lack of efforts, in part, may be attributed to "Customer-specified design" nature of the trailer manufacturing industry, and the lack of efficient and user friendly analytical tools. Some of the earlier studies have investigated the improvements in "ladder-type" structures used in truck, and bus applications [22-38]. Typically, a ladder structure, as the name implies comprises of rugged side

frames coupled through many cross members arranged in a ladder fashion. The structural members are generally made of thin walled beam type structures of open cross-section. While ladder type structures are frequently used in trailer and bus chassis applications, numerous variations in the configuration layout exist to satisfy specific application requirements, such as passenger and cargo transportation. The cross members are arranged in different manners and varying methods of joining the cross members are employed.

Figure 1.1 illustrates typical ladder type trailer structures which are employed in the industry. The semi-trailer structure comprises two rugged beams, referred to as main beams (essentially, those attached to wheel assembly units transmitting the loads to the terrain) placed in the middle of the trailer structure along the longitudinal axis. Side beams are generally provided outside of the main beams to provide a platform bed. The four beams are joined through end members and number of cross members, as shown in the Figure 1.2. Typical fastening arrangements for the cross members [22,27] are illustrated in Figure 1.3.

The articulated freight vehicle trailers are designed to carry heavy cargo (up to 40 tons), and are subject to excessive dynamic loads arising from directional maneuvers and tire-road interactions. Articulated vehicles employed in logging operation are specifically subject to high dynamic loads caused by vehicle interactions with unpaved forestry roads. The design of such trailers is thus carried out with appropriate considerations of flexural and torsional rigidity of the members. Different design methods based upon empirical and semi-empirical relations, derived from simple beam theory considerations, and extensive field tests, have been proposed to enhance the torsional rigidity of the structure[22-26].

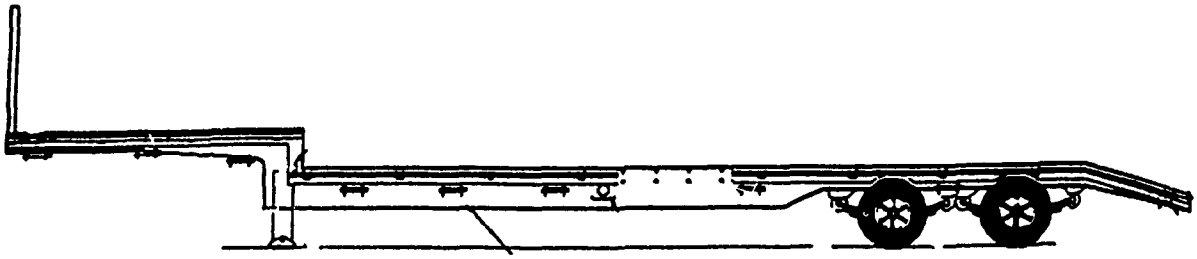

(b) Semi-trailer 30T Capacity, 14.6m (48ft.) long and 2.59m (102") wide

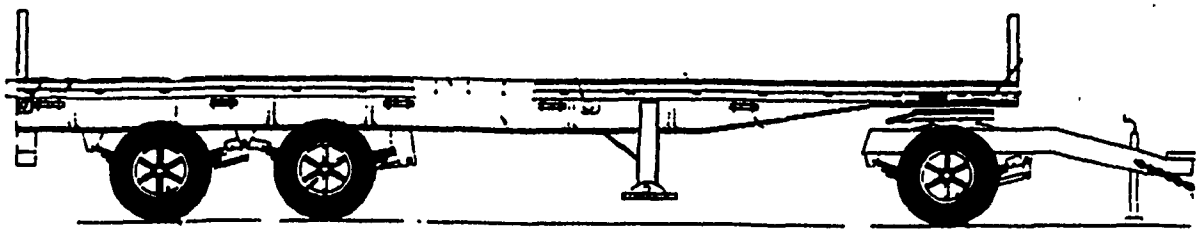

(c) Semi-trailer 30T capacity, 9.144m (30ft.) long and 2.59m (102") wide

Figure 1.1 Configurations of Semi-trailers commonly used in freight transportation

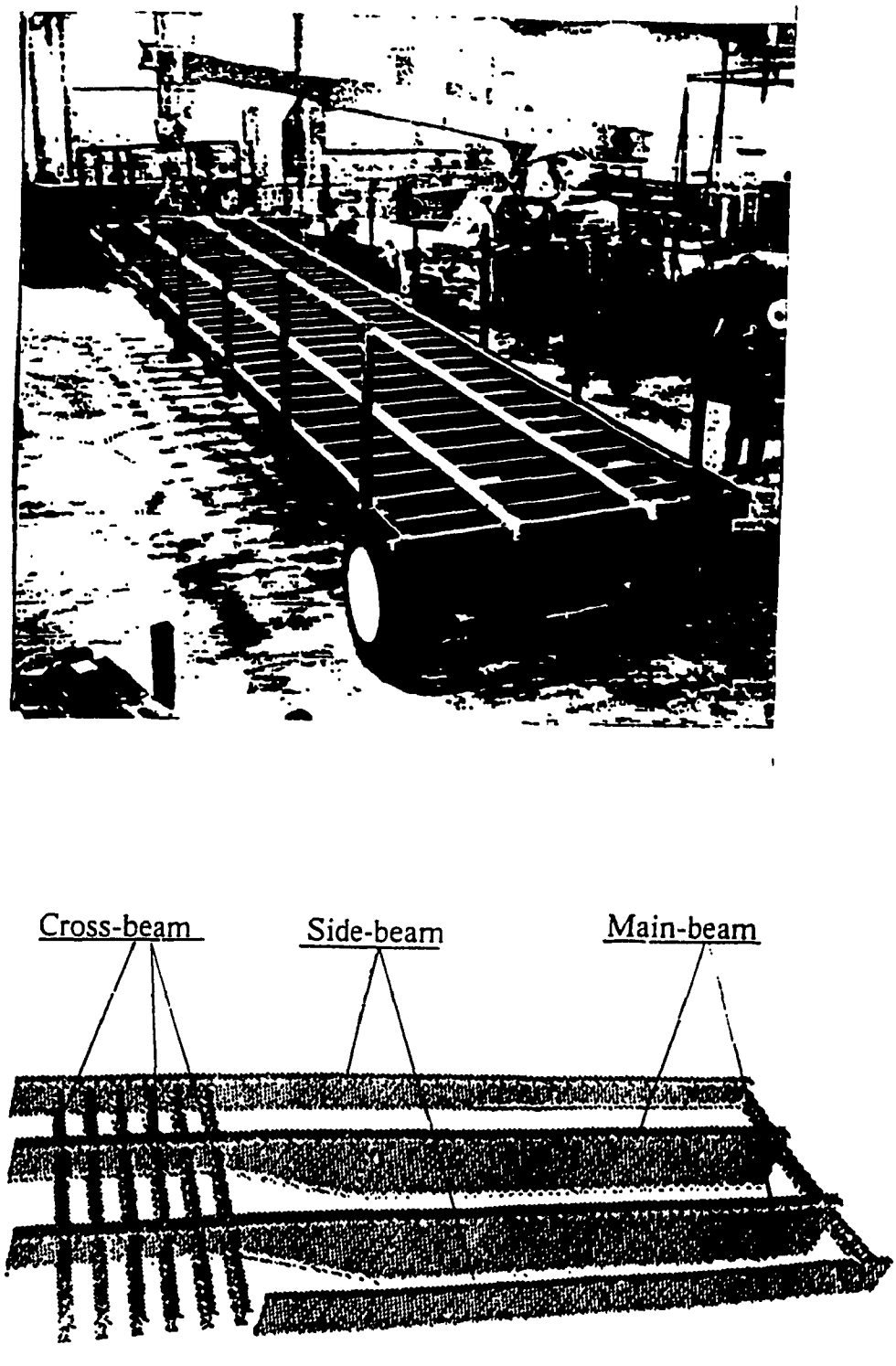


Figure 1.2 A pictorial view and schematic of a semitrailer illustrating the ladder-type design.

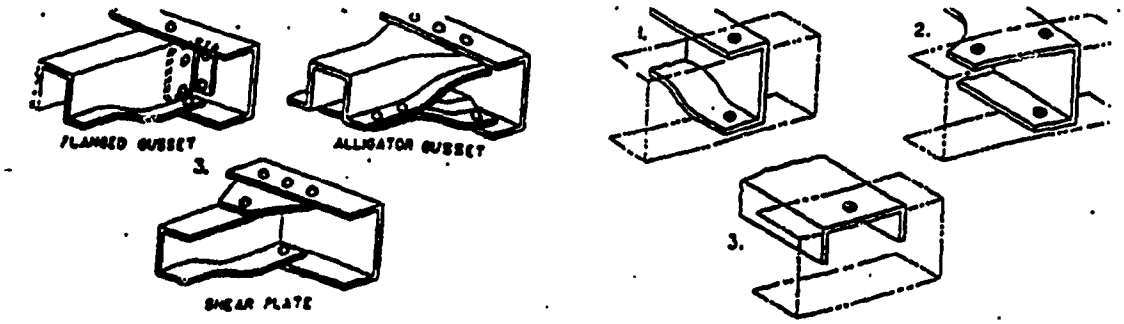


Typical cross member-side member fastening arrangement

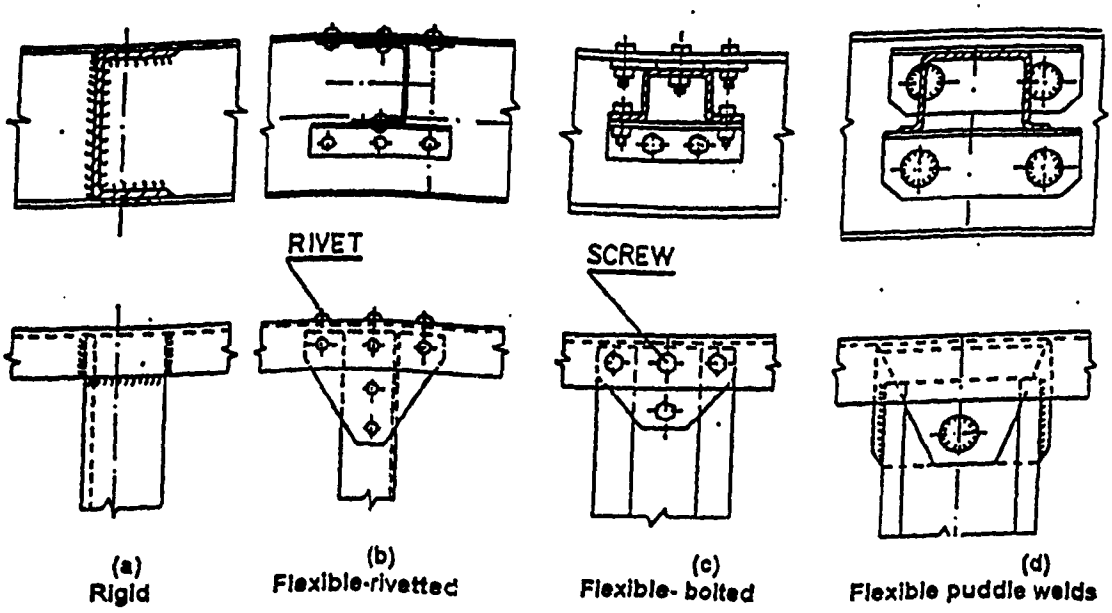


Figure 1.3: Schematics of various cross-member fastening and joints used in trailer design [22,27].

Methods to achieve frame rigidity and their distribution in overall configuration under different operating conditions have been described by Exler [22]. The study in particular, outlines various guidelines and practices for attaching cross members to side members, and describes methods to improve overall frame rigidity to minimize the problems associated with parallelogramming, torsion, warping and lateral deflection modes of vibration. Shomberger et al. [23] and Carver [24] proposed design methods to achieve improved fatigue life of truck frame side rails. The strength improvement was achieved by appropriate stiffening of critical locations, while adopting a basic section of high-strength steel. The proposed design was derived upon consideration of resistance to bending moment and flange buckling. Alternatively, variable depth side rail was proposed to achieve the desired rigidity, which resulted in increased fabrication cost [24].

McNitt [25] discussed the side rail buckling stresses from test studies performed on various specimens representing truck frame assemblies. The experimental study presented the effects of cross member spacing and attachment on the critical buckling stress of a typical truck frame side rail. Based upon the evaluation of different methods of attachments, such as bolting the cross members to flange only, cross member bolted to web only, and a combination of flange and web mounting (Figure 1.3), the study recommended that, the cross members be riveted to only the web of the side rail and the vertical input loads were to be introduced into frame assembly through the side rail shear centre. High vertical load to a side rail is to be introduced to the web through shear attachment to avoid local flange radius failure. Beerman [26] performed the structure analysis by incorporating the flexibility of the joint using discretization of the nodal (joint) region and substructure techniques to study the torsional characteristics of the

frame. The study emphasized the importance of joint flexibility and the associated stresses on the vehicle frame.

While bolted and riveted connections are commonly used in the truck and bus industry for their advantage of low maintenance costs and the flexibility to mount auxiliary systems, the trailer type vehicle structures are often fabricated using welded joints, as shown in Figure 1.3. Rusinski and Teisseyre [27] investigated the behavior of frames with certain welded joints and their influence on torsional stiffness. The study, however, focused on the effectiveness of puddle welded joints as shown in the Figure. Making allowances for puddle welds in the formulation of the stiffness matrix enables one to make decisions on design factors such as, number and diameter of each puddleweld. The study presented the thermal and mechanical analyses of stress concentration, residual stress and their effect on fatigue life of chassis structures with welded joints. Nippon Heavy Industries [28] have reported on the fatigue performance of spot welds as influenced by both magnitude of loading and the quality of weld. Lawrence et al. [29] have developed a three stage crack initiation propagation model of fatigue failure in spot welds loaded in tensile-sheer. The three stages included: Crack initiation, crack growth through the sheet thickness to the surface, and crack growth across the specimen. The study concluded the presence of residual stress as prestress on the spot weld.

Finite element techniques have been used for analyses of chassis and body of automobiles and commercial vehicles, such as, buses and trucks. Monasa and Chipman [30] developed a three dimensional elasto-plastic structural model to study the deformation of small passenger bus-compartment, modeled as a space frame, subject to frontal and side impact loads. Beerman [31] presented a hybrid-

method for analysis of chassis frames using a finite element idealization of the joint area of the cross member with the side rail, coupled with the warping-torsion-force displacement relationships. Yoshikawa et al. [32] studied side bending stress of heavy duty trucks, using FEM analysis, and compared the results derived from a simple bar idealization and plate elements. The study concluded that the analysis based upon bar elements yields effective estimation of trends, while the plate element analysis provides good correlation with the experimental results.

Dynamic analysis of bus-body configurations using beam and plate elements for the finite element modeling have been reported by Ramamurti and Sujatha [33]. The study presented eigensolutions and the response characteristics of the vehicle under random road-loads. The transient dynamic analysis of a truck structure composed of interconnected rigid and flexible bodies has been reported by Kim et al. [34]. The study based upon a simplified planar model described a methodology to compute the reference motion of vehicle, while including the effects of elastic deformations of the structure.

Crash worthiness of vehicles has received special attention in recent years due to extensive developments in light weight automobiles and the associated concerns related to crash safety. Tidbury [35] investigated the truck and bus structures by considering the collapse properties of the members and developed the CRASHD finite element program to depict the deformed structural shape under roll-over and side impact conditions. Winter et al. [36] performed the crash analysis of an automobile body made of fiberglass resin, using the FEM code DYCAST with nonlinear structural element formulation, to determine the load path, material failure and individual components behavior. The crash performance of a vehicle subject to 30 km/h frontal impact was carried out using the code.

The fatigue life estimate of the structure and the influence of road loads on the vehicle structures have also been addressed in some studies. Matyas and Sheth [35] described the use of Extreme Value analysis technique for determining the service loads in operation. A methodology to compute the effects of long term service loads from the short term load measurements was proposed. Sharmann [38] performed the fatigue life estimation of a semi-trailer chassis using dynamic strain records measured on different classes of roads. The fatigue life of the structure for a typical load cycle was estimated from the statistical analysis with design factors and load spectra as variables, and Miner's cumulative damage theory.

### 1.2.2 Finite Element Modeling and Analysis

It is worthwhile to review briefly the evolution of the analysis methods using discretization techniques in seeking solutions for physical problems. The behavior of the physical phenomenon such as displacement of a structure, or the free/forced vibration of a member can be expressed by means of differential equations governing the related quantities. The equations may be solved by expressing the differentials by the finite differences or by using the equivalent variational formulation, which involving the discretization of the continuous domain into finite elements, such as beams, plates, or shells, and using appropriate shape functions to describe the displacement behavior within the finite element. Over the past two decades, many general purpose FEM packages have been developed such as, NASTRAN, ANSYS etc. The FEM packages interfaced with drafting software, have served as standard tools for modeling and analysis of engineering components. Such software tools often lack the flexibility desired by

the user and require high degree of effort from the user, specifically when large scale structures are analyzed. Furthermore, the commercial FEA software packages do not allow structural modifications in an interactive manner to carry out trend analysis. The use of such packages is severely limited when large scale structures need to be analyzed using a personal computer. These software packages are known to be highly inefficient for design of complex structures with several design variables, which involve several modifications and repetitive analyses. Alternatively, reanalysis methods have been developed to enhance the efficiency of the FE analysis.

### 1.2.3 Reanalysis Techniques

Design of complex structures involving choice of several design variables require repeated design modifications and analyses. Such design methodology poses unreasonable demands on the computing and the designer's efforts. The lack of flexibility in commercial software further deteriorates the efficiency of the design process. Many analysis methods have been proposed to efficiently analyze the modified design using the information derived from a previous design. The reanalysis methods, in general, are formulated to utilize the results of a previous design and to reduce the computational effort. Such methods are generally implemented in the intermediate stages of design iterations, in order to seek approximate solutions based on the information of the previous analysis. In static analysis applications matrix-displacement and matrix-force methods and mixed formulations have been frequently used to perform efficient reanalysis of structures. Many reanalysis algorithms have been developed by various researchers with objectives to reduce the computational effort and to improve the

numerical accuracy. A comprehensive review of these algorithms has been reported [12,13].

Based upon the method of solution, the reanalysis techniques can be grouped in three broad classes: (1) Direct method; (2) Iteration method; and (3) Approximate method. The direct methods, as the name implies, provide exact closed-form solutions and are applicable to situations where a relatively small portion of the structure is modified [14,15]. The iterative methods are considered effective for design problems involving minor modifications of large structures. The original displacement vector, derived from a previous design analysis is used as a starting estimate and an iterative solution algorithm is applied to seek solutions for the modified structure and associated system of equations [15]. Approximate methods derive the solutions using Taylor series expansion based on the earlier set of solutions (solution vectors) obtained for different design parameters. The approximate methods are considered adequate for analysis of intermediate designs, where an exact analysis is not essential. Table 1.1 summarizes the general reanalysis techniques along with the brief description and potential applications.

Argyris et al. [14], Jalon and Viadero [15] used direct method of computing the displacements of the modified structure through direct inversion of the modified stiffness matrix using the Sherman-Morrison formula. In the direct solution, the change in displacements was computed by carrying out a series of decomposition and operations on the original and modified stiffness matrices and load vectors. Phansalkar [16] achieved improved and rapid convergence by

**Table 1.1: A summary of Various Reanalysis Methods Reported in the Literature.**

| Reanalysis Method | Brief Description of | Applications Demonstrated (if any) | Comments |
|---|---|---|---|
| Direct Method [14] | An algorithm to compute modified displacements by triangularizing the modified stiffness and original decomposed stiffness matrix | A simple bar structure to illustrate the methodology | Useful for changes affecting a small portion of a structure |
| Direct Method [15] | An algorithm very similar to [13], but with an improvement by creating an augmented matrix to include modified stiffness and using skyline vector solution | Plane frame structure | Numerical efficiency is higher than that of the method reported in [14]; may not be applicable for large modifications |
| Iterative method [16] | Gauss-Seidel iterative solutions are shown to be effective for reanalysis | Continuous beam structure | Useful for simple structure |
| Iterative method [17] | Series expansion formulation of the modified stiffness matrix | Continuous beam structure | Useful for simple structural configurations |
| Approximate method [18] | Taylor series single and two terms expansions solutions and Reduced basis vector solutions are compared | Transmission tower (space truss) | Modified reduced basis technique is better for solutions where many design variables are involved |
| Approximate method [19] | A mixed method involving both displacements and forces as unknowns is discussed | Space truss with 124 bar elements | Require large computer memory |

adopting a judicious grouping of the coefficient matrix, comprising the original and modified stiffness, into blocks and by performing a series of Gauss-Seidel iterative operations on the blocks for achieving convergent solution of the problem. Kirsch and Rubinstein [17] proposed an algorithm using series expansion based on the changed stiffness, as a linear combination of the original and modified matrices, to compute the approximate solution. While the proposed iterative technique required more operations it resulted in improved convergence. Noor and Lowder [18] compared the approximate solutions obtained through the Taylor series expansion and reduced basis vectors, derived from the previous solutions for the structure with different design parameters. The study demonstrated the merits of the reduced basis vector approximation method in achieving computational efficiency through analysis of a space truss.

### 1.2.4 Substructuring and Reanalysis

Analysis of large structures using personal computers has been severely limited due to complexities associated with memory management with large size matrices. Substructuring techniques are known to be quite effective, specifically when the structure is of repetitive or of similar configurations. Local design modifications can easily be analyzed by creating refined and analysis of the modified structure alone [39]. The derivation of total structure response through combination of individual substructure solutions, however, poses complexities with standard packages due to constraints imposed in managing the input/output file information [41]. The published studies on structures using substructure technique are summarized in Table 1.2 together with the applications.

**Table 1.2: Summary of Published Studies on Reanalysis Using Substructuring Techniques.**

| Reanalysis Method | Brief Description of | Applications Demonstrated (if any) | Comments |
|---|---|---|---|
| Approximate Method [19] | Reduced basis vector method in conjunction with substructuring and sensitivity vectors | 219 bar transmission tower with 4 design variables | Problem size was manageable due to substructuring |
| Approximate Method [18] | Optimization is performed successively on substructures, using direct search method and penalty functions | six equal span beam structure | Reduction in problem size and computational time are reduced |
| Approximate Method [39] | An algorithm is developed to evaluate only critical design sensitivity vectors combined with substructure | 200 member, 150 DOF plane truss structure | Reduction in computer time was achieved |
| Approximate Method [41] | A black box approach using the analysis results from a standard commercial package and using static condensation for sensitivity analysis for a limited part of a structure | Stick frame model of an automobile | Significant reduction in computer time was achieved |
| Approximate Method [46] | A different method of partitioning using the symmetry and asymmetry loading conditions | Rectangular shell structure | May have very limited application depending on the loading situations |

Noor and Lowder [19] described the reanalysis methods using substructuring and reduced basis vectors for analysis of large scale structures, such as transmission tower. In the reduced basis approach, it is assumed that the

displacement vector of a new design can be approximated by a linear combination of linearly independent vectors of previously analyzed designs. The authors presented a mixed-method formulation, by considering both displacement and force as unknowns, for solving a 124 bar space truss problem [20]. While the benefits of the method were clearly demonstrated for the example cases, the application to structures requiring more degrees-of-freedom at a node may pose memory problems [20]. The matrix size may approach extremely large, since it involves a combination of both stiffness and flexibility matrices of the entire structure in a single global matrix. Gupta [36] analyzed the static behavior of a liquid -tank -structure loaded by liquid pressure, using substructure and reanalysis techniques, where the initial solution was obtained using ANSYS computer code.

In computing the reanalysis solution, the evaluation of design sensitivity is implied. Sensitivity can be defined as the ratio of the change in response of a structure, such as stress, deformation, frequency obtained due to change in one or several design variables from the existing design space. The simplest technique in calculating them is through finite difference techniques. However, this can be computationally expensive. The other method is to directly seek the derivative of the performance variable with respect to the design variable using appropriate equilibrium equations. In seeking reanalysis solutions for large structure it is advantageous to combine the information of sensitivity and substructuring, since the computation can be restricted to few substructures affected by design modifications. Literature based on this approach of analyses in structural problems with application are summarized in Table 1.3. Arora and Govil [39] have sought an optimal structural design for a large truss structure of 200 members, by substructuring and design sensitivity in the formulation. The authors claim the algorithm is 66% more efficient than conventional approach. Gangadharan et al.

[41] used a static condensation method for sensitivity analysis of structures to calculate the sensitivity of the joint displacements with respect to the stiffness of welded joint of car frame. The car structure was based on a stick-model and the information of displacements was obtained from general purpose software ANSYS.

**Table 1.3: Summary of Published Studies on Reanalysis and Sensitivity Analysis.**

| Reanalysis Method | Brief Description of | Applications Demonstrated (if any) | Comments |
|---|---|---|---|
| Approximate Method [52] | FEM analysis with Taylor series approximation | Stringer-Frame fuselage | Good approximations for deflections and stresses |
| Iterative Method [40] | Algorithm uses an iterative technique using design variable perturbation and forward difference algorithm | Static analysis of thin plates and eigenvalue analysis of plane frame | Good convergence was achieved |
| General study [43] | Three methods, namely, virtual load, state space variable and design space variable, are compared | A general study. | Design sensitivity analysis for structural optimization are discussed |
| Iterative Method [17] | Discusses method for computing finite difference derivatives | Static analysis of a 72 bar space truss analysis | Method permits independent control of accuracy of a variable and its derivative |
| Rational approximant Method[63] | Superior convergence behavior of rational approximants is exploited. | Static and free vibration analysis of a beam structure | Method permits large variations of design variables and fewer terms for achieving convergence |

### 1.2.5 Reanalysis using Transfer Matrices Method

The design and analysis methods based upon finite-element, reanalysis and substructuring techniques, reviewed in the previous subsection, result in excessive problem size, specifically for large scale structures. In view of the increasing trends towards the use of personal computers, a reduction in the problem size is considered highly desirable. The cargo trailer industry has, specifically, identified need for PC based design tools, since the industry is involved in fabrication of numerous configuration of Custom trailers. A number of alternate methods of structure analysis with an objective to reduce the problem size have thus been explored. Dokainish [11] demonstrated the potential benefits of a using Finite Element-Transfer Matrix approach for the vibration analysis of a clamped plate. The method referred to as 'Finite Element Transfer Matrix' (FETM) combines the compactness of transfer matrix solution and efficiency of the finite element method. In this approach the complete structure is partitioned into strips connected in a chain-like manner and the stiffness matrix generated for each strip is rearranged in order to relate the performance or behavior vectors of the adjacent strips at the connections. The advantage of the method is readily appreciated as the size of the problem is considerably reduced. The author demonstrated the effectiveness of the method through an example case using the 18 x 18 matrix instead of 108 x 108 generated with the conventional finite element approach. Sankar and Hoa [10] proposed an extended transfer matrix method for free vibration analysis of a plate. The method utilized an extended state vector comprising the vector of displacements and forces and the sensitivity vector, their derivatives with respect to the circular frequency. The study demonstrated considerable improvement in the computational efficiency of the method through eigensolutions for a clamped plate. The method of combining the FETM and

sensitivity vectors in seeking reanalysis solution through an extended finite element transfer matrix formulation thus becomes an attractive approach for PC-based application.

## 1.3 Scope and Layout of the Thesis

From the review of the relevant literature presented in the previous section it is apparent that the finite-element based methods (FEM) provide the most efficient analysis of structures, including those of the vehicles. Such methods, however, pose unreasonable demands on computing and human resources, specifically when large scale trailer structures are involved. A need to improve the efficiency and compactness of such tools has thus been identified in order to implement the design and analysis tool in a personal computer environment. The design process associated with large scale vehicular structures frequently involves repetitive analyses to identify near optimal design compromises. The limitations posed by the memory requirements and speed of FEM analysis can be conveniently addressed through development of reanalysis methods, which are ideally suited for vehicular structures with ladder-type design configurations. Although methods based upon reanalysis, substructuring and sensitivity analyses have been proposed to enhance the computational efficiency of large scale structures, these methods do not take advantage of the repetitive design features of a trailer structures. A combination of these techniques, referred to as extended finite element-transfer matrix method, has also been proposed to improve the computational efficiency. The proposed method, however, has been applied for free vibration analysis of simple structures.

The review of published literature further revealed that the reanalysis methods have been extensively applied for large structures such as bridges and transmission towers. The studies on vehicular structures have been, invariably, limited to automobile structures, which may be attributed to their large production volume and well established research and development support The similar studies on truck-trailer structures, however, are limited to only a few. The lack of such studies may be attributed to the small to medium-size of the trailer manufacturing industries, and extensive design variations arising from different road laws, applications and customer requirements. A need to develop efficient reanalysis methods that can be generally applied to trailer structure design is thus identified in this study, in order to derive light weight, cost efficient and reliable trailer structures. The overall objective of this investigation is to contribute towards attainment of energy efficient light weight designs of trailers employed in freight transportation. The specific objectives of this investigation are to develop design-reanalysis tools to perform efficient assessment of design and design modification in a personal computer environment. The detailed objectives of the present investigation are as follows:

a. Develop a reanalysis methodology using substructuring of large scales in conjunction with Potters' method of solution in order to reduce the overall matrix size and to enhance the numerical efficiency of the solution.
b. Develop a reanalysis methodology upon integrating the compactness of substructuring and transfer matrix techniques by extending the station vectors to include the design sensitivity vector.
c. Develop a methodology to derive the change in stiffness matrix of the substructure affected by a local design modification and propose methods to

integrate this modification into the overall problem thus eliminating the need for total re-evaluation of the entire structure.

d. Perform a study of design details of most commonly used trailer structures and identify representative candidate structures.

e. Develop a performance criteria to assess the flexural and torsional deflections and stresses of the trailer structures.

f. Propose a methodology to assess the performance characteristics of the structures subject to dynamic road loads arising from directional maneuvers and tire-road interactions.

g. Validate the developed reanalysis methodologies through analysis of selected bench mark structures and investigate the numerical efficiency of the reanalysis techniques.

h. Perform experimental modal analysis of a candidate trailer structure and compare the experimental results with those derived from the developed analysis methods to demonstrate their validity.

i. Validate the analysis methods by comparing the solutions with those obtained from a commercial finite-element software.

j. Perform a comprehensive parametric study involving local design modifications in the design parameters of key members, using the reanalysis methods and design sensitivity vector. Investigate the influence of design modifications on the performance criteria under normal and twist loads.

k. Determine the dynamic response characteristics of the trailer structures subject to suspension loads arising from tire-terrain interactions as a function of the vehicle speed and road roughness.

The design of various trailer configurations used in freight transportation are briefly reviewed in Chapter 2, and two candidate semi-trailer structures are identified for the present study. The design details of the candidate structures are described and performance indices are formulated to study the structure behavior under static and dynamic loads. The pre- and post-processor requirements for compilation of design data and interpretation of the response are discussed.

Chapter 3 describes the finite element and substructuring concepts for analysis of large scale structures in view of their implementation in a personal computer environment. Two methods of reanalysis are developed based upon Potters' method of solution and extended transfer matrix approach. The significance of design sensitivity and solution techniques is discussed. The influence of a local design modification is incorporated into the overall problem through derivation of the change in stiffness sub-matrix with variations in the design variable using first order Taylor's series approximations.

In Chapter 4, the reanalysis methods are extensively validated through analysis of selected bench mark and candidate trailer structures. Bench mark structures, such as, planar bar structure and a space truss structure are analyzed using the two reanalysis techniques, and the solutions are compared with those reported in published studies to demonstrate the validity of the proposed methods. The reanalysis methods are further validated for large scale trailer structures using the results derived from experimental modal analysis and those derived from ANSYS software. The computation efficiency of the proposed methods is investigated for different structures.

In Chapter 5, the design sensitivity analyses are performed to study the influence of selected design variations on the performance indices for the candidate trailer structures.

The dynamic response characteristics of the trailer structure subject to suspension loads arising from tire-terrain interactions are evaluated in Chapter 6. Two distinct road profiles are identified from published studies and equivalent suspension forces are estimated from a simplified uncoupled vertical mode model. The method of modal superposition is used to determine the dynamic response as function of road roughness, speed, modal damping and suspension stiffness. The simultaneous matrix iteration technique is employed to identify the first 25 deflection modes of the structure.

The conclusions drawn from the study are finally summarized in Chapter 7, together with recommendations for further studies in the area.

# CHAPTER 2

# DESCRIPTION OF STRUCTURE AND ANALYTICAL REQUIREMENTS

## 2.1 Introduction

The design and analysis of automotive structures has been supported by extensive research and development efforts in view of the large volume productions and competitive demands. The design of heavy vehicle structures, however, has received only minimal support due to the small scale nature of the industry and extensive variations in the design configurations. The developments in design and analysis tools for the large scale trailer structures have been mostly limited by the lack of PC-based user friendly and efficient design tools to effectively analyze the large scale structures and design modifications. In this study, design and reanalysis method are developed for applications to large scale trailer structures.

The development of an analysis tool for such applications, primarily, requires the formulation of PC-based finite element analysis applicable to standard cross sections used in trailer-type large structures. The computational and the user-friendliness of the tool in reanalysis of structure form the primary concerns of the users. A pre-processor and the post-processor, therefore, must be designed for enhancing the efficiency and user-friendliness in formulating the model, analyses, reanalyses, and interpretation of the results. Appropriate performance indices also need to be selected for effective evaluation of a design and design modification.

In this section, the trailer structures are described to formulate the essential features of the pre-processor. The design details of two candidate trailers are presented and various design and analysis requirements are discussed.

**Table 2.1 Population of the Heavy Vehicles Combinations Present in Various Centers Across Canada [44].**

| Vehicle Combination | % Distribution of Vehicle Combination | | | | | |
|---|---|---|---|---|---|---|
| | Vancouver | Calgary | Winnipeg | Toronto | Montreal | Moncton |
| Tractor Semitrailors | 60 | 80 | 60 | 70 | 90 | 98 |
| A-Doubles | 32 | 8 | 25 | 25 | 8 | 1 |
| B-Doubles | 8 | 10 | 14 | 5 | 2 | 1 |
| C-Doubles | 0 | <2 | <1 | <1 | <1 | 0 |
| Triples | 0 | <1 | <1 | 0 | <1 | 0 |
| Total | 100 | 100 | 100 | 100 | 100 | 100 |

## 2.2 Description of Candidate Trailer Structures

A large number of commercial vehicle configurations are used in general purpose transportation. Figure 2.1 presents the schematics of some of these vehicle configurations and Table 2.1 summarizes the percentage population of different vehicle combinations used across Canada. A Survey of vehicle configurations, conducted by the University of Michigan Transport Research Institute [44], concluded that approximately 77% of all heavy vehicles operating in

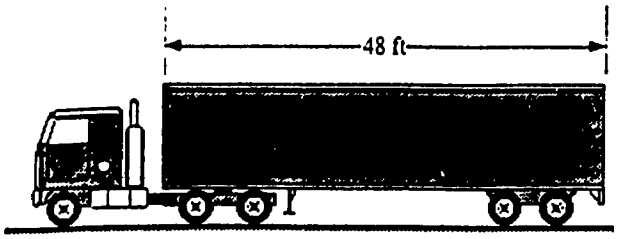


(a) Tractor-semitrailer

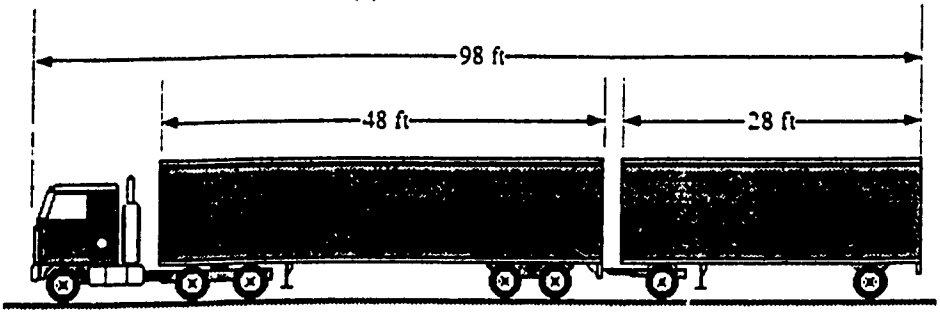


(b) Rocky Mountain Double

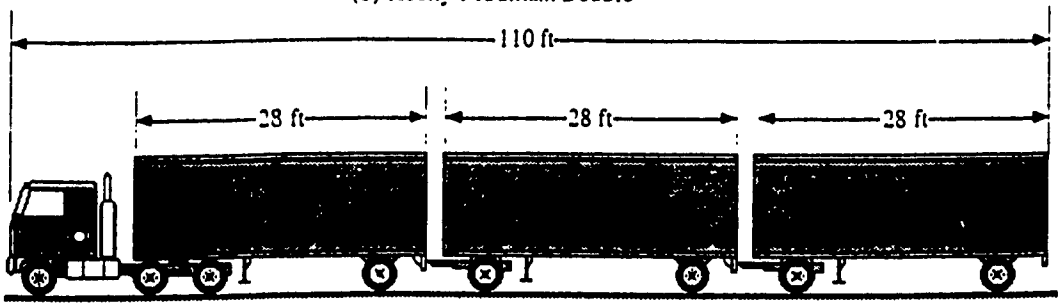


(c) Triple Trailer

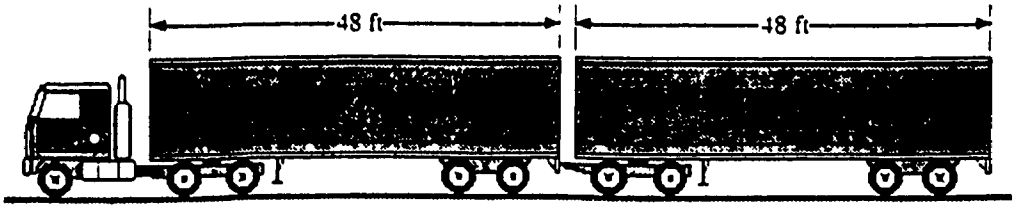


(d) Turnpike Double

Figure 2.1: Schematics of vehicle configurations [66].

Canada are tractor-semitrailers. The semitrailer structures are thus selected as the candidate structures for this study.

The semitrailer/trailer structures used in freight transportation or logging operations are large size structures with ladder-type repetitive configurations. The typical base structure used in truck/trailer industry is referred to as "ladder-type" configuration, which comprises a pair of main beams and a pair of side beams interconnected through a number of cross beams. The beam members are either fabricated or extruded structural members with varying web-depth along the trailer length to accommodate the fifth wheel pivot and suspension arrangements. A schematic of a typical semitrailer structure with two main beams, two side beams and number of cross beams is shown in Figure 2.2. Two candidate trailers are selected for this investigation based upon the commonly used configurations and different applications:

Trailer A: A trailer employed in five-axle tractor-semitrailer combination operating in on-road load conditions. The wheel base of this candidate trailer is relatively short (9.29 m) and is equipped with 2-axle tandem suspension with a payload capacity not exceeding 250 kN.

Trailer B: A trailer employed in a six-axle tractor-semitrailer combination designed for forestry or logging sector. The wheel base of this trailer is 14.62 m which is equipped with a tridem axle suspension with a load carrying capacity of nearly 350 kN. The lead axle of the trailer comprises a liftable mechanism. This candidate trailer is designed to operate on road as well as forestry terrain. Since the lift-axle is used only during tight turns, the candidate trailer is modeled as a three-axle trailer in this study.

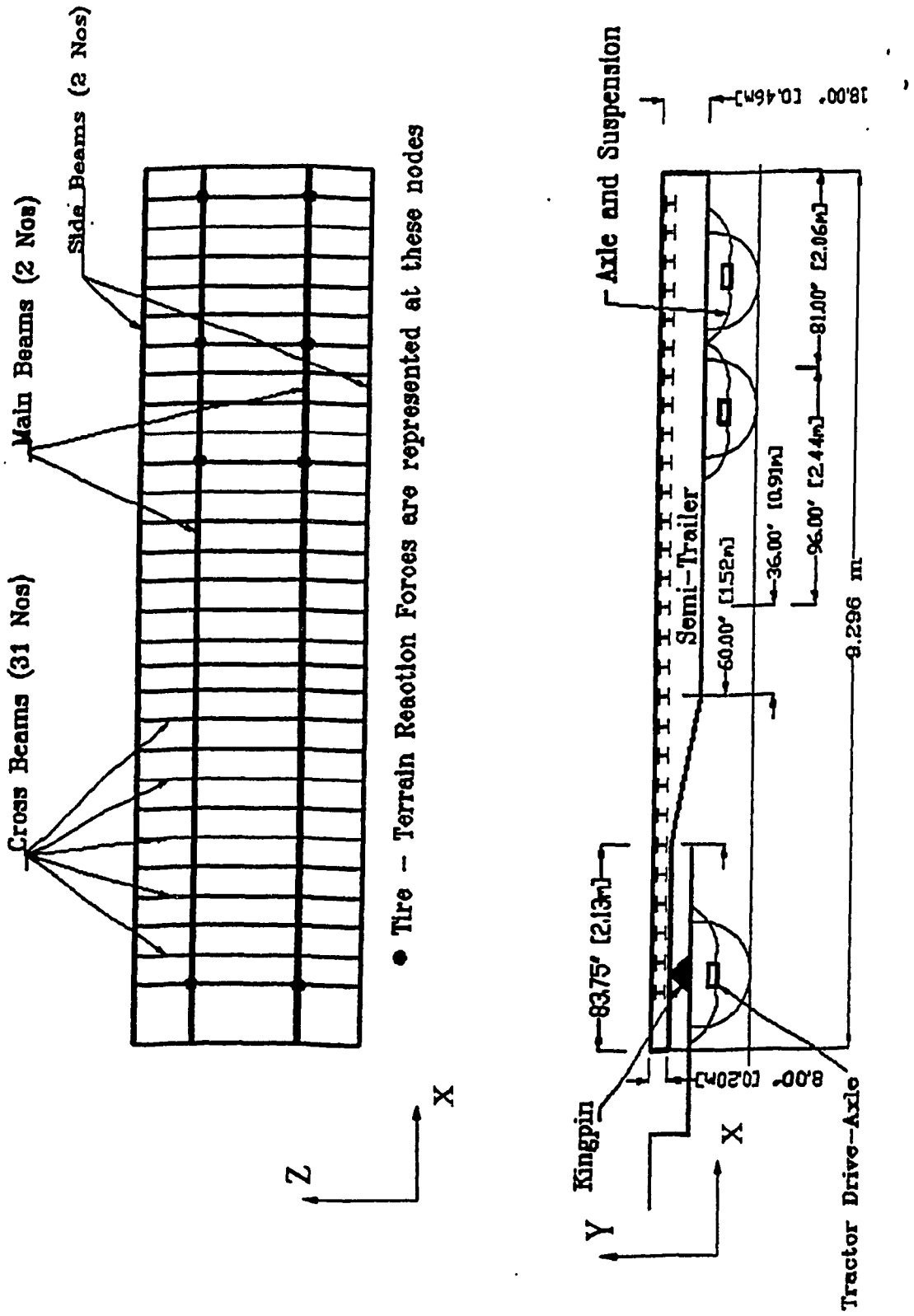


Figure 2.2: Schematic of a semi-trailer structure illustrating the arrangement of main- side- and cross-beams.

The two trailer structures are quite similar in configuration, their dimensions and the load carrying capacities, however, differ in many features. The structure comprises two main-beams and two side-beams interconnected through several cross-beams forming a framed structure fabricated of structural steel, as illustrated in Figure 2.2. The cross beam constructional arrangements vary widely in the industry as illustrated in the Figure 2.3 for trailers A and B. The cross-sections of the main and side beams of the structure may also differ with the designer's preferences and load carrying capacities. The cross-section of the members of the candidate trailers considered in this study are summarized in Table 2.2.

**Table 2.2: Summary of Cross-Section of Structural Members of the Trailers.**

| | Candidate Trailer | |
|---|---|---|
| | Trailer - A | Trailer - B |
| Main Beam | I - Section | I - Section |
| Side Beam | C - Section | I - Section |
| Cross-member | I - Section | C - Section |

The depth of the main-beam, in-general is varied along the length of the trailer in order to accommodate the fifth wheel, and suspension, and to achieve desired ground clearance, as shown in Figure 2.3. The detailed geometry of the beams used in trailer-A with section and physical dimensions are summarized in Table 2.3. The material properties of the structured members are also summarized in Table 2.3. Table 2.4 describes the geometry and cross-sectional properties of the members used in trailer-B [46]. A comparison of the design details of the two trailers reveals that the trailers A and B employ C- and I- section side beams,

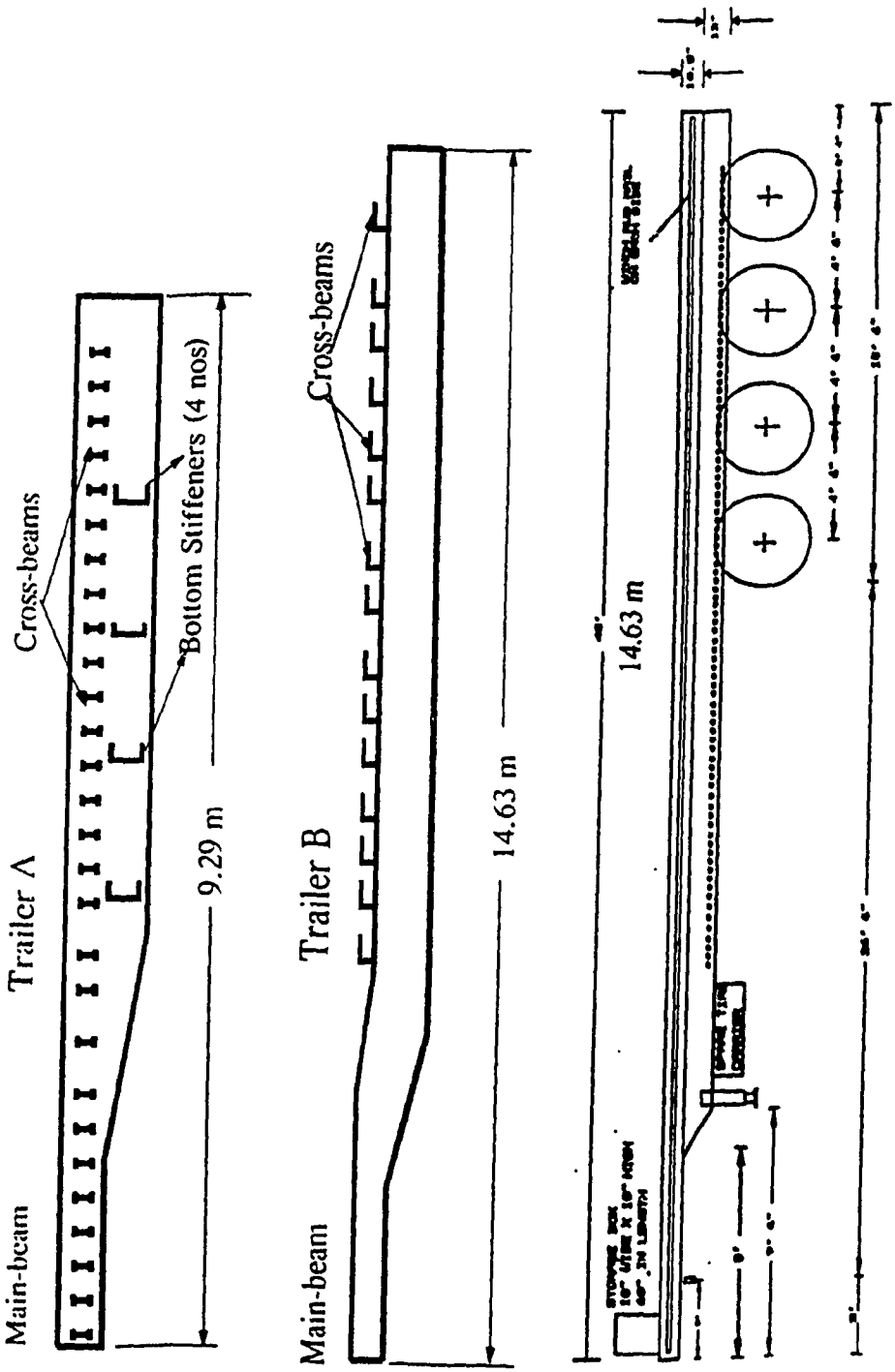


Figure 2.3: A Plane view of the trailer structure and main-beams used in trailer A and B.

## Table 2.3: Material and Sectional Properties of Structural Members (Trailer A)

| Material: Structural Steel | |
|---|---|
| E Young's modules | $2.1 \times 10^{11}$ Pa |
| G Shear modules | $1.05 \times 10^{11}$ Pa |
| Yield Strength | $1.75 \times 10^{8}$ Pa |
| Density | $7.86 \times 10^{3}$ kg/m$^3$ |

MAIN BEAM

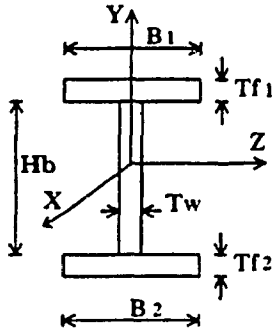


SIDE BEAM

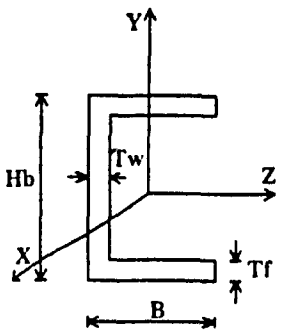


CROSS BEAM

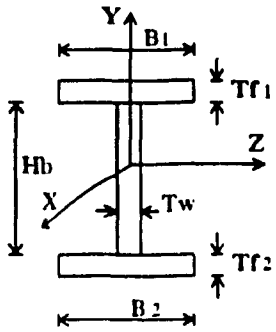


MAIN BEAM

| Section | Length (m) | Hb (m) | Tw (m) | $B_1$ (m) | $Tf_1$ (m) | $B_2$ (m) | $Tf_2$ (m) |
|---|---|---|---|---|---|---|---|
| I | 2.1336 | 0.20320 | 0.63500E-02 | 0.12700 | 0.01905 | 0.12700 | 0.01905 |
| II Variable Hb | 1.5672 | 0.41402 | 0.47943E-01 | 0.17018 | 0.06223 | 0.17018 | 0.06223 |
| III | 5.4102 | 0.45720 | 0.47625E-02 | 0.12700 | 0.01905 | 0.12700 | 0.01905 |

SIDE BEAM

| Section | Length (m) | Hb (m) | Tw (m) | B (m) | Tf (m) |
|---|---|---|---|---|---|
| I | 0.21336E+01 | 0.10160E+00 | 0.47625E-02 | 0.76200E-01 | 0.47625E-02 |
| II | 0.15240E+01 | 0.10160E+00 | 0.47625E-02 | 0.76200E-01 | 0.47625E-02 |
| III | 0.54102E+01 | 0.10160E+00 | 0.47625E-02 | 0.76200E-01 | 0.47625E-02 |

CROSS BEAM

| Section | Length (m) | Hb (m) | Tw (m) | $B_1$ (m) | $Tf_1$ (m) | $B_2$ (m) | $Tf_2$ (m) |
|---|---|---|---|---|---|---|---|
| Left | 0.68580 | 0.08890 | 0.63500E-02 | 0.057150 | 0.63500E-02 | 0.057150 | 0.63500E-02 |
| Middle | 0.91440 | 0.08890 | 0.63500E-02 | 0.057150 | 0.63500E-02 | 0.057150 | 0.63500E-02 |
| Right | 0.68580 | 0.08890 | 0.63500E-02 | 0.057150 | 0.63500E-02 | 0.057150 | 0.63500E-02 |

## Table 2.4: Material and Sectional Properties of Structural Members (Trailer B)

| Material: Structural Steel | |
|---|---|
| E Young's modules | $2.1 \times 10^{11}$ Pa |
| G Shear modules | $1.05 \times 10^{11}$ Pa |
| Yield Strength | $1.75 \times 10^{8}$ Pa |
| Density | $7.86 \times 10^{3}$ kg/m$^3$ |

MAIN BEAM

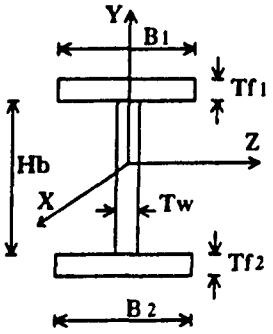


CROSS BEAM

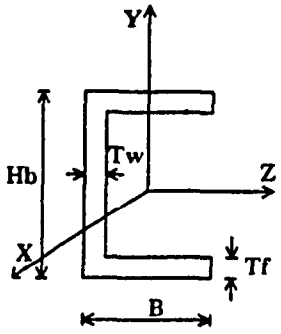


SIDE BEAM

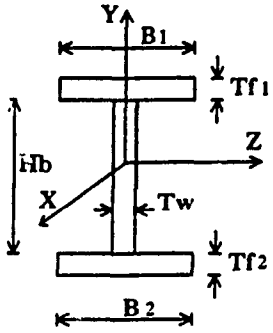


MAIN BEAM

| Section | Length (m) | Hb (m) | Tw (m) | $B_1$ (m) | $Tf_1$ (m) | $B_2$ (m) | $Tf_2$ (m) |
|---|---|---|---|---|---|---|---|
| I | 2.190 | 0.2413 | 1.27e-02 | 0.1778 | 1.27e-2 | 0.1778 | 1.27e-2 |
| II Variable Hb | 1.336 | 0.2413 0.4572 | 1.27e-02 | 0.1778 | 1.27e-2 | 0.1778 | 1.27e-2 |
| III | 11.104 | 0.420 | 1.27e-02 | 0.1778 | 1.27e-2 | 0.1778 | 1.27e-2 |

SIDE BEAM

| Section | Length (m) | Hb (m) | Tw (m) | $B_1$ (m) | $Tf_1$ (m) | $B_2$ (m) | $Tf_2$ (m) |
|---|---|---|---|---|---|---|---|
| I | 2.190 | 0.2413 | 1.016e-02 | 0.1524 | 1.016e-02 | 0.1524 | 1.016e-02 |
| II | 1.336 | 0.2413 | 1.016e-02 | 0.1524 | 1.016e-02 | 0.1524 | 1.016e-02 |
| III | 11.104 | 0.2413 | 1.016e-02 | 0.1524 | 1.016e-02 | 0.1524 | 1.016e-02 |

CROSS BEAM

| Section | Length (m) | Hb (m) | Tw (m) | B (m) | Tf (m) |
|---|---|---|---|---|---|
| Left | 0.863 | 0.1524 | 6.35e-03 | 4.45e-02 | 6.35e-03 |
| Middle | 0.863 | 0.1524 | 6.35e-03 | 4.45e-02 | 6.35e-03 |
| Right | 0.863 | 0.1524 | 6.35e-03 | 4.45e-02 | 6.35e-03 |

respectively. The cross members of trailers A and B, however, are of I- and C-sections, respectively.

In addition to the static forces and moments arising from the cargo load, king-pin reaction and the suspension reactions, a trailer structure is subject to dynamic forces arising from tire-road interaction. The magnitude of dynamic forces transmitted to the trailer structure is strongly related to the geometric and inertial properties of the vehicle combination, tire and suspension properties, and axle and suspension configurations. The trailers employ a wide range of axle suspensions, such as air, elastomeric and leaf springs, in varying kinematics configuration. Since heavy vehicles employ only lightly damped suspension, the forces arising from the tire-road interactions can be primarily related to the force-deflection properties of the suspension springs. In view of the wide variations in suspension springs used in trailers and their nonlinear force-deflection characteristics, the dynamic loads are estimated using equivalent linear spring rates of typical springs. The two candidate trailers considered in this study employ four- and six- leaf spring suspension with equivalent spring rate of 1342.2 kN/m/spring for the rear suspension springs.

## 2.3 Analysis Requirements

From the review of literature presented in Chapter 1, it is apparent that there exists a need to develop a simplified but comprehensive analytical methods to specifically address the design and analysis large scale trailer structures. The current designs of trailers are considered to be highly conservative with excessive tare weight [1]. The development of a simplified analysis tool can provide significant insight into the design of cost effective light weight trailers. The

weight optimization of the large scale trailer structures using the FEA methods, however, may be highly cumbersome. Alternatively, parameter sensitivity analyses in conjunction with reanalysis algorithms can be employed to derive near optimal light weight trailer designs in a highly efficient manner. A design software comprising reanalysis methodology thus needs to be developed for design and analysis of such structures. The pre-and post-processors also are considered highly desirable to facilitate the reanalysis and interpretations. A pre-processor is developed to model the conceptual designs loading, constraints and to describe the geometric and material properties of the structural members in an inter-active manner. The post-processor is developed to summarize the selected performance indices extracted from the results of the analysis.

### 2.3.1 Preprocessor

The analytical methods developed in this study are integrated into the design software comprising pre-and post-processor modules developed at CONCAVE Research Centre. The FEA methods, in-general, pose severe demands on the designer's efforts to describe the geometry, loading and section properties of a large scale structure. The computation of physical parameters of beam sections, such as areas, and moments of inertias of various sections further require considerable effort from the designer. The analysis of a design modification, such as changes in the physical dimensions of a member (web height, flange width or thicknesses) requires repetitive computations on the physical parameters. Variations in the location and number of structural members, such as cross beams would involve recreation of new data sets for the analysis. The processor developed in this study permits, the definition of the conceptual designed configuration, and the geometric, sectional and material properties of the structure

in an interactive manner. The menu-driven preprocessor then generates the input data required for the analysis program in the desired format. Figures 2.4 through 2.8 show typical terminal screen information displayed for carrying out different tasks, in describing the model for the analysis. Display of certain selected preprocessor screens are discussed below.

#### 2.3.1.1 INTERACTIVE SELECTION OF THE LAYOUT OF THE TRAILER CONFIGURATION

Figure 2.4 displays the first screen input asking the user to identify the nature of the task. The analysis program comprises the following three modules to carry out the different tasks.

Module 1- Build trailer structure: This module permits the user to define the configuration and geometry of the structure from either conceptual or engineering drawings. This module invokes the preprocessor to describe or select the detailed section and material properties. The preprocessor outputs the data file in a specified format for the analysis of the structure.

Module 2 - Analysis of the structure: This module may comprise FE analysis and reanalysis algorithms, developed in this study to perform the static and dynamic response analysis. The analysis module utilizes the data files compiled by the preprocessor, which may include the complete structural properties or the local design variations. The structures behavioral vectors are stored in a number of direct access files for later reanalysis and interpretations.

Module 3 - View Results (Post-processor): The data files generated by the analysis module are manipulated to display the structural response in terms of deflections and stresses in a graphical manner.

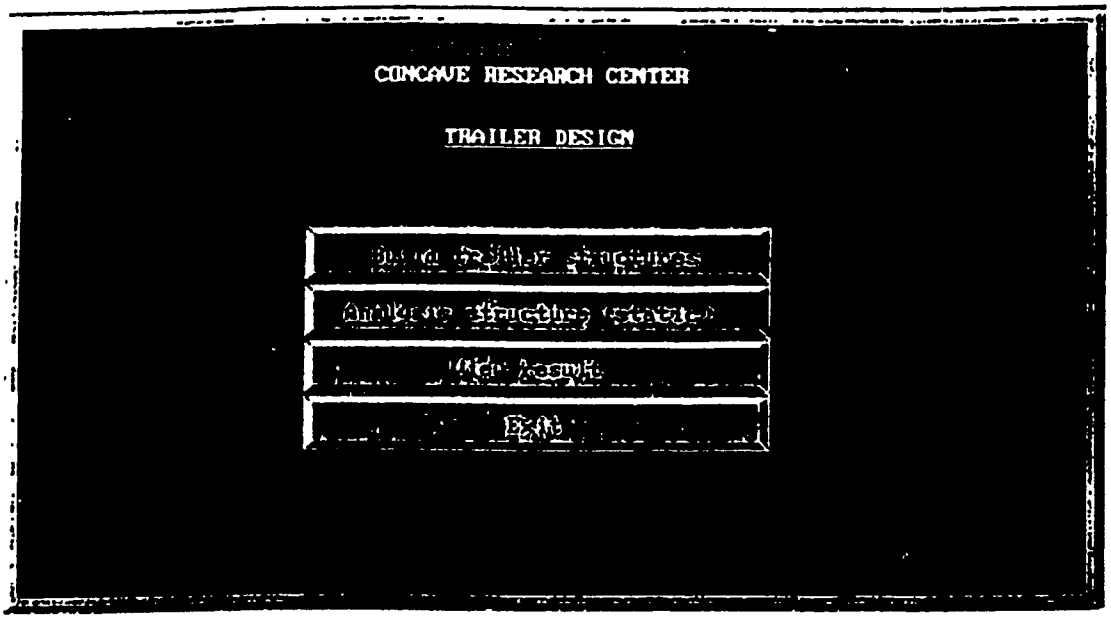


a. Components of the analysis software.

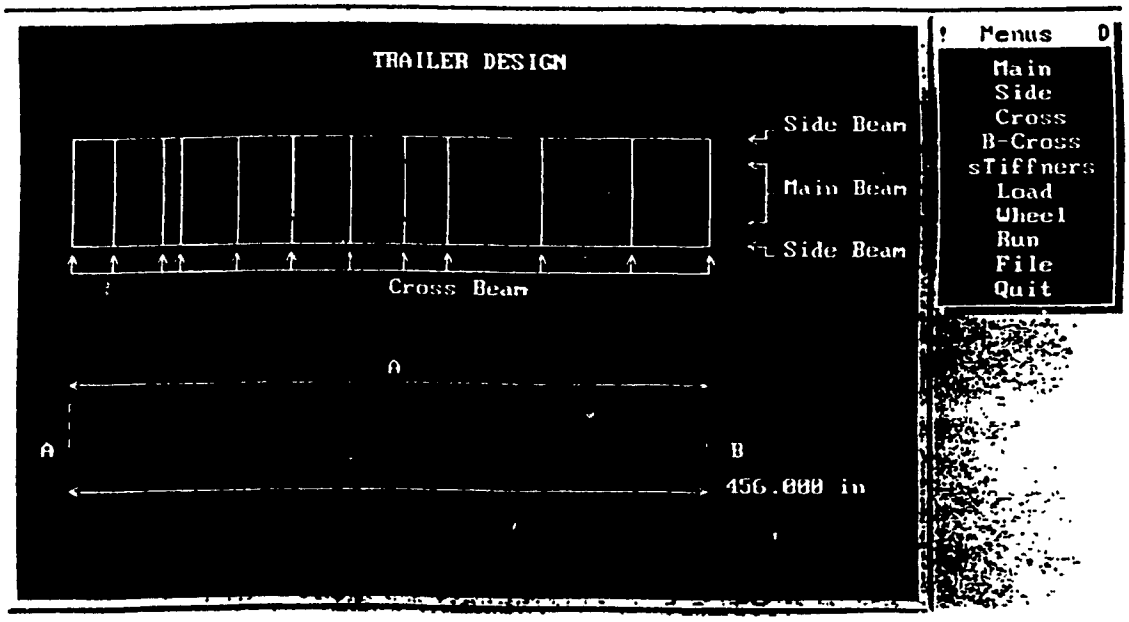


b. Outline of the structure design realized from the pre-processor.

Figure 2.4: Sample screen of the pre-processor developed at CONCAVE.

The design configurations of trailer structures, previously defined by the user, are defined by the user, and are displayed when the pre-processor module is invoked, as shown in Figure 2.4. The display describes the nomenclature adopted for modeling, and identifying the side-, main- and cross-beams with a sample lay-out, which can be modified by the user by selecting the appropriate item from the menu list. In this application, the side-beams denote the outboard longitudinal members of the ladder configurations, and main-beams denote the inner pair of the longitudinal members in the ladder structure. In the general configuration, a dotted line representation refers to the absence of that particular member. In the design configuration, shown in the Figure, item *SIDE* may be selected from the menu screen to describe/modify its geometric, sectional and material properties, which results in the screen menu illustrated in Figure 2.4. Since the primary load carrying members of a trailer are invariably designed with variable depth beam to accommodate for suspensions and other auxiliaries, the preprocessor allows the designer to specify the variations using the *six predefined primitives* shown in the Figure 2.5. The user makes a choice by typing "Type:" and providing details of length, height at both ends. The section properties of the beams are then defined by activating the *SECTION* option in the menu. The sectional geometry is defined by selecting the standard sectional details illustrated in Figure 2.6. The preprocessor comprises four standard I-, L-, C- and rectangular tube. The following physical dimensions of the selected cross-section are defined by the user:

| | |
|---|---|
| Hb - Web height; | Tw - Web thickness; |
| B1 - Flange width at top: | B2 - Flange width at bottom; |
| Tf1 - Flange thickness at top; | Tf2 - Flange thickness at bottom. |

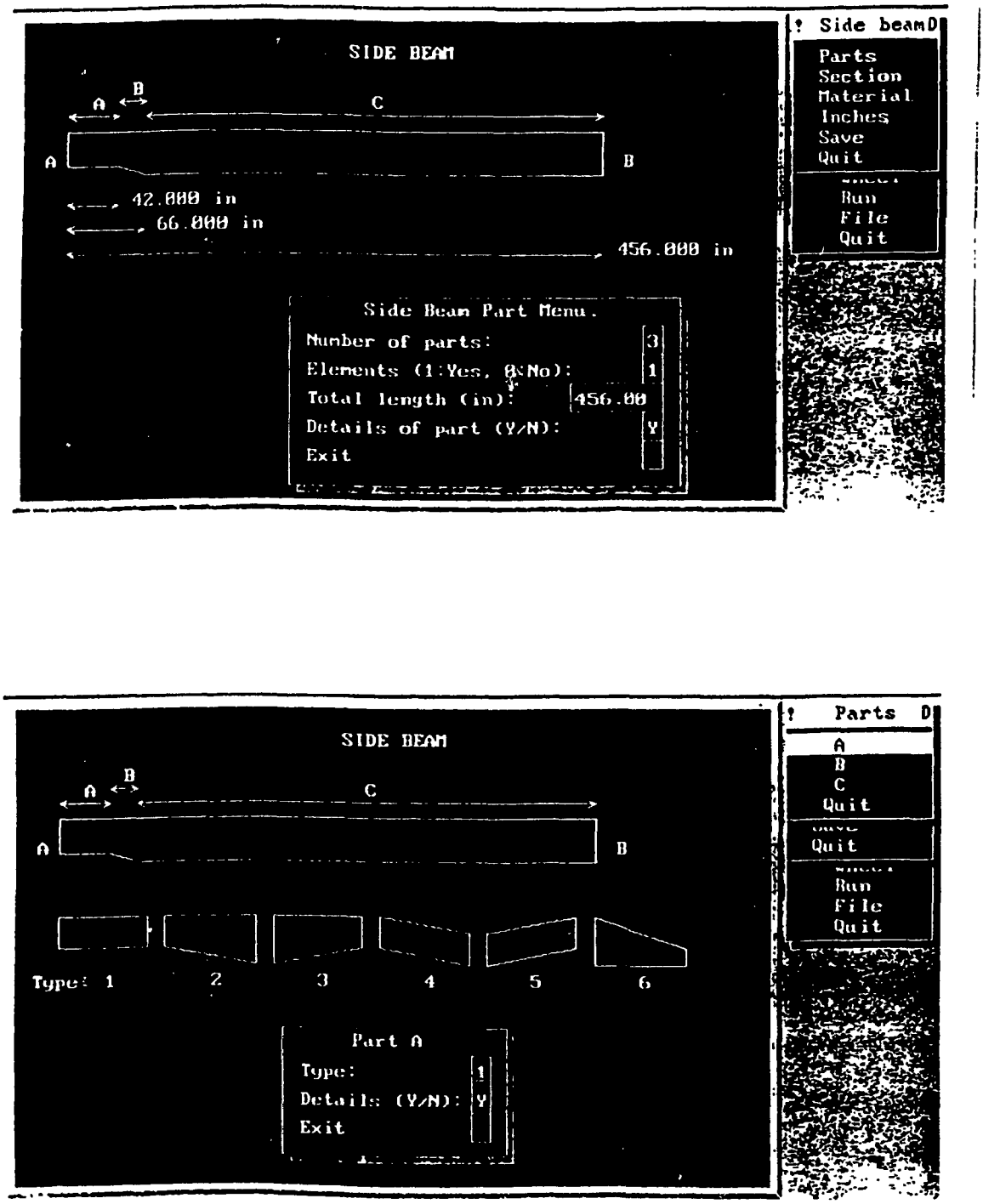


Figure 2.5: Sample screen displaying the side-beam geometry and predefined primitives.

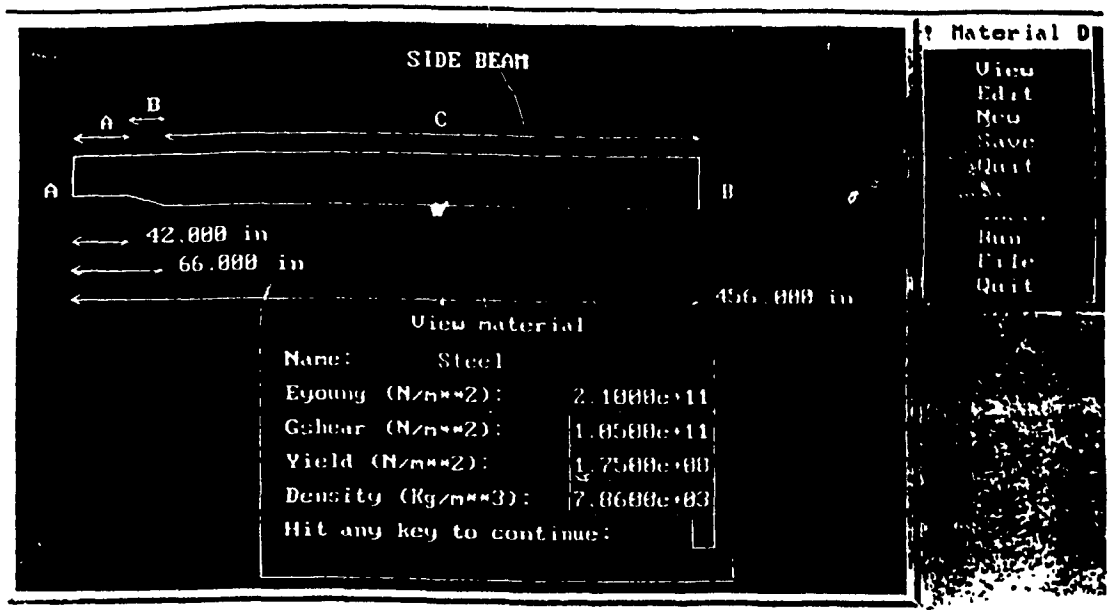


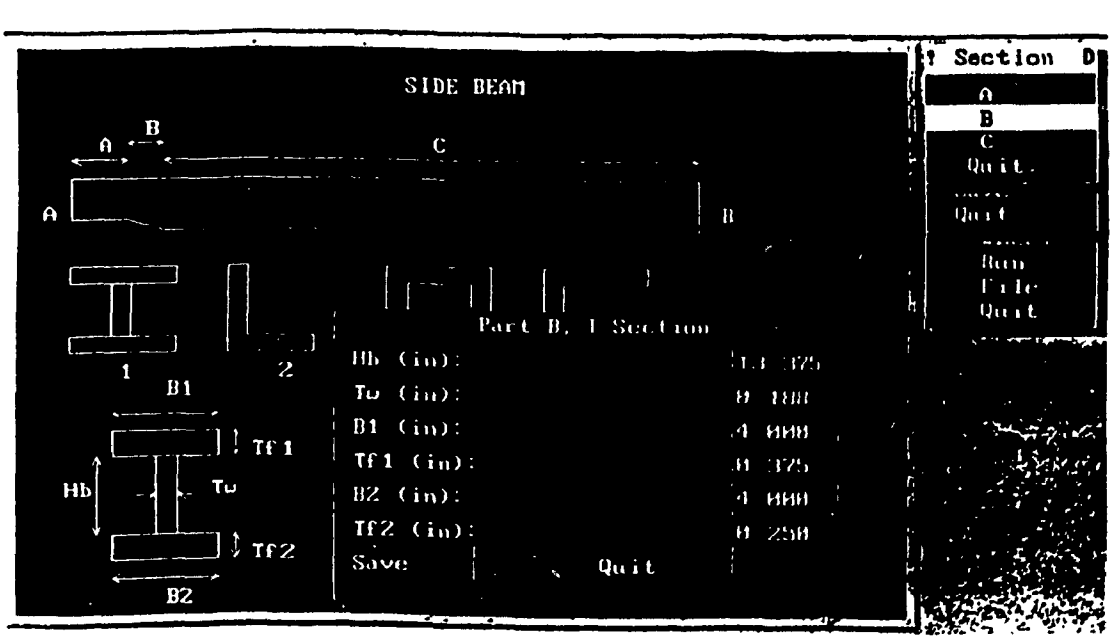


Figure 2.6: Sample screen displaying the geometry and material properties of different section.

The physical properties of the structural members, such as area of cross sections, and the moments of inertia about three perpendicular axes are computed by the module, which are used in formulating the element stiffness matrix and for computation of the deflections and stresses in the analysis stage. The material properties of the selected sections are defined by selecting the *MATERIAL* option in the menu, as shown in Figure 2.6. This menu displays typical material properties which may be edited by the user and saved for building the material property library. The geometric and material properties of cross-beams can be defined in a similar manner, by selecting the *CROSS* option in the pre-processor menu, illustrated in Figure 2.4. Figure 2.7 illustrates the screen displays for defining the positions of the cross-beams and the stiffness properties of the suspension beams. Additional stiffeners can also be defined and integrated into the structure using the prompt *STIFFENERS* in the pre-processor menu (Figure 2.4). The static loads applied on different nodes are defined by activating the *LOAD* option in the menu.

The properties of suspension springs are described by the user by selecting the *WHEEL* option in the trailer design menu (Figure 2.4). The user is required to describe the following:

(i) The location of suspension springs to determine the coordinates of tire forces transmitted to the structure. The location of the suspension element is described by identifying the node by the corresponding row and column of the ladder type structure, as shown in Figure 2.7.

(ii) The stiffness of the equivalent suspension springs.

(ii) The boundary restraints on the structural nodes.

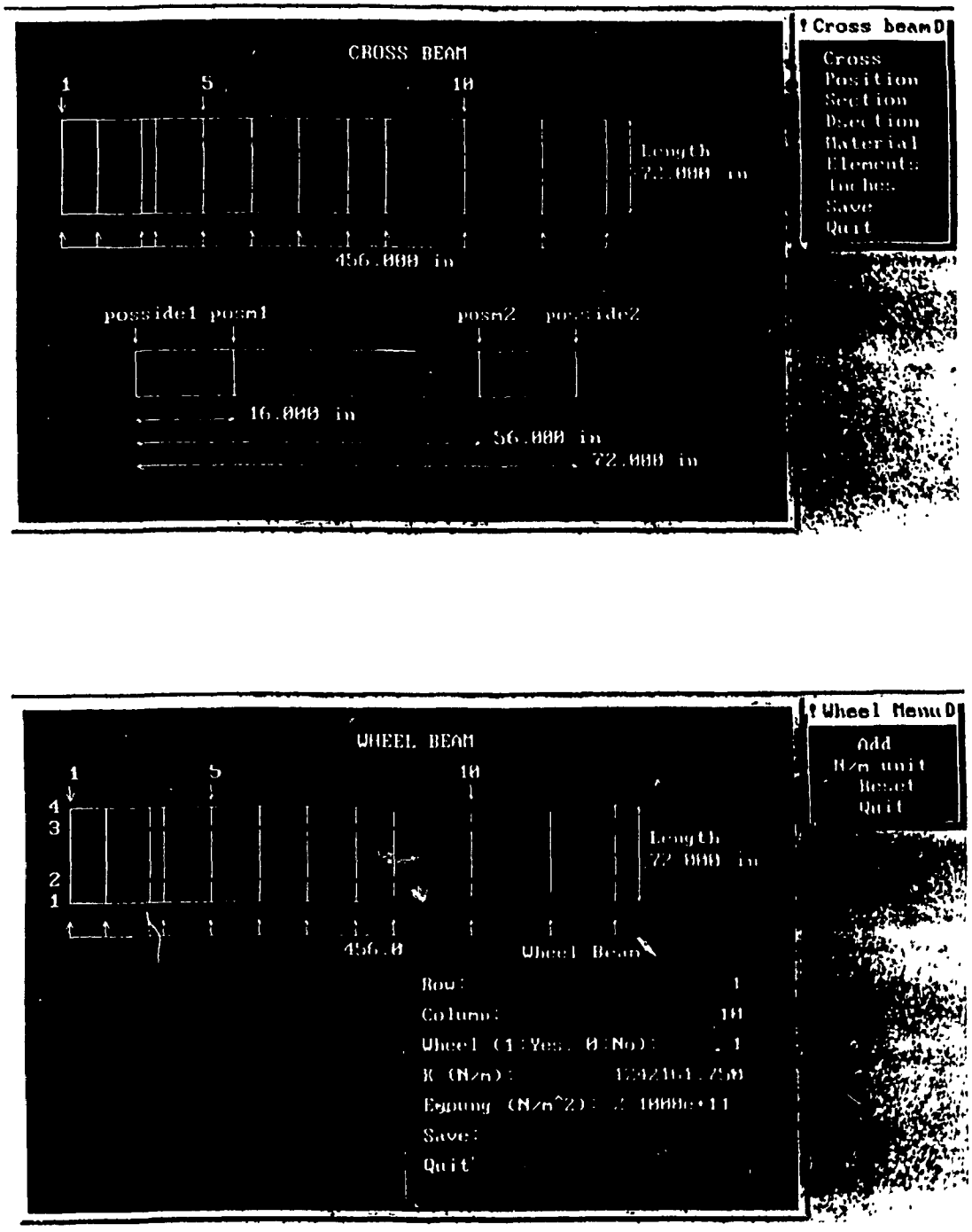


Figure 2.7: Sample screen displaying the position of the cross-beams and properties of the wheel support.

The model data is stored in an input file by activating the *RUN* option in the menu. The user specifies the input file name as prompted by the pre-processor module. The *FILE* option can also be activated to retrieve/edit the model data of a predefined structure. The data file comprises the following data for the structure:

(i) Coordinates of the nodes.

(ii) Structure partitioning and nodal connectivity of elements.

(iii) Elements and nodes contained in each partition.

(iv) Coordinate transformation matrix for each element.

(v) Cross section of each element and associated properties (cross-section area and moments of inertia about three perpendicular axes).

(vi) Loads acting on various nodes.

Upon defining the structural design, the structure analysis may be performed by activating the *ANALYSIS* option in the main menu. This option requires the specification of the input file containing the structure model data. The output file generated by the analysis module are further analyzed in the post-processor module, as shown in Figure 2.8. Desired performance characteristics such as deflections and stresses may be selected and viewed for the main- side-, or cross-beam

## 2.4 Performance Indices

The design and analysis of a structure, in-general, involves a number of performance objectives and criteria. The primary performance criteria for the design of a trailer structure may comprise: (i) the tare weight to reduce the manufacturing cost and to allow maximum payload; (ii) service life as determined

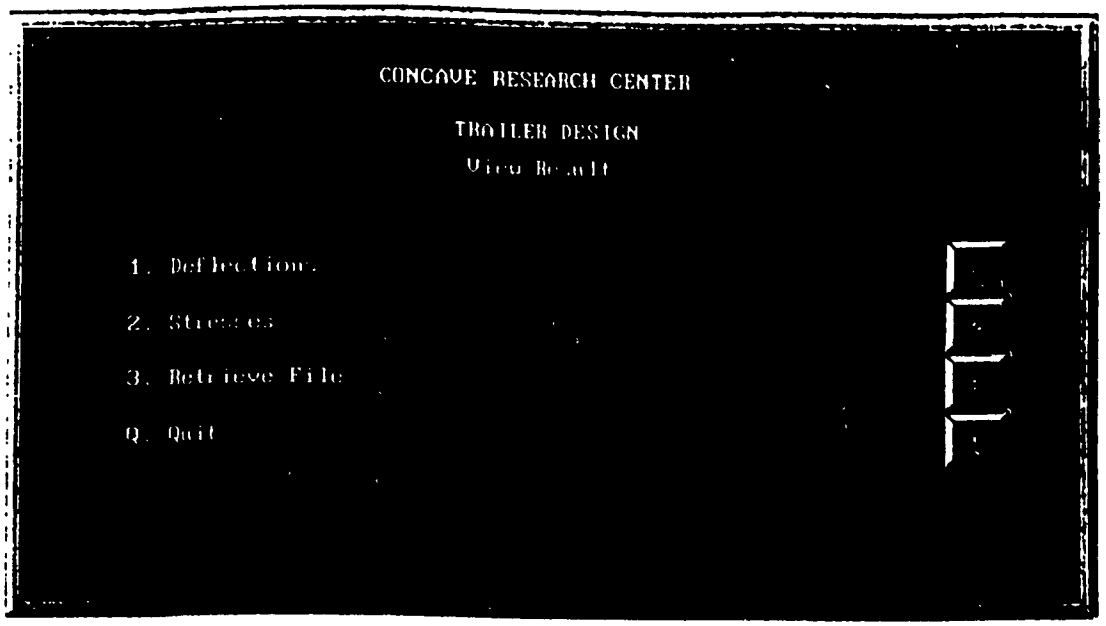


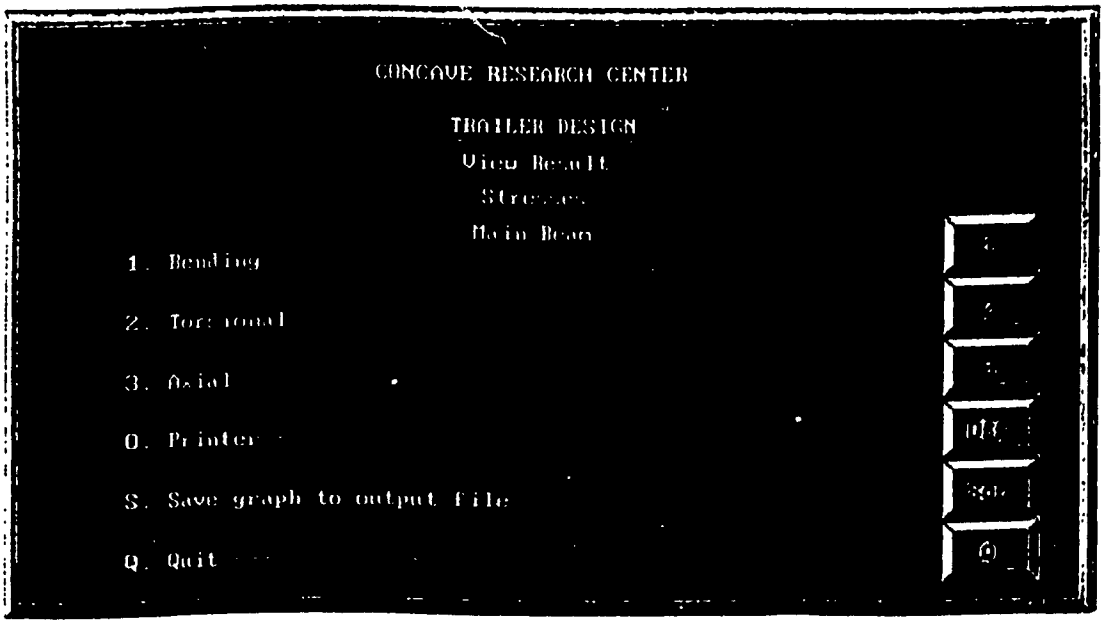


Figure 2.8: Sample screen displaying the post-processor menu.

from the dynamic stresses of the members; and (iii) weights and dimensions to conform with the provincial road laws. Commercial considerations directly relate to the cost effectiveness as derived form the weight saving and service life expectancy. Legal considerations involve total trailer weight, and its overall dimensions and road clearances. The performance objectives of a trailer design may thus be formulated as follows:

(i) Minimize the maximum deflections of structure to maintain the required ground clearances.

(ii) Minimize the static and dynamic working stress of the structure to enhance the life expectancy.

(iii) Minimize the tare weight of a particular design to reduce the manufacturing cost and to enhance the transport economy by increasing the payload.

In this study three different performance criteria are formulated to determine and assess the above design objectives. The influence of design modifications is specifically investigated using the following performance indices under static and dynamic loading:

1. Deflection Performance Index (DPI): The deflection performance of the trailer structures is assessed in view of variations in the trailer length, trailer weight and the payload. The DPI is thus characterized by the peak bending deflection normalized with respect to the trailer length, tare weight and the payload, in the following manner:

$$DPI = \frac{(\text{Peak deflection in bending, m})\ (\text{Tare weight, N})}{(\text{Overall length, m})\ (\text{Payload, N})}$$

2. Torsional Performance Index (TPI): The torsional performance is evaluated in terms of maximum twist angle of the structure subject to extreme twist load imposed on the trailer. The extreme twist loads, encountered during a severe directional maneuver, can be incorporated within analytical model by considering one side of the rear wheels off the ground. The TPI is thus expressed as:

$$TPI = \frac{\text{Maximum Twist angle, rad}}{\text{Maximum twisting moment on the trailer, kNm}}$$

3. Stress Performance Index (SPI): The stress performance index, is assessed by the ratio of the peak flexural stress, normalized with respect to material yield strength, Tare weight and the payload in the following manner:

$$SPI = \frac{(\text{Yield strength of the material, MPa})(\text{Payload, N})}{(\text{Peak stress, MPa})(\text{Tare weight, N})}$$

## 2.5 Summary

The design details of two candidate trailers, employed in tractor-semitrailer combinations, are discussed in view of their configuration, weights and dimensions. The limitations of implementing FEA software for design/re-design of large scale structures are briefly discussed to emphasize the need for development of simplified and efficient analysis methodologies. A design analysis software comprising menu-driven pre- and post- processors, and the design and reanalysis algorithms is configured to: (i) define the structure model in a graphical

and interactive manner; (ii) to analyze the design and re-design in an efficient manner using the substructuring and rear ..is techniques developed in this study; and (iii) to asses the response ch ..eristics through graphical displays. The primary requirement and highlights of the pre- and post- processors are described through sample screens and three design performance indices are identified from the legal and commercial design objectives.

# CHAPTER 3

# REANALYSIS TECHNIQUES FOR LARGE STRUCTURES

## 3.1 Introduction

Finite element based methods have proven to be highly reliable and efficient to model and analyze large scale complex structures. The use of such methods, however, poses considerable demands associated with modeling of structures with excessively large number of degrees-of-freedom (DOF) to perform accurate analyses. The design of structures frequently involves repetitive analyses with only local changes in the design parameters. The use of finite element analysis methods for repetitive analyses of modified designs to seek an optimal or near optimal design thus poses severe demands on the designer's efforts. The use of personal computers for analysis of large structures has thus been limited due to the large memory requirement and management associated with large size matrices. The implementation of the FE based analysis techniques thus necessitates the development of alternate efficient methods for analyzing large scale structures through modeling of the entire structure by various sub-structures.

Methods based upon substructuring and transfer matrix analyses have been proposed to carry out efficient analysis of large scale structures [9,44]. Substructuring techniques are specifically suited for structures with repetitive or similar configurations. The generation of additional stiffness matrices is thus avoided in such cases. Transfer-matrix methods also provide efficient analysis of structures with repeatable sub-structures, where the structures can be represented

as 'line-type'. The influence of local design modifications on the response behavior of the entire structure can be easily performed through analysis of that substructure alone. The major advantage of the substructuring technique is that the computation can be limited to a few substructures only. Both the techniques based upon substructuring and transfer-matrix methods employ a common methodology to partition the structure into several substructures. Reanalysis methods are used to derive the response behavior of a modified structure from the existing or original response by combining the Taylor series expansion about the present design space and the information derived from the design sensitivity vector [12-18]. Several approximate reanalysis techniques have been developed as summarized earlier in Chapter 1.

Substructuring in combination with reanalysis algorithms can considerably reduce the design cycle time in arriving at acceptable design. The transfer matrix approach combines the efficiency of finite element method and the compactness of transfer matrix solution. In the 'Finite Element-Transfer Matrix' (FETM) method, the complete structure is partitioned into strips connected in a chain-like manner and the stiffness matrix generated for each strip is rearranged in order to relate the performance/behavior vectors of the adjacent strips. The advantage of the method is demonstrated for a plate vibration problem [10], where an 18 x 18 matrix is used instead of 108 x 108 required in a conventional finite element approach. Sankar and Hoa [11] used an extended transfer matrix method for vibration analysis of a plate by extending the state vector comprising displacements and forces, together with their derivatives with respect to the circular frequency. Application of this method has been, however, limited to simple elements.

In this study, two reanalysis solution methods combining the substructuring with FETM and Potters' method, are formulated. The methods are developed for structures characterized by beam elements with three-DOF. Furthermore, reanalysis in combination with substructure and FEM are developed, where the design sensitivity vectors with respect to the design variables are computed simultaneously while seeking the first solution. The following subsections present the techniques of substructuring, reanalysis and FETM towards the development of the proposed methods.

## 3.2 Substructure Technique

Substructuring techniques have been extensively used for efficient analysis of large scale structures as discussed in the literature review [12,17,19]. In this formulation, the large structure, idealized by, finite element approximation, is grouped into many sub-structures. The studies on substructuring methods, reported in the literature [14,15,16], make use of the conventional matrix partition method and boundary nodes, which are commonly shared by the adjacent sub-structures, and the internal nodes defined within the sub-structure alone. The substructuring technique employed in the analyses is formulated using an example space truss structure comprising repetitive subsections.

Figure 3.1 represents a typical structure idealized into a finite element model using bar elements. The space truss model comprises 124 bar elements and 36 nodes, where X, Y and Z represent the global Cartesian coordinates. The members are oriented parallel to X, Y, Z axes and along the diagonal directions. All the members (elements), however, are not shown in the figure to enhance the visual clarity. The structure is divided into 5 substructures as identified by

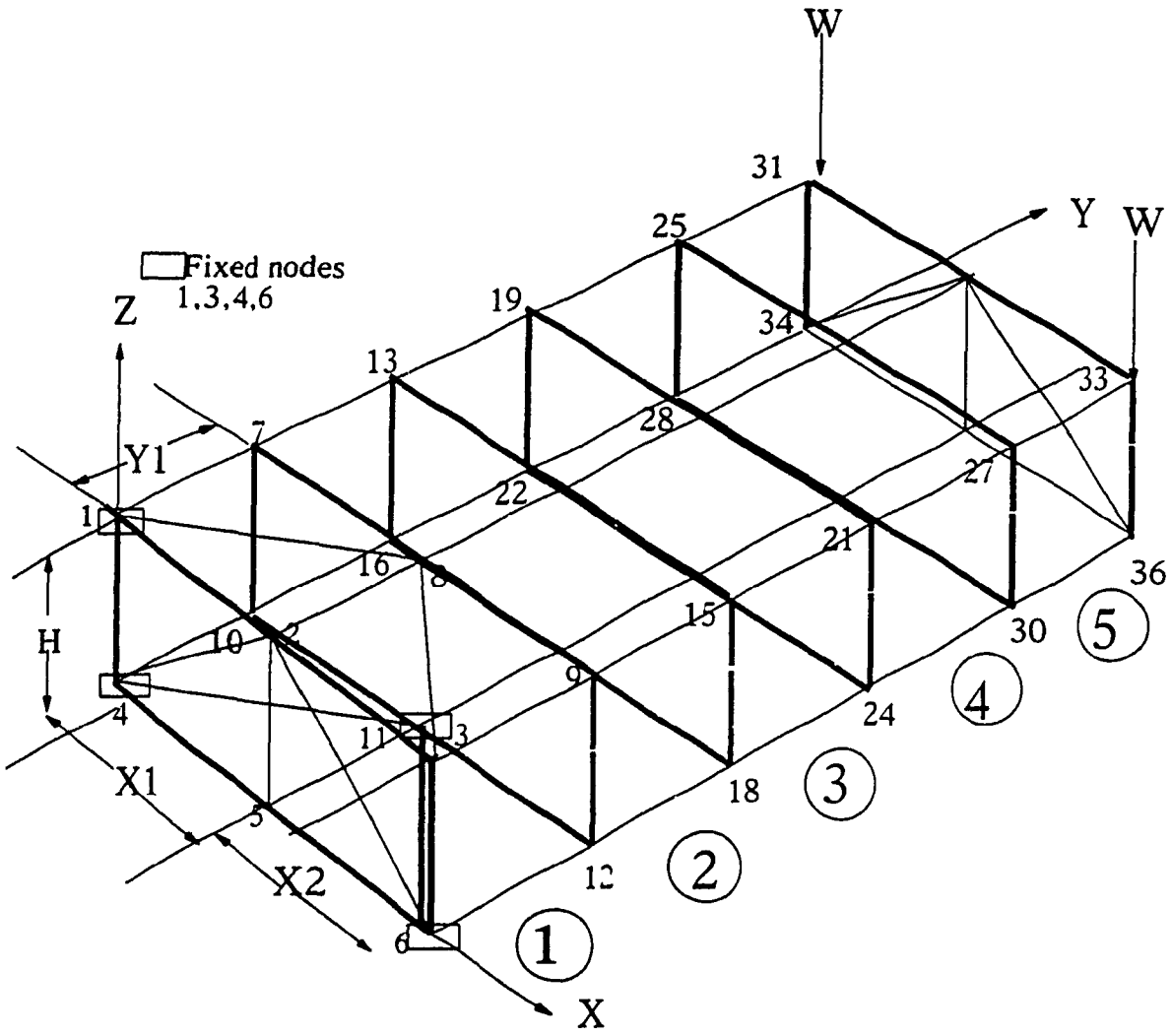


Figure 3.1: Schematic of the space truss structure showing substructures and the finite element model.

members represented by thick lines. Thin bar lines oriented along X, Y, Z and diagonals are the truss members *within* a substructure. Considering one such substructure, such as ①, the nodes 7, 9, 12 and 10 represent the boundary nodes, which are common between adjacent substructures ① and ②. The nodes (1, 11, 6, 4) and (31, 33, 36, 34) are also considered as boundary nodes of the two substructures on the extremities (1 and 5, respectively). The nodes (2, 8, 11, 5) are internal nodes within the substructure 1 as shown in the Figure. The space structure used in the formulation is subject to loads W as shown and the extreme boundary nodes of the first substructure nodes (1, 3, 4, 6) are constrained along the X, Y, and Z directions. Since each node allow 3-DOF motion, the structure can be modeled with an overall stiffness matrix of size for the stiffness matrix of (108 x 108).The static equilibrium equation for the structure can be expressed as:

$$[K]\{U\} = \{F\} \tag{3.1}$$

where [K] is the global stiffness matrix.

{U} is the displacement vector.

{F} is the external force vector.

The equilibrium equations are solved in the following two stages:

1) The internal forces and displacements for the internal nodes are expressed in terms of the boundary nodes or master nodes. The global stiffness matrix, composed of master nodes alone, is then assembled and the corresponding equilibrium equation is solved using either matrix inversion, or by Cholesky's decomposition techniques.

2) The response behavior of the internal nodes is computed from the response vectors of the boundary nodes using the matrix partition equations for each substructure.

The equilibrium equation for a substructure can be expressed in the following manner:

$$[K_{sub}]\ \{U_{sub}\} = \{F_{sub}\} \tag{3.2}$$

where $[K_{sub}]$ is the (36x36) stiffness matrix of the substructure, and $\{U_{sub}\}$ and $\{F_{sub}\}$ are the displacement and force vectors, respectively. Equation (3.2) can be represented in the following partitioned matrix form:

$$\begin{bmatrix} K_{BB(24x24)} & K_{BI(24x12)} \\ K_{IB(12x24)} & K_{II(12x12)} \end{bmatrix}_i \begin{Bmatrix} U_{B(24x1)} \\ \hline U_{I(12x1)} \end{Bmatrix}_i = \begin{Bmatrix} F_{B(24x1)} \\ \hline F_{I(12x1)} \end{Bmatrix}_i \tag{3.3}$$

where subscript 'B' denote the quantities associated with boundary nodes and the subscript 'I' denote the quantities associated with internal nodes of the *sub-structure 'i'*. Expanding the matrix equation and collecting the like terms, the displacement vector quantities of internal nodes, $U_I$ can be expressed in terms of the displacement vector $U_B$ associated with the boundary nodes, as:

$$U_{I_i} = \left(K_{II}^{-1}F_I\right)_i - \left(K_{II}^{-1}K_{IB}U_B\right)_i \tag{3.4}$$

where the internal node forces $F_I$ can be expressed in terms of $U_B$ by expanding the second row in Equation (3.3) as:

$$F_{I_i} = (K_{IB}U_B)_i + (K_{II}U_I)_i \tag{3.5}$$

Expanding the first row of Equation (3.3) and substituting for $U_I$ from. Equation (3.4) yields the relationship between the master stiffness matrix and master force vectors as:

$$\overline{K_{B_i}}U_{B_i} = \overline{F_{B_i}} \tag{3.6}$$

where, $\overline{K_{B_i}}$ and $\overline{F_{B_i}}$ are referred to as master stiffness matrix and force vector, respectively, and are given by:

$$\overline{K}_{B_i} = (K_{BB})_i - (K_{BI}K_{II}^{-1}K_{IB})_i \quad \text{and} \quad \overline{F}_{B_i} = (F_B)_i - (K_{BI}K_{II}^{-1}F_I)_i \tag{3.7}$$

The sizes of $\overline{K_{B_i}}$ and $\overline{F_{B_i}}$ vectors are identical to those of the partitioned $K_{BB}$ and $F_B$. The above formulation thus leads to considerable reduction in size of the problem. Equations (3.6) and (3.7) describing the equations for substructure 'i' are systematically combined to formulate the equilibrium of the entire structure. Equation (3.6) is used to describe the equivalent stiffness and forces reflected on the boundary nodes, given by:

$$\begin{bmatrix} \overline{K_{B1}} & & & & \\ & \overline{K_{B2}} & & & \\ & & \overline{K_{B3}} & & \\ & & & \overline{K_{B4}} & \\ & & & & \overline{K_{B5}} \end{bmatrix} \begin{Bmatrix} U_{B1} \\ U_{B2} \\ U_{B3} \\ U_{B4} \\ U_{B5} \end{Bmatrix} = \begin{Bmatrix} \overline{F_{B1}} \\ \overline{F_{B2}} \\ \overline{F_{B3}} \\ \overline{F_{B4}} \\ \overline{F_{B5}} \end{Bmatrix} \tag{3.8}$$

The size of global stiffness matrix in equation (3.8) is apparently dependent on the number of substructure considered. For the example structure considered, the size of the global stiffness matrix reduces to (72x72). The size of $\overline{K}_B$ is (72x72) as compared to (108x108) to be used in conventional FE analysis. The decomposed global stiffness matrix $\overline{K}_B$ can be saved for further analyses with different load conditions. The size of global stiffness matrix, $\overline{K}_B$ is, however, equal to the global boundary nodes of the structure which can be quite large in different applications.

Alternatively, the matrix solution and sensitivity vectors can be obtained using Potters' method [47], where the size of the stiffness matrix associated with boundary nodes can be reduced within a substructure. This method, therefore, can yield significant advantage in terms of memory management. This alternate approach is formulated and discussed in the following subsection.

## 3.3 Substructure Analysis Using Potters' Method

Although conventional methods of substructure analysis have been widely employed to reduce the problem size associated with analysis of large scale structures, only limited efforts have been made to further reduce the size of the global stiffness matrix determined by the number of global boundary nodes of the total structures. The substructure analysis using matrix decomposition based upon Potters' method has been proposed to reduce the size of the global stiffness matrix. It has been established that the use of Potters' method can reduce the size of stiffness matrix equal to the highest number of boundary nodes of a substructure. This method further provides the flexibility to add or delete substructures as desired and removes the constraint of renumbering the global nodes, and

assembling the global stiffness matrix and force vector. Formulation of the method along with submatrices elimination procedure is described below.

Figure 3.2 illustrates the example space truss structure with two typical partitions shown in dotted lines. The two arrow-heads pointing to left represent the stiffness contributions of the members sharing the nodes to the left of each partition line. In the illustration, for substructure 1, the sharing nodes 1 to 6 alone contribute to the stiffness matrix, while the members sharing nodes 7 to 12 contribute to the stiffness matrix for the following substructure.

### 3.3.1 Mathematical Formulation

As presented in equation (3.1), the equilibrium equation for a structure can be represented by:

$$[K]\ \{U\} = \{F\}$$

where the global stiffness matrix is of the banded form. The above equation thus can be rewritten as :

$$\begin{bmatrix} B_1 & A_1 & .. & .. & .. \\ C_2 & B_2 & A_2 & .. & .. \\ & C_3 & B_3 & A_3 & .. \\ .. & .. & .. & .. & .. \\ & & & C_n & B_n \end{bmatrix} \begin{Bmatrix} z_1 \\ z_2 \\ z_3 \\ .. \\ z_n \end{Bmatrix} = \begin{Bmatrix} g_1 \\ g_2 \\ g_3 \\ .. \\ g_n \end{Bmatrix} \qquad (3.9).$$

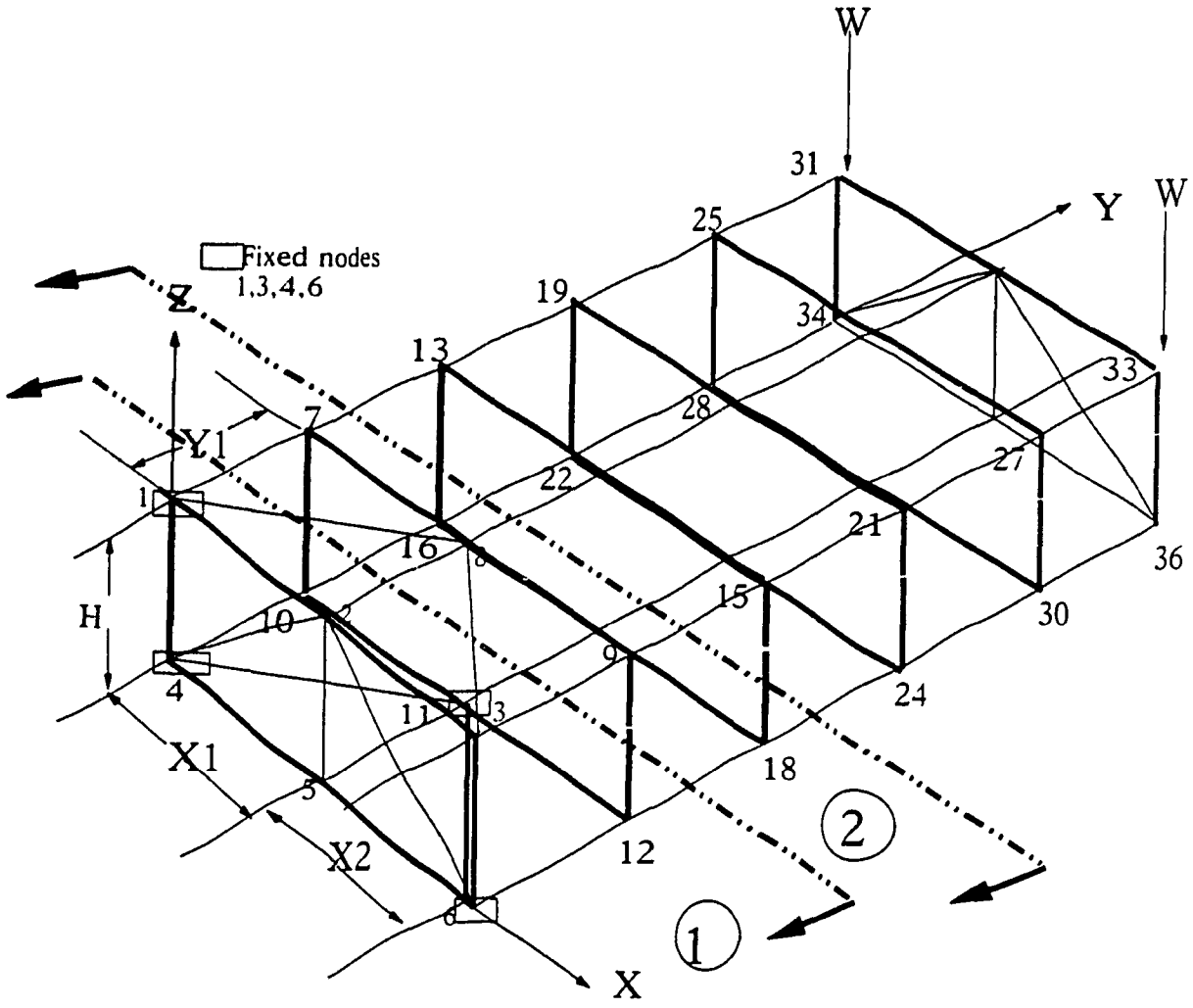


Figure 3.2: Partitioning scheme employed in the Potters' method.

where $A_i$, $B_i$ and $C_i$ (i=1,2,....,n) are stiffness matrices representing the contribution of the elements within the partition 'i', and:

$$\{U\} = \begin{Bmatrix} z_1 \\ z_2 \\ z_3 \\ .. \\ z_n \end{Bmatrix} : \text{and } \{F\} = \begin{Bmatrix} g_1 \\ g_2 \\ g_3 \\ .. \\ g_n \end{Bmatrix} \tag{3.10}$$

Since the stiffness matrix [K] is symmetric and positive definite, the matrix element groups are related in the following manner:

$$[C_2] = [A_1]^T \ , \ [C_3] = [A_2]^T \text{ etc.}$$

This property can be expressed in a general form as:

$$[C_{i+1}] = [A_i]^T \quad i=1, 2, ....., n-1 \tag{3.11}$$

where superscript 'T' designates the transpose. This above relationship is used in the substructure solution scheme in order to eliminate submatrices from the equilibrium equation, as described in the following sub-section.

### 3.3.2 Elimination of Submatrices

Upon substituting the Maxwell's relationship of equation (3.11) into (3.9), the equilibrium equation can be rewritten as:

$$\begin{bmatrix} B_1 & A_1 & .. & .. & .. \\ A_1^T & B_2 & A_2 & .. & .. \\ .. & A_2^T & B_3 & A_3 & .. \\ .. & .. & .. & .. & .. \\ .. & .. & .. & A_{n-1}^T & B_n \end{bmatrix} \begin{Bmatrix} z_1 \\ z_2 \\ z_3 \\ .. \\ z_n \end{Bmatrix} = \begin{Bmatrix} g_1 \\ g_2 \\ g_3 \\ .. \\ g_n \end{Bmatrix} \tag{3.12}$$

Using the Cholesky's matrix decomposition method, the diagonal and off-diagonal elements in the banded matrix of equation (3.12) can be expressed as:

$$\begin{bmatrix} L_1L_1^T & L_1P_1 & & & \\ & L_2L_2^T & L_2P_2 & & \\ & & L_3L_3^T & L_3P_3 & \\ & & & .. & \\ & & & & L_nL_n^T \end{bmatrix} \begin{Bmatrix} z_1 \\ z_2 \\ z_3 \\ .. \\ z_n \end{Bmatrix} = \begin{Bmatrix} L_1q_1 \\ L_2q_2 \\ L_3q_3 \\ .. \\ L_nq_n \end{Bmatrix} \tag{3.13}$$

Expanding the first rows of Equations (3.12) and (3.13) result in the following two expressions, respectively:

$$[B_1]\{z_1\} + [A_1]\{z_2\} = \{g_1\}$$

and $$[L_1][L_1]^T\{z_1\} + [L_1][P_1]\{z_2\} = [L_1]\{q_1\}$$

Comparison of the above two equations yields:

$$[L_1][L_1]^T = [B_1]: \quad [L_1][P_1] = [A_1]: \quad [L_1]\{q_1\} = \{g_1\} \tag{3.14}$$

Further simplification of the first row of equation (3.13) yields:

$$[L_1]^T\{z_1\}+[P_1]\{z_2\}=\{q_1\} \tag{3.15}$$

Equation (3.15) thus describes the relationship between the nodal displacement vectors $\{z_1\}$ and $\{z_2\}$:

$$\{z_1\}=[L_1]^{-T}\{q_1\}-[L_1]^{-T}\{P_1\}\{z_2\} \tag{3.16}$$

The expansion of the second rows of equations (3.12) and (3.13) in a similar manner results in the following expressions.

$$[A_1]^T\{z_1\}+[B_2]\{z_2\}+[A_2]\{z_3\}=\{g_2\}$$

and

$$[L_2][L_2]^T\{z_2\}+[L_2][P_2]\{z_3\}=[L_2]\{q_2\} \tag{3.17}$$

Substituting for $\{z\}$ from Equation (3.16) and for $[A_1]$ from Equation (3.14) in (3.17) yields:

$$\left[[B_2]-[P_1]^T[P_1]\right]\{z_2\}+[A_2]\{z_3\}=\{g_2\}-[P_1]^T\{q_1\} \tag{3.18}$$

A comparison of Equations (3.17) and (3.18) yields following relationships:

$$[L_2][L_2]^T=[B_2]-[P_1]^T[P_1]$$

$$[L_2][P_2]=[A_2]$$

$$[L_2]\{q_2\} = g_2 - [P_1]^T\{q_1\} \tag{3.19}$$

The application of the above formation to the successive substructures results in a recursive relation between the adjacent substructures:

$$[L_i][L_i]^T = [B_i - P_{i-1}^T P_{i-1}]$$

$$[A_i] = [L_i][P_i]$$

$$\{g_i\} - [P_{i-1}^T]\{q_{i-1}\} = [L_i]\{q_i\}$$

$$[L_i]^T\{z_i\} + [P_i]^T\{z_{i+1}\} = \{q_i\} \quad (i = 2,\ldots.n-1) \tag{3.20}$$

Similarly, the above relations for the last substructure are derived as:

$$[L_n][L_n]^T = [B_n - P_{n-1}^T P_{n-1}]$$

$$[L_n]\{q_n\} = \{g_n - P_{n-1}^T P_{n-1}\}$$

$$[L_n]^T\{z_n\} = \{q_n\} \tag{3.21}$$

The submatrices elimination scheme thus makes use of the matrix decomposition technique, and evaluates [P] and {q}, for all substructures to compute the response characteristics of the substructures successively.

## 3.4 Reanalysis and Evaluation of Design Sensitivity Vectors

Design sensitivity can be defined as the ratio of the change in response of a structure, such as stress, deformation, and frequency caused by variations, in one or several design variables from the existing design space. Taylor series expansion can be conveniently employed to achieve a first order approximation of the sensitivity vectors, which can be effectively used in achieving an optimal solution. Although the design sensitivity can be conveniently analyzed using finite difference techniques, the method may pose severe demands on computing. Alternatively, the sensitivity vectors may be derived directly from the derivatives of the performance variables with respect to the design variables using the equilibrium equations. The static equilibrium equation of the structure as described in Equation (3.1), is rewritten:

$$[K]\{U\} = \{F\} \tag{3.22}$$

When a design modification is carried out, an approximate solution is sought by a truncated first order Taylor series expansion about the original solution $\{U\}$ to derive a new displacement vector, $\{U^*\}$, given by:

$$\{U^*\} = \{U\}_0 + \sum_{j=1}^{j=r} (d_j^* - d_{j0}) \left\{ \frac{\partial U}{\partial d_j} \right\}_{d_j = d_{j0}} ; \tag{3.23}$$

where $d_j^*$ and $d_{j0}$ are the new and initial design variables and $\frac{\partial U}{\partial d_j}$ are first-order design sensitivity vectors evaluated about the original design vector $d_{j0}$. 'r' is number of design variable to be considered in the sensitivity analysis. Since the stiffness matrix changes with a change in a design variable, the sensitivity vectors can be obtained by differentiating Equation (3.22) with respect to a design variable $d_j$:

$$[K]\left\{\frac{\partial U}{\partial d_j}\right\}+\left[\frac{\partial K}{\partial d_j}\right]\{U\}=\left\{\frac{\partial F}{\partial d_j}\right\};\quad j=1.....r \tag{3.24}$$

Assuming that applied loads do not vary with the change in design variables, such that $\left\{\frac{\partial F}{\partial d_j}\right\} = 0$, the Equation (3.24) reduces to:

$$[K]\left\{\frac{\partial U}{\partial d_j}\right\}=-\left[\frac{\partial K}{\partial d_j}\right]\{U\} \tag{3.25}$$

Equations (3.22) and (3.25) reveal that the design sensitivity vector $\{\partial U/\partial d_j\}$ is akin to the displacement vector $\{U\}$, and the right hand side matrix product $\{\partial K/\partial d_j\}\{U\}$, is a vector akin to $\{F\}$, which may be considered as a 'pseudo-force' vector. It is apparent that the solutions derived from the Potters' partitioning concept can be directly used to compute the design sensitivity vectors using the above formulation. Since the stiffness matrix [K] for each partition has already been decomposed and stored from the substructure analysis, the corresponding variations in stiffness matrix, $\{\partial K/\partial d_j\}$ can easily be derived. The formulation thus provides a highly convenient and efficient method to directly compute the

design sensitivity vectors from the original solutions derived from the substructure analysis.

### 3.4.1 Design sensitivity vector using Potters' Method

In the preceding discussion of Potters' Method in Section 3.2, the submatrix elimination procedure led to equation (3.12). Expanding the first two rows of this equation result in:

$$\begin{aligned} B_1 z_1 + A_1 z_2 &= g_1 \\ A_1^T z_1 + B_2 z_2 + A_2 z_3 &= g_2 \end{aligned} \tag{3.26}$$

Now differentiating the above relation for the first partition with respect to a design variable $d_j$ yields:

$$B_1 \frac{\partial z_1}{\partial d_j} + \frac{\partial B_1}{\partial d_j} z_1 + A_1 \frac{\partial z_2}{\partial d_j} + \frac{\partial A_1}{\partial d_j} z_2 = 0 \tag{3.27}$$

The above equation can be rearranged to separate the response sensitivity to yield:

$$B_1 z_1 + A_1 z_2 = \bar{f}_1$$

where $[z_1] = \partial z_1 / \partial d_j$ is the response sensitivity with respect to design variable $d_j$, and $\bar{f}_1$ represents the 'pseudo force' given by:

$$\bar{f}_1 = -\frac{\partial B}{\partial d_j} z_1 - \frac{\partial A_1}{\partial d_j} z_2 \qquad (3.28)$$

Similarly the second matrix relation of Equation (3.26), after differentiation with respect to the design variable will take the form as:

$$A_1^T z_1' + A_1'^T z_1 + B_2 z_2' + B_2' z_2 + A_2 z_3' + A_2' z_3 = 0$$

The above equation can be rearranged in a similar manner to yield:

$$A_1^T z_1' + B_2 z_2' + A_2 z_3 = -\bar{f}_2. \qquad (3.29)$$

where

$$\bar{f}_2 = \frac{\partial A_1^T}{\partial d_j} z_1 + \frac{\partial B_2}{\partial d_i} z_2 + \frac{\partial A_2}{\partial d_i} z_3 \qquad (3.30)$$

As stated earlier, the right hand side of Equation (3.29) is termed as 'pseudo force' vector. The vectors $z_1$, $z_2$,....., $z_n$ are the design sensitivity vectors describing the sensitivity of displacement performance with respect to variations. The applications of the above method yields a recursive relationship to determine the design sensitivity vectors for the remaining partitions.

## 3.4.2 Reanalysis Solution Algorithm

Based on the solution techniques for basic static analysis and reanalysis of structural configurations as described in previous sections, the sequence of seeking the solution and design sensitivity vector is summarized as follows:

(i) Divide the structure into convenient partitions.

(ii) Number the nodes and elements.

(iii) Identify the nodes, elements and nodal forces for each partition.

(iv) Compute for each partition the overall stiffness matrix and formulate matrices $A_i$.and $B_i$, i = 1,....., n, as defined in equation (3.12). Store the matrices in indexed files for later retrieval.

(v) Formulate the forcing vector {g} and store.

(vi) Formulate the stiffness derivatives matrices for the partitions affected by certain design variation. Compute $\partial A_i/\partial d_j$ and $\partial B_i/\partial d_j$, only for the affected partitions, and store in indexed files, DA and DB. The matrices DA and DB for unaffected partition are defined as *null matrices*.

(vii) Compute the displacement response vector U, using forward and backward substitution in conjunction with Cholesky's decomposition for each partition using equations (3.19), (3.20) and (3.21) derived using Potter's method. Store decomposed matrices of $A_i$ and $B_i$ and the response vector $U_i$ for later reanalysis solution.

(viii) If the reanalysis is desired to assess the influence of a local design variation, formulate the pseudo force vector, $\bar{f}_i$ , for different partitions. Equations (3.28) and (3.30) are solved using the displacement response vector $Z_i$ and the corresponding stiffness matrices derivatives to determine the vector $f_i$ It should be noted that the vector $\bar{f}_i$ for unaffected partitions is zero.

(ix) Compute the design sensitivity vector $(\partial z_i/\partial d_j)$ upon substituting for $f_i$, $z_i$ and the stiffness matrices in relation described equation (3.27) and (3.28).

(x) Compute the new response vector, $U^*$ using the Taylor series approximation in equation (3.23).

## 3.5 Reanalysis using Extended FETM approach

Although the reanalysis techniques yield rapid convergence of the solution, the problem size associated with large structures often poses a major constraint, specifically, when personal computers are used. Dokainish [10], analyzed the free vibration of a clamped plate using finite element transfer matrix method by combining the efficiency of the finite element method and the compactness of transfer matrix solution. The structure was partitioned into strips connected in a chain-like manner and the stiffness matrix generated for each strip was rearranged to relate the behavior vectors (displacement, moment, etc.) of adjacent strips using the simple transfer matrix relation. The method demonstrated considerable reduction in problem size. Sankar and Hoa [11], used an extended transfer matrix method for vibration analysis of a plate by extending the state vector comprising displacements and forces, with additional vectors of the derivatives with respect to the circular frequency. The study showed further reduction in the problem size and considerable improvement in the computational efficiency for simple structures. A reanalysis algorithm based upon extended FETM and the design sensitivity vectors, described in Section 3.3, is formulated to perform the reanalysis solution of structures modeled using three-DOF beam elements. The proposed technique is applied to seek the reanalysis solution of large scale trailer structures in Chapter 5.

### 3.5.1 Mathematical Formulation

The mathematical formulation for the extended FETM method is illustrated for a simple line structure arranged in a chain-like manner, as shown in 3.3.

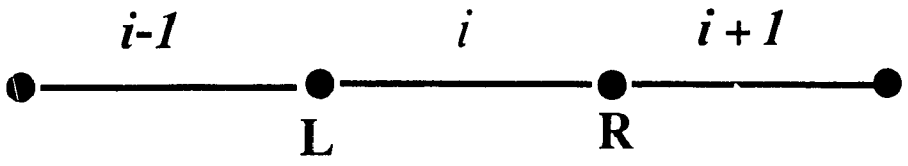


Figure 3.3: Schematic representation of elements arranged in a Chain-like manner.

For a linear structure, subject to a given set of loading and boundary conditions, the displacement vector {U} is computed from the equilibrium equations, represented in the matrix form:

$$[K]\ \{U\} = \{F\} \tag{3.31}$$

An approximate solution of the modified structure resulting from certain variations in one or more design variables, may be derived from the truncated first order Taylor series expansion about the original solution {U}. The displacement response vector of the modified structure is thus determined from:

$$\{U^*\} = \{U\}_0 + \sum_{j=1}^{j=r} (d_j - d_{j0}) \left\{ \frac{\partial U}{\partial d_j} \right\}_{d_j = d_{j0}} \tag{3.32}$$

where, $d_j$ and $d_{j0}$ are design variables of the modified and initial structures respectively. $\left\{ \frac{\partial U}{\partial d_j} \right\}$ are first-order design sensitivity vectors evaluated about the original design vector $d_{j0}$. 'r' represents the number of design variables and $\{U\}_0$ refers to the displacement response vector of the original structure. In a finite element formulation with the elements arranged in a chain-like fashion, as shown in Figure 3.3, the force-displacement relationship for a typical element 'i' may be expressed as :

$$[K]_i \left\{ \frac{U_L}{U_R} \right\}_i = \left\{ \frac{F_L}{F_R} \right\}_i \quad i=1,.....,n \tag{3.33}$$

where n is the number of elements and $[K]_i$ is the element stiffness matrix, given by:

$$[K]_i = \begin{bmatrix} K_{LL} & K_{LR} \\ K_{RL} & K_{RR} \end{bmatrix}_i$$

In the transfer matrix method, the equation of equilibrium are rearranged to relate the state vectors at the right and the left nodes of the element. Each state vector comprises the displacement and force vectors, such that $\{U_R \;\; F_R\}_i$ and $\{U_L \;\; F_L\}_i$ refer to the respective state vectors at the right and left nodes, respectively, of element i, where subscripts L and R refer to behavior vectors at the left and right nodes of the element *i*. Equation (3.33) can be solved to describe the relationship between the state vectors at the right $\{U_R \; F_R\}^1$ and left $\{U_L \; F_L\}^1$ nodes:

$$\begin{aligned} F_R &= \left[K_{RL} - K_{RR}K_{LR}^{-1}K_{LL}\right]U_L + K_{RR}K_{LR}^{-1}F_L \\ U_R &= -K_{LR}^{-1}K_{LL}U_L + K_{LR}^{-1}F_L \end{aligned} \tag{3.34}$$

Equation (3.34), when expressed in the matrix form, yields the transfer-matrix relating the state vectors at right and left nodes of the element *i*:

$$\begin{Bmatrix} U_R \\ F_R \end{Bmatrix}_i = \begin{bmatrix} T_{11} & T_{12} \\ T_{21} & T_{22} \end{bmatrix}_i \begin{Bmatrix} U_L \\ F_L \end{Bmatrix}_i \tag{3.35}$$

where $[T]_i$ is the transfer matrix for the element 'i' given by:

$$[T]_i = \begin{bmatrix} K_{LR}^{-1}K_{LL} & K_{LR}^{-1} \\ K_{RL} - K_{RR}K_{LR}^{-1}K_{LL} & K_{RR}K_{LR}^{-1} \end{bmatrix} \tag{3.36}$$

The design sensitivity vectors required for the reanalysis solution are easily incorporated in the state vector. An extended state vector thus comprises the displacement and force vectors, and their derivatives with respect to the design variation is thus formulated. An *Extended Finite Element Transfer Matrix* (EFETM) is thus formulated to study the response characteristics corresponding to variations in a design variable, '$d_j$' The EFETM is constructed incorporating design derivatives of the transfer-matrix, [T]i, and the approximate solutions derived from the first order Taylor series reanalysis formulation. The derivative matrix of [T]i is formed for each element 'i', by differentiating the elements of the [T]i matrix, which are essentially the derivatives of the partitioned matrix with respect to the design variable '$d_j$' given by:

$$\left[\frac{\partial T}{\partial d_j}\right]_i = \begin{bmatrix} \partial T_{11} & \partial T_{12} \\ \partial T_{21} & \partial T_{22} \end{bmatrix}_i$$

The individual elements of the above matrix are derived in the following manner:

$$\frac{\partial T_{11}}{\partial d_j} = \frac{\partial\left(\left[-K_{LR}^{-1}K_{11}\right]\right)}{\partial d_j}$$

The EFETM for a design variable relating the station vectors, between the left and right nodes of an element 'i' is expressed as:

$$\begin{Bmatrix} U_R \\ F_R \\ \frac{\partial U_R}{\partial d_j} \\ \frac{\partial F_R}{\partial d_j} \end{Bmatrix}_i = \begin{bmatrix} T_{11} & T_{12} & 0 & 0 \\ T_{21} & T_{22} & 0 & 0 \\ \frac{\partial T_{11}}{\partial d_j} & \frac{\partial T_{12}}{\partial d_j} & T_{11} & T_{12} \\ \frac{\partial T_{21}}{\partial d_j} & \frac{\partial T_{22}}{\partial d_j} & T_{21} & T_{22} \end{bmatrix}_i \begin{Bmatrix} U_L \\ F_L \\ \frac{\partial U_L}{\partial d_j} \\ \frac{\partial F_L}{\partial d_j} \end{Bmatrix}_i \qquad (3.37)$$

Equation (3.42) may be expressed in the form, $\{Z_R\}_i = [\bar{T}]_i \{Z_L\}_i$, where, $[T]$ is the extended transfer-matrix. $\{Z_R\}$ and $\{Z_L\}$ are right- and left- station vectors respectively, comprising state vectors and design sensitive vectors. The sensitivity vectors at all stations can be conveniently formulated by progressively moving across the elements of the structure. The station vectors of the extreme elements (first and last) of the structure are related through the global extended transfer-matrix :

$$[Z_R]_n = [\Gamma][Z_L]_1 \tag{3.38}$$

where $[\Gamma] = [\bar{T}]_n [\bar{T}]_{n-1} \ldots\ldots \ldots\ldots [\bar{T}]_1$. The structural analysis is initiated by incorporating the known vectors at one end of the structure. The EFETM $[T]_i$ for the subsequent elements are then formulated while progressing toward the other end of the structure. Equation (3.43) is solved together with the known boundary conditions and applied loads to determine the station vectors.

## 3.5.2 Analysis Algorithm

An algorithm is developed to carry out reanalysis of structures using the proposed EFETM methodology. The algorithm may be expressed as follows:

(a) Partition the structure into substructures arranged in a chain-like manner.

(b) Compute the stiffness matrices for each substructure, using finite element method.

(c) Compute the elements of $\left[\bar{T}\right]_l$ using Equations (3.36).

(d) Compute the derivatives of the elements $\left[\bar{T}\right]_l$ with respect to design variables and formulate the EFETM, $\left[\bar{T}\right]_l$, using equation (3.37).

(e) Group the station vector, starting from one end of the structure into two distinct blocks: $\left[\{\text{Known}\} \quad \{\text{Unknown}\}\right]^T$.

(f) Formulate global extended transfer matrix $[\Gamma]$ relating the station vectors of the two ends using equation (3.38)

(g) Solve for the {Unknown} components of the station vector using $\left[\bar{T}\right]_l$ and the boundary constraints.

(g) Evaluate all station vectors by proceeding in a systematic manner.

(h) Obtain reanalysis solution for behavior vectors using equation (3.32).

## 3.6 Application of Reanalysis Methods for Large Scale Trailer Structures

The reanalysis solutions based upon Potters' method and EFETM can be effectively applied for analysis of large scale trailer structures. The trailer structures described in Chapter 2, are ideally suited for the proposed reanalysis solution due to their repetitive and in-line type configurations. The advantages of reanalysis solutions become quite apparent for such large structures involving large number of possible variations in the design variables and configurations. The design of such large scale structures involving variations in several design parameters through finite element analysis is known to be demanding on the computing as well as human resources. The methods based upon substructure and

EFETM permit the design in a highly efficient manner using the design sensitivity vectors and reanalysis algorithms.

### 3.6.1 APPLICATION OF POTTERS' METHOD

The candidate trailer B structure, presented in Figure 2.3 and 2.4, comprises two main-beams and two side-beams of an I-section, which are coupled through several cross members of C-section. The trailer structure represents repetitive in-line type construction, which can be conveniently represented by the substructures in the analysis. Figure 3.4 illustrates the trailer structure idealized by n partitions. Each substructure is represented by the members lying on the left of the partition lines indicated by dotted lines. The structure members can be modeled comprising finite elements, which may be of beam, plate, or other element type, that can best describe the desired DOF and response. The trailer structure model is formulated assuming 3-D beam-type elements to describe the flexural and torsional behavior of the structure. The tridem axle suspension is represented by six 3-D spar elements with linear stiffness equivalent that of the suspension springs, assuming negligible contribution of the unsprung masses and elastic properties of the tires. The reaction force at the king-pin support is considered to be equally distributed at two nodes located on the main beam. The reaction forces are modeled by equivalent linear springs represented by spar elements. The model, thus formulated, is generally applicable to ladder-type trailer structures frequently used in freight and log transportation. The model further provides the added flexibility to add or delete one or more substructures to adequately represent a specific design configuration. The addition or removal of the substructures, however, does not affect the problem formulation and the solution methodology in terms of the assembled substructure matrix size, which is a distinguishing advantage of the

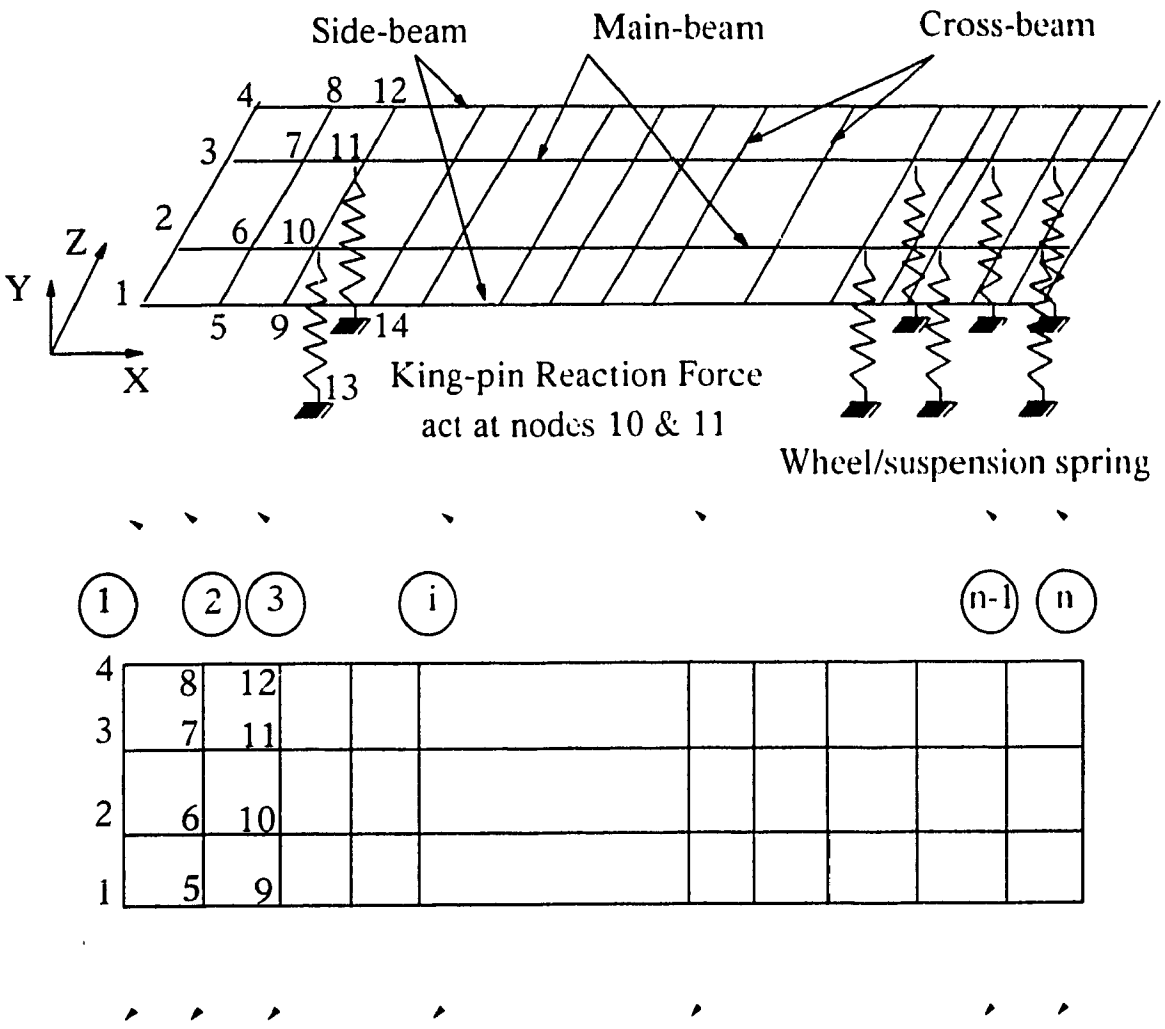


Figure 3.4: Schematic of the substructure model idealized by $n$ partitions.

Potters' method when compared to the conventional substructure method of analysis. The general modeling consideration of a substructure " i " are as follows:

a. Each substructure must be represented by a minimum of four nodes. The substructure comprising the king-pin support or suspension spring incorporates a higher number of nodes as illustrated in the Figure 3.4. The recursive relations described in Equations (3.20) and (3.21), are used to formulate the stiffness matrix of a substructure. Equation (3.30) is then used to determine the design sensitivity and pseudo force vectors, which are used in conjunction with the Taylor's series approximation to derive the reanalysis solution.

b. The matrix size of the problem is thus determined by the number of active DOF in a substructure. (Active DOF = Total DOF - number of Constrained DOF).

c. Each node possesses 6 DOF motion, 3 translations and 3 rotations.

d All external forces and moments acting on the structure can be represented by their appropriate contributions at the nodes.

e. One end of the suspension element is connected to the unsprung mass and the tire. While the unsprung mass is considered to be extremely small compared to trailer and tire stiffness is of the order of ten times of the suspension stiffness. The node which transmits the tire-terrain reaction is completely restrained.

The above modeling considerations result in all substructures with a total of 24 DOF, and stiffness matrix of size (24 x 24). Although a design configuration may be represented by varying number of substructures, the size of the matrix used to solve one substructure at a time remains always for (24 x 24 ). Both the candidate trailer structures are represented by their substructure models for reanalysis solutions using Potters' method. Table 3.1 summarizes the design and modeling

details for both the trailers. It should be noted that the structure design involves analyses with several design variables, including: material and sectional properties of the main-, side- and cross- members; and number of location of cross-members.

**Table 3.1: Summary of Candidate Trailer Design.**

| | TRAILER-A | TRAILER-B |
|---|---|---|
| Overall Length | 9.29 m | 14.62 m |
| Overall Width | 2.438 m | 2.59 m |
| Number of Wheel sets | Two-axle | Tridem-axle |
| Suspension spring rate | 1342 kN/m | 1342 kN/m |
| Number of Main-beams | 2 | 2 |
| Number of Side-beams | 2 | 2 |
| Number of substructures | 31 | 37 |
| Tare weight | 1.99 metric tons | 5.0 metric tons |
| Pay load | $\leq$ 250 kN | $\leq$ 350 kN |
| King-pin Reaction force | 55kN | 74kN |
| Axle load | $\leq$ 33kN | $\leq$35kN |
| Application | Cargo transportation | Log-hauling |

### 3.6.2 APPLICATION OF EFETM

The method discussed earlier is applicable for large scale in-line type ladder structures. An application of this technique for seeking design analysis and reanalysis of the candidate trailer A has been made. The method of solution is similar to the Potters' method of substructuring discussed above. The difference is in identifying the substructure and the DOF considered. Figure 3.5 represents a typical substructure " i " with respective nodes. Each substructure has left- and right- side stations located on either sides of the substructure. Using the methodology and algorithm discussed in section 3.5, reanalysis solutions are sought for the structure. The method is sufficiently general and is applicable for all large scale structures. The DOF for each substructure is 24 for analysis and 48 for EFETM when the station vector comprises the derivative of the behavior vectors with respect to design variable.

## 3.7 Summary

The method of substructure analysis and the finite element-transfer matrices are investigated for their efficiency of solution and compactness in handling large matrix sizes and in seeking the reanalysis solutions in conjunction with first-order Taylor's series approximation. The substructure method utilizes Potters' method of solution together with Cholesky's decomposition. Reanalysis method of solution including design sensitivity has been developed for static analysis of large structures. This method provides significant advantage over the traditional substructure analysis methods in terms of convenience and faster computation. This is shown to be achieved by formulating the global stiffness matrix irrespective of the partitioning used. Partitions can be increased or

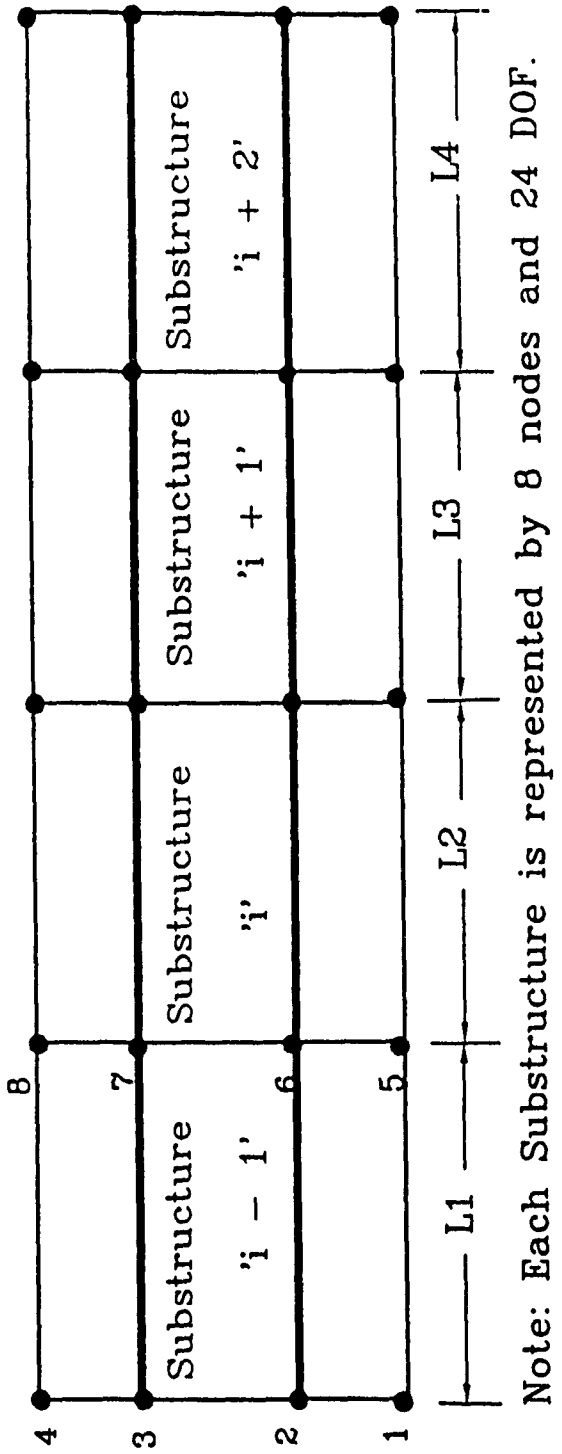


Figure 3.5: Chain-like arrangement of the semitrailer substructure.

decreased as desired and the solution algorithm allows for the change without changing the size of the global stiffness matrix in contrast with the traditional substructure analysis. In the Transfer-matrix approach, the station vectors are extended to include derivatives of the behavior vectors at each station and a reanalysis solution is sought in the first solution stage itself. The reanalysis solution techniques developed in this chapter enhance the efficiency and compactness of the matrices, such that the proposed algorithm can be conveniently applied to large structures using a Personal Computer.

# CHAPTER 4

# THE REANALYSIS METHODS: VALIDATIONS AND EVALUATIONS

## 4.1 Introduction

Finite element modeling is widely considered as a reliable analysis and design tool because of its efficiency in representing mechanical or structural configurations with ease and its ability to invoke appropriate elements for describing the physical behavior of the structure in analyzing a design. The methods can be easily implemented through development of analysis software customized to design and analyze typical structures, rather than using a commercial package, which may pose difficulties to perform desired manipulations. While the custom designed software offers significant flexibility, such software needs to be validated against some standards or measurements to enhance the reliability of the methodology used.

In the present investigation, the analyses and reanalyses tools are developed in Chapter 3, need to be evaluated for their computational efficiency and validated for their reliability. The methods based upon substructure method of solution using FEM, and Transfer Matrix method of solution using the stiffness matrix of the substructure, are validated through analysis of example structures in many stages. The validation in general, may be carried using one or more of the following approaches: (i) Validation through simulation of a bench mark problem and comparing with known results; (ii) Validation through simulation of an

example problem and comparing the results with those deri' ed from other well established tools; and (iii) Validations through comparison of simulation results for a given problem with those derived from experimental studies. Further to validation it is necessary to assess the performance of the developed tools pertaining to their efficiency when compared with other commercial tools. This chapter describes the methodology used to validate the reanalysis tools developed in Chapter 3. The method based upon substructuring is implemented to analyze a large scale candidate trailer structure. The method is validated by comparing the results with those derived from ANSYS software and experimental modal analysis. The proposed analysis method is assessed in view of its computational efficiency with a personal computer.

## 4.2 Validation of Developed Tools

In the present investigation, two distinct analysis/reanalysis tools are developed, namely: Substructure method of solution using FEM; and Transfer Matrix method of solution using stiffness matrix of the substructure. The validation of the developed methodology is carried out in three stages: using published results for selected bench mark problems; simulation results of the candidate trailer structure obtained using commercial software ANSYS; and the results derived from experimental modal analysis of a candidate trailer structure.

### 4.2.1 Validation using bench mark structures

The two analysis methods are initially validated for three example structures referred to in the published literature. These structures are:

a) Plane ten-bar cantilever truss [47]

b) Space truss [35, 48]

c) Plane frame structure [49].

The selected planar ten-bar cantilever truss [47], corresponds to a fully stressed design (FSD) shown in Figure 4.1, comprises aluminum bar elements with members arranged in two spans. The structure model consists of 6 nodes and 10 members as shown. The member sizes in terms of cross-section areas and material properties are illustrated in Table 4.1. A static load of 444.8 kN is applied at nodes 1 and 3 in the negative direction along Y-axis, while the nodes 5 and 6 are constrained along both the coordinates. The schematic of a three dimensional space truss structure model, considered for validation of the developed tools, is shown in Figure 4.2. This example structure comprises 124 bar members and 36 nodes, where the members are oriented parallel to the three Cartesian coordinates X, Y, and Z, and diagonal directions, as shown in the Figure. The members 1-18, 19-42, 43-72 are placed along the Z, X, and Y-axes respectively, while members 73-124 are oriented along different diagonals. A number of design configurations, described in Table 4.2 are considered for validating the proposed analysis and reanalysis algorithms. The nodes 31 and 33 are subject to a vertical load of 444.8 kN and the nodes 1, 3, 4 and 6 are constrained in all directions as shown. The plane frame structure, considered for validation, is a support structure used for a boiler in a power generation station. The example structure is idealized as a plane frame structure as shown in Figure 4.3 [49]. The structure is modeled with 10 nodes and 10 members, where each node is allowed 3 DOF motion. The nodes 4, 5, 6 and 7 are subject to static loads as shown in the Figure. The geometric and sectional properties of the structure are summarized in Table 4.3.

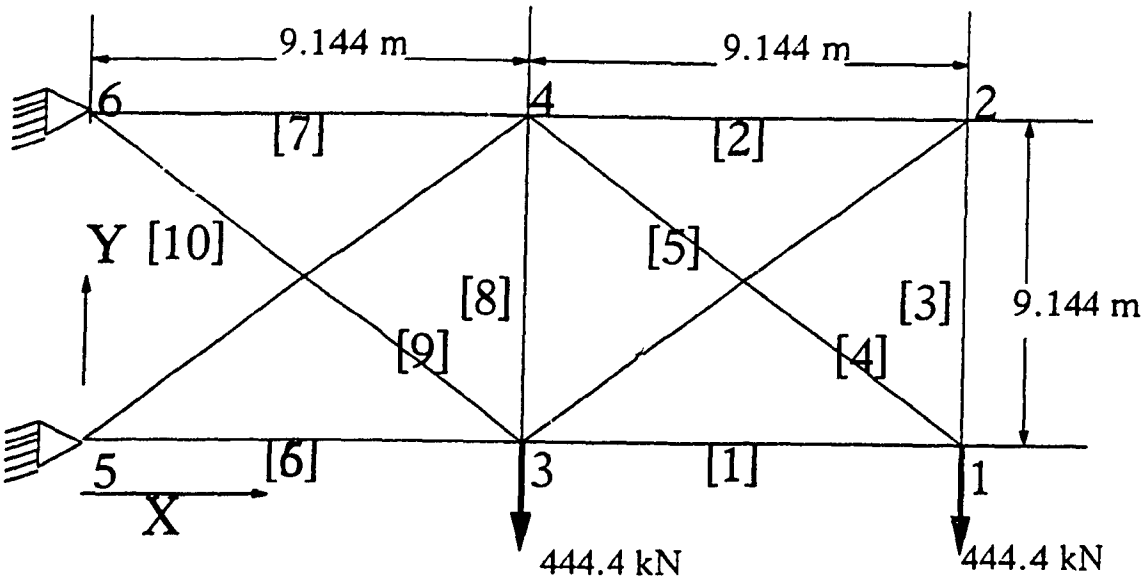


Note: Numbers with in [] denote Element numbers
Numbers at joints indicate Nodes

Figure 4.1: Schematic of a planar ten-bar cantilever truss model [47].

**Table 4.1: Design Details of Ten-Bar Cantilever Truss [47].**

MATERIAL: Aluminum E = 0.7 E11 MPa

| Member No. | Area ($cm^2$) | Member | Area ($cm^2$) |
|---|---|---|---|
| 1 | 0.7096 | 6 | 76.69 |
| 2 | 25.09 | 7 | 26.51 |
| 3 | 25.09 | 8 | 0.645 |
| 4 | 0.645 | 9 | 71.98 |
| 5 | 35.54 | 10 | 0.9675 |

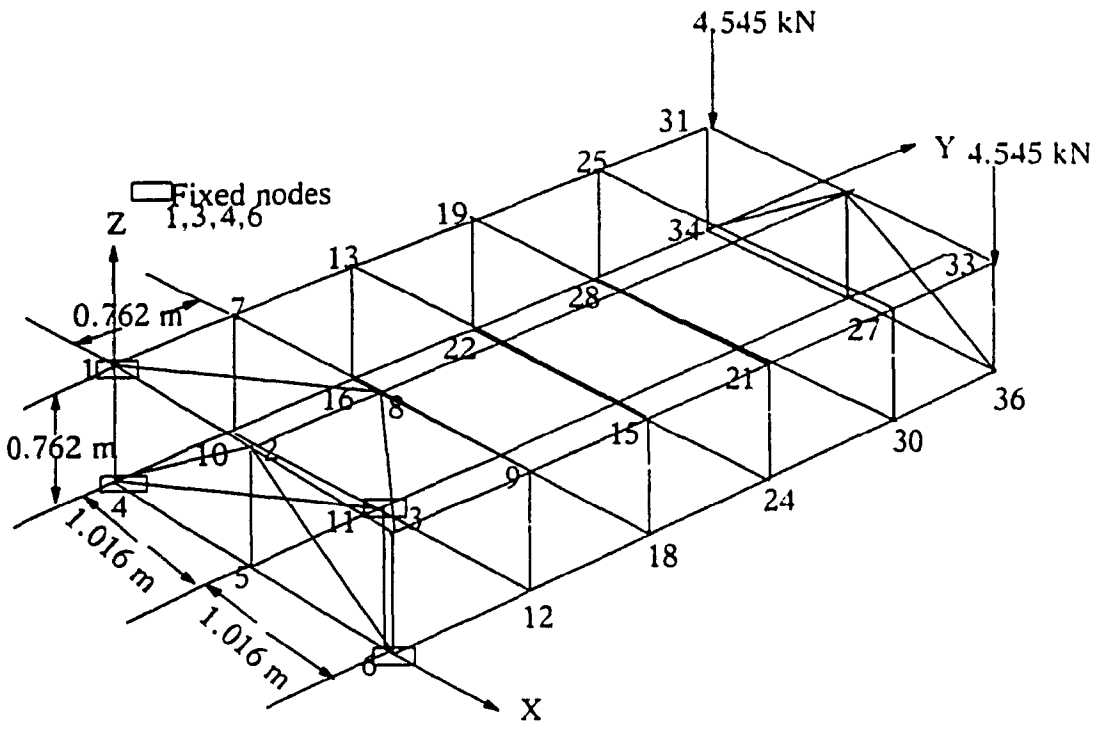


Figure 4.2: Schematic of the three dimensional space truss model [48]

**Table 4.2: Design Configurations of the Three-Dimensional Space Truss [48].**

| | | Cross-section Areas ($cm^2$) | | | |
|---|---|---|---|---|---|
| Member Numbers | Direction | Design 1 | Design 2 | Design 3 | Design 4 |
| 1-18 | Z-axis | 6.45 | 1.29 | 6.45 | 6.45 |
| 19-42 | X-axis | 6.45 | 6.45 | 1.95 | 6.45 |
| 43-72 | Y-axis | 12.90 | 12.90 | 12.90 | 12.90 |
| 73-124 | Diagonals | 3.23 | 3.23 | 3.23 | 0.65 |

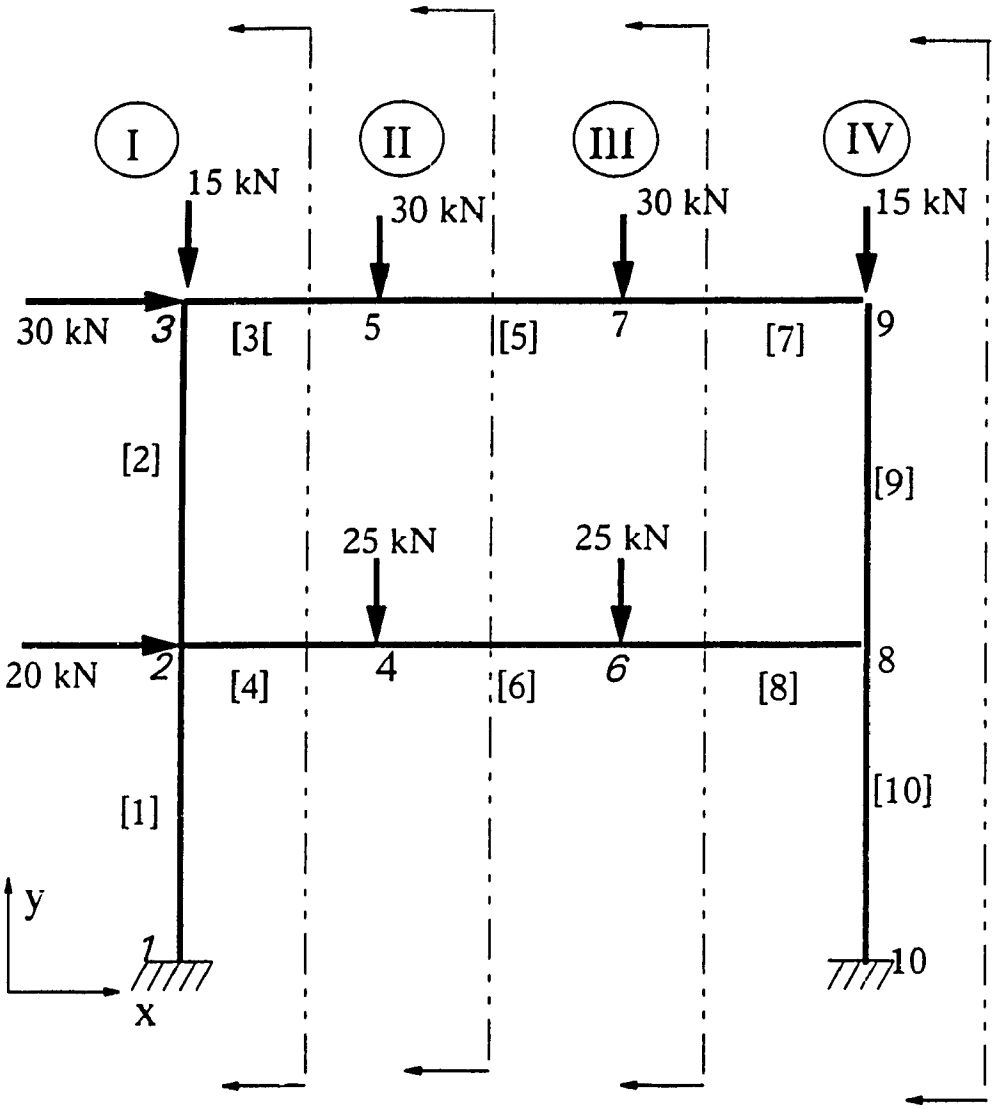


Note: I, II, III, IV denote partitions

Each partition includes elements[] and nodes to the left of dotted lines

Figure 4.3: A schematic of the boiler frame structure [49].

**Table 4.3: Sectional properties of Plane Frame [49].**

Material: Structural steel Young's modulus: 2.1e11MPa

| Member connecting nodes | Area ($cm^2$) | Length (cm) | Flexural Rigidity N $cm^2$ |
|---|---|---|---|
| 1-2 | 45 | 200 | 1e11 |
| 2-3 | 45 | 200 | 1e11 |
| 2-4 | 60 | 100 | 2e11 |
| 4-6 | 60 | 100 | 2e11 |
| 6-8 | 60 | 100 | 2e11 |
| 3-5 | 60 | 100 | 2e11 |
| 5-7 | 60 | 100 | 2e11 |
| 7-9 | 60 | 100 | 2e11 |
| 9-8 | 45 | 200 | 1e11 |
| 8-10 | 45 | 200 | 1e11 |

#### 4.2.1.1 VALIDATION OF FETM METHOD

In order to validate FETM method developed in Chapter 3, the example structure referred to as space truss, shown in Figure 4.2, is selected. The structure can be conveniently represented by five substructures arranged in "in-line" type manner. It should be noted that all the members are not shown in the figure in order to improve the visual clarity. It is evident that the structural members connecting nodes 1 to 12 form the first substructure comprising three dimensional spar elements. The nodes 7 to 18 in a similar manner form the subsequent substructure. This structural configuration is ideally suited for transfer matrix method, since the stiffness matrix of each substructure is identical. The method thus requires formulation of the stiffness matrix for only one substructure.

Fox and Miura [48], and Noor and Lowder [35] have analyzed the space truss using matrix methods. Noor and Lowder [35], however, did not report the absolute deflection response in their study. The geometric and loading conditions

specified in the study of Fox and Miura [48], are thus used to compare the results of the FETM method. The method of solution based upon FETM, outlined in section 3.7, is used to analyze the structural model and the response characteristics computed are compared with those reported in [48] to demonstrate the validity of the developed methodology. Since the deflection response is reported only for the nodes 21 and 33, the validation is demonstrated by comparing the deflection at these two nodes in Table 4.4. The comparison reveals very good agreement with the reported data, while the deviations are about 1%.

**Table 4.4: Comparison of Nodal Displacement Response with the data reported in [48].**

| | | Nodal Displacement (cm) | | |
|---|---|---|---|---|
| Node | Coordinate | FETM method | Reference [48] | % error |
| 21 | X | 0.000 | 0.000 | 0.00 |
| | Y | 0.1905 | 0.1874 | 1.00 |
| | Z | -1.808 | -1.797 | 0.50 |
| 33 | X | 0.0500 | 0.0530 | 0.00 |
| | Y | 0.2310 | 0.2272 | 1.00 |
| | Z | -3.8430 | -3.799 | 1.00 |

### 4.2.1.2 VALIDATION OF EFETM TECHNIQUE

Since the primary objective of the study is to develop efficient reanalysis method, the validity and efficiency of the above method is investigated through reanalysis solutions of two different structures: (i) A planar ten-bar cantilever truss as shown in Figure 4.1; and (ii) 124 bar space truss with various design modifications. The EFETM method of reanalysis is used to analyze different example structures and the results are compared with those derived from the FEM

analysis. The computing efficiency and the accuracy of the reanalysis method are further presented. Both structures are of "repeated-type" and are best suited for transfer matrix treatment. In the first structure cross-sectional areas of different members in a specific substructure are varied, whereas properties of members oriented along a specific axis in all the substructures within the second substructure are varied simultaneously.

The transfer matrix for each substructure is derived from FEM formulation using bar elements, using Equation (3.36). For studying the design sensitivity, the variation of the structural behavior (nodal displacements) as a consequence of a change in *reciprocal of the member cross-sectional area*, rather than the area itself has been considered. This approach resulted in enhanced sensitivity behavior. The geometry and loading condition of the base cantilever truss structure are represented in Figure 4.2 and in Table 4.2. The design modification were performed by varying the cross-section area of a specific member in a specific substructure. The method of reanalysis, based upon EFETM, and described in section 3.7, was used to evaluate the response behavior of the modified structure.

The deflection at nodes 3 and 4, evaluated for various design modifications using the reanalysis method, are compared to those derived from the FETM analysis, as illustrated in Table 4.5. The table illustrates a comparison of the results derived from analysis and reanalysis solutions, when the cross-section areas of members 2, 3 and 5 are varied from 5% to 20%. The results show that EFETM method can provide a reasonable estimate of the structural response via reanalysis solution. The reanalysis method, however, is extremely efficient to evaluate the influence of a design modification. The reanalysis solution corresponding to a design modification requires 5 s execution time with a personal computer (80486

DX 33 MHz. processor), while FETM analysis requires for each analysis 8 s. Since this particular structure is simple and requires small order of matrix size (12x12), both FEM and FETM require similar execution time. It is apparent that the execution time for each reanalysis reduces by approximately 38% when compared to that for the solution using FETM and FEM.

**Table 4.5:Comparison of Displacement Response derived from FETM and EFETM Reanalysis Solutions. (continued..)**

| | | | Nodal Displacement (cm) | | | | | |
|---|---|---|---|---|---|---|---|---|
| | | | X- DOF | | | Y-DOF | | |
| ELEM. No. | %Area Change | NODE | FETM | EFETM | % error | FETM | EFETM | % error |
| 2 | 5 | 3 | 2.299 | 2.290 | 0.0 | -6.933 | -6.933 | 0.0 |
| | | 4 | 2.301 | 2.2800 | <1.0 | -6.904 | -6.55 | 5.0 |
| | 10 | 3 | 2.287 | 2.260 | <1.0. | -6.933 | -6.933 | 0.0 |
| | | 4 | -2.283 | 2.07 | 9.0 | -6.904 | -6.07 | 12.0 |
| 3 | 5 | 3 | 2.286 | 2.28 | <1.0 | -6.933 | -6.59 | 5.0 |
| | | 4 | -2.283 | -2.30 | 0.4 | -6.904 | -6.4 | 7.0 |
| | 10 | 3 | 2.30 | 2.28 | <1.0 | -6.989 | -6.704 | 4.0 |
| | | 4 | -2.301 | -2.25 | 2.0 | -6.903 | -6.35 | 7.0 |
| 5 | 5 | 3 | 2.30 | 2.28 | 0.4 | -6.989 | -6.70 | 4.0 |
| | | 4 | -2.30 | -2.29 | <1 | -6.903 | -6.44 | 6.7 |
| | 10 | 3 | 2.3 | 2.29 | 0.5 | -7.081 | -6.62 | 6.5 |
| | | 4 | -2.301 | -2.275 | <1.0 | -6.902 | -6.07 | 12.0 |

**Table 4.5: Comparison of Displacement Response derived from FETM and EFETM Reanalysis Solutions.**

| | | | Nodal Displacement (cm) | | | | | |
|---|---|---|---|---|---|---|---|---|
| | | | X- DOF | | | Y-DOF | | |
| ELEM. No. | %Area Change | NODE | FETM | EFETM | % error | FETM | EFETM | % error |
| 2 | 15 | 3 | 2.299 | 2.290 | 0.0 | -6.933 | -6.933 | 0.0 |
| | | 4 | -.2.301 | -2.050 | 11.0 | -6.904 | -6.50 | 6.0 |
| | 20 | 3 | 2.287 | 2.260 | <1.0. | -6.933 | -6.933 | 0.0 |
| | | 4 | -2.283 | 2.00 | 14..0 | -6.904 | -6.10 | 11.0 |
| 3 | 15 | 3 | 2.2867 | 2.25 | 1.3 | -6.933 | -6.495 | 6.2 |
| | | 4 | -2.283 | -2.26 | <1.0 | -6.904 | -6.15 | 10.5 |
| | 20 | 3 | 2.30 | 2.24 | 2.00 | -6.989 | -6.704 | 4.0 |
| | | 4 | -2.301 | -2.25 | 2.0 | -6.903 | -5.886 | 15.0 |
| 5 | 15 | 3 | 2.30 | 2.26 | 2.0 | -6.989 | -6.70 | 4.0 |
| | | 4 | -2.30 | -2.29 | <1 | -6.903 | -6.10 | 11.5 |
| | 20 | 3 | 2.3 | 2.29 | 0.5 | -7.081 | -6.50 | 8.2 |
| | | 4 | -2.301 | -2.275 | <1.0 | -6.902 | -5.2 | 23.0 |

The results tabulated in Table 4.5 clearly illustrate that the EFETM reanalysis solution yields an accurate estimate of the deflection response along X-axis for small variations in cross-section. The corresponding estimation error in deflection of node 3 is well below 3% for 5% variation in the cross-section areas of members 2, 3 and 5. While 10% area change of member 2 yields a deflection error of node 4 of approximately 9%, the similar variations in members 3 and 5 yield errors well below 1%. A large change in the cross-section areas yields somewhat increased error in the deflection response of node 3, which is directly subjected to the static load. The reanalysis solution, however, yields an accurate estimate of node 4 deflection response corresponding to 20% change in the cross section. From the results it can be concluded that EFETM reanalysis solution yields a reasonably good estimation of the structure response in a highly efficient manner irrespective of the variations in the members oriented along X, Y and diagonal directions.

The results summarized in Table 4.5 also reveal small estimation errors in vertical (Y-axis) deflection response of node 3 for variations in the cross-section areas. The error is observed to be below 4% for 5% change in the areas, and below 10% corresponding to 15% change in the areas. The error in the vertical deflection of node 4 , however, is larger, which tends to increase in the magnitude of variation in the cross-section areas. The estimation error is observed to be nearly 12% for 10% area change, and in the 16-23% range for 20% change in the area. This may be attributed to the significant reduction in the cross section area of the structural member 1 connecting node 4 is very thin (38 times lesser in area) compared to member 2.

The results derived from the EFETM reanalysis solution of different design configurations described in Table 4.2 are further compared with those established from direct FETM solution for the space truss to demonstrate the validity and efficiency of the proposed reanalysis technique. Table 4.6 illustrates the vertical deflection response of nodes 15, 19, 21 and 25 of the different design configurations, as derived from the FETM and EFETM reanalysis methods. As discussed earlier, the validation of the FETM solutions was verified with those reported in the literature. It should be noted that the different design configurations represent excessive variations in the cross-section areas of different members with respect to the base design (Design 1). The design 2 configuration represents 80% reduction in the cross-section areas of all the vertical members of the space truss, while the design 3 is realized by reducing the cross-section areas of all members, oriented along X-axis, by 70%. The design configuration 4 corresponds to 80% reduction in cross-section areas of all members oriented along the diagonal directions. The results summarized in Table 4.6 clearly illustrate that the reanalysis solution provides an accurate estimate of deflection response when the members along X- and Z-axes are varied, although the magnitudes of design variations are quite large. The advantages of the reanalysis solution in terms of computing efficiency are quite apparent, since the EFETM requires only 40 s of execution time in comparison with 70 s required by the FETM analysis. The results, however, reveal larger errors for the design configuration 4, where the cross-section area of the diagonally oriented members are reduced by 80%. While the deflection response of nodes 13 and 15 is considerably small (<1.2%), the deflection response of nodes 19, 21 and 25 exhibit large errors as high as 60%.

**Table 4.6: Comparison of Vertical displacement Response of the Space Truss [48].**

| | Design 1 | DESIGN 2 | | | DESIGN 3 | | | DESIGN 4 | | |
|---|---|---|---|---|---|---|---|---|---|---|
| NODE | (Base Design) | FETM | EFETM | % error | FETM | EFETM | % error | FETM | EFETM | % error |
| 13 | 5.2959 | 6.238 | 6.238 | 0.0 | 22.40 | 22.39 | 0.0 | 5.496 | 5.496 | 0.0 |
| 15 | 5.334 | 6.175 | 6.172 | 0.0 | 22.34 | 22.33 | 0.0 | 6.035 | 6.802 | 12.0 |
| 19 | 11.00 | 13.17 | 13.17 | 0.0 | 45.49 | 45.49 | 0.0 | 13.11 | 17.65 | 34.0 |
| 21 | 11.61 | 13.10 | 13.10 | 0.0 | 45.44 | 45.41 | 0.0 | 12.82 | 19.53 | 50.0 |
| 25 | 11.69 | 20.61 | 20.61 | 0.0 | 69.11 | 69.11 | 0.0 | 20.41 | 33.95 | 64.0 |

### 4.2.1.3 VALIDATION OF SUBSTRUCTURE TECHNIQUE

A direct and reanalysis substructuring technique employing Potters' method of solution, described in Chapter 3, are validated for static as well as free-vibration response. The direct method is initially validated for static analysis using the plane frame example structure presented in Figure 4.3. The static and dynamic response behavior of the structure are reported [49]. The structure is partitioned into 4 substructures as described in Figure 4.3, and each node is considered to have 3 DOF motion: displacement along X-axis, displacement along Y-axis, and rotation about XY plane. The static response characteristics of the structure derived from the Potters' solution are compared with those reported in [49], as illustrated in Table 4.7. The results clearly demonstrate the validity of Potters' solution. The peak error in deflection is observed to be well below 3% for all nodes, except nodes 4 and 6. Solutions were obtained by standard FEM solutions without partitioning and the deflection response obtained were similar to Potters' solution.

**Table 4.7: Comparison of Static Deflection Response Derived from Potters' Solution with those Reported in [49].**

| NODE | Potters' method | | | Reference [49] | | | % error | |
|---|---|---|---|---|---|---|---|---|
| | X (mm) | Y (mm) | Rotn (rad) | X (mm) | Y (mm) | Rotn (rad) | X (mm) | Y (mm) |
| 2 | 2.556 | -.076 | -.0011 | 2.548 | -.073 | -.0011 | <.02 | 4.0 |
| 3 | 4.959 | -.148 | -.0010 | 4.948 | -.0148 | -.0010 | <.02 | 0.0 |
| 4 | 2.554 | -.665 | 0.000 | 2.547 | -.617 | 0.000 | <.02 | 7.7 |
| 5 | 4.939 | -.920 | -.0003 | 4.927 | -.932 | -.0003 | <.02 | 1.2 |
| 6 | 2.552 | -.339 | .0005 | 2.545 | -.307 | .0005 | <.02 | 10 |
| 7 | 4.918 | -.795 | .0005 | 4.905 | -.812 | .0005 | <.02 | 2.0 |
| 8 | 2.550 | -.219 | -.0006 | 2.543 | -.227 | -.0006 | <.02 | 3.5 |
| 9 | 4.897 | -.338 | .0006 | 4.884 | -.352 | .0006 | <.02 | 3.9 |

The validity of the Potters' method is further examined through analysis of the example structure. An eigenvalue analysis is performed to determine the modal frequencies and deflection modes of the structure. The method of solution is by using simultaneous iteration technique which is described later in Chapter 6 for the study of Candidate trailer structure. The eigenfrequencies and corresponding dominant deflection modes, derived from the Potters' solution, are compared with those reported in [49] to demonstrate the validity of the direct solution method. Table 4.8 illustrates a comparison of the natural frequencies and dominant deflection modes with those reported [49]. The results clearly illustrate the validity of the Potters' method for dynamic response analyses. The peak error in natural frequency is observed to be 1.4% for the first mode, and well below 1% for the remaining modes. Figure 4.4 illustrates the deflection modes of the structure corresponding to modes 1, 2, 4 and 8, which correspond to the frame lateral sway modes, and vertical vibration modes of the members.

**Table 4.8: Comparison of Natural Frequencies and Dominant Deflection Modes [49].**

| | Potters' method | | Reference [49] | | |
|---|---|---|---|---|---|
| Mode | Natural Frequency (rad/s) | Dominant Deflection mode | Natural Frequency (rad/s) | Dominant Deflection mode | % error in Natural Frequency |
| 1 | 143.6 | lateral sway | 145.0 | lateral sway | 1.4 |
| 2 | 475.1 | lateral | 476.2 | lateral | 0.2 |
| 3 | 768.7 | | 770.3 | | 0.3 |
| 4 | 963.5 | vertical top frame | 972.0 | vertical top frame | 1.0 |
| 5 | 1353.7 | | 1360.0 | | 0.5 |
| 6 | 2677.9 | | 2680.0 | | 0.05 |
| 7 | 3249.0 | | 3255.0 | | 0.05 |
| 8 | 3347.3 | vertical bottom frame | 3350.0 | vertical bottom frame | 0.01 |
| 9 | 4006.7 | | 4015.0 | | >0.05 |
| 10 | 4066.7 | | 4077 | | >0.05 |
| 11 | 4083.4 | | 4095 | | >0.05 |
| 12 | 6536.9 | vertical and lateral | 6555.0 | vertical and lateral | >0.05 |

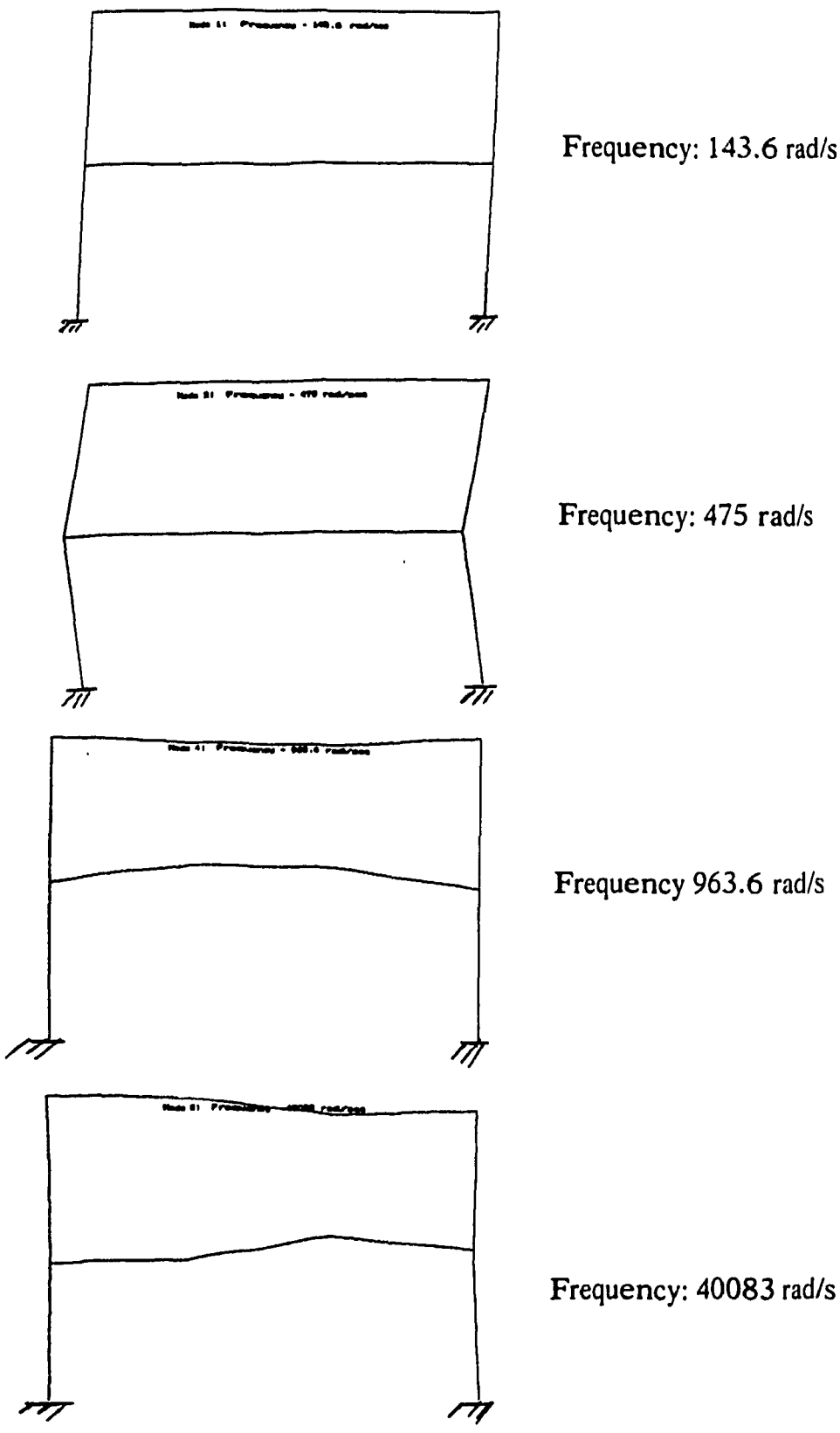


Figure 4.4: Deflection modes of the boiler frame structure [49].

### 4.2.2 Validation against ANSYS

The Potters' method is further validated through comparing the response characteristics of a large scale trailer structure (Trailer B, described in Chapter 2 (with those derived from ANSYS software, PC version 5.0). A finite element model of the trailer structure is developed to perform analyses using the ANSYS software. The main-, side- and cross-beams of the trailer structure, shown in Figure 2.2 are characterized by three dimensional elastic beam elements (BEAM 4 of the ANSYS element library) with six DOF at each node. The spring elements characterizing the trailer suspension are represented by 3-D spar elements (LINK 8 of the ANSYS element library). The FE model, is thus formulated with a total of 156 nodes, 355 beam elements, and 936 DOF. The model also comprises 8 spring elements. The rated trailer payload of 350 kN is uniformly distributed over all the nodes, except the reaction nodes with all their DOF constrained.

The substructure model of trailer B is formulated using the methodology presented in section 3.8. The details of the model are presented in Table 3.1. The substructure model is solved using Potters' method and the results are compared to those derived from ANSYS solution. Figures 4.5 and 4.6 illustrate a comparison of the vertical deflection and bending stress distribution respectively of the main-beam derived from the two solutions. While the response behavior derived from the two methods reveal a reasonable agreement, certain discrepancies exist as shown in the Figures. The deflection response established from Potters' method is observed to be slightly larger than that derived from ANSYS software, over the

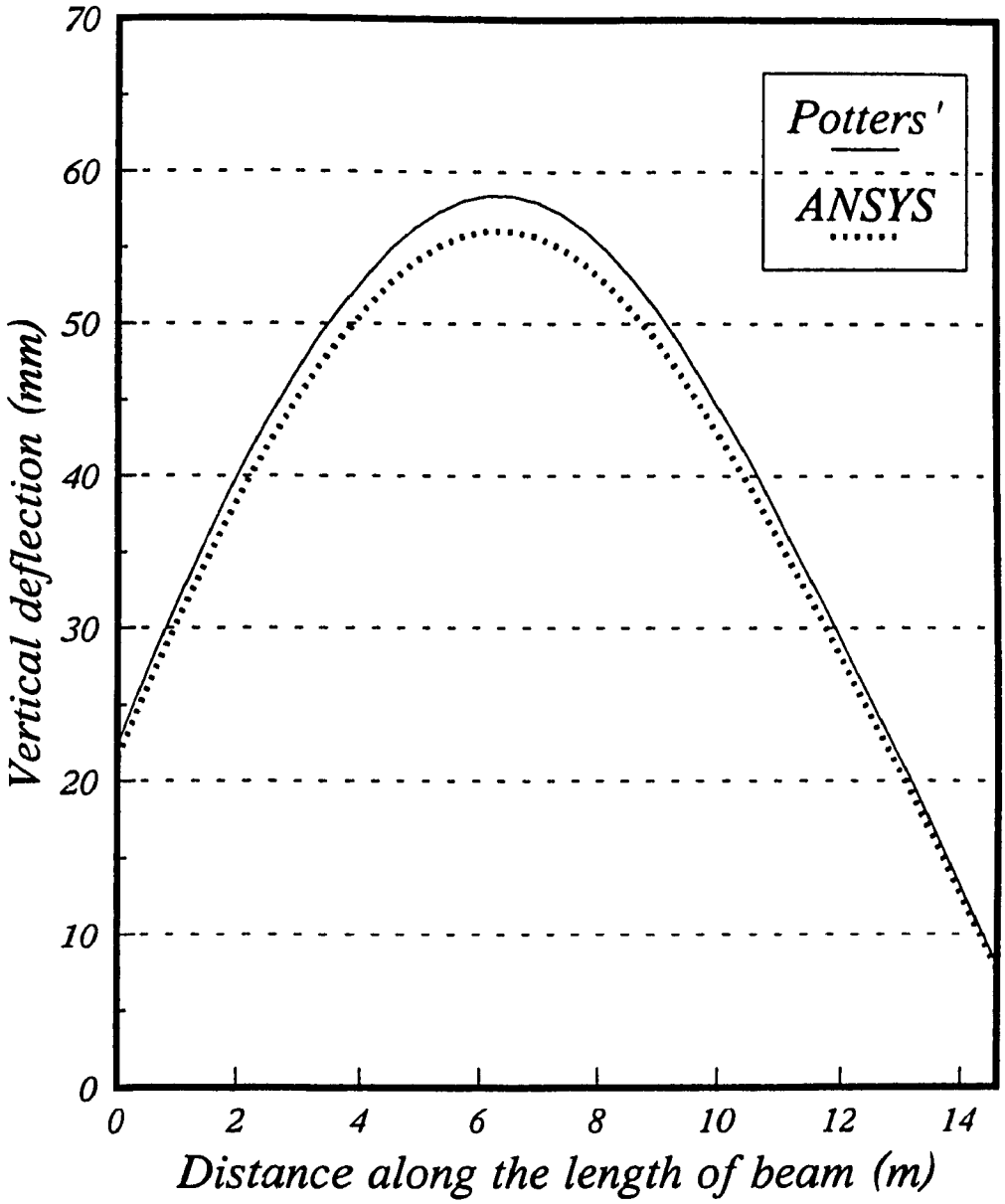


Figure 4.5: Comparison of deflection response of the main-beam derived from Potters'solution and the ANSYS software.

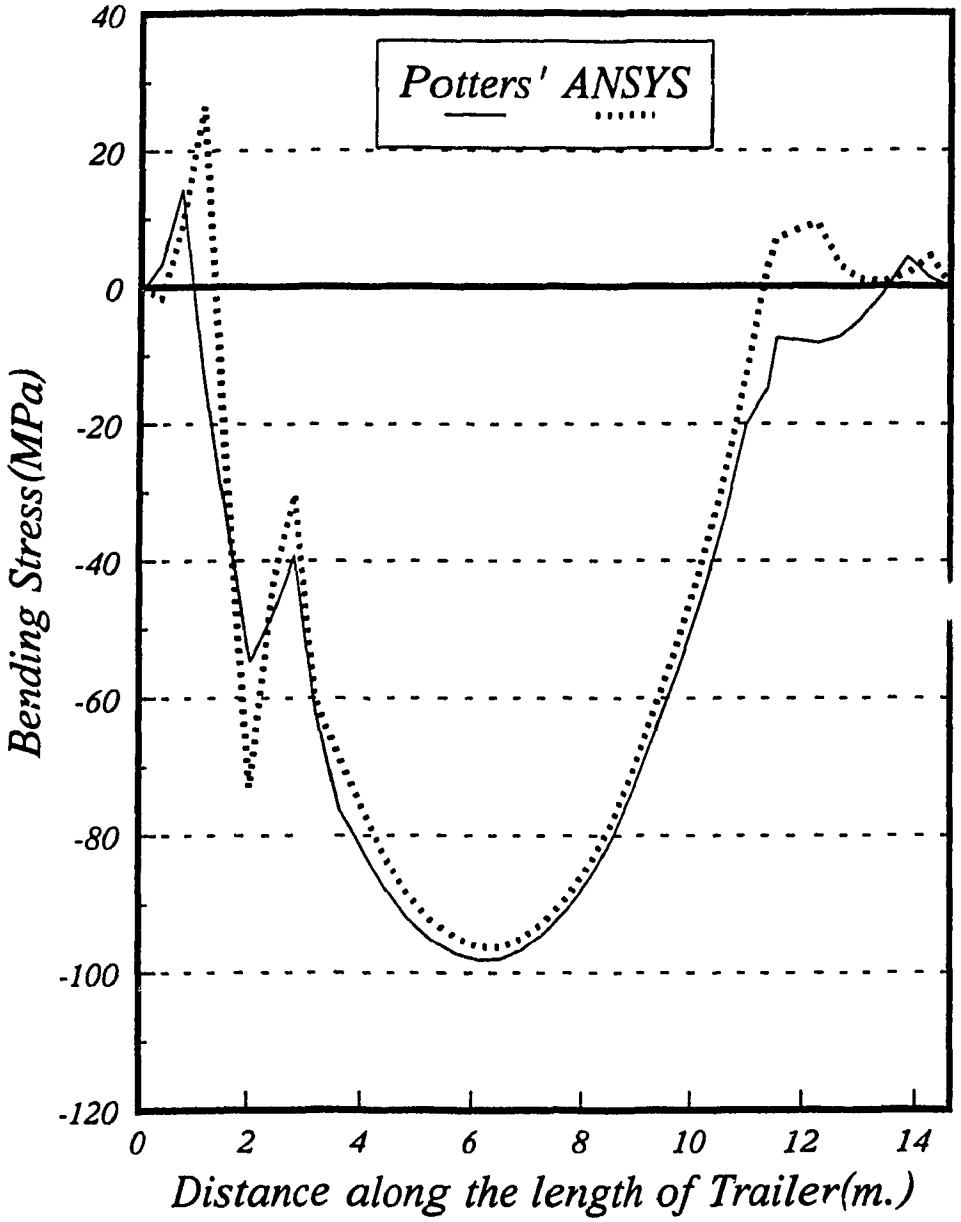


Figure 4.6: Comparison of flexural stress response of the main-beam derived from Potters' solution and the ANSYS software.

entire length of the trailer. The magnitude of the peak deviation between the two solutions is well below 6%. The response reveals large stresses near the king-pin support and the goose-neck region, and the peak stress occurs near the middle of span between the king-pin and suspension supports. The error in the solutions, corresponding to the peak stress, is below 2%, the error in the peak stress near the king-pin support is considerably large.

The ANSYS solution yields larger bending stresses in the leading and trailing edges of the goose-neck region with varying cross-section area. The stress distribution over the span between the king-pin and suspension supports, estimated from Potters' method agree very well with that derived from ANSYS solution. The Potters' method, however, yields a slightly larger value of bending stress, as illustrated in Figure 4.6.

Figures 4.7 and 4.8 illustrate the comparison of vertical deflection and flexural stress distribution of the side-beam derived using two methods. The results clearly demonstrate the validity of the Potters' method. While the displacement plot in Figure 4.7 depicts a very close agreement, with a maximum % error less than 7%, the stress distributions predicted by both the methods tend to compare very well for the beam length. The Potters' method tend to predict the maximum stress level slightly on the higher side with the maximum % error less than 5%.

### 4.2.3 Validation Through Modal Analysis

The substructure analysis based upon Potters' method is further validated by comparing the modal frequencies of the substructure model with those derived

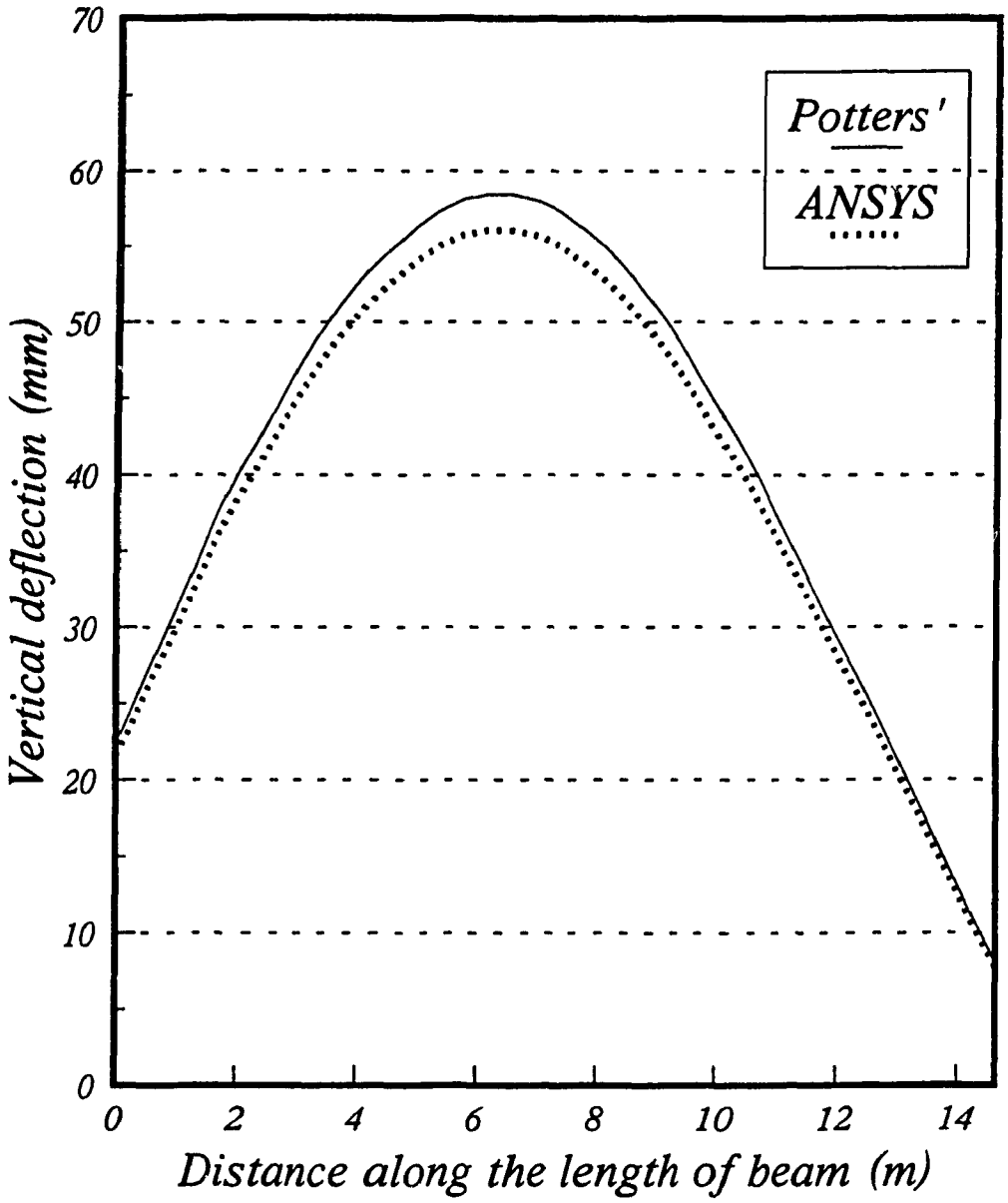


Figure 4.7: Comparison of deflection response of the side-beam derived from Potters' solution and the ANSYS software.

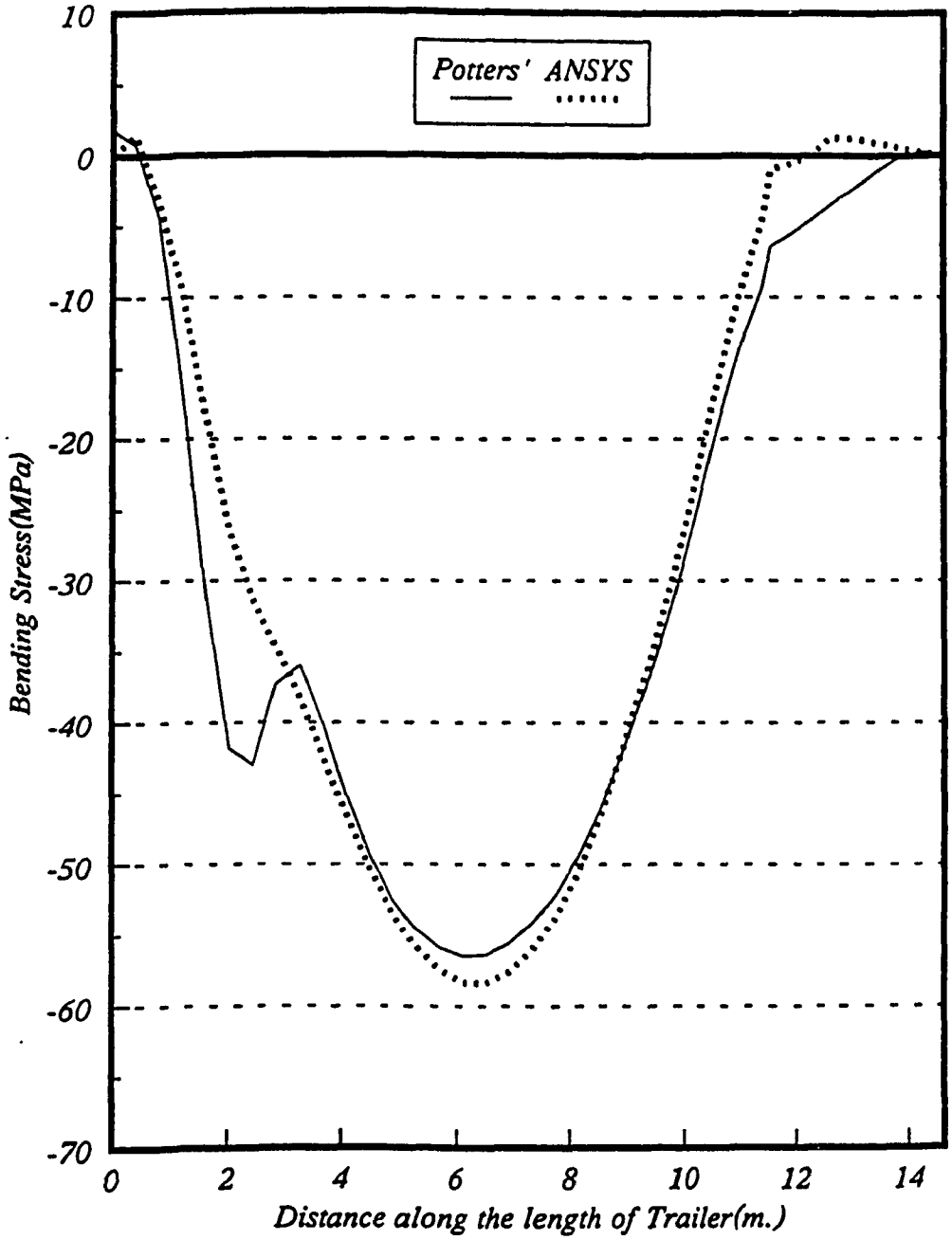


Figure 4.8: Comparison of flexural stress response of the side-beam derived from Potters' solution and the ANSYS software.

from ANSYS solution and experimental modal analysis. The eigenvalues and eigenvectors corresponding to the lowest 25 modes are determined using the method of simultaneous iteration [49]. The method is further described in Chapter 6. The eigenfrequencies are further compared with those derived from the ANSYS model in Table 4.9. It should be noted that the extraction of eigensolution in ANSYS solution requires selection of master DOF to reduce the size of the problem. In view of the limitations of the wave front equations of the PC-version of ANSYS software used, the eigensolutions associated with vertical and lateral DOF alone were extracted. The results summarized in the table demonstrate that the eigenfrequencies and the dominant deflection modes of the substructure model correlate reasonably well with those established from ANSYS solution. Figures 4.9 to 4.12 illustrate a qualitative comparison of selected deflection modes from the substructure and ANSYS solutions. The deflection mode associated with dominance of trailer roll occurring at 5.05 Hz (Potters') and 5.00 Hz (ANSYS) are illustrated in Figure 4.9. The dotted representation of the geometry depicts the undeformed structure and the deformed shape is represented by solid lines. While the ANSYS solution exhibits pure roll deflection, the substructure analysis yields dominantly roll motion constrained near the king-pin support. The deflection behavior near the trailing edge, however, exhibits dominantly roll motion. Both ANSYS and substructure analyses predict a lateral translation mode occurring at 5.68 Hz and 5.88 Hz respectively. Figure 4.10 illustrates the first flexural mode as predicted by Potters' analysis and ANSYS. While ANSYS predicts it as 13.7 Hz, substructure analysis estimates at 13.90 Hz. The second flexural frequency are predicted at 24.73 Hz and 28.19 Hz by Potters' analysis and ANSYS respectively. The torsional modes exhibited by Potters' and ANSYS are presented in Figure 4.11. A combined flexural and torsional mode occurring at higher frequencies of 35.5 and 38.3 Hz for Potters' and ANSYS solutions, respectively, is shown in

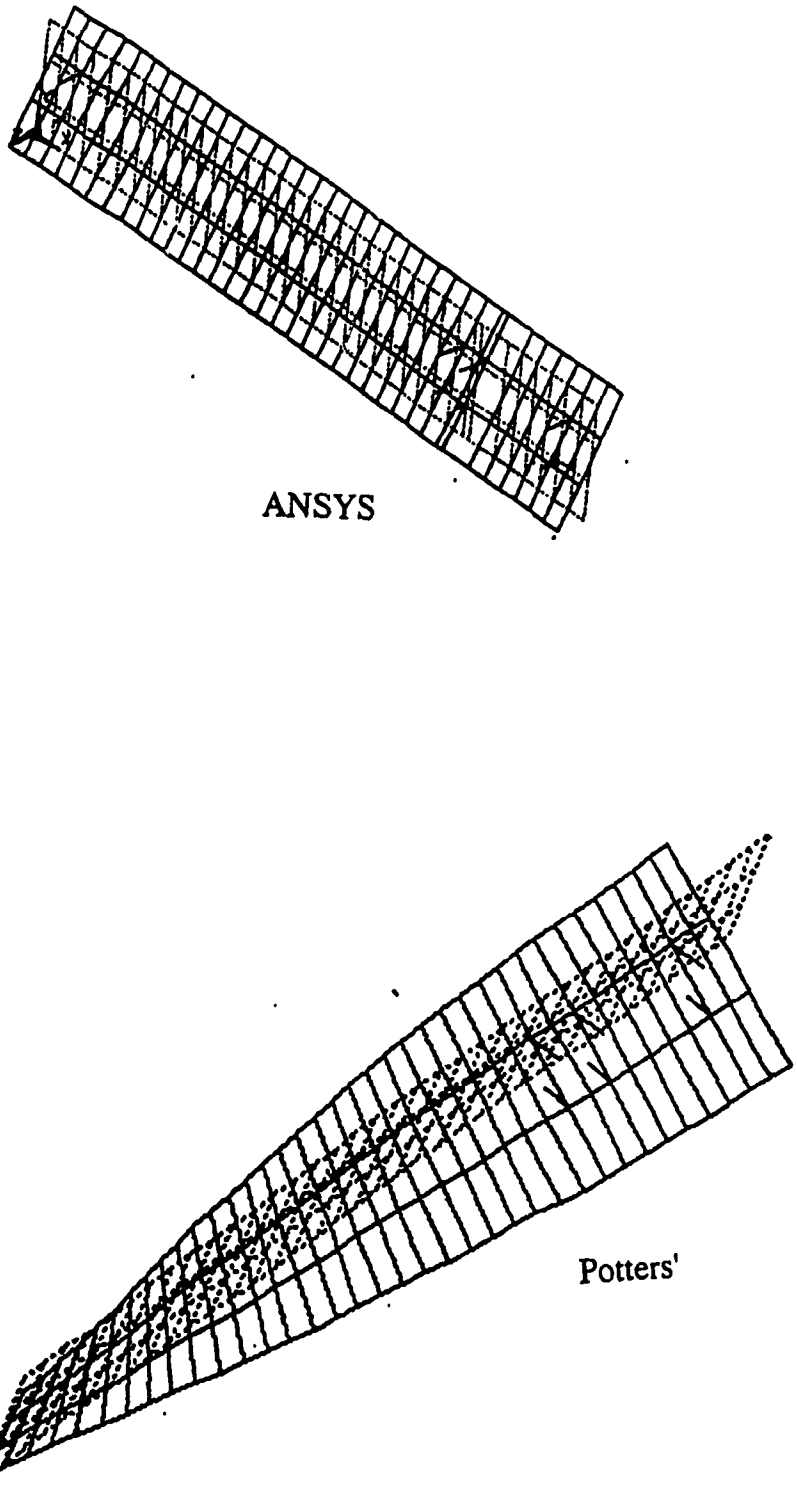


Figure 4.9: The roll deflection mode of the trailer structure derived from Potters' solution and ANSYS.

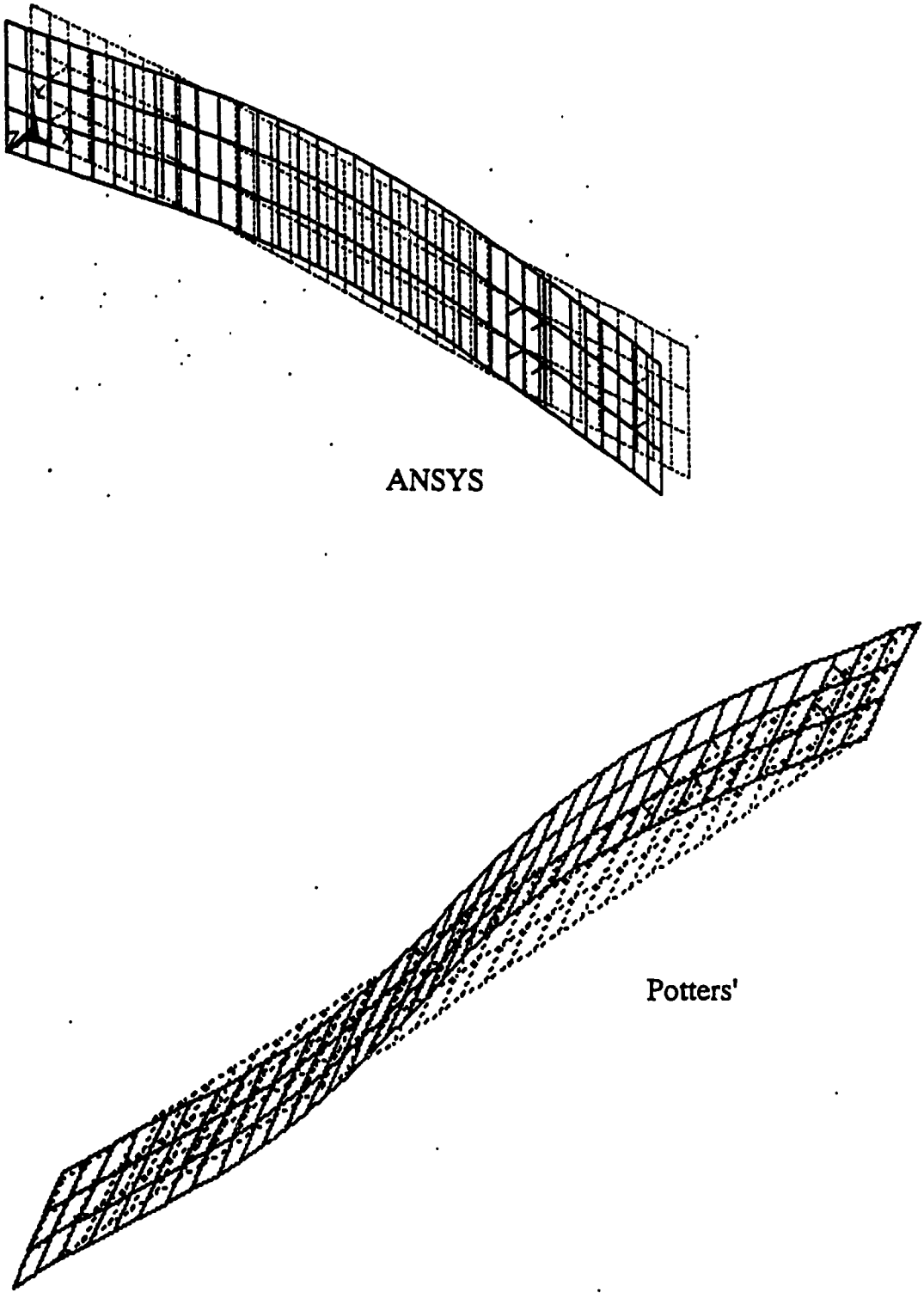


Figure 4.10: First flexural mode of the trailer structure derived from Potters' solution and ANSYS.

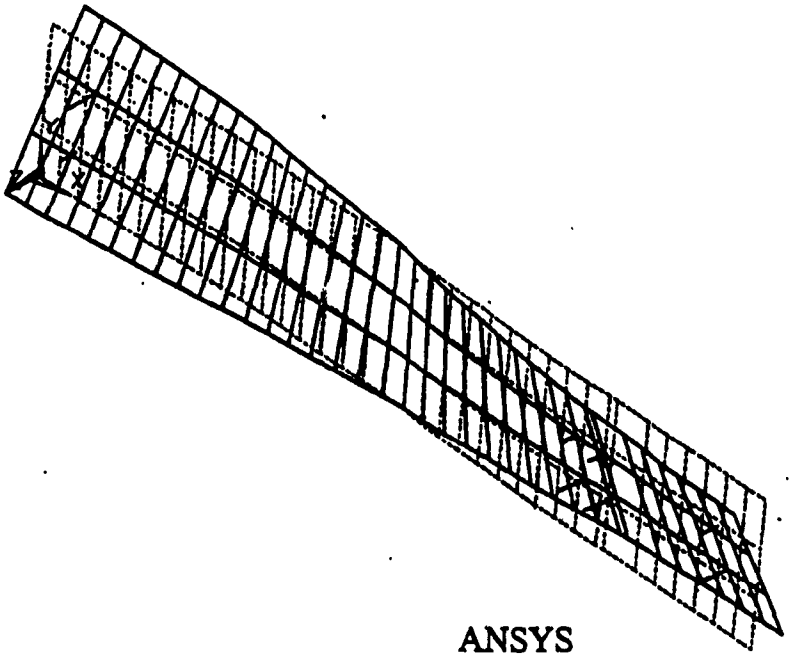

ANSYS

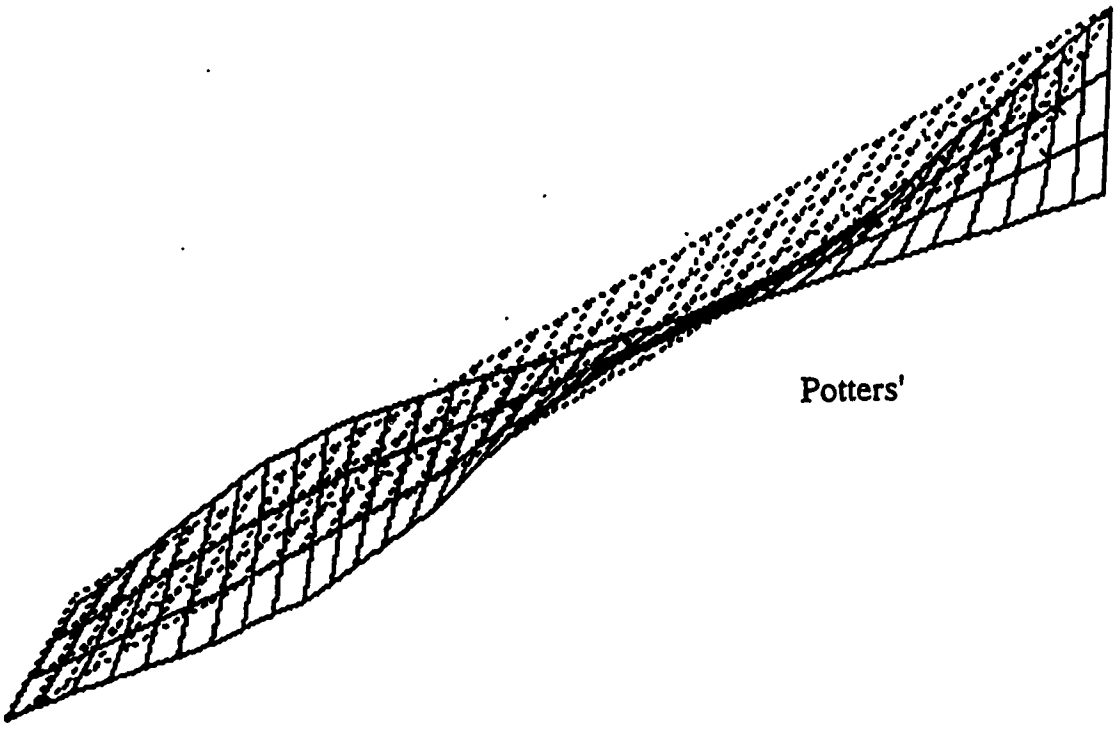

Potters'

Figure 4.11: First torsional mode of the trailer structure derived from Potters' solution and ANSYS.

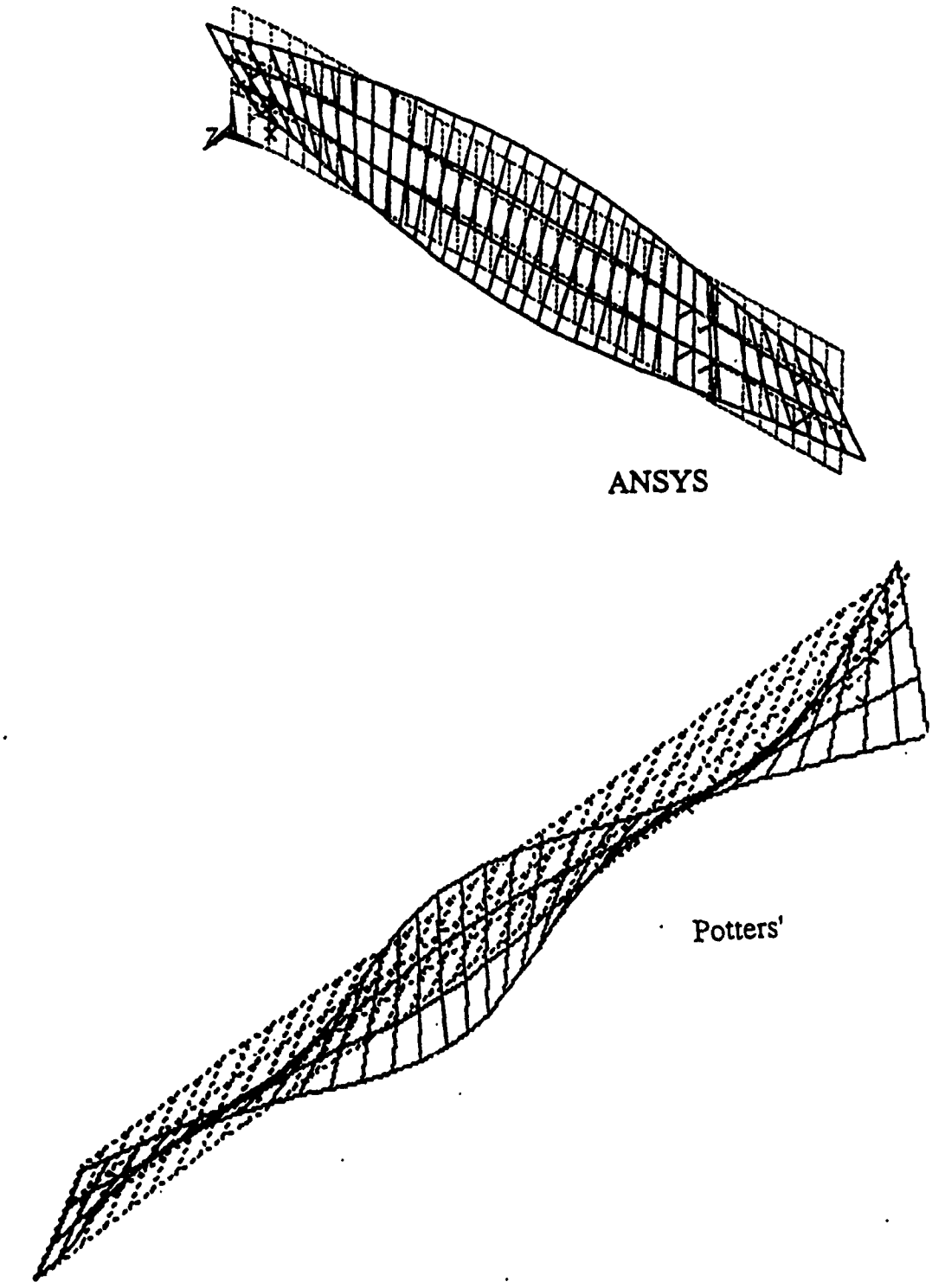


Figure 4.12: Combined flexural and torsional mode of the trailer structure derived from Potters' solution and ANSYS.

**Table 4.9: Comparison of Modal Frequencies Derived from Potters' method, ANSYS and Experimental Modal Analysis.**

| Potters' method | | ANSYS Software | | EXPERIMENTAL MODAL ANALYSIS | |
|---|---|---|---|---|---|
| Frequency (Hz) | Dominant Mode | Frequency (Hz) | Dominant Mode | Frequency (Hz) | Dominant Mode |
| 3.25 | | | | 2.72 - 2.75 | Bounce |
| 4.00 | Bounce | 3.85 | Bounce | 4.27 - 4.52 | Roll |
| 5.05 | Roll | 5.15 | Roll | | |
| 5.88 | Lateral Translation | 5.68 | Lateral Translation | 7.45 - 7.50 | Yaw |
| 10.05 | | 10.10 | Pitch - Front | 8.37 - 8.38 | Lateral Bending |
| | | 12.79 | Pitch -Rear + Translation | | |
| 13.92 | First Flexure | 13.70 | First Flexure | 9.52 | Vertical Bending |
| 20.35 | Rear Torsion | 20.32 | Torsion | 13.33 - 13.90 | Torsion |
| 24.73 | Second Flexure | 28.19 | Second Flexure | 20.38 - 20.34 | Torsion & Vertical Bending |
| 28.50 | Second Torsion | | | 23.56 - 23.68 | Torsion & Lateral Bending |
| 39.09 | Flexure and Torsion | 39.18 | Torsion | | |
| 61.00 | Flexure and Torsion | 59.36 | Flexure and Torsion | | |

Figure 4.12. The higher value predicted by ANSYS is due to its limited master DOF representation in the model. A combination of flexure and torsional modes are predicted by both the methods at quite close frequencies as represented in the Table. The % error difference is less than 2% and the substructure model is able to analyze the natural frequencies and mode shapes effectively as demonstrated.

### 4.2.3.1 EXPERIMENTAL MODAL ANALYSIS

Analytical vehicle structure models in general are validated through static tests performed in the laboratory. The forced response behavior of the structure, however, necessitates further validation under dynamic loads. Rakheja and Sankar [50] discussed different options to achieve dynamic validation of a structural model, both qualitatively and quantitatively as illustrated in Figure 4.13. The authors reported an integrated computer-aided modal analysis and testing technique for achieving acceptable dynamic verification of a snowmobile chassis structure. The approach enabled the verification of the FE model and allowed for modification to be incorporated in the analytical model from the quantitative and qualitative feedback obtained from experimental results, such as modal frequencies as modal damping and mode shapes.

One of the candidate trailers, Trailer-B was selected for carrying out experimental modal analysis. The test was carried out at the Transport Canada Automotive Test centre, Blainville, Quebec in collaboration with Forestry Engineering Research Institute of Canada. The detail test methodology, instrumentation and analysis are described in an internal CONCAVE report [51].

The test trailer is a quad-axle semi-trailer comprising three axles mounted on pneumatic suspensions, is used for transportation of logs. The design

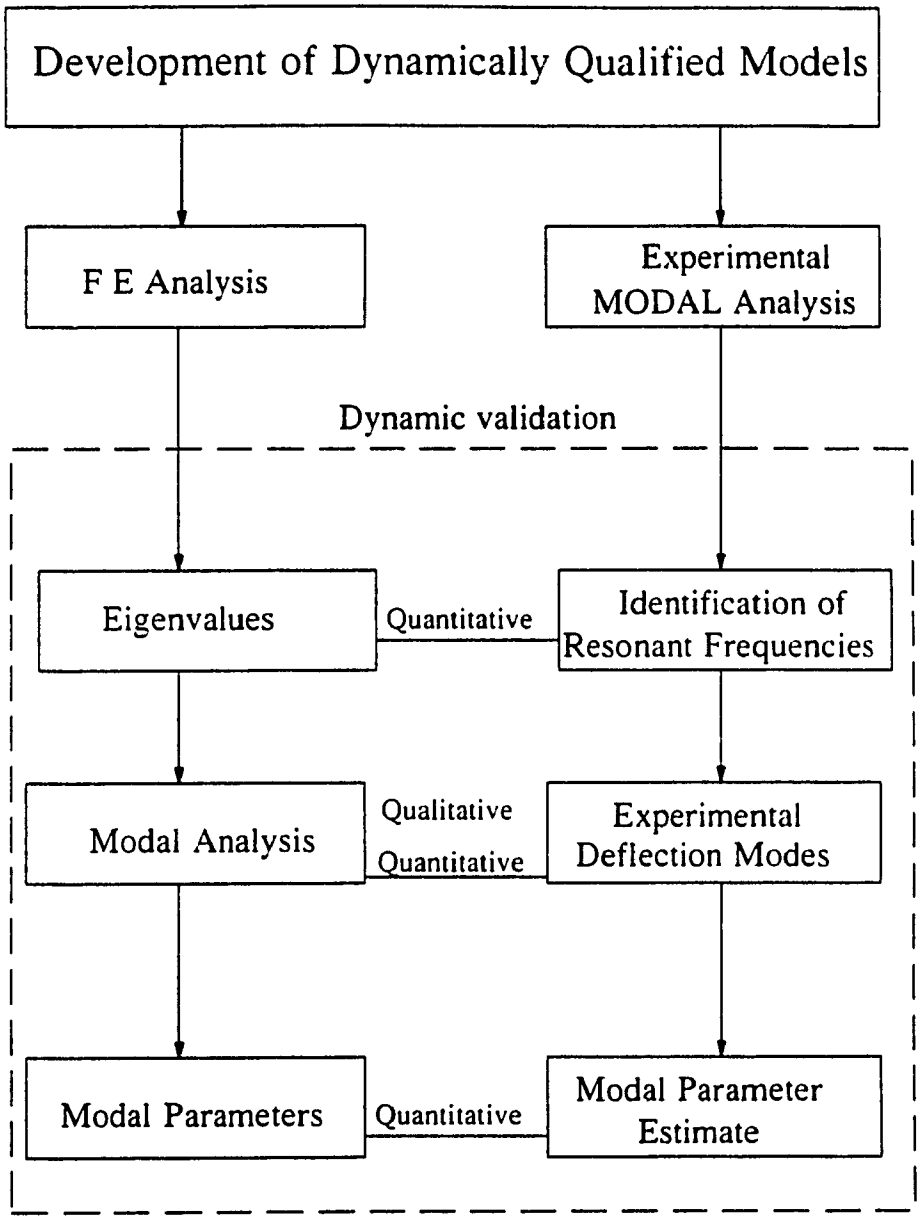


Figure 4.13: Methods to validate the structural models [50].

configuration of the trailer (trailer-B) is described in Chapter 2, where the front axle of the semitrailer axle group is liftable. The experiments were performed on the unloaded semitrailer without pickets, while coupled with a three-axle tractor. The tests were carried out in two stages: (i) with the semitrailer liftable axle up; and (ii)with lift- axle down. The location of accelerometers is presented in Figure 4.14 and Table 4.10

The semitrailer was excited using a servo-hydraulic shaker with pseudo-random signal generator in the frequency range 0-25 Hz. An Aries TRD-1000 force transducer of load capacity 1000 kgf, was mounted between the shaker and the structure, to measure the excitation force. Two accelerometers of PCB make (model 308B) and signal conditioners were used to monitor the vertical and lateral acceleration response of the structure at different locations. A Bruel and Kjaer 2032 dual signal analyzer was used to analyze the frequency response spectrum at different nodes from the measured force and acceleration. The frequency response which is a function of excitation frequency is defined as the ratio of output acceleration over the input force is expressed as :

$$H_1(\omega) = \frac{G_{FX}(\omega)}{G_{FF}(\omega)}$$

where $G_{FX}$ is the cross spectrum of the acceleration response and force, and $G_{FF}$is is the auto spectrum of the force. The modal analysis was carried out on a HP-9000 workstation with the *SMS 3.0 Structural Analysis Software* [49]. The modal parameters in terms of modal frequency, mode shape and modal damping were extracted. The modal frequencies and associated deflection modes of the trailer with lift-axle up are compared with those derived from the substructure solution to demonstrate the validity of the analysis method.

Table 4.10: Geometry of the Measurement Nodes of Trailer used in Experimental Modal Analysis

| Position | X location (m) | Y location (m) | Z location (m) | Position | X location (m) | Y location (m) | Z location (m) |
|---|---|---|---|---|---|---|---|
| #1 | 0.0 | 0.0 | 0.0 | #11 | 0.0 | 0.8 | 0.0 |
| #2 | 3.2 | 0.0 | 0.0 | #12 | 3.2 | 0.8 | 0.0 |
| #3 | 6.58 | 0.0 | 0.0 | #13 | 6.58 | 0.8 | -0.6 |
| #4 | 9.96 | 0.0 | 0.0 | #14 | 9.96 | 0.8 | -0.6 |
| #5 | 14.58 | 0.0 | 0.0 | #15 | 14.58 | 0.8 | -0.6 |
| #6 | 14.58 | 2.44 | 0.0 | #16 | 0.0 | 1.64 | 0.0 |
| #7 | 9.96 | 2.44 | 0.0 | #17 | 3.2 | 1.64 | 0.0 |
| #8 | 6.58 | 2.44 | 0.0 | #18 | 6.58 | 1.64 | -0.6 |
| #9 | 3.2 | 2.44 | 0.0 | #19 | 9.96 | 1.64 | -0.6 |
| #10 | 0.0 | 2.44 | 0.0 | #20 | 14.58 | 1.65 | -0.6 |

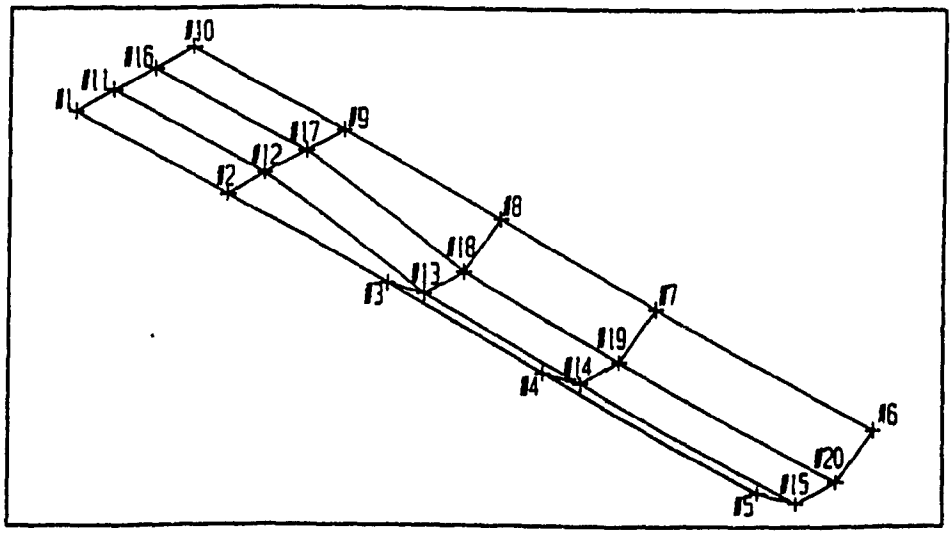


Figure 4.14: A schematic of the experimental modal analysis model highlighting the measurement nodes.

## 4.3 RESULTS AND DISCUSSION

The typical response of the structure as measured and analyzed in terms of the frequency response function is presented in Figure 4.15 together with the schematic of the undeformed structure. The results of the modal analysis revealed the trailer bounce mode near 2.72 Hz, as shown in Figure 4.16. The deflection mode reveals trailer bounce towards the trailing edge, which can be attributed to the suspension and tires. The leading edge of the trailer exhibits only small deflection due to the highly rigid king-pin articulation. Although the model yields an eigenfrequency neat 3.25 Hz, the corresponding deflection mode is rigid body bounce attributed to the flexible king-pin support. The differences in the deflection mode may thus be related to the two different king-pin supports used in the analytical and experimental studies. Figure 4.17 demonstrates the experimental roll mode of the trailer near 4.52 Hz, which correlates with analytical solution shown in Figure 4.9. The discrepancies in the frequencies, in general, may be attributed to rigid king-pin support, axle suspension, tires, lift-axle, the coarse modal model (20 nodes, with 3 DOF each) of the trailer, and additional exciter mass attached to the trailer.

## 4.4 Numerical Efficiency

The numerical efficiency can be compared in terms of the matrix operations, computation of stiffness matrices for a new design associated with new variables, and the decomposition of matrices of partitions. The EFETM analysis, involves mostly matrix multiplication of intermediate field matrices and station vectors and one final matrix decomposition performed on a smaller sized matrix.

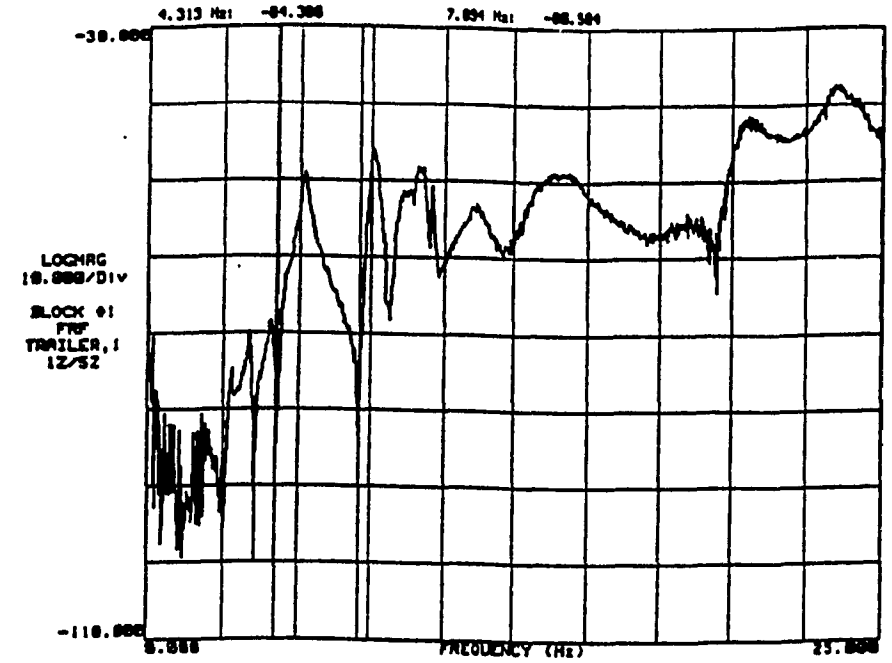


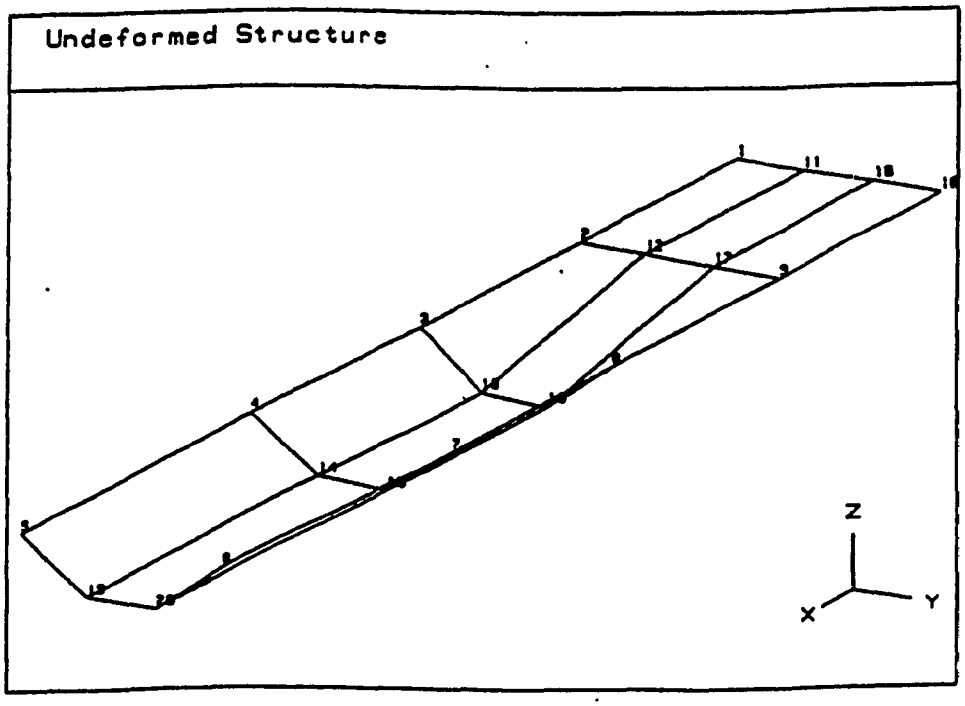


Figure 4.15: Schematic of the undeformed structure and a sample frequency response function measured at node 1.

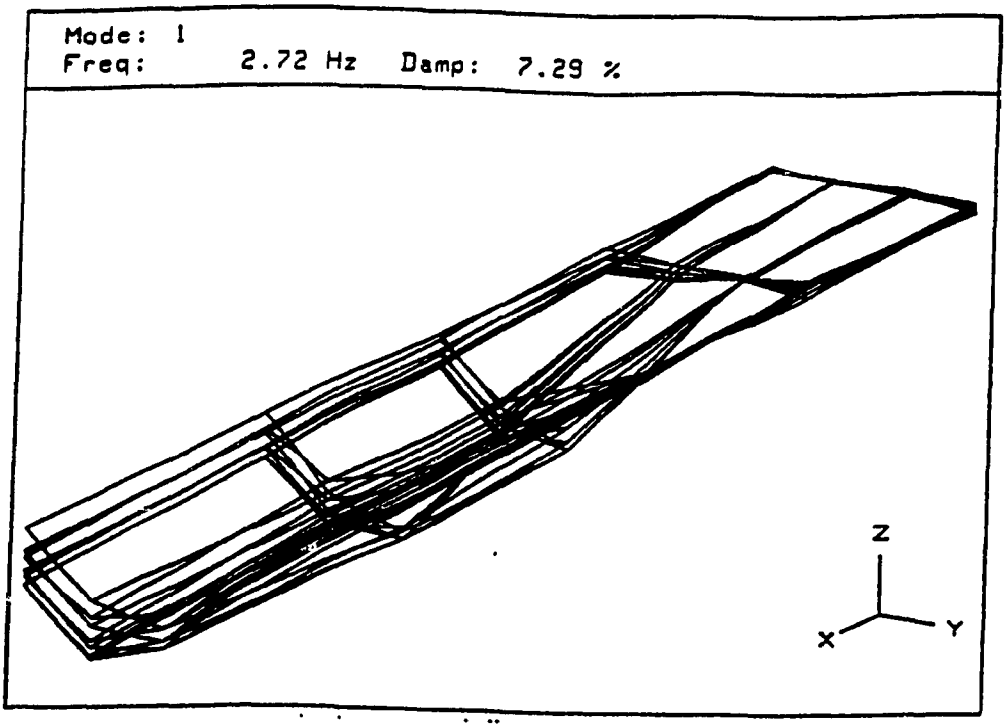


Figure 4.16: Experimental bounce mode of the trailer structure (2.72 Hz).

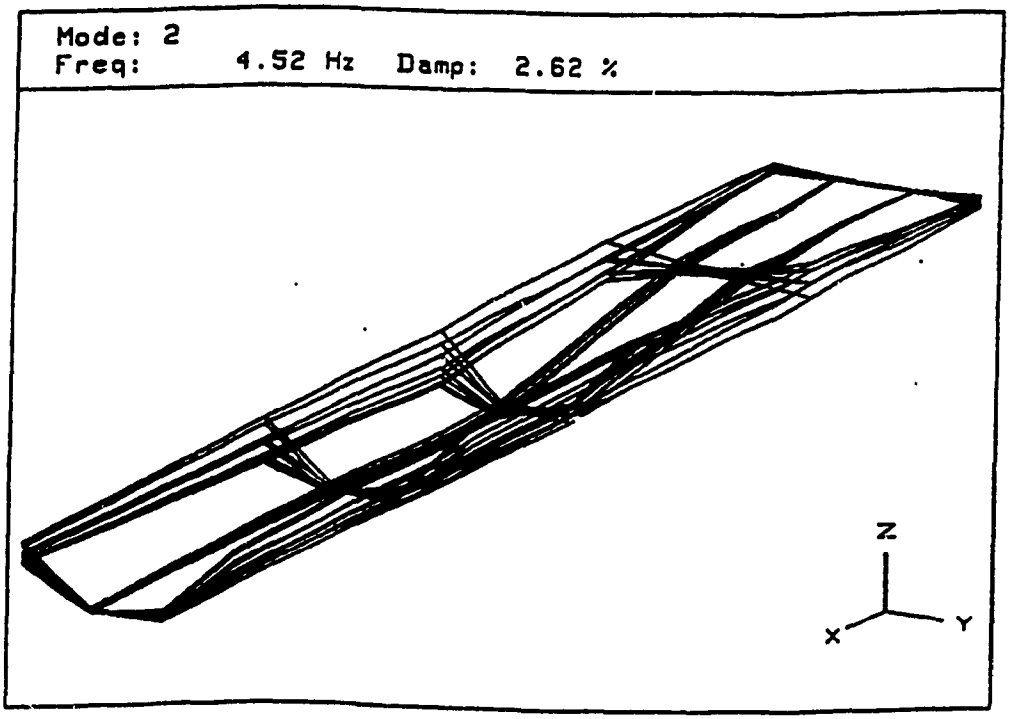


Figure 4.17: Experimental roll mode of the trailer structure (4.52 Hz).

Here the inversion of the matrix is done for a much smaller size, using Cholesky's decomposition. In case of reanalysed solution the basic matrix size is only increased by 2 in order to accommodate the design derivatives. Whereas, in case of the conventional method the decomposition is sought for the entire matrix, which is N times ( N= number of substructures). Table 4.11 summarizes the execution time required for analysis of benchmark and trailer structures by different methods using a 486 DX 33 PC. In the present analysis, the time for direct computation and reanalysis solution performed on trailer A, resulted in a saving of 70% time for reanalysed solutions.

**Table 4.11: Comparison of Numerical Efficiency.**

| | | Execution Time (80486 DX 33 Hz PC) | | | |
|---|---|---|---|---|---|
| Structure | Problem Size | FETM Analysis | EFETM Reanalysis | Potters' Analysis | Potters' Reanalysis |
| Ten bar Cantilever | 12 x 12 | 5 s | 5 s | -- | -- |
| Space Truss | 96 x 96 | 70 s | 40 s | -- | -- |
| TRAILER-A | 810 x 810 | 170 s | 50 s | 220 sec | 90 s |
| TRAILER-B | 936 x 936 | -- | -- | 240 sec | -- |

## 4.5 Summary

The analysis methods based upon EFETM and substructure techniques are thoroughly validated through analysis of bench mark structures and a trailer structure. Substructure technique in conjunction with Potters' method of solution utilizing Cholesky's decomposition method is validated for static and dynamic analyses of large structures and bench mark structures. The design sensitivity analysis is carried out for design changes in the structure and reanalysis solution are compared with the direct solutions to demonstrate the numerical efficiency and validity of the reanalysis algorithm. The reanalysis solution revealed good agreement with the direct solution, while the associated execution time was reduced by 70%.

# CHAPTER 5

# STATIC RESPONSE AND REANALYSIS OF CANDIDATE TRAILERS

## 5.1 Introduction

Static response of the structure is an essential part of structural analysis for evaluation of deflection and stresses throughout the structure for a given design configuration and prescribed load. Such analysis also aid in configuring the structure in terms of shape, size and properties of the members to effectively resist a prescribed system of forces. The process of seeking an efficient design, therefore, requires numerous reanalyses. In this investigation analytical technique based upon substructure analysis and FETM are used to derive the design sensitivity vectors from base design solution. The analytical methods, presented in Chapter 3, and validated in Chapter 4 are applied to evaluate static response of the candidate trailer structures A and B described in Chapter 2. Reanalysis methods are applied to study the influence of design changes in the section modulus of the main beams, the primary load bearing members, to derive an efficient design with reduced structural weight.

The static analysis of trailer A is performed using both methods. Influence of variations in the section modulus of the main-beams on the static response behavior is derived using EFETM reanalysis algorithm. The effectiveness of the reanalysis method is demonstrated by comparing the response characteristics in terms of bending displacement and stress distribution on those derived from direct

computation using FETM. The reanalysis method based upon Potters' solution is applied to investigate the influence of variations in design parameters of main-beam on the static response behavior of the trailer A. Reanalysis solutions are also obtained for various design perturbations in the design variables the main-beam sections. A limited parametric study is also performed to investigate the influence of variations in design parameters of main and side beams of trailer-B on the static response characteristics and corresponding weight reductions.

## 5.2 Reanalysis of Candidate Trailer Structure Using EFETM

The reanalysis algorithm based upon EFETM is applied to determine the static response behavior of the candidate trailer A and its sensitivity to variations in different design variables. The geometry, configuration and the base line parameters of this candidate trailer have been described in Figure 2.2 and Table 2.3. The trailer is a flat-bed 9.29 m x 2.44 m structure of ladder-type configuration comprising two main-beams of I cross-section and two side-beams of C cross-section. A total of 31 cross beams of I cross-sections are used to join the two main-and side-beams, as illustrated in Figure 5.1. The trailer structure is supported on a leaf-spring tandem axle suspension. The king pin reaction loads and the tandem-axle suspension is represented by four linear springs located towards the rear section of the trailer as illustrated earlier in Figure 3.4. The trailer is designed to carry a load not exceeding 250kN. The cargo loading is assumed to be distributed uniformly along the length of the trailer. The contributions due to the weight of the structure and those of other auxiliaries, such as suspension springs, the torque rods and linkages are considered to be negligible when compared to the cargo load. The tare weight of this trailer structure is approximately 19.0 kN. The suspension and king-pin reaction forces, and the spring rates are computed from

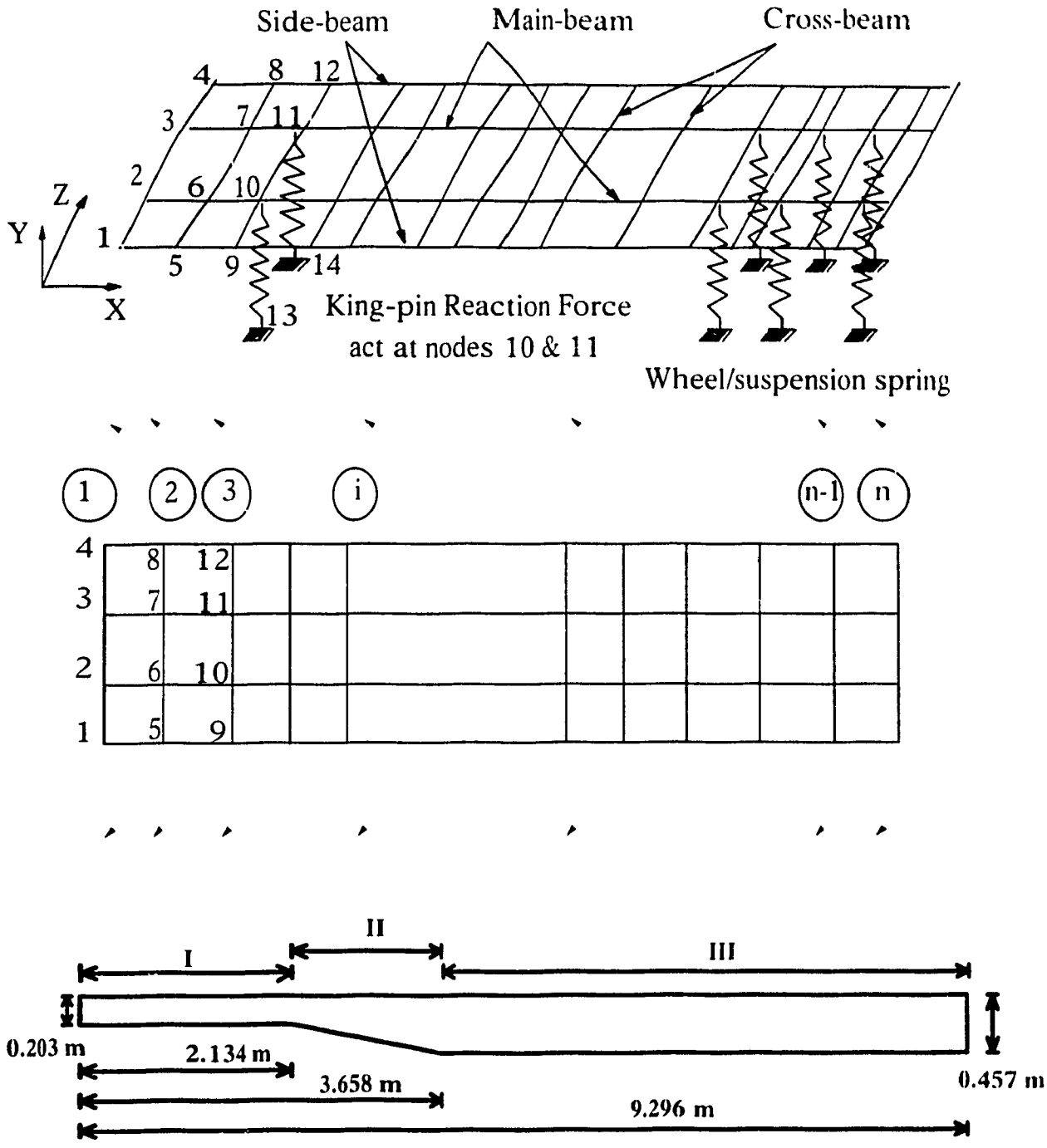


Figure 5.1: A substructure model of candidate trailer A.

the static force and deflection equilibrium. The suspension reaction loads are derived from the rated axle loads in the following manner:

$$W_{sus} = W_{axle} - W_u \tag{5.1}$$

where $W_{sus}$ is the suspension reaction force, $W_{axle}$ is the rated axle load, and $W_u$ is the unsprung weight due to axle, wheel and the tire assembly. The king pin reaction force distributed equally between the two linear springs is then derived from

$$W_k = 0.5\left[W_c - 2(W_{axle} - W_u)\right] \tag{5.2}$$

where $W_k$ is the reaction force due to each king-pin spring and $W_c$ is the total cargo load. The suspension spring rate is selected close to 1340 kN/m (7500 lb/in.) from the published data [52], to represent the equivalent linear spring rate of typical leaf spring suspension. To conform to the legal regulation of not to load the axles beyond permissible limits and to ensure uniform level of the trailer bed in the X-Y plane corresponding to static equilibrium:

$$K_k = \frac{0.5\,W_c - W_{axle} + W_u}{W_{axle} - W_u} * K_s \tag{5.3}$$

where $K_s$ and $K_k$ are the linear rates of axle suspension and king-pin reaction springs. The trailer is represented analytically, as described in Chapter 3, by 29 sub-elements. Each sub-element is represented by 8 nodes and two stations at its left and right ends. Each node posses 3 DOF motion and is described by a (24 x 1)

behavioral vector, comprising 3 displacements (vertical displacement in Z axis, 2 rotations about the X-Y plane $\theta_x$ and $\theta_y$ and 3 forces (vertical force $F_z$ and moments about X - Y plane $M_x$ and $M_y$) associated with each node. Each station have 6 behavioral vectors, representing 3 displacements (one vertical displacement in the Z axis, and two inplane rotations in the X-Y plane to account for flexural and twisting behavior of the trailer bed) and 3 force vectors representing the vertical force and inplane moments, designated by:

$\left\{\frac{U}{F}\right\} = \{w, \theta_x, \theta_z, \mid F_z, M_x, M_y\}$. The station vector is extended to include the derivatives of the behavioral vector with respect to any design variable 'd' resulting in (48 x 1) extended station vector, $\left\{U \quad F \quad \frac{\partial U}{\partial d} \quad \frac{\partial F}{\partial d}\right\}$ where " ' " designates the transpose. The cargo trailers are, invariably, designed such that the main-beams serve as the primary load bearing members. The main-beams thus, the primary contributor to the total weight. A design variation associated with the main-beam will yield the most pronounced influence on the structural behavior and its weight. It is desirable to realize a trailer design with adequate structural integrity and minimal tare weight. A parametric study is thus performed to investigate the influence of variations in the main-beam design parameters on the behavior vectors and the corresponding trailer weight. The reanalysis algorithm can be effectively applied to carry out the parametric study in a highly efficient manner. EFETM method is applied to obtain reanalysis solution for changes in the main beam dimensions, resulting in variations in the effective modulus of the cross-section of the main beam. The schematics of the basic trailer structure, and the main beam with three distinct segments is illustrated in Figure 5.1. The reanalysis solutions are derived for following modifications of the main beam,

while the geometric configuration and the other parameters are held same as the base structure:

(i) A reduction in section modulus of segment III of the main beam: A 35% reduction in the overall modulus of rigidity is achieved by reducing the web height, H, from the base line value of 0.4572 m(18 in) to 0.381 m (15 in).

(ii) A reduction in section modulus of segment II of the main beam: A 35% reduction in overall value of modulus of rigidity is realized by reducing the web height, H, by .05 m on the taper segment.

(iii) A reduction in section modulus of segment I of the main beam: A 35% This is upto 35% reduction in overall value of modulus of rigidity is realized by due to reducing the web height, H, from the base line value of 0.1524 m (8 in) to 0.1270 m (5 in).

For carrying out the reanalysis solution, the sensitivity vectors of behavior performance with respect to changes in design variables are computed as change in reciprocal of section modulus to change in deformations. This approach is found to yield a better measure of the change in structural stiffness than that predicted by a derivative of the change in the modulus.

### 5.2.1 Discussion of Results

The reanalysis solutions for the above case studies have been carried out for the normal loading conditions and the results are presented in Figures 5.2 to 5.9. The dominant characteristics of the trailer are characterized by the vertical deflection and the flexural stress levels distributed along the length of the trailer. The base design of the trailer is first analyzed using FETM and the static response characteristics in terms of vertical deflection and bending stress distribution of the main- and side- beams are illustrated in Figures 5.2 and 5.3, respectively. The

vertical displacements in mm and the flexural stresses in MPa are represented along the length of the trailer. In the base design configuration, the main- and side- beams exhibit maximum vertical deflections 48.5 mm and 51.0 mm, respectively. The peak deflections occur near the mid-span between the king-pin and suspension supports, at a distance of 3.2m from the leading edge of the trailer. The maximum deflection point however, is not exactly the centre of the king pin and first wheel set axis, as can be expected in a beam of uniform section modulus. The peak deflection occurs closer to the king-pin support due to relative low section modulus of the main beam segments I and II. Figure 5.3 represents the flexural stress distribution along the main- and side- beams of the trailer A. The results show that the main-beam experiences considerably larger stress than the side-beam, which is attributed to the concentration of the uniformly distributed cargo load on the nodes, located at the main-beam. The two-beams, however, exhibit similar trends in view of the distribution of the stress. The peak stress values occurring along the main- and side- beams are 82 and 59 MPa, respectively. The maximum stress occurs at the beginning of tapering section segment II, frequently referred to as *goose neck* at a distance of 2.134 m from the leading edge.

The flexural stress of the main-beam tends to increase nearly linearly with X-axis, starting from the leading edge. The stress value grows rapidly in the low modulus segment I, specifically after the king-pin support, when the magnitude of the moments become dominant. The main-beam stress approaches a peak value near the goose neck, beyond which it tends to decrease along the X-axis. The stress value approaches the lowest corresponding to the peak deflection point and then starts to increase slightly. A second peak (magnitude- 71MPa) is observed near X = 5m. A trailer structure with uniform cross-section main-beam may yield

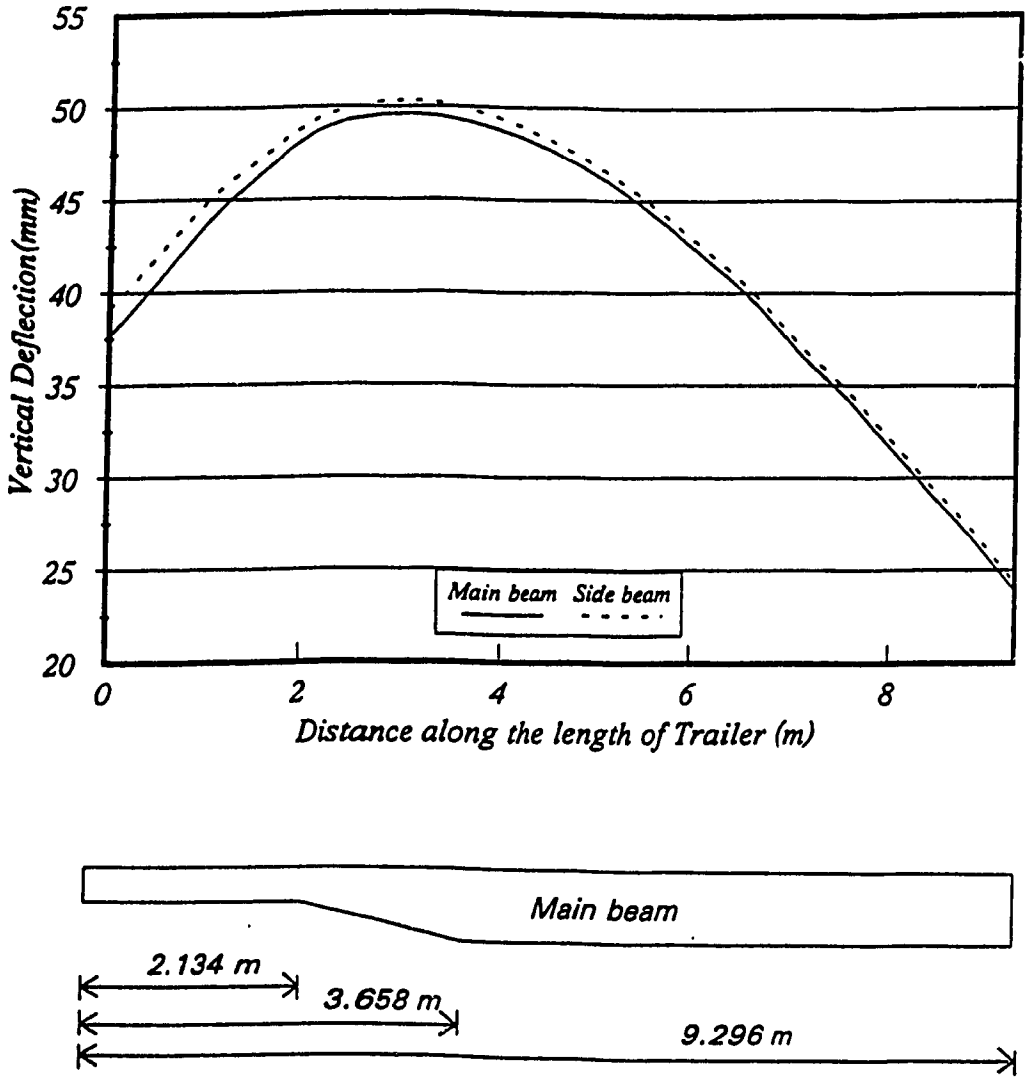


Figure 5.2: Static deflection response of the main- and side-beam trailer A.

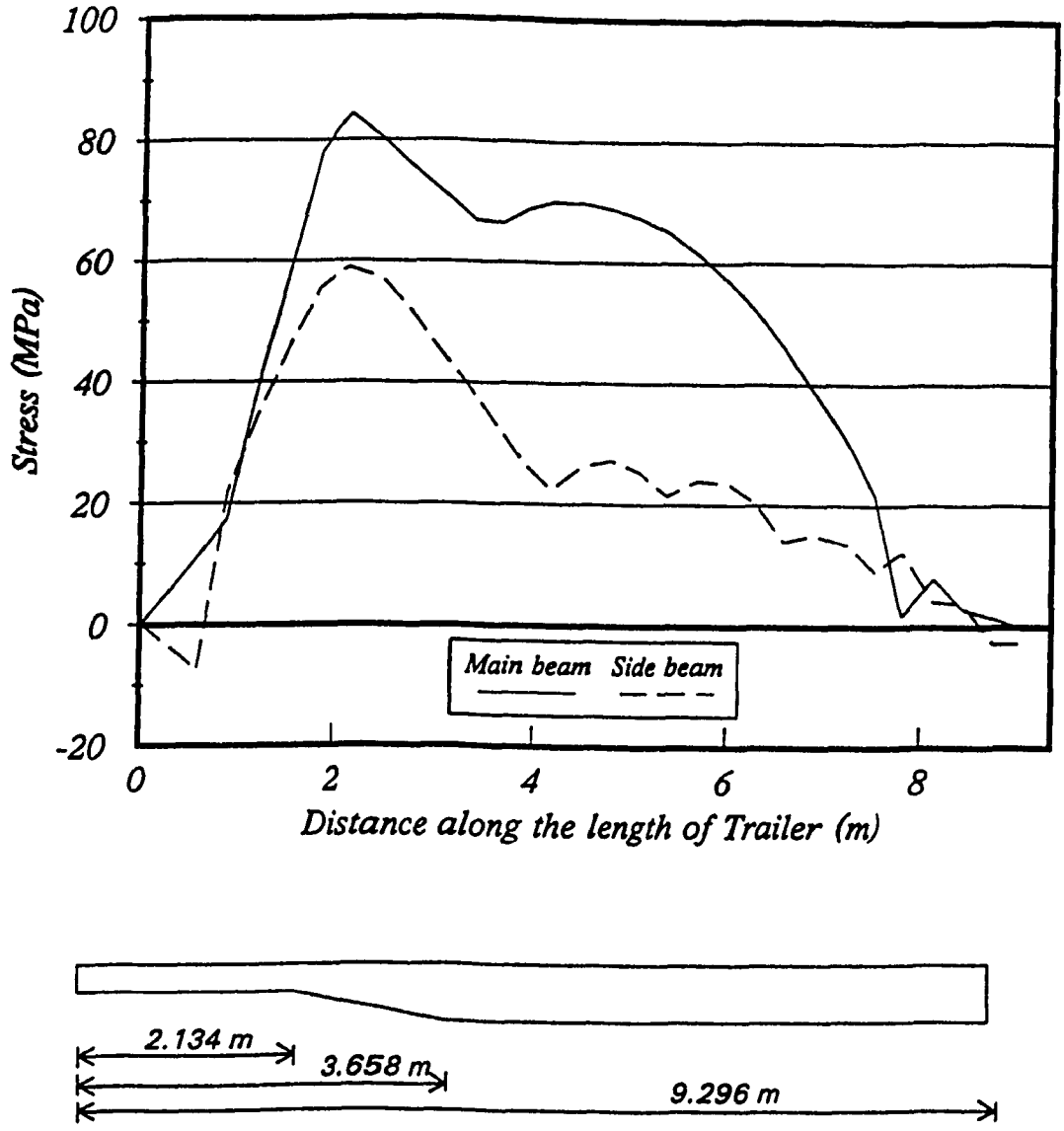


Figure 5.3: Stress response of the main- and side-beam trailer A.

the peak stress in the vicinity of X = 5m. A comparison of response characteristics of the main- and side- beams reveals that the side beam experiences slightly larger deformation and considerably lower stresses. The flexural stresses of both the beams gradually diminishes near the suspension supports and the trailing edge of the trailer as shown in the Figure. The reduction in the stress levels in the vicinity of suspension supports is attributed to four additional stiffeners connecting the main- and side- beams at prescribed intervals, as described earlier in Figure 2.3.

The influence of variations in the overall section modulus of the main-beam on the static response behavior is investigated using EFETM reanalysis algorithm. The results derived from the reanalysis solution are compared with those established from FETM direct computation to illustrate the accuracy and efficiency of the reanalysis algorithm. Figures 5.4 and 5.5 illustrate the deflection and stress distribution of the main- and side- beams, derived from the reanalysis solution of the trailer structure, when the segment III of the main-beam is modified to yield 35% reduction in the overall modulus of rigidity. The response characteristics established through direct computation are also presented in the same Figures. As may be expected, the overall response has changed to higher values in the stresses and deflections caused by the reduction in the section modulus. A comparison of the response behavior with that of the base design (Figure 5.2 and 5.3) clearly illustrate an increase in stresses and deflection caused by the reduction in section modulus. The patterns of the defection and stress distribution along the main- and side- beams however, are observed to be similar to those of the base design. The peak deflections and stresses of both beams of the modified structure occur at similar locations observed for the base design. The magnitudes of peak response, however, differ considerably from the base design. The peak flexural stresses of the main-beam occurring near the goose neck increases from 82 MPa to 102 MPa.

when the structure is modified. The corresponding peak stress near the suspension support increases from 71 MPa to 88 MPa. The peak deflection response of the main-beam of the modified structure is observed to be 52.5 mm, while that of the base design was 51 mm. A comparison of the response behaviors of the modified structure, derived from EFETM reanalysis and FETM analysis, reveals only slight differences, as shown in the Figures. The analysis and reanalysis methods yield peak stresses of main -beam as 102 and 98 MPa, respectively. The corresponding values for the side--beams are 60 MPa and 58 MPa. The two methods exhibit identical patterns of deflection and stress response, the reanalysis tends to provide a slight overestimate of the stress throughout the length of the beams. The peak error, however, is nearly 4%. The peak deflection response of the main - and side- beams also increase from 48.5 to 51 mm and 51.0 to 52.0 mm, respectively, when design modification is made. The reanalysis method provides an overestimate of deflection 2.5 to 3%.

Figures 5.6 and 5.7 illustrate the response behavior of the modified structure with 35% of the section modulus of segment II of the main-beam (modification-ii). The values of flexural stresses and vertical deflections are computed directly (FETM) and using EFETM. The deflection and stress distribution patterns of both the beams are again similar to those of the base design. The deflection levels however, are slightly higher than those of the base design, but smaller than those obtained corresponding to modification-i., where the section modulus of longer segment III was changed. The two methods of analysis (FETM) and reanalysis (EFETM) yield nearly identical deflection response as shown in Figure 5.6. The maximum deflection for the main- and side- beams are 51 mm and 52 mm, respectively. The peak stresses encountered by the main- and side- beams, however, are considerably larger than those of the base design. The

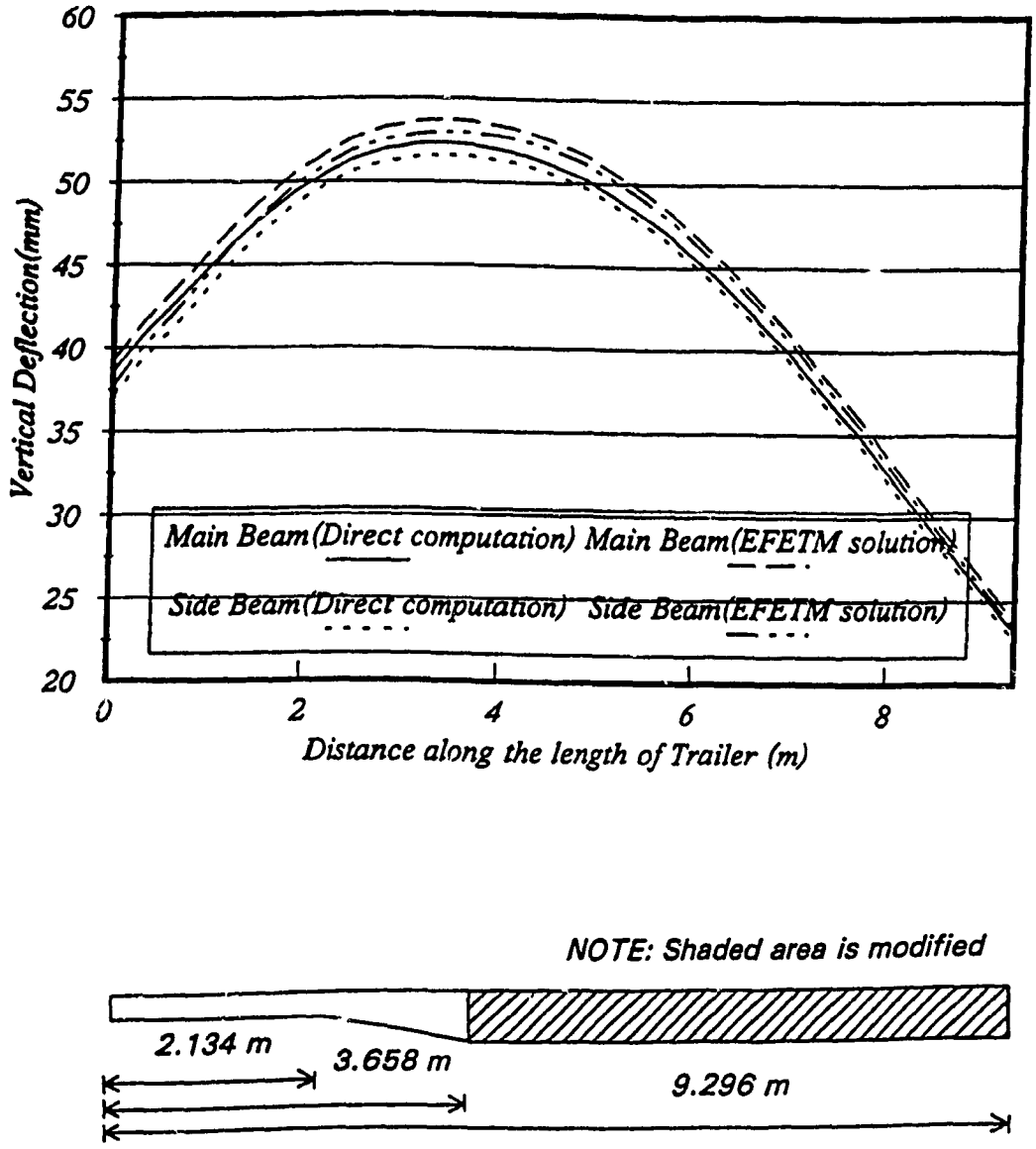


Figure 5.4: Static deflection response of the main- and side-beam derived from the reanalysis solution (35% reduction in section modulus of segment III).

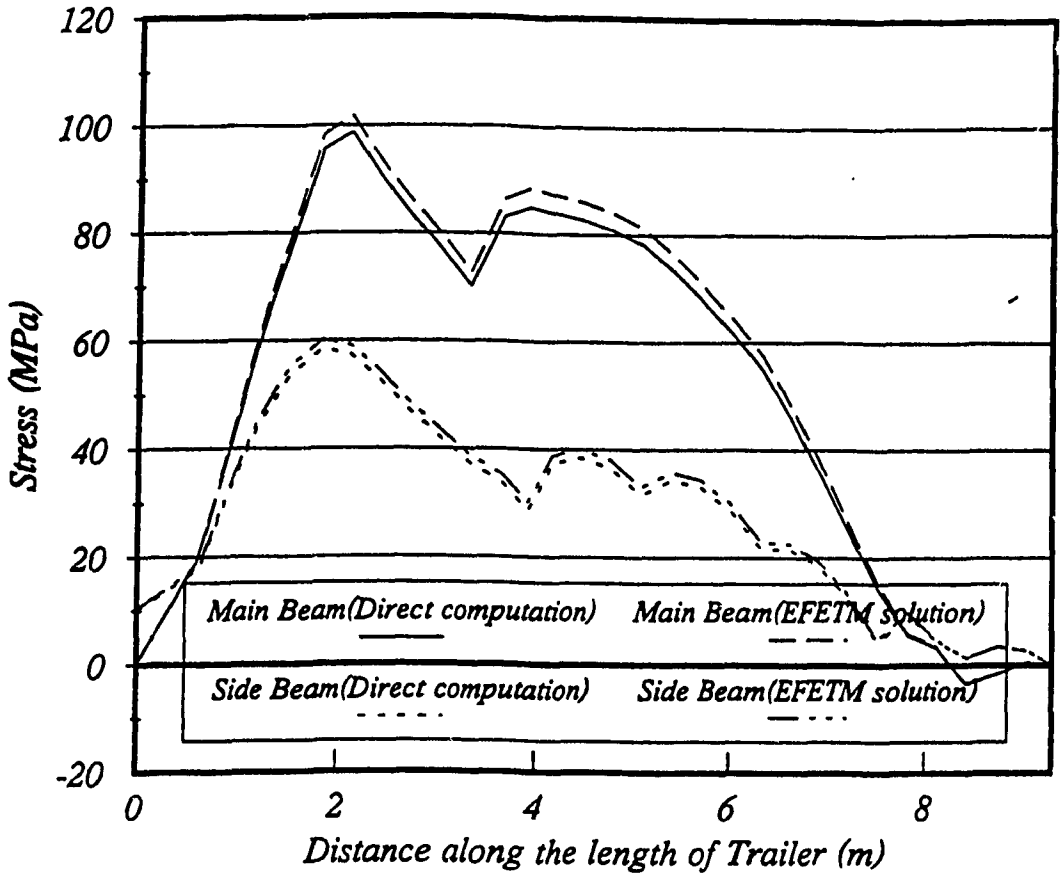


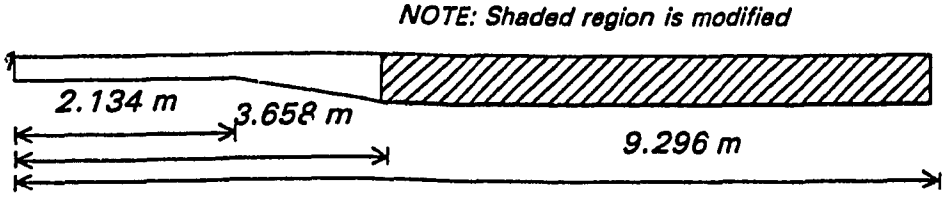


Figure 5.5: Stress response of the main- and side-beam derived from the reanalysis solution (35% reduction in section modulus of segment III).

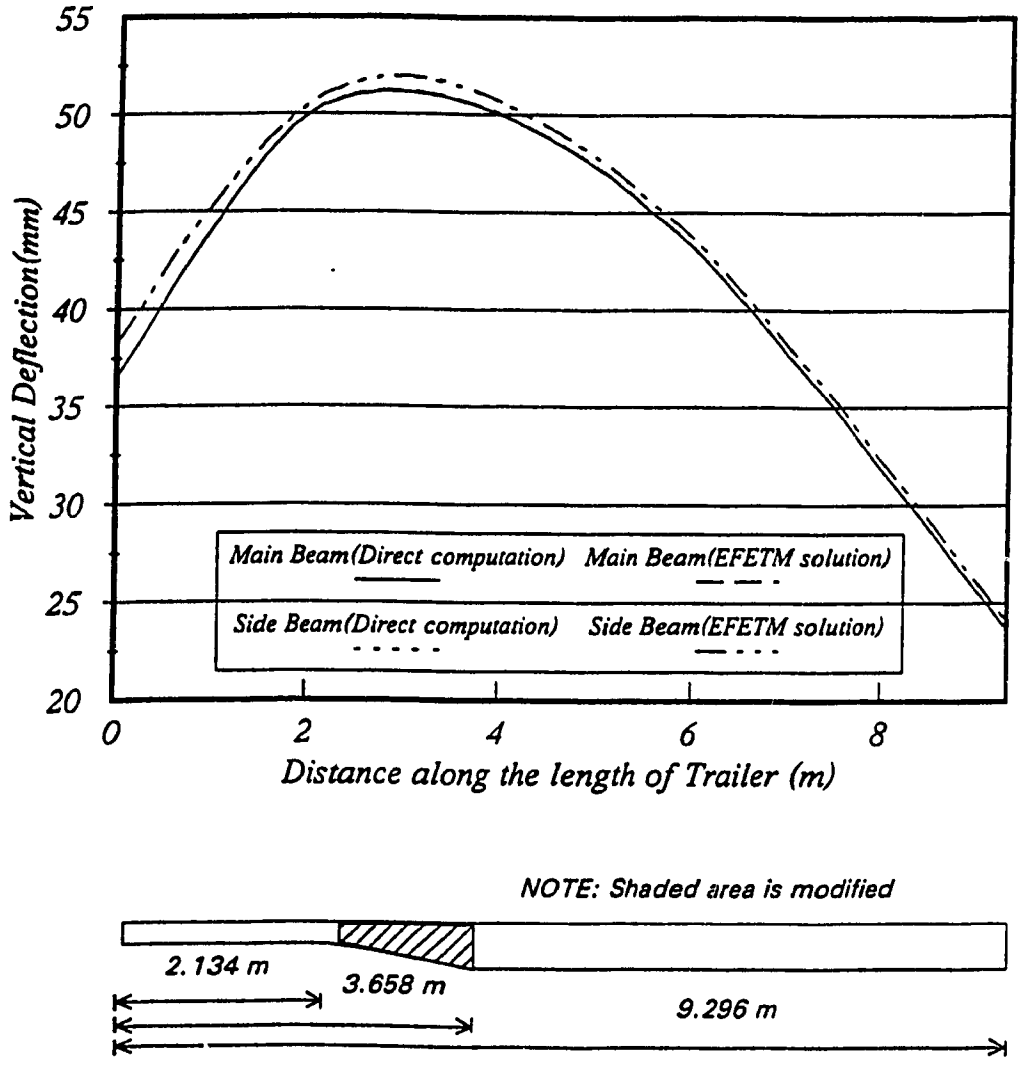


Figure 5.6: Static deflection response of the main- and side-beam derived from the reanalysis solution (35% reduction in section modulus of segment II).

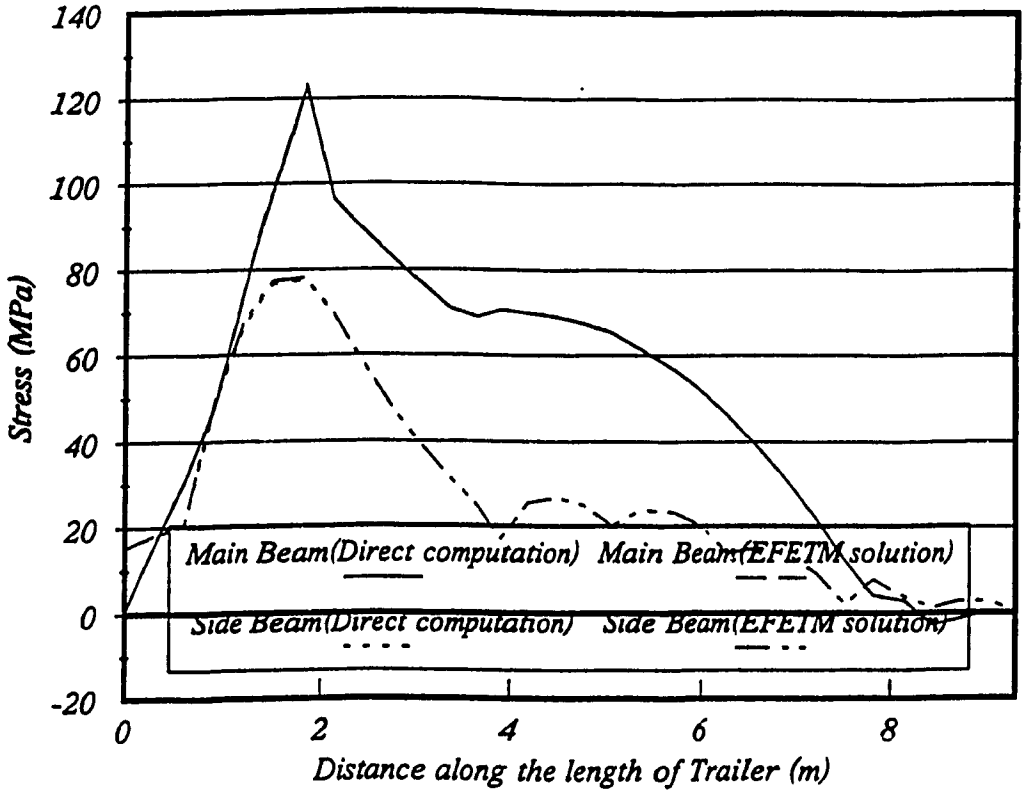


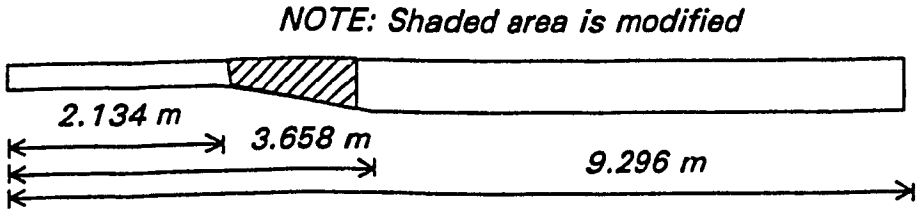


Figure 5.7: Stress response of the main- and side-beam derived from the reanalysis solution (35% reduction in section modulus of segment II).

maximum flexural stress of the main beam is 122 MPa and that for the side beam is 78 MPa (base design values are 82 MPa and 58 MPa respectively). This considerable increase in the peak stress is attributed to the significant reduction in segment II modulus. The method of reanalysis yields results almost identical to those derived from direct computation.

A very similar behavior is observed for the design modification (iii) carried out on the segment I of the main-beam as shown in Figures 5.8 and 5.9. The design modification involving 35% reduction in modulus of rigidity of segment I has slightly larger deflection and stress response, when compared to those of the base design. The deflection and flexural stress distribution of the two beams, presented in Figures, further reveal the accuracy of the reanalysis solution. The maximum flexural stresses obtained for main- and side- beams are 110 MPa and 65 MPa, respectively, and corresponding peak vertical deflections are 50.5 mm and 51.5 mm. The weight reduction realized by the three modifications are also computed and summarized in Table 5.1 together with the peak stress and deflection response.

The static response characteristics of the base and modified design of trailer A, presented in Figures 5.2 to 5.9, clearly demonstrate the accuracy of the reanalysis solution. The reanalysis method further yields significant enhancement of computing efficiency, attributed to the following:

(i) While carrying out the design modifications, since it was already known that segments, I, II, and III of the main beam will be subjected to modification, the elements of the extended transfer matrices are computed and stored for each subelement during the initial computation of the

element submatrices as discussed in the algorithm (step -b ), in previous section 3.8.

(ii) The above results in a considerable savings in terms of computation time, since the reanalysis solution only requires is sensitivity vectors, which are readily computed during the first iteration of solution.

(iii) The reanalysis solution for a design change in the segment III of the main-beam required an execution time of 50 s on an IBM 486 DX 33 PC, while the direct solution based upon FETM necessitated 170 s execution time. The reanalysis algorithm thus enhances the numerical efficiency by 70%. The numerical efficiency can be further enhanced, when the modifications are performed on relatively smaller segments (fewer sub-elements) of the base design.

**Table 5.1: Summary of Design Modification and Peak Stress and Deflection Response**

| Design | Peak stress (MPa) | Peak deflection (mm) | Weight (Kg) | Weight Reduction % |
|---|---|---|---|---|
| Base | 82 | 48.5 | 1977 | - |
| Modification in segment I | 110 | 51.5 | 1800 | 9 |
| Modification in segment II | 122 | 51 | 1890 | 4 |
| Modification in segment III | 102 | 52.5 | 1682 | 15 |

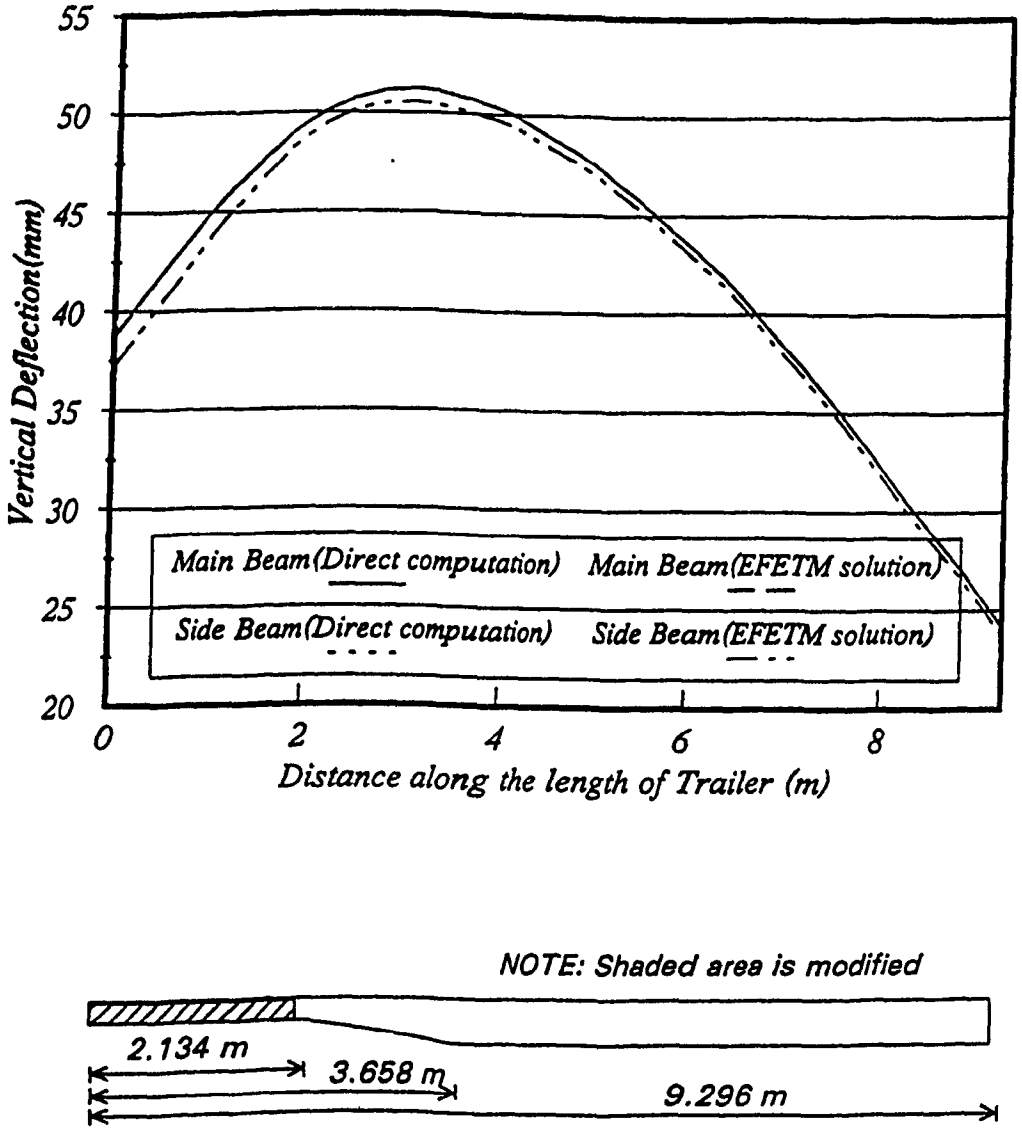


Figure 5.8: Static deflection response of the main- and side- beam derived from the reanalysis solution (35% reduction in section modulus of segment I).

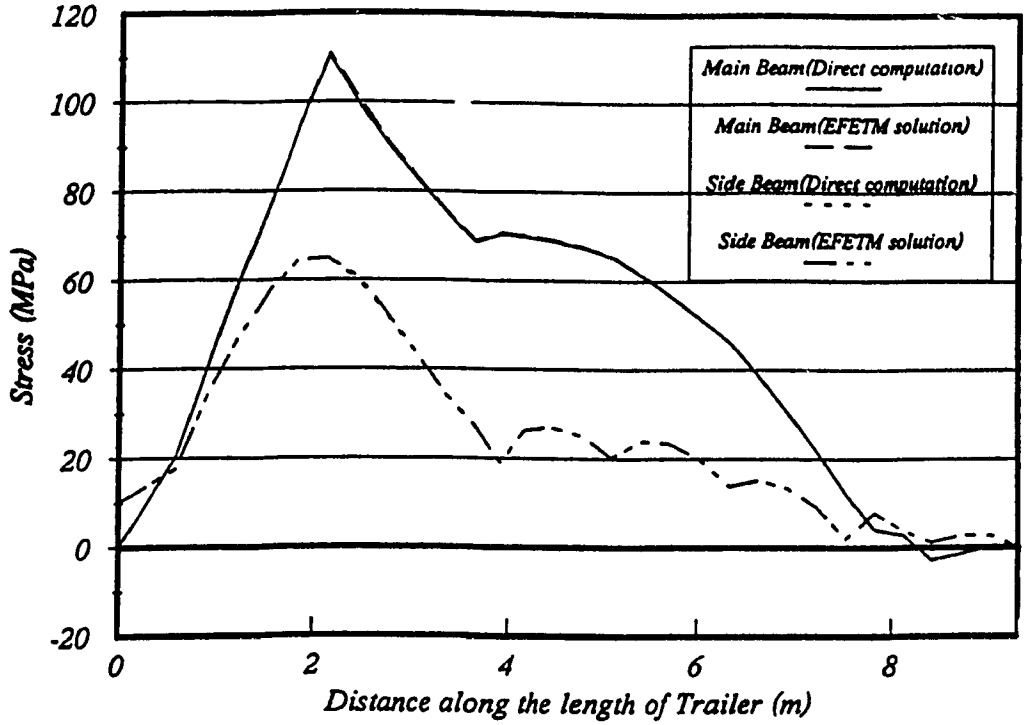


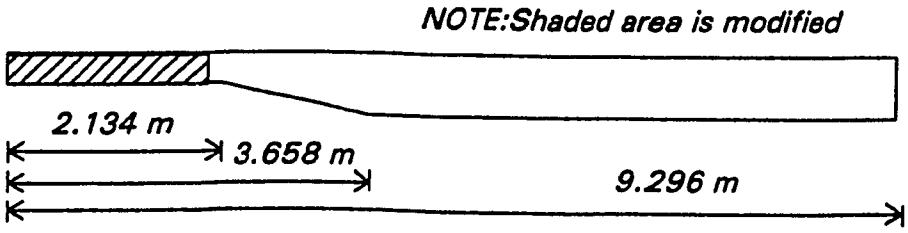


Figure 5.9: Stress response of the main- and side-beam derived from the reanalysis solution (35% reduction in section modulus of segment I).

## 5.3 Reanalysis of Candidate Trailer Structures by Potters' method

Potters' method of analysis and reanalysis, discussed in section 3.2 is used to determine the static response behavior of several design options of the candidate trailers A and B. Trailers A and B are analytically modeled using substructure analysis described in section 3.4. The configuration, details of substructuring, type of finite elements, number of elements, total nodes, payload on the structure and operating conditions are summarized in Table 5.2. Two distinct cases of loading simulations are considered for relative performance evaluation of both the trailers:

(i) Normal load condition.

(ii) Maximum twist load condition.

The twist load condition represents the loads caused by excessive lateral load transfer encountered during highway speed directional maneuver or wheel lift-off. The response analysis under such loading condition can provide a measure of the torsional and flexural integrity of the trailer structure subject to extreme lateral load transfers encountered in motion. The twist load in this study was realized by eliminating the suspension spring reactions being transmitted to one side of the trailer frame.

A design sensitivity analysis is initially performed for trailer A to investigate the influence of primary design variables associated with the main-beam. The segment of the main beam starting at the end of the tapered beam and until the first wheel-set from the leading edge, as shown in Figure 5.10, is considered for design modification and design sensitivity study. The following design variables that affect the mass and stiffness properties of the structure, and the behavioral vectors are considered for the analysis: (i) H- web height

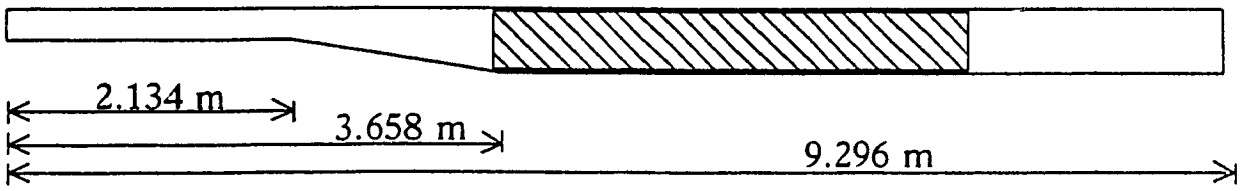


Note: Hatched area is design modified

Figure 5.10: Schematic of the segment of main-beam of trailer A considered for design sensitivity analysis.

(ii) B- flange width (iii) Tf- flange thickness (iv) Tw- web thickness. The influence of these design variables on the response characteristics of the trailer structure A is therefore investigated using reanalysis algorithm based upon Potters' method. The design values and the range of variations considered for the analysis are summarized in Table 5.2

**Table 5.2: Parameters Considered for Design sensitivity Analyses (Trailer A).**

| Design Variables | Base Design | Variation range |
|---|---|---|
| H | 457.2 mm (18 in) | 406.4mm- 508.0 mm (16 in- 20 in) |
| B | 127.0 mm (5 in) | 76.2 mm- 177.8 mm (3 in - 7 in) |
| Tf | 19.05 mm (0.75 in) | 12.7 mm- 25.4 mm (0.5 in - 1.0 in) |
| Tw | 4.7624mm (3/16 in) | 3.175 mm - 6.35 mm (1/8 in-1/4 in) |

Different analysis/reanalysis solutions are performed with design variables assuming the upper and lower values in the Table. Only one design parameter, however, is varied while the other variables are held as their baseline values. A limited parametric study is also carried out to evaluate the various design options for the trailer B using Potters' reanalysis method to evaluate the behavioral responses in terms of deflections and stresses achieved with the design perturbations around the base design, including the associated weight savings. Table 5.3 summarizes the design perturbations used in the case of the trailer B structure about the base design configuration.

**Table 5.3: Summary of Design Variations Analyzed for Trailer B.**

| Design | Structural Member | Design Variable | Base Design Value | Variation |
|---|---|---|---|---|
| Base design | - | - | - | - |
| Design 1 | 2 Main-beams | Tw | 12.70 mm | ± 6.35 mm |
| Design 2 | 2 Main-beams | Tf | 12.70 mm | ± 6.35 mm |
| Design 3 | 2 Side-beams | Tw | 10.16 mm | ± 4.25 mm |
| Design 4 | 2 Side-beams | Tf | 10.16 mm | ± 4.245 mm |
| Design 5 | 2 Main-beams | B | 127.0 mm | ±50.8 mm |

## 5.3.1 Results and Discussion

The candidate trailers are analyzed for both normal and twist load conditions and results are presented to assess the flexural and torsional response behavior of the structures. The response characteristics of the base design are initially discussed followed by the design sensitivity analysis.

### 5.3.1.1 RESPONSE TO NORMAL LOADING CONDITION

The reanalysis solutions for the above variations in the trailer structure design were carried out for normal and twist conditions. The results in terms of behavioral response, namely, deformations and stresses, are presented for both candidate trailers A and B. The results are obtained for various members of the structures such as the side-beams, main beams and cross beams. The response characteristics of the candidate trailers derived under different loading conditions are compared to highlight the influence of loading. Figure 5.11 and 5.12 represent

the vertical deflection and flexural stresses experienced by trailer-B (base-design), subject to a uniformly distributed normal static load of 350 kN. The deflection values of the side-and main-beams of both right and left sides are illustrated as function of the longitudinal coordinate-x as shown in Figure 5.11. The deflection pattern is observed to be symmetric under the symmetric normal load condition. The peak deflection of the main beam is nearly 58 mm and side beams exhibit only slightly higher deflection response. Both, th main- and side- beams, exhibit peak deflection at an identical location (x = 6mm) along the longitudinal axis, which lies approximately mid-way between the king-pin location and the first wheel-set axis. While the main- and side- beams of the trailer B design exhibit quite similar deflection response, the deflection response of the side-beam of trailer A is observed to be larger than that of the main-beam as shown in Figure 5.2. A comparison of deflection response of behavior of the two candidate trailers (Figures 5.2 and 5.11) reveals considerably larger deflection of trailer B. It should be noted that the trailer B is a tri-axle semi trailer with length significantly larger than the 2-axle trailer A.

The distribution of flexural stress of main- and side- beams of trailer B are illustrated in Figure 5.12 . The peak flexural stresses of the main- and side- beams of the base design are obtained as 98 MPa and 58 MPa, which occur at x = 6 m with reference to the leading edge of the trailer. The peak stresses occur at a location of the beams, which is nearly midway between the king-pin location and the first wheel-set from the left. The results also reveal occurrence of the peak stress near the beginning of the goose-neck region , with the peak value being 81 MPa and 42 MPa respectively. A comparison of stress distribution of main- and side- beams of trailers A (Figure 5.3) and B reveals considerable differences. The trailer B, with longer span between the king-pin and axle supports reveals peak

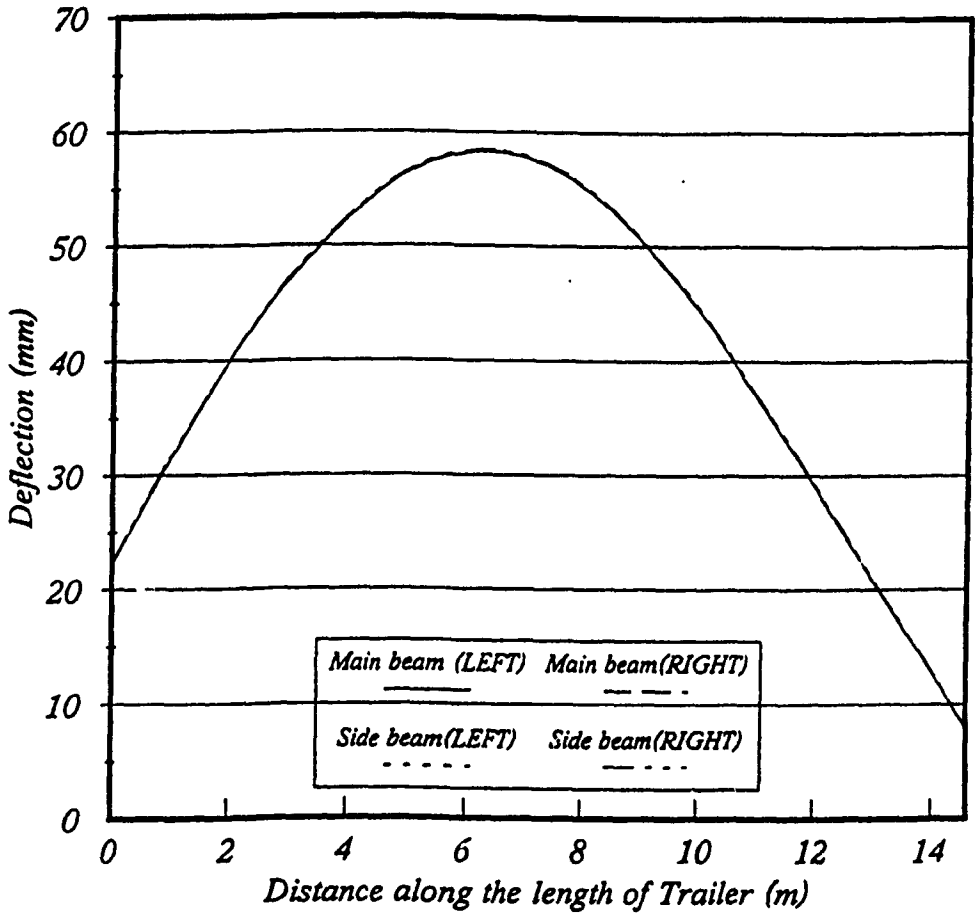


Figure 5.11: Deflection response of the main- and side-beam of trailer B structure derived from Potters' solution (Base design ).

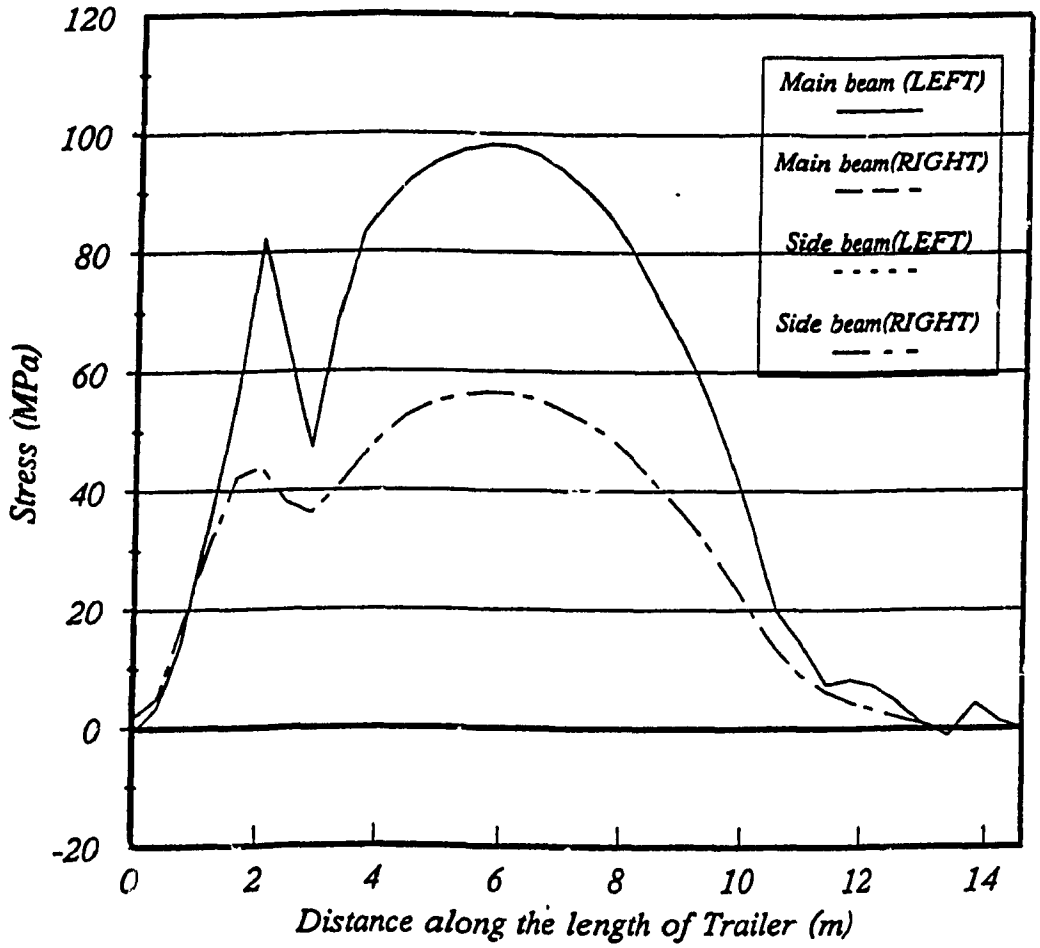


Figure 5.12: Stress response of main- and side- beams of trailer B structure derived from Potters' solution (Base design).

stress near the mid-span, while the peak stress in trailer A occurs near the goose-neck. This is primarily governed by the modulus of section resisting the maximum flexural moment for the applicable structure and the behavior is attributed to the distinct feature of individual design and involving, the configuration, the geometry and location of structural members, and the cargo loading. The side-beams experience a similar stress pattern but the magnitudes are much lower than those of the main beams.

Figure 5.13 illustrates the peak flexural stresses experienced by the three sections of the 37 cross-beams of the base design. Although the magnitudes of the bending stresses are relatively smaller than those experienced by the main- and side- beams, the cross beams located closer to the king-pin and the suspension supports experience higher stresses. The peak stress of the right and left sections of the cross-beam located near the last axle suspension is observed to be nearly 55 MPa. The mid-sections connecting the two main-beams, however experience, less bending stress, when compared to the corresponding outboard sections connecting the main-beams to the side-beams.

### 5.3.1.2 RESPONSE TO TWIST LOADING CONDITION

The torsional behavior of the trailer B structure is investigated under twist load condition, realized by shifting the entire suspension reaction force to only one side of the trailer. The resulting load condition represents the extreme lateral load transfer caused by either a high speed directional maneuver or the wheel lift-off. This extreme load condition is achieved in the mathematical model by making the

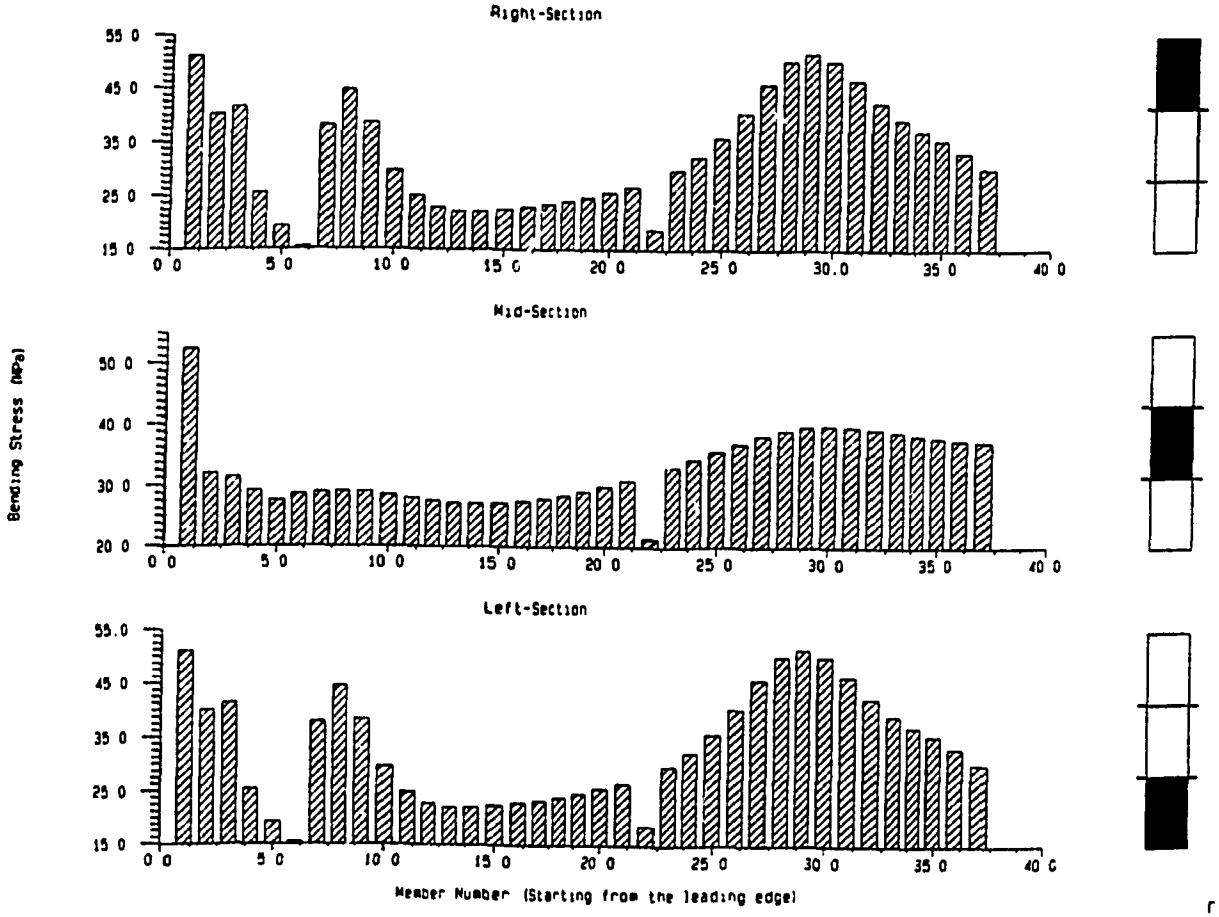


Figure 5.13: Flexural stress response of the cross-beams derived from Potters' solution (Base design).

spring members to carry null reactions. The results derived from Potters' solution are presented in terms of vertical deflections, and flexural and torsional stresses of various members of trailers A and B, as shown in Figures 5.14 to 5.17. Figure 5.14 illustrates the vertical deflection patterns of trailer B, when the reaction forces of right-side suspension springs are reduced to zero. The resulting asymmetric loading about the longitudinal axis yields considerably different deflections of the left- and right- side members, as shown in the Figure. The main- and side- beams located near the right-side track exhibit considerably larger deflections when compared to those of the left-side members. The maximum deflection of the main-beams on the left- and right- sides are observed to be 52 mm and 130 mm, respectively, while the peak deflections of the corresponding side-beams are (+)100 mm and (-) 220 mm. The peak vertical deflections of the side-beams are opposite in phase and occur at different locations.

The flexural stress distribution of the main- and side- beams along the longitudinal axis of the trailer B, subject to twist loading are presented in Figure 5.15. Although the stress pattern appear to be similar to those obtained under normal load condition; the magnitudes of the flexural stresses are considerably different. Both left- and right- main-beams exhibit higher stresses than those experienced under normal loading. The right-side main-beam, subject to zero suspension reaction force contributes to unbalanced torsional stresses on the members of the main- and side- beams. Figure 5.16 presents the behavior of the trailer in terms of torsional stresses distributed along the length of the trailer. The main-beams exhibit considerably larger stresses than the side-beams. The right-side beams are subject to increased stresses than the left-side counter parts due to asymmetric suspension loads. The right-side-beam reveals a peak stress of 75 MPa occurring at a location .4 m from the leading edge, in the vicinity of goose-

neck and suspension support region. The two main-beams exhibit similar stress levels for $x \leq 2m$, the right-beam stress grows rapidly in the goose-neck region due to excessive twist around the king-pin. The peak value approaches 138 MPa and reduces to 120 MPa after the goose-neck. This level of stress varies only slightly until the suspension supports. It should be noted that the torsional loading of this nature represents the extreme twist condition that may be experienced by the trailer structures. Although the cross-beams are only lightly stresses under normal loading condition, their significant role becomes apparent under the twist loads. Figure 5.17 illustrates the distribution of flexural stresses experienced by the various cross-beams. The figure illustrates the only the peak stress experienced by the right-, left- and mid- sections of each cross-beam. The results clearly illustrate the asymmetric stress distribution along the cross-beams, where the right-sections located near the king-pin and suspension supports exhibit considerably large stresses than the corresponding left-sections. The mid-sections of these cross-members also exhibit increased stresses in the vicinity of king-pin and the suspension support, and the corresponding peak values are 160 MPa and 120 MPa, respectively.

### 5.3.1.3 PERFORMANCE INDICES FOR CANDIDATE TRAILERS

The performance characteristics of the candidate trailer structures are evaluated in terms of the performance indices established in section 2.4. The performances indices describe the ability of the structure to withstand the vertical deflection (DPI), ability to resist torsional moment (TPI), and the strength margin in relation to the material yield strength (SPI). The torsional performance indices (TPI) of the candidate trailers A and B are evaluated for toque loading of 270.99 kNm and 393.80 kNm respectively. The prescribed torque loading yields

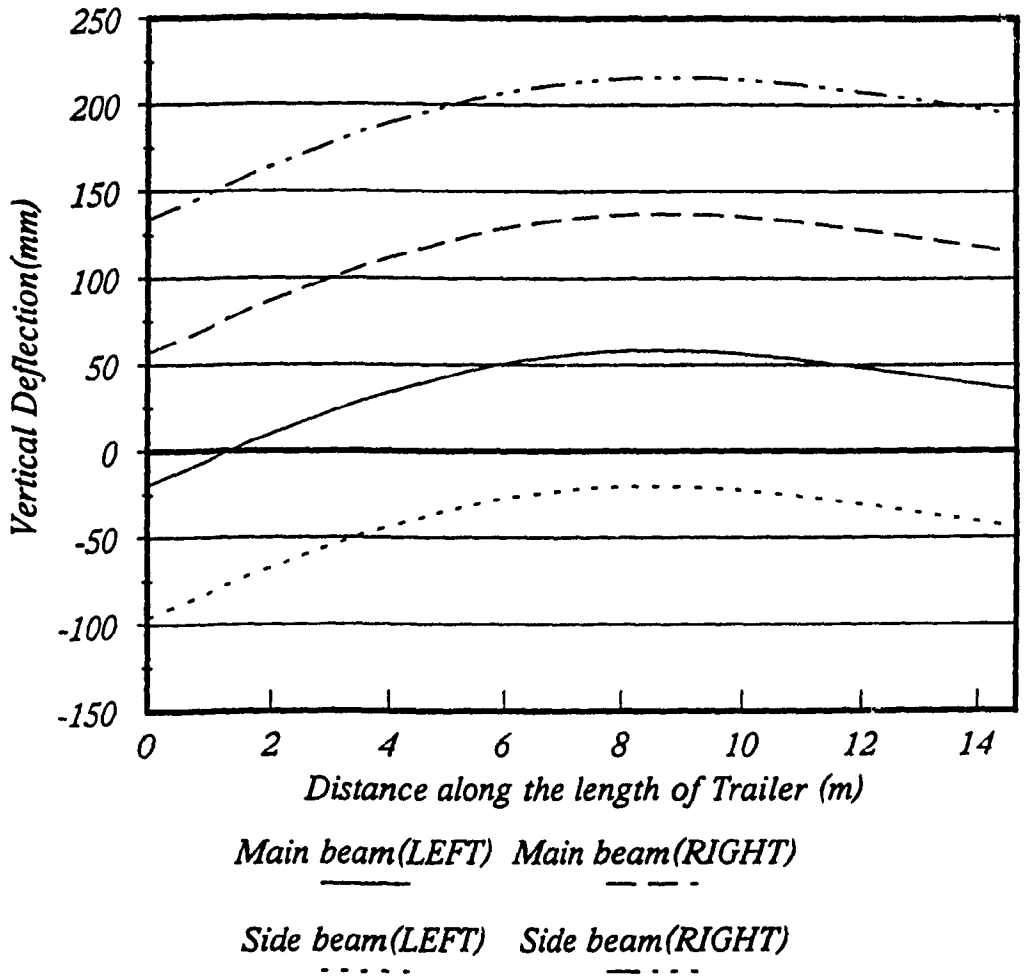


Figure 5.14: Vertical deflection response of main- and side-beams of trailer B subject to twist loads (Base design).

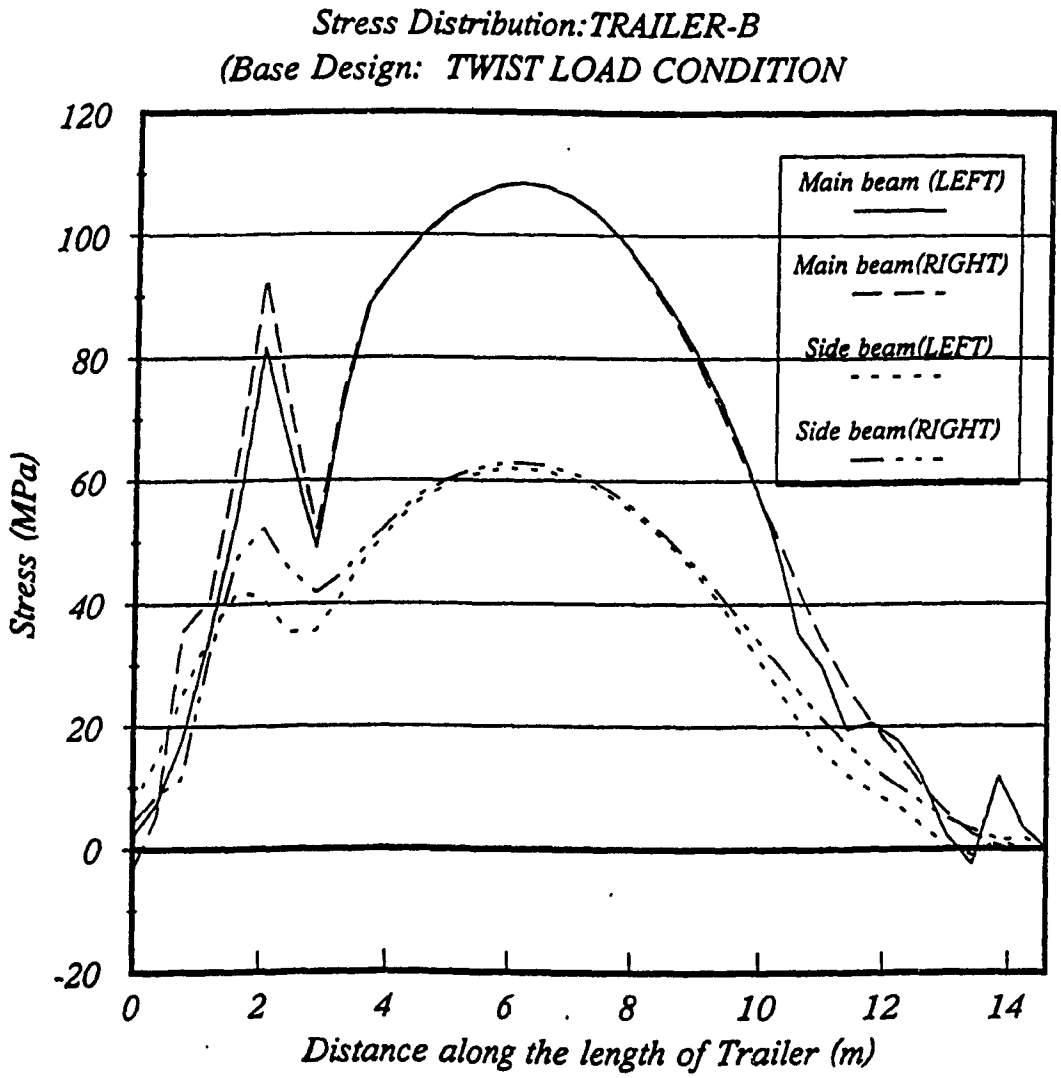


Figure 5.15: Flexural stress response of main- and side-beams of trailer B subject to twist loads (Base design).

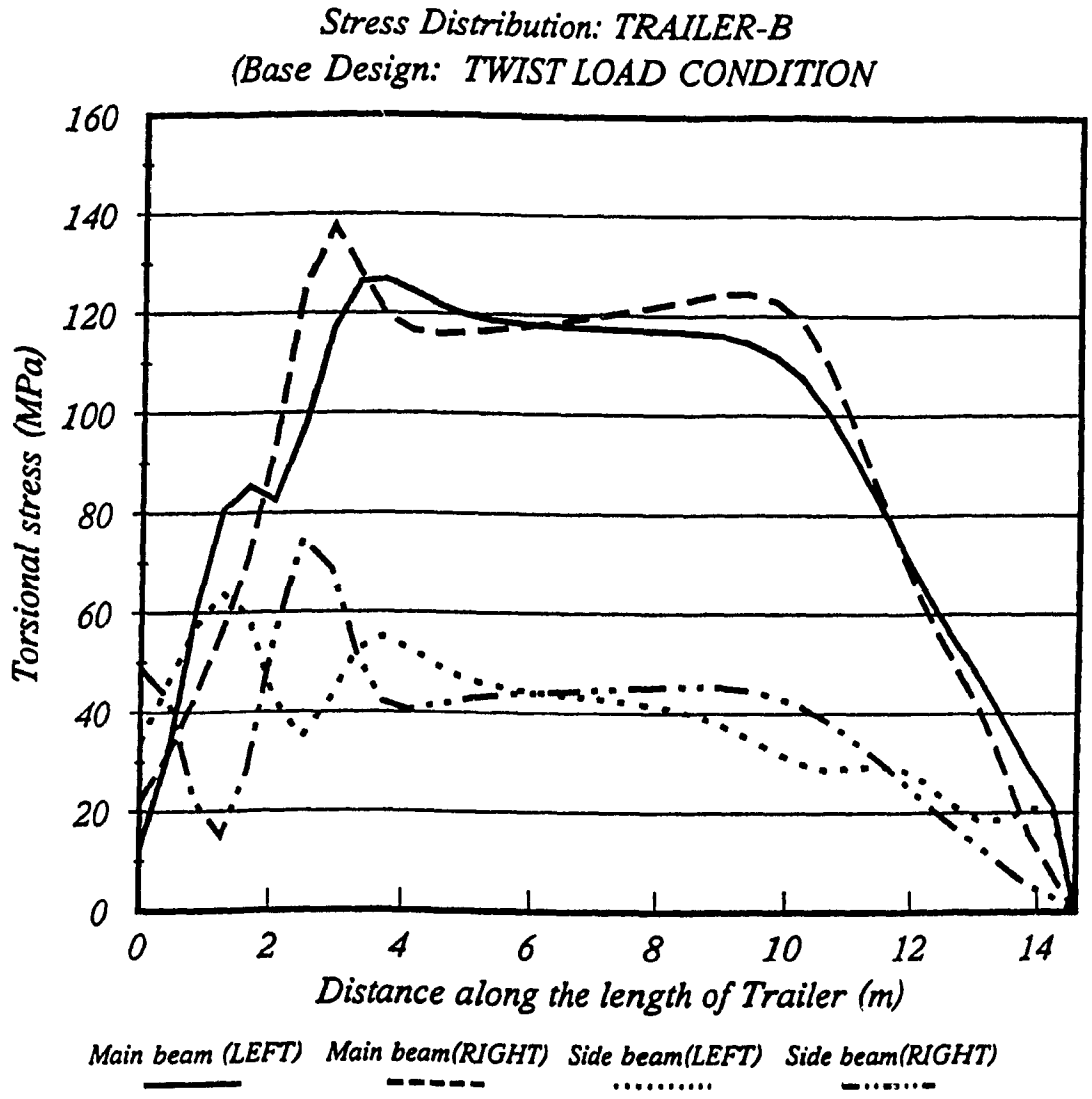


Figure 5.16: Torsional stress response of main- and side-beams of trailer B subject to twist loads (Base design).

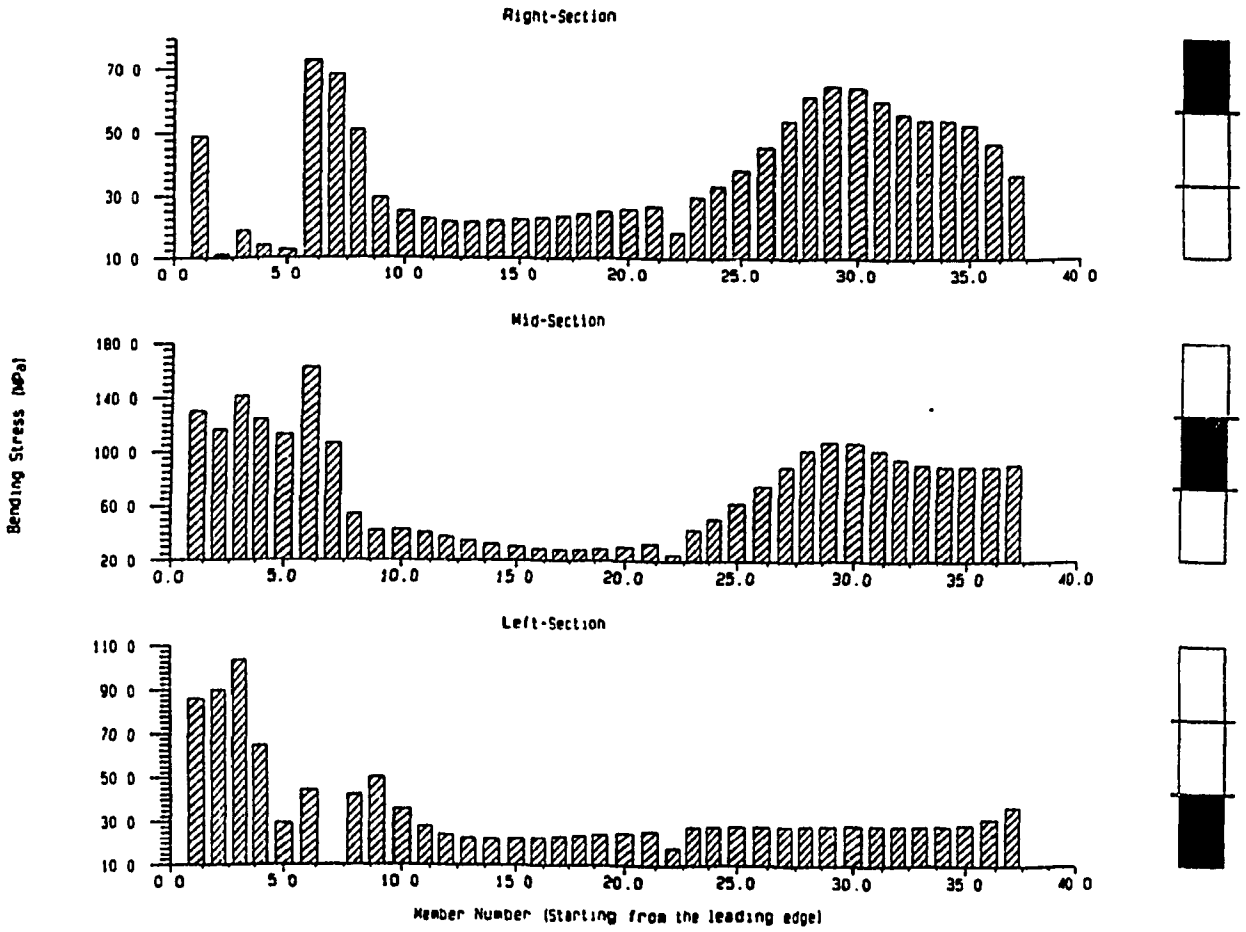


Figure 5.17: Flexural stress response of cross-beams of trailer B subject to twist loads (Base design).

maximum twist angles of 0.0065 and 0.018 radians respectively, of trailers A and B, as shown in Figures (5.17 and 5.18) The figures further reveal that both trailer will encounter maximum twist moment near the king-pin support. The performance indices evaluated for both the candidate trailers are summarized in Table 5.4.

**Table 5.4: Performance Indices of the Candidate Trailers.**

| Performance Index | Trailer A | Trailer B |
|---|---|---|
| DPI | 415.5e-6 | 566.0e-6 |
| TPI | 5.73e-9 rad/Nm | 6.09e-9 rad/Nm |
| SPI | 45.96 | 21.42 |

It is desirable to maximize both DPI and SPI to reduce the maximum deflection and enhance the structural integrity and fatigue life. A comparison of the performance indices of the two trailers reveals that both trailers exhibit similar torsional performance index(TPI). The trailer A design exhibit superior stress margin (SPI) and poor deflection performance index(DPI), when compared to those of the trailer B.

### 5.3.1.4 DESIGN SENSITIVITY RESULTS

The reanalysis solution based upon Potters' method yield the sensitivity vector, which can provide significant insight into desirable design modifications to achieve performance indices. The design sensitivity analysis is thus performed to study the influence of various beam design variables on the performance characteristics of the structures. The dimensions of the main-beams, which are the

primary load carrying members, are known to affect the performance indices in most significant manner. The design sensitivity analyses are thus performed to study the sensitivity of vertical deflection response with variation in the design variables $(\partial W/\ \partial d)$, using the design variations summarized in Table 5.2. The design variations in all cases are made with the main-beam segment ranging from the rear end of the goose-neck to the first axle suspension support, as reflected by the shaded region in Figure 5.10. This particular segment of the main-beams were selected due to their relatively high deflection and stresses, as demonstrated in the base design analysis.

Figure 5.18 illustrates the deflection response of the main- and side- beams of trailer A derived from the direct computation and reanalysis solution, when the selected main-beam segment height is reduced from 457.2 mm (18 in) to 406.64 mm(16 in). The remaining dimensions of the members are maintained as the base line values. The results illustrate the behavior pattern is similar to that obtained for the base design presented in Figure 5.2. The comparison with the base design, however, reveals an increase in the response caused by the reduction in the cross-sectional properties. The results further show an excellent agreement between the reanalysis and direct methods of solution. The reanalysis solution however yields a slight underestimate of the peak deflection and an overestimate of the deflection response near the leading and trailing ends. Figure 5.19 presents the comparison of the deflection response derived from two methods of solution, when the beam height is increased to 508 mm (20 in). The figure depicts a good agreement between the two solutions, while the trend in reanalysis solution is reversed. The maximum difference however, it is observed to be less than 3%. This reversal in estimation of the deflection is attributed to the change in sign contributed by the factor $(d\text{-}d_{j0})$ in Equation (3.32).

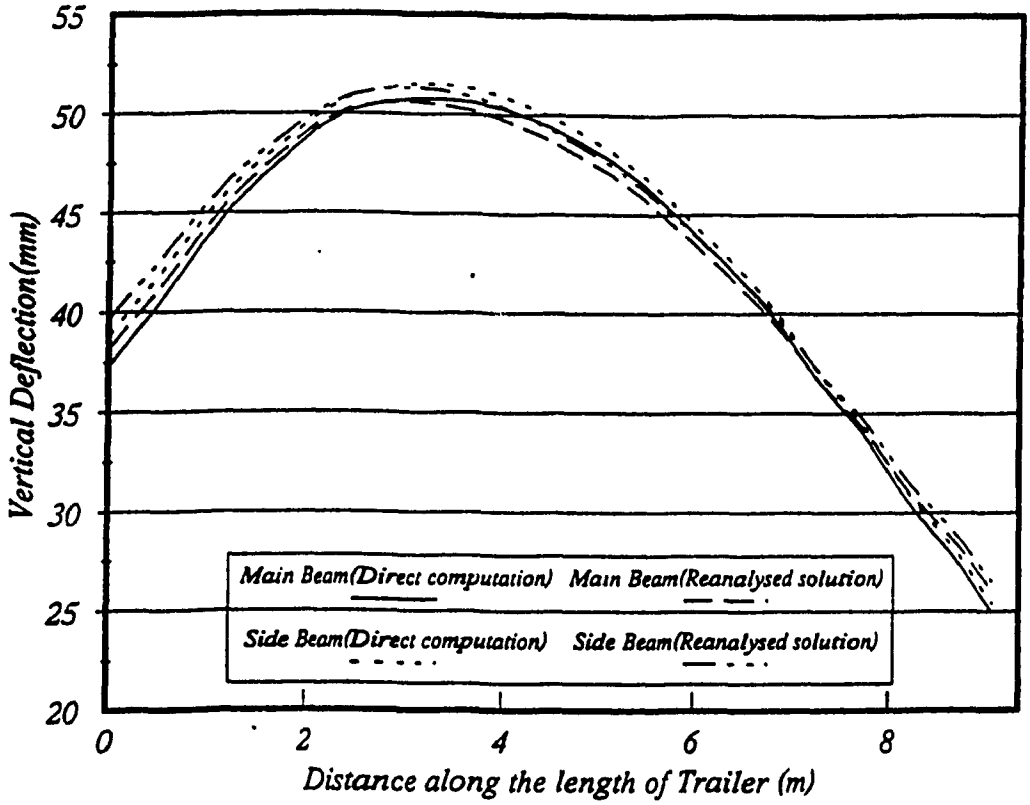


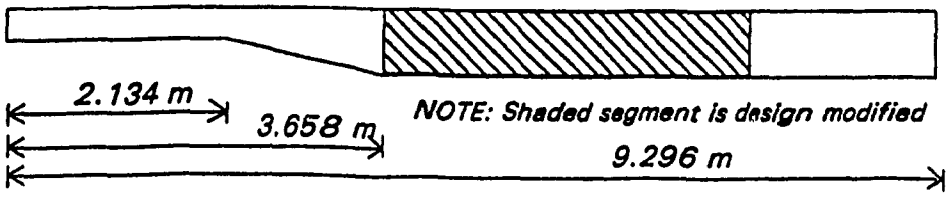


Figure 5.18: Deflection response of main- and side- beams derived from direct and reanalysis solution (H = 406.64 mm).

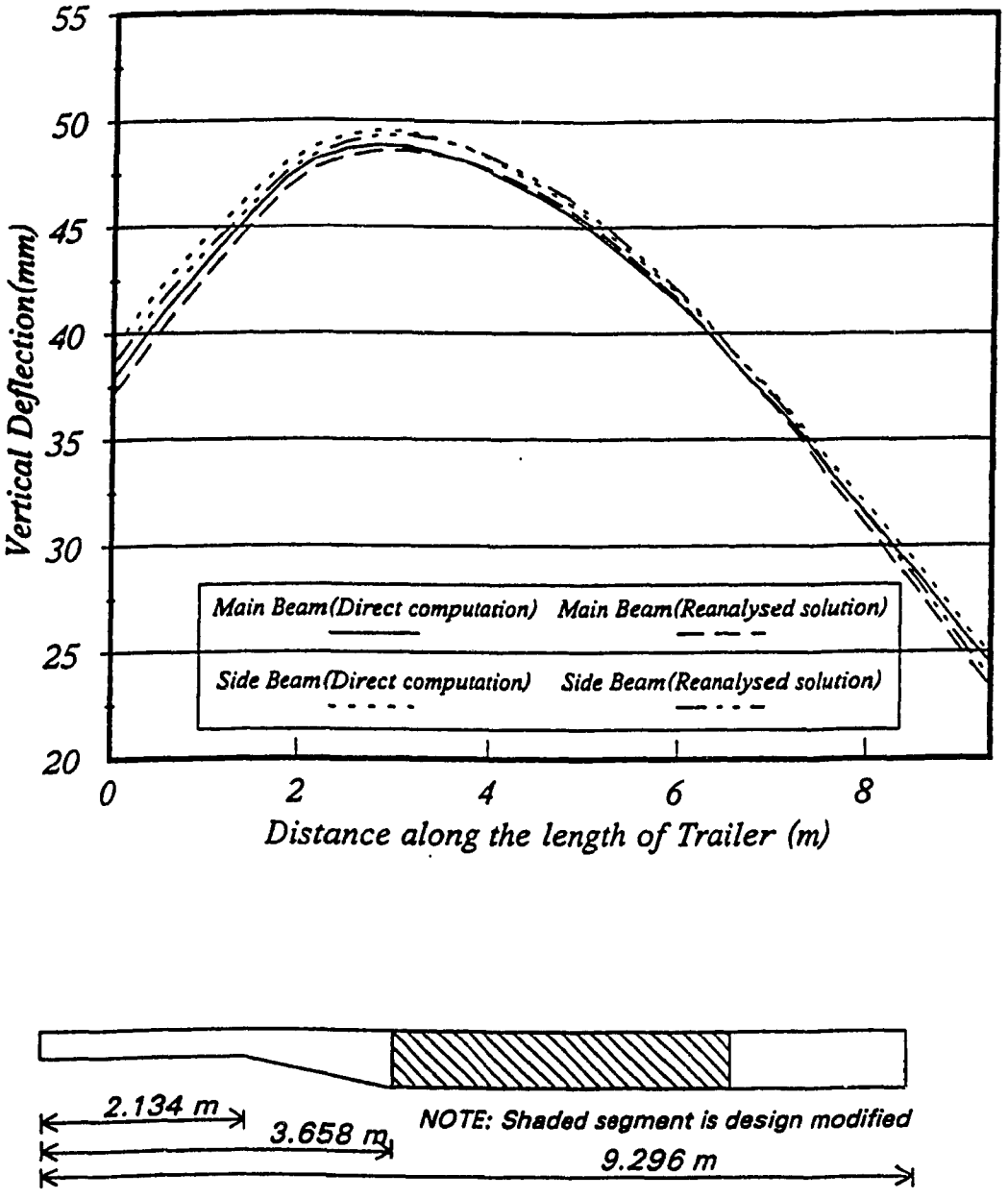


Figure 5.19: Deflection response of main- and side- beams derived from direct and reanalysis solution (H = 508 mm).

The bending stress along the length of main- and side- beams are computed using reanalysis and direct computations by Potters' method, when the main-beam height is varied to 406.4 mm (16 in) and 508 mm (20 in). Figure 5.20 and 5.21 illustrate the stress response derived from the two methods. A comparison with the stress response of base design (Figure 5.3) reveals an increase in the flexural stress with reduction in the section height and reduced stress with increased section height. The response behavior derived from reanalysis solution compares very well with those derived from the direct solution, while the reanalysis solution tends to overestimate and underestimate for increase and decrease in the section height, as discussed above. The peak error, however, is near 6%. Figure 5.22 and 5.23 illustrate the deflection and stress response of the main- and side- beams derived from two methods of solutions, when the web thickness of main-beam is varied from the base design to 3.175 mm (1/8 in) and 6.35 mm (1/4 in). The results clearly demonstrate the numerical effectiveness of the reanalysis solution. The structural response in terms of deflection and stress decreases with increase in the web thickness. The change in the response values, however, is considerably small. The reanalysis solution further reveals similar trends in estimating the deflection and stress response.

Figure 5.24 presents the deflection response of the main- and side- beams, when the flange thickness is increased from 19.05 mm(0.75 in) to 25.4 mm(1 in). A comparison of the deflection response with that of the base design reveals that the variation in the flange thickness pose only insignificant effect on the structure response. The reanalysis solution, however, yields a slightly higher value (50 mm) of the peak deflection resulting in peak error of 3%. Figure 5.25 illustrates the stress distribution for the design modification, showing the behavior in flexural and shear mode of the main beam. A comparison with the response of the base

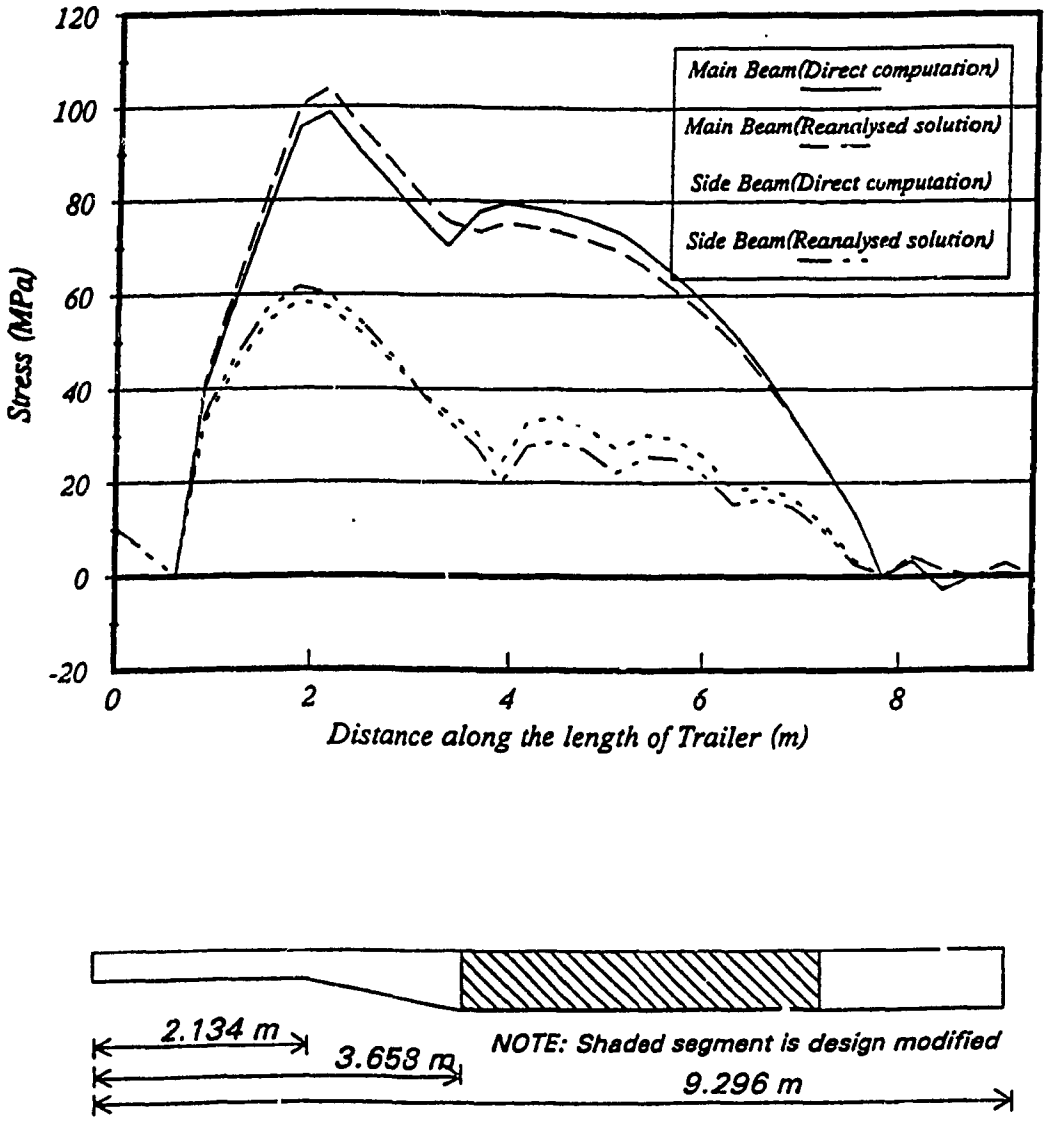


Figure 5.20: Flexural stress response of main- and side- beams derived from direct and reanalysis solution (H = 406.64 mm).

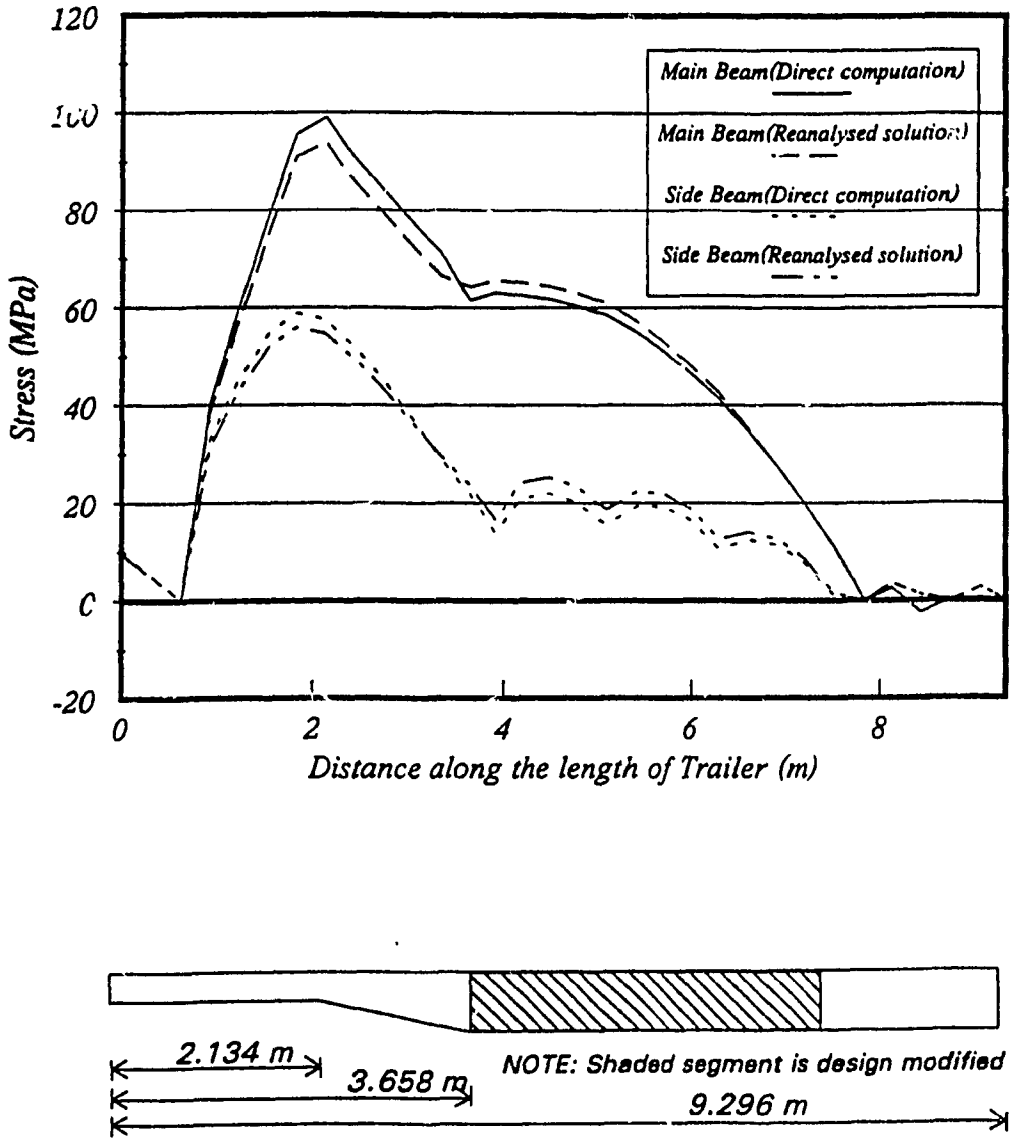


Figure 5.21: Flexural stress response of main- and side- beams derived from direct and reanalysis solution (H = 508 mm).

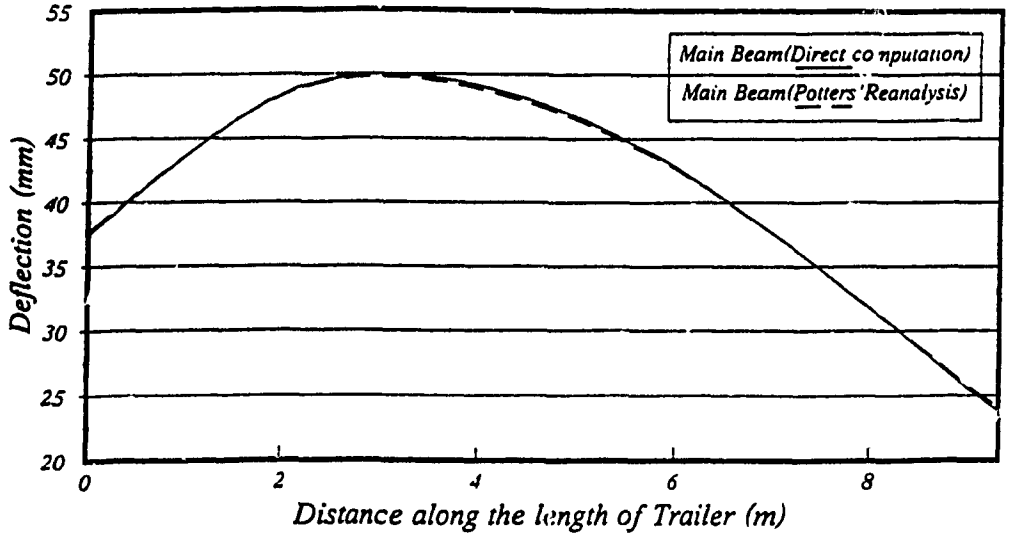


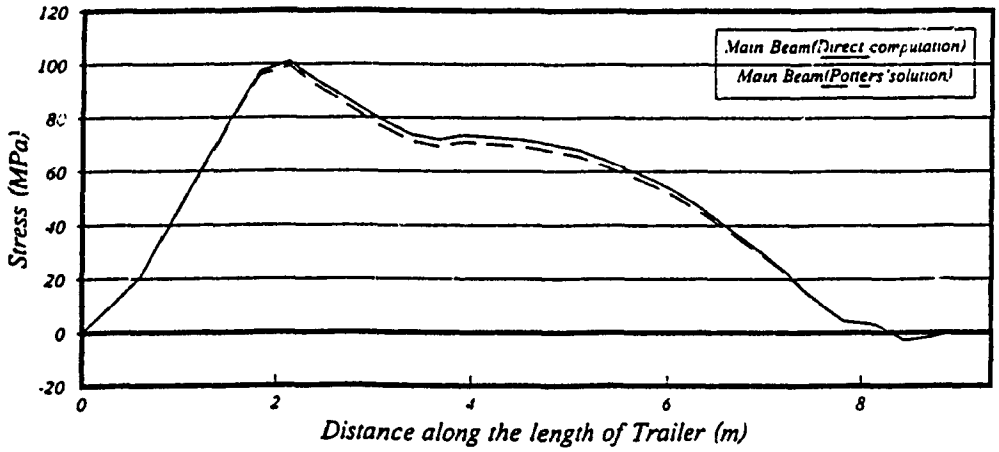


Figure 5.22: Deflection and stress response of main-beam derived from direct and reanalysis solution (Tw = 3.175 mm).

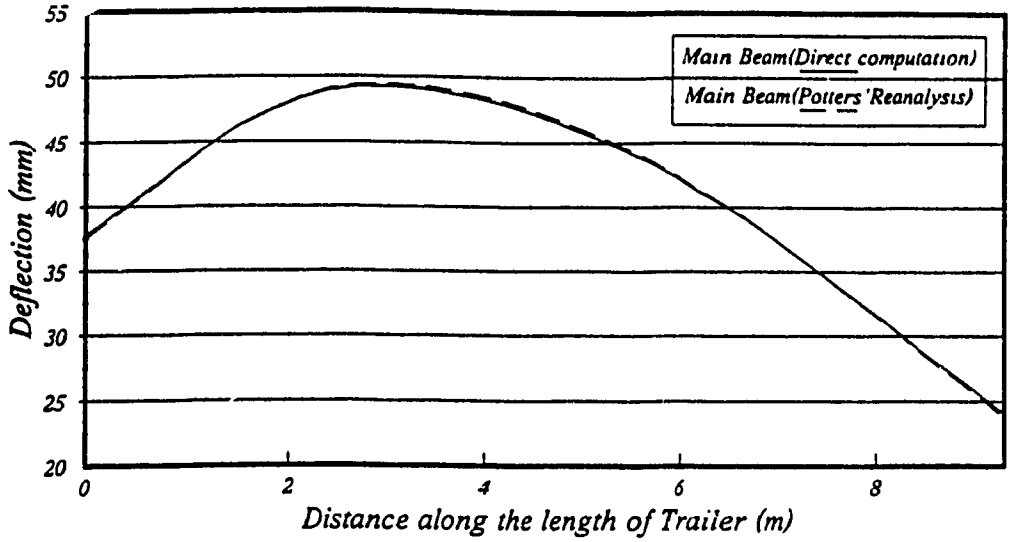


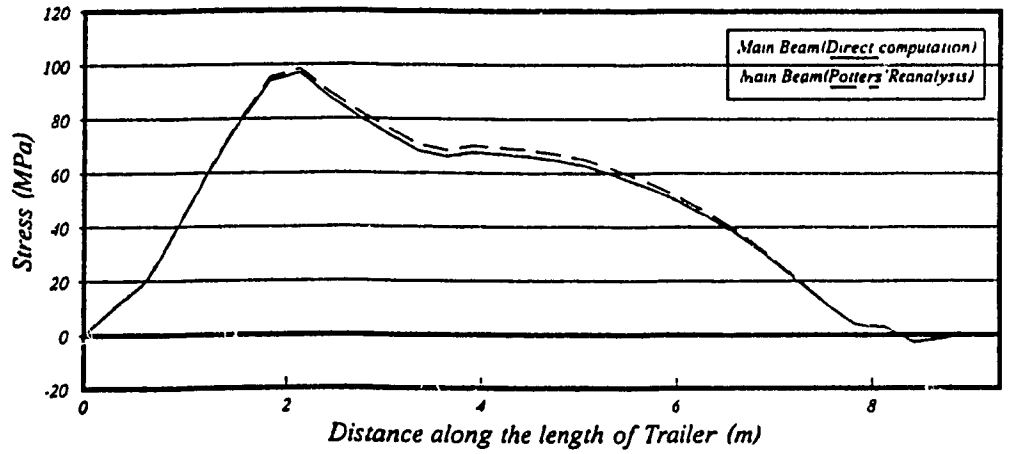


Figure 5.23: Deflection and stress response of main-beam derived from direct and reanalysis solution (Tw = 6.35 mm).

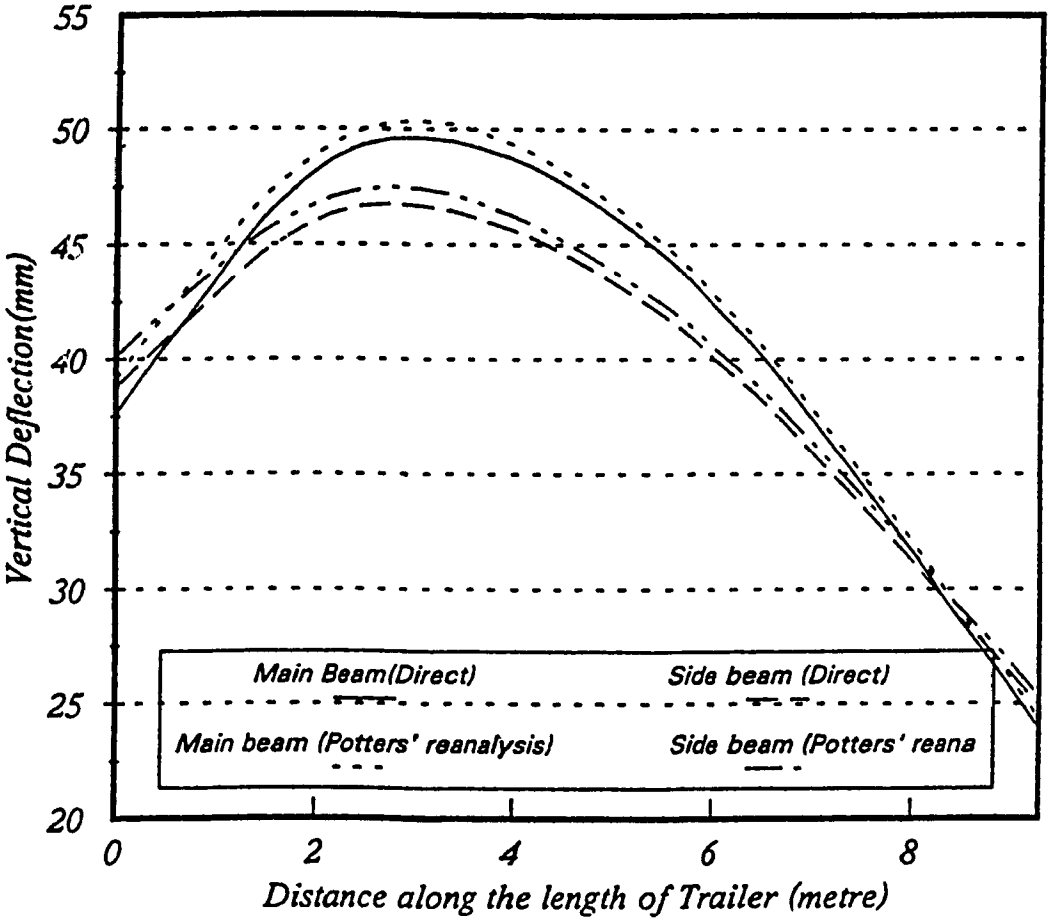


Figure 5.24: Deflection response of main- and side- beams derived from direct and reanalysis solution (Tf = 25.4 mm).

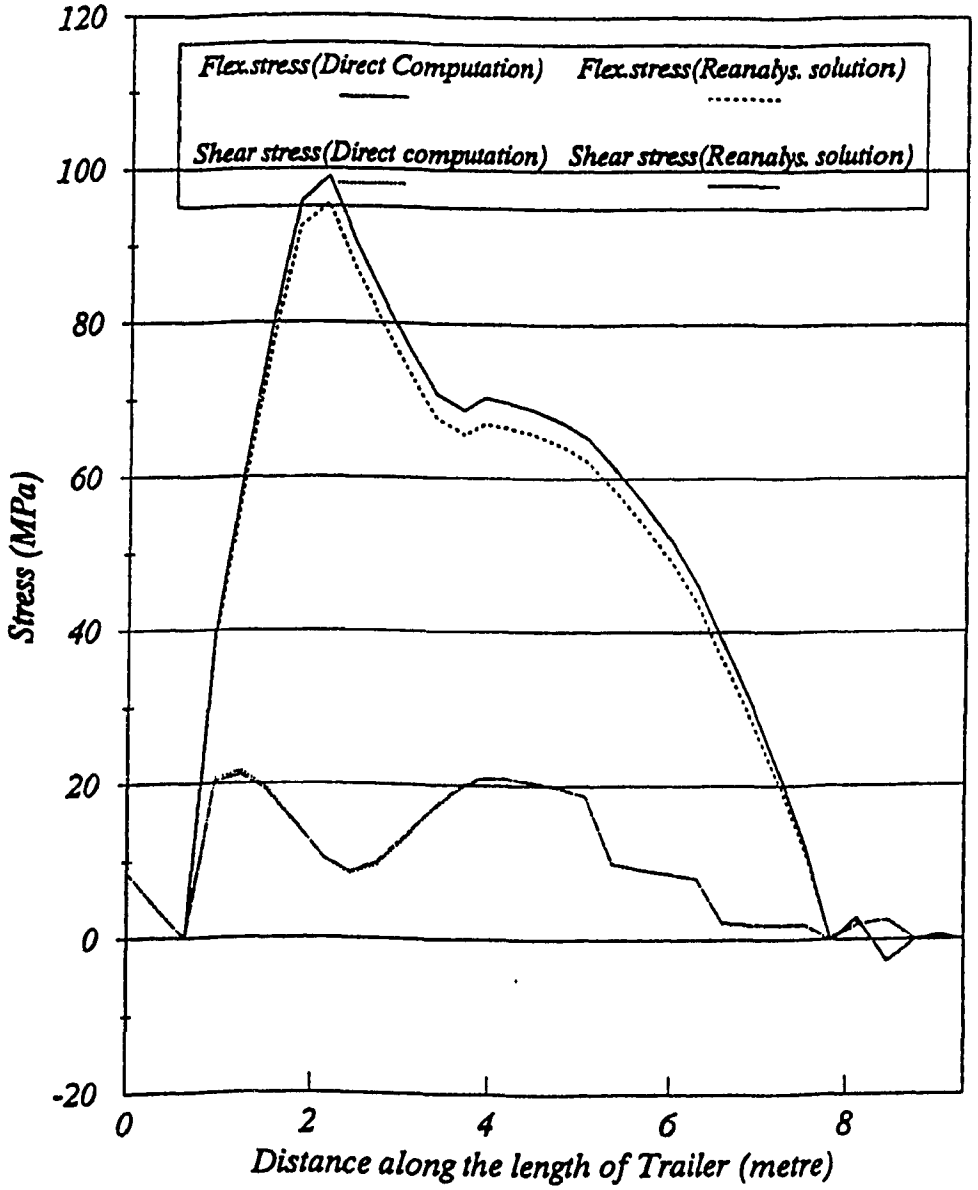


Figure 5.25: Flexural and torsional stress response of main-beam derived from direct and reanalysis solution (Tf = 25.4 mm).

design reveals that the peak stresses increases to 98 MPa (Peak stress of the base design= 82 MPa). This can be attributed to the reduced web height and thus the modulus caused by an increase in the flange thickness.

Figure 5.26 illustrates the sensitivity of deflection response with respect to variations in the web height-H, web thickness-Tw, flange width-B and flange thickness Tf. The influence of variations on the deflection sensitivity is more pronounced in section of the main-beam affected by the design modification (shown by the hatched area in the Figure). The sensitivity of the stress response with respect to design variation can be derived from the reanalyzed displacement solutions.

### 5.3.1.5 PARAMETRIC STUDY OF TRAILER-B DESIGN

A parametric study is performed to evaluate the influence of variation in the selected design variables of the trailer B on the tare weight and using Potters' method of direct computation. various design options are considered to provide the basis for designing a near optimal trailer structure in view of its tare weight and stress performance index (SPI). A total of five design alternatives are formulated by varying different section properties of the entire main- and side- beams. The response characteristics are evaluated in terms of the distribution and peak values of deflection and flexural stress of the main- and side- beams. The design options and associated design modifications are summarized in Table 5.5 together with % weight reduction, peak deflection, peak stress and deflection and stress performance indices. The objective of the design process is to maximize both DPI and SPI. The results summarized in the Table illustrate that the Design-2, involving a reduction in the main-beam web thickness, yields a relatively high value of SPI and 11% reduction in the tare weight with increased deflection

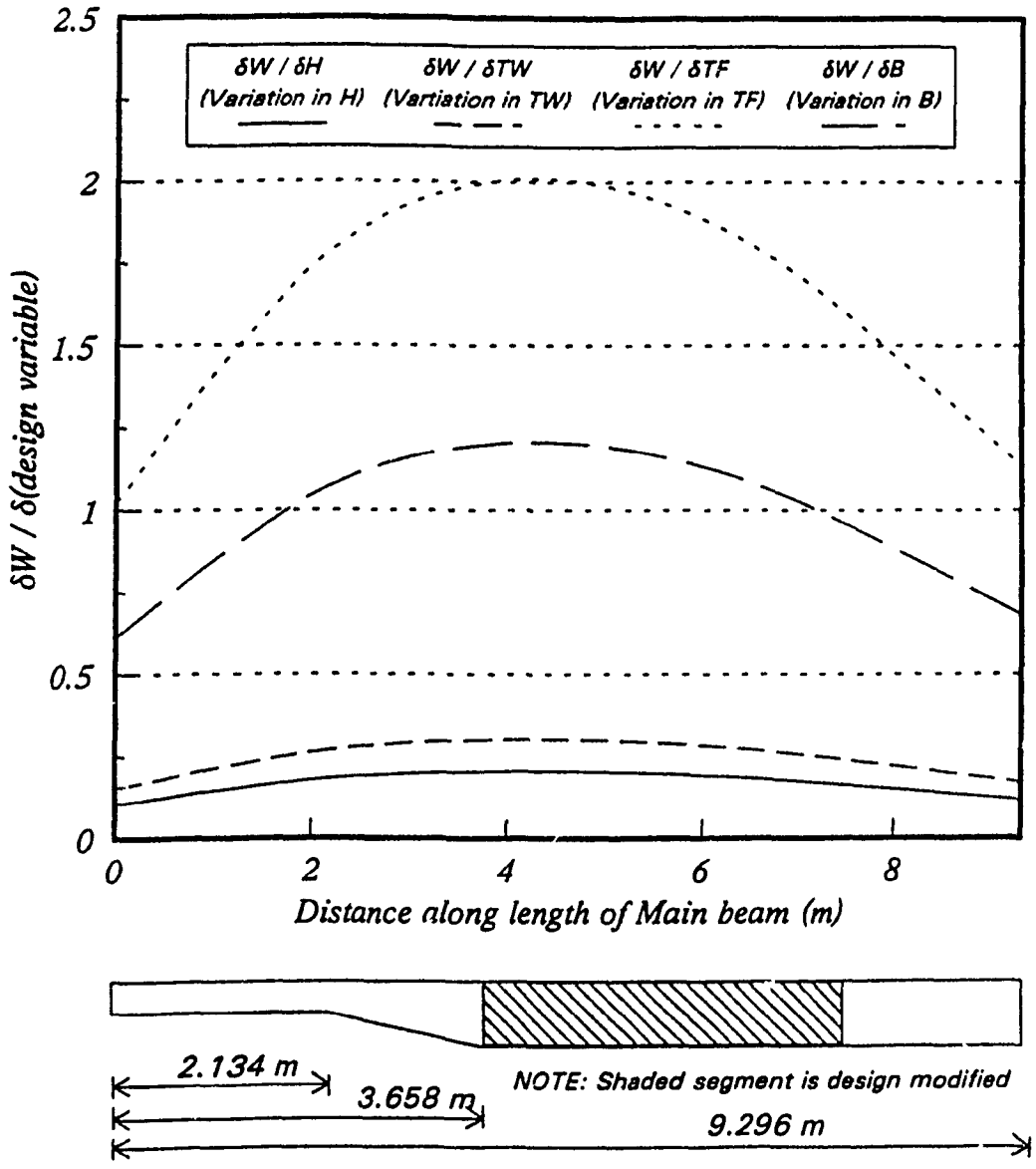


Figure 5.26: The deflection sensitivity response to variation in the main-beam design parameters.

**Table 5.5: Summary of Performance Indices of Different Design Options (Trailer B).**

| DESIGN OPTION | Change in Variable (% redn.) | Max Stress MPa | SPI | Max Deflect. mm | DPI value x E-6 | Tare Weight Kg | % Weight Reduction |
|---|---|---|---|---|---|---|---|
| Base Design | - | 98 | 21.42 | 58 | 566.0 | 5000 | - |
| Design 1 | Main-beam -Tf (50.0) | 108 | 21.94 | 62 | 536.0 | 4430 | 11.4 |
| Design 2 | Main-beam- Tw (37.5) | 100 | **23.59** | 58 | **504.0** | 4450 | 11.0 |
| Design 3 | Side-beam -Tf (50.0) | 135 | 16.72 | 63 | 572.0 | 4650 | 7.0 |
| Design 4 | Side-beam- Tw (37.5) | 108 | 20.64 | 62 | 570.0 | 4710 | 5.8 |
| Design 5 | Main-beam -B (28.5) | 118 | 20.93 | 67 | 556.0 | 4250 | 15.0 |

performance index (DPI). The results further reveal that a reduction in sectional properties of the side- beams yields a considerably lower SPI with only marginal reduction in the weight. Although the reduction in flange width (Design 5) yields significant reduction in the tare weight (15%), the corresponding DPI values increases considerably. The earlier design sensitivity studies, in conjunction with the performance indices, have helped in arriving at a near optimal design satisfying tare weight and performance considerations.

### 5.3.1.6 COMPARISON OF EFETM AND POTTERS' METHOD OF REANALYSIS

The EFETM and Potters' methods of analyses are based upon substructuring techniques, which involve the operations with considerably reduced size matrices when compared to those used in conventional FEM analysis. The FETM analysis, and Potters' method of analysis and reanalysis formulated in this study involve the solution of a (24 x 24) matrix. The matrix size, however, increases to (48 x 48) in the EFETM reanalysis due to addition of the design sensitivity vector. The results presented in Chapters 4 and 5 clearly demonstrated the validity and numerical efficiency of both methods for structures ranging from simple bench mark problems to large size heavy vehicle trailers. The FETM and EFETM methods use a series of matrix multiplications followed by a single matrix decomposition operation, while, the Potters' method involves decomposition of matrix for each partition followed by multiplications for forward- and backward-substitution operations to arrive at the final solution. Another difference that distinguishes the FETM solution technique is that the station vectors, comprising the displacement and force vectors, are evaluated simultaneously at each station. The stresses and displacements of all the stations are thus computed

simultaneously. In the Potters' method, the displacement vector is initially computed, and the forces and stresses are derived from the displacement vectors. Intermediate forces can be conveniently introduced arbitrarily in both the analyses methods, although the imposition of restraints needs to be introduced at the formulation stage in the Potters' solution technique. Figure 5.27 illustrates the deflection and stress response of the main-beam of the trailer A derived using the two methods. The results clearly demonstrates that both methods yield similar solutions. Table 5.6 presents a comparison of the computing time required by the two methods with the 80486, DX, 33 MHz. PC system, for the static analysis of the trailer A (design modification-I, discussed in section 5.2). The table reveals that the FETM/EFETM method is more efficient numerically than the Potters' method for both direct and reanalysis solutions.

**Table 5.6: Computational Time for EFETM and Potters' method**

| Operation | FETM/EFETM | Potters' |
|---|---|---|
| Direct Analysis | 170 s | 220 s |
| Reanalysis | 50 s | 90 s |

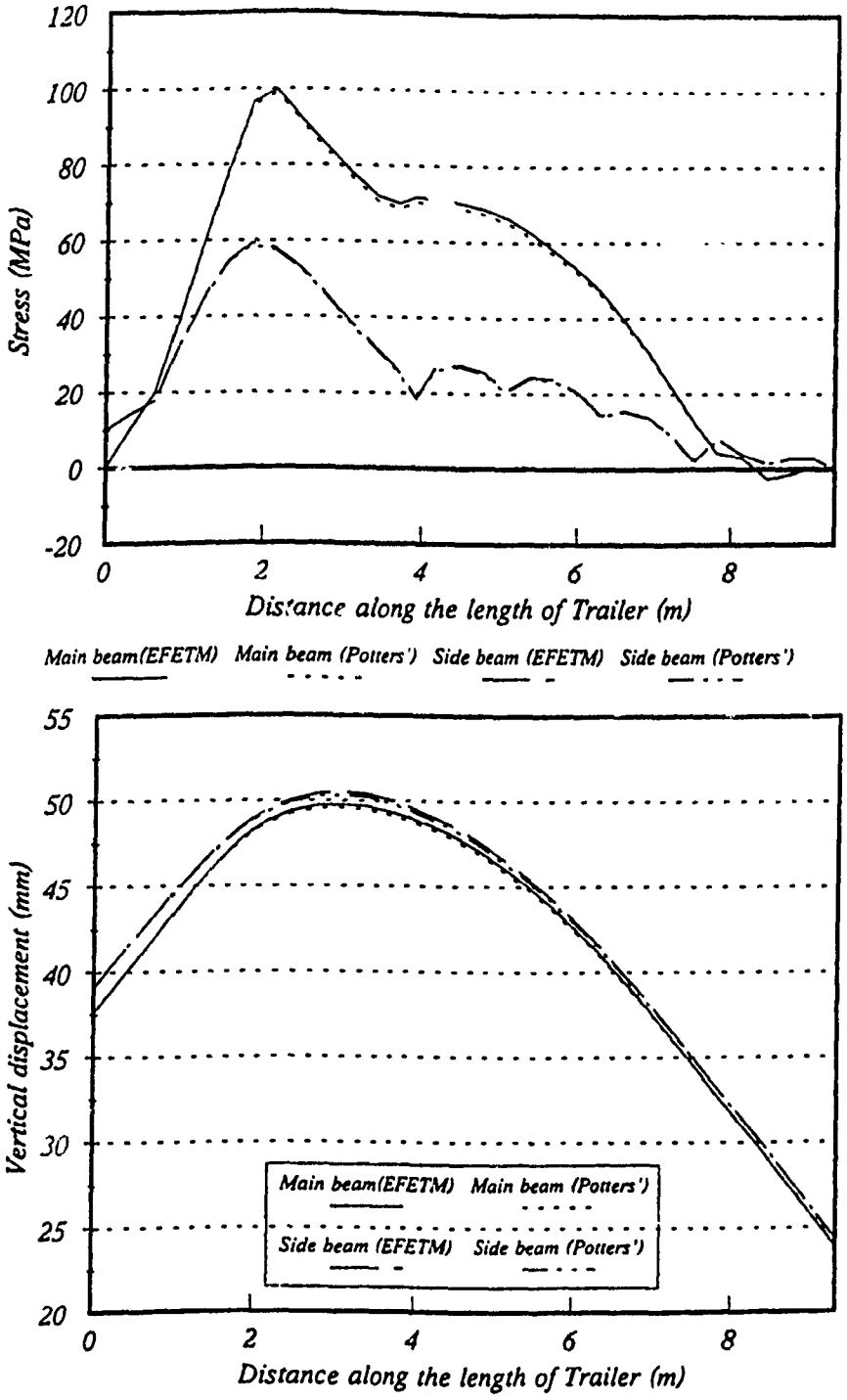


Figure 5.27: Comparison of deflection and stress response characteristics derived from EFETM and Potters' methods of solution

## 5.4 SUMMARY

Static analyses of the candidate trailers A and B are performed using the analysis and reanalysis techniques based upon Potters' and FETM solutions. Design sensitivity of reanalysis solutions to illustrate the influence of design variables and to demonstrate the effectiveness of the reanalysis solution. The effectiveness of the reanalysis solution is further demonstrated by comparing the response behavior with those derived from direct analyses. The EFETM and Potters' solutions predict reasonably accurate solutions with maximum errors not exceeding 4% and 6% respectively. A design parametric study is carried out using Potters' substructure method to provide the basis for the realization of an optimal design of trailer B. Various design options were evaluated in terms of weight reduction, and deflection and stress performance indices. Both reanalyses methods exhibit superior numerical efficiency in comparison with direct solutions.

# CHAPTER 6

# DYNAMIC RESPONSE ANALYSIS OF CANDIDATE TRAILER STRUCTURE

## 6.1 Introduction

Vehicle structures are invariably subjected to time-varying loads arising from tire-terrain interactions, cargo interaction and dynamics of the vehicle. The response analysis of the trailer structures to dynamic loads thus forms an important design consideration. Vehicle response to time varying road excitations, in-general, is evaluated through analysis of multi-degrees-of freedom models [55, 56, 57, 58]. Such studies, however, provide important insight into the vibration modes of the lumped-parameter vehicle models related to ride, handling and directional performance characteristics [59]. The analytical models of the trailer structures developed in this investigation can be effectively employed to evaluate the dynamic response of the flexible structure subject to road loads arising from the tire-terrain interactions.

This chapter describes the analytical representations of the candidate trailer structures for dynamic response analyses. Road-loads transmitted to the trailer structure or the sprung mass are characterized for smooth and rough roads using the quarter-vehicle formulation proposed by Rakheja and Woodroofe [60]. The methodology described in their study is used to derive the dynamic tire forces as

functions of the vehicle speed, and suspension and tire properties. In this study, the dynamic tire loads are evaluated for two road profiles reported in [61], and referred to as 'smooth' and 'rough' roads. The smooth road profile corresponds to an *International Roughness Index* (IRI) of approximately 1.0, while the IRI value of rough road profile is approximately 4.75. The dynamic response of the trailer structure models is evaluated for dynamic loads corresponding to equivalent suspension spring rates and modal damping parameters. The response characteristics, presented in terms of dynamic displacement and stress behavior, are discussed in view of the design parameters.

## 6.2 Estimation of Dynamic Loads

Figure 6.1 illustrates the schematic of a typical tractor-semitrailer configuration. The dynamic loads transmitted to the trailer structure are highly complex function of the vibration behavior of the coupled vehicle system, tire loads, road roughness, suspension and tire properties, structural deflection, cargo loads, speed, etc.. The dynamic forces to the trailer structure, however, are primarily transmitted near the trailer axle mountings and the king-pin supports. The inertia force due to the sprung mass (cargo and trailer) further contribute to the dynamic loads. The determination of dynamic loads thus necessitates the analysis of the coupled vehicle under specified road roughness and speed conditions. Alternatively, the dynamic loads transmitted by the axle assemblies may be estimated through analysis of a simplified uncoupled lumped-parameter model, similar to the quarter-vehicle models reported in literature [56-58]. This approach can provide a reasonable estimate of transmitted forces assuming negligible interaction among the different axles and vehicle pitching. Such simplified models have been extensively used to estimate dynamic tire loads and to evaluate

suspension performance associated with uncoupled vertical dynamics of the vehicle. Figure 6.2 illustrates quarter-vehicle model used to estimate the tire loads as a function of the suspension and tire properties, and the ride quality performance of the suspension system. The vehicle model comprises the sprung mass $m_s$ supported on the vehicle suspension represented by a parallel combination of energy restoring and dissipative elements. The unsprung mass due to the axle, $m_u$, is supported on the tire characterized by linear spring and damping elements in a point-contact manner.

Since the primary objective of the present study is to investigate the response behavior of the structure under dynamic chassis loads, the suspension and the tire damping is assumed to be negligible, which are of importance for ride quality analyses. The effects of structural damping, however, are incorporated into the dynamic analysis through inclusion of modal damping. The undamped quarter-vehicle model is thus used to characterize the trailer supported on the rear-axle assembly. The corresponding sprung mass is derived from the rated axle load and the weight of the axle assembly. A tridem trailer axle assembly is expressed as an equivalent single composite axle by lumping the suspension and tire properties. The masses due to the trailer axles are lumped together and represented by the unsprung mass, $m_u$. The dynamic forces transmitted to the structure from the road undulation are derived from the following equilibrium equations:

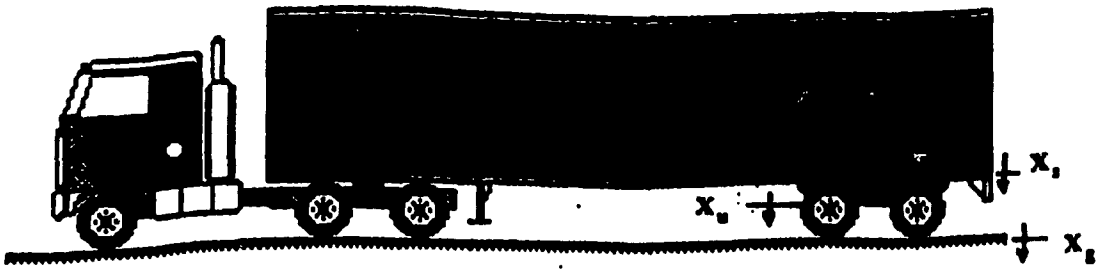


Figure 6.1: Schematic of a tractor-semitrailer vehicle.

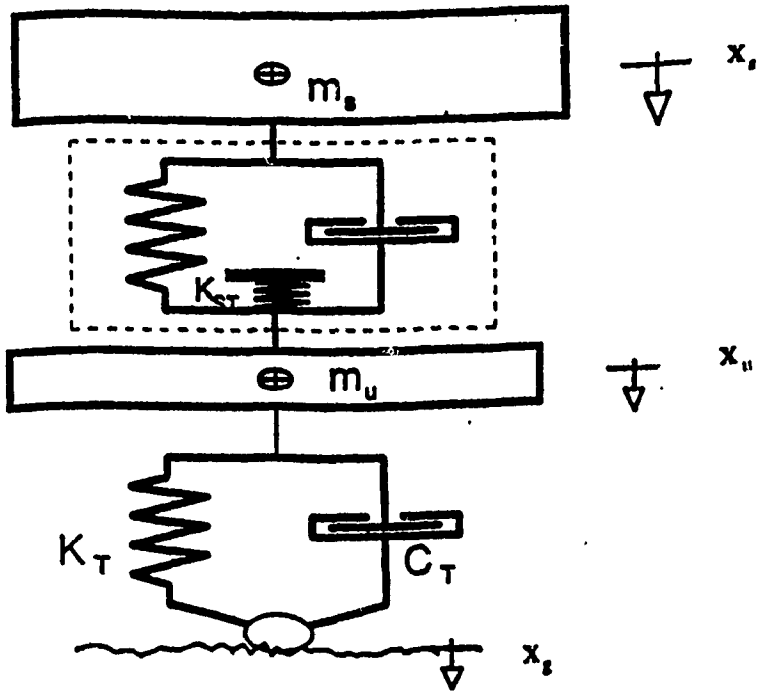


Figure 6.2: Vertical mode quarter-vehicle model of the vehicle.

$$m_s \ddot{x}_s + K_s (x_s - x_u) = 0 \tag{6.1}$$

$$m_u \ddot{x}_u + K_T (x_u - x_g) - K_s (x_s - x_u) = 0 \tag{6.2}$$

where,

$x_s$ = Sprung mass displacement

$x_u$ = Unsprung mass displacement

$x_g$ = Road undulation

$K_T$ = Tire stiffness

$K_s$ = Suspension stiffness

In heavy vehicle trailers the sprung mass is considerably larger than the unsprung mass. The unsprung mass inertia force can thus be considered negligible when compared to tire and suspension forces. Equation (6.2) thus yields that the dynamic tire and suspension forces are approximately equal.

$$K_T (x_u - x_g) \approx K_s (x_s - x_u) \tag{6.3}$$

Equation (6.3) is further simplified to yield:

$$x_u - x_g = \frac{K_s}{K_T} (x_s - x_u) \tag{6.4}$$

Since the vehicle suspension is considerably softer than the tire, the ratio of the stiffness coefficients ($K_s/K_T$) is extremely small. The relative deflection of the tire can thus be considered small, implying that $x_u \approx x_g$. The resulting suspension force, $F_s$, can then be approximated as :

$$F_s \approx K_s(x_s - x_g) \tag{6.5}$$

The above equation provides an estimate of the suspension force transmitted to the trailer structure. This method of approximation eliminates the necessity to analyze the quarter vehicle model and the axle response, and provides an estimate of the dynamic force directly from the road roughness data. The resulting reaction force at the king-pin support is then derived from:

$$R_{K_{Dyn}} + R_{K_{Stat}} = 0.5\left[W_c - n(W_{axle} - W_u) - F_s - \sum m_i \ddot{x}_{si}\right] \tag{6.6}$$

where, $R_{K_{Dyn}}$ is the reaction force at each of the two king-pin support nodes. $W_c$ is the cargo weight, $F_s$ is the dynamic suspension force, and $(m_i \ddot{x}_{si})$ is the inertia force due to the spring mass at node i. Using the static vertical force equilibrium, the above equation can be expresses as:

$$R_{K_{Dyn}} = -0.5\left[F_s + \sum m_i \ddot{x}_{si}\right] \tag{6.7}$$

## 6.3 Dynamic Response Analysis

The equation of motion for the trailer structure subject to dynamic forces can be expressed in the following matrix form:

$$[M]\{\ddot{U}\} + [C]\{\dot{U}\} + [K]\{U\} = \{F\} \tag{6.8}$$

where,

[M] is the mass matrix.

[C] is the structural damping matrix.

[K] is the stiffness matrix.

$\{\ddot{U}\}$ is nodal acceleration vector.

$\{\dot{U}\}$ is the nodal velocity vector.

$\{U\}$ is the nodal displacement vector.

$\{F\}$ is the *time varying* nodal force vector.

The solution of equation (6.8) using modal superposition method involves eigen analysis. The eigen analysis of the equation for trailer B involving the stiffness matrix (936 x 936), however, may be demanding on the computing and human resources. Since the vehicle structures exhibit high deflections and stresses corresponding to lower frequency modes, only lower 25 modes are extracted using an iterative algorithm.

## 6.3.1 EIGENVALUE ANALYSIS

The equations of motion characterizing the free vibration behavior of the structure can be expressed as :

$$[K]\{U\} = \omega^2[M]\{U\} \tag{6.9}$$

where, [K] and [M] are the global stiffness and mass matrices, $\omega$ denotes the natural frequency of the structure and is related to the eigenvalue, and {U} denotes the corresponding displacement or eigenvector. The mass matrix can be derived in terms of consistent mass matrix or, can be represented as lumped masses along the

diagonal of the global mass matrix. The lumped mass representation offers significant saving in memory requirements since the diagonal elements of the mass matrix [M] can be conveniently presented as a column vector. The Potters' method of solution used for static analysis of the structure is employed in the iteration technique, while retaining the decomposed stiffness matrices of the substructures as discussed in Chapter 3. The simultaneous matrix iteration procedure is employed to derive the lower 25 vibration modes of the trailer structure [1]. However, only 15 modes were selected to compute the dynamic response in the 0-45 Hz frequency range. Since the stiffness matrix [K] in Equation (6.9) is symmetric Cholesky's decomposition can be employed to represent the matrix in the following manner:

$$[K] = [L][L]^{t} \tag{6.10}$$

Equation (6.9) and (6.10) yield:

$$[L][L]^{t}\{U\} = \omega^{2}[M]\{U\} \tag{6.11}$$

The displacement vector {U} is expressed by the following matrix relation:

$$\{U\} = [L]^{-T}\{q\}, \tag{6.12}$$

Upon substituting the above relation, Equation (6.11) can be written as:

$$\frac{1}{\omega^{2}}\{q\} = [L]^{-1}[M][L]^{-t}\{q\} \tag{6.13}$$

The method of simultaneous matrix iteration is employed to solve Equation (6.13), which yields the natural frequencies and associated eigenvectors, {q} [49]. The method permits the evaluation of number of modes simultaneously. In the iterative procedure, a trial vector $U^1$ of size (p x n), where p is the number of modes to be derived, is initially assumed. The right hand side of Equation (6.9) is then solved to yield:

$$[M]\{U^1\} = \{x\} \tag{6.14}$$

Equation (6.11) can be represented as:

$$[K]\{V\} = \{x\} \tag{6.15}$$

Equation (6.15) is then solved using the Potters' method discussed in Chapter 3, to solve for {V}. Using the relation described in Equation (6.12), the vector {V} may be expressed as:

$$[L]^{-1}\{V^1\} = \{r\} \tag{6.16}$$

Pre-and post multiplication of [M] by transpose of $\{r\}^T$, and {r}, respectively, yields:

$$[L]^{-1}\{V^1\}^T[M]\{V^1\}[L]^T = [B] \tag{6.17}$$

If $\{U^2\}$ is the desired eigenvector at the second iteration stage, then orthonormalizing with respect to [M] will yield an identity matrix. Equations (6.15) and (6.17) result in the diagonal matrix of eigenvalues:

$$[B] = \{U^2\}^T [M] \{U^2\} = [\omega^2] \tag{6.18}$$

This iterative procedure is terminated when the matrix [B] in Equation (6.18) is fully converged to yield eigenvalue solution for the lowest 25 modes.

## 6.3.2 MODAL SUPERPOSITION ANALYSIS

The principle of modal superposition can be conveniently applied to determine the forced response characteristics of the structure. Although a total of 25 vibration modes were identified using the method of simultaneous matrix iteration, only 15 modes with frequency range of 0-45 Hz were used to determine the dynamic response using the mode superposition analysis [49]. The modal coordinates, $Y_i$, and the modal vector, $\{\Phi\}_i$, corresponding to mode i, are related the displacement vector $\{U\}$ in the following manner:

$$\{U\} = \sum_{i=1}^{n} \{\Phi_i\} Y_i \tag{6.19}$$

The equation of motion for the trailer structure, Equation (6.8), can thus be expressed as:

$$[M]\sum_{i=1}^{n}\{\Phi_i\}\ddot{Y}_i + [C]\sum_{i=1}^{n}\{\Phi_i\}\dot{Y}_i + [K]\sum_{i=1}^{n}\{\Phi_i\}Y_i = \{F\} \qquad (6.20)$$

Premultiplying Equation (6.20) by $\{\Phi_j\}^T$ and applying the principle of orthogonality, yields the following uncoupled equations of motion for the mode j:

$$\ddot{Y}_j + 2\omega_j\varsigma_j\dot{Y}_j + \omega_j^2 Y_j = f_j \; ; j = 1.....n \qquad (6.21)$$

where,

$$f_{j=}\{\Phi_j\}^T\{F\} \qquad (6.22)$$

$\varsigma_j$ is the modal damping ratio corresponding to the mode j, derived upon assuming proportional damping. Equation (6.21) is solved for the 15 selected modes and the structural response is computed using Equation (6.19). Since the dynamic response characteristics are strongly related to the modal damping, different representative values of modal damping are selected for the analysis. The damping properties of structural steels and cast iron have been reported in many published studies[64]. These studies, however, frequently report the damping ratio corresponding to the fundamental mode of vibration, ranging from 2% to 10% In the present analysis three values of modal damping ratios, 1%, 3% and 5% are considered.

## 6.4 Results and Discussion

The dynamic response behavior of the candidate trailer structure (trailer B) subject to equivalent suspension forces arising from tire-terrain interactions is evaluated using mode superposition method. Equation (6.21) is solved to determine the modal response and the total dynamic response is evaluated by combining the contribution due to all participating modes. The stress response behavior of the structure is then evaluated from the material and sectional properties of the structure. The dynamic response characteristics of the trailer structure are evaluated under the following dynamic loading conditions:

- Vehicle traversing at 120 km/h on a smooth road
- Vehicle traversing at 120 km/h on a rough road.
- Vehicle traversing at 100 km/h on a smooth road.
- Vehicle traversing at 100 km/h on a rough road.

The response characteristics are further evaluated for different suspension stiffness and modal damping parameters. Two typical road profiles, representing smooth and rough road surfaces, are obtained from the test results reported in the literature [61]. Table 6.1 summarizes operating and design parameters considered for the evaluation of dynamic response behavior of the candidate trailer B. Figures 6.3 illustrate the displacement coordinates of the two roads. The spatial power spectral density (PSD) displacement of the two road profiles is presented in Figure 6.4. The forces transmitted to the trailer structure at the king pin and at the attachments to the wheel axle sets are derived from vehicle speed, suspension, stiffness, and the deflection response of the structure, using Equations (6.5) and (6.6). The dynamic response characteristics of the candidate trailer structure (B) are presented in terms of vertical deflections and flexural stress at the selected nodes, illustrated in Figure 6.5. Since the trailer structure is symmetric along its

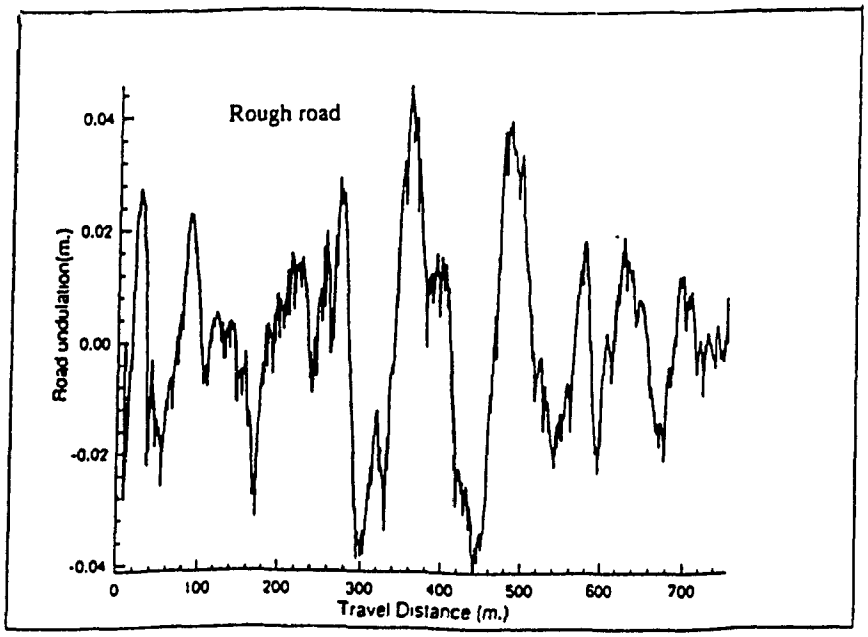


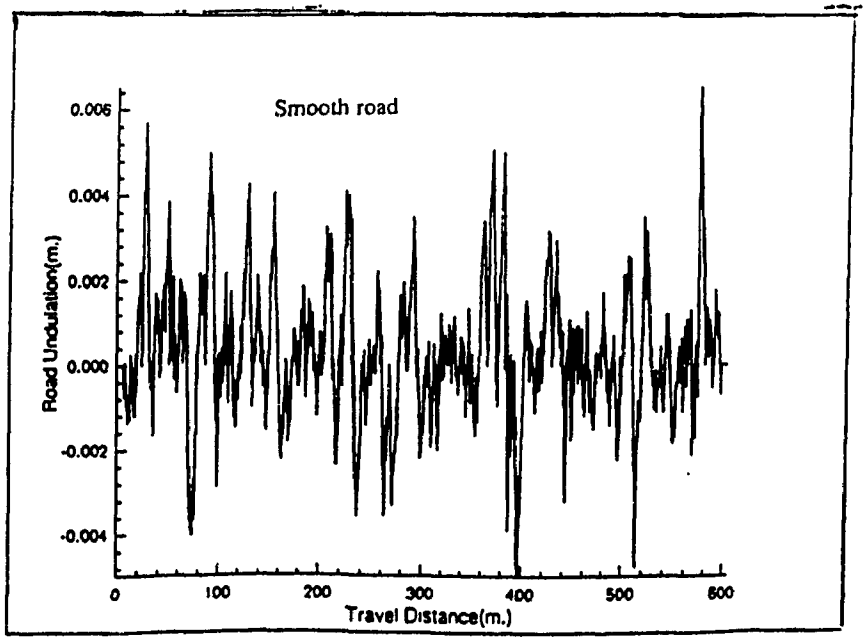


Figure 6.3: Displacement coordinates of of the road profiles.

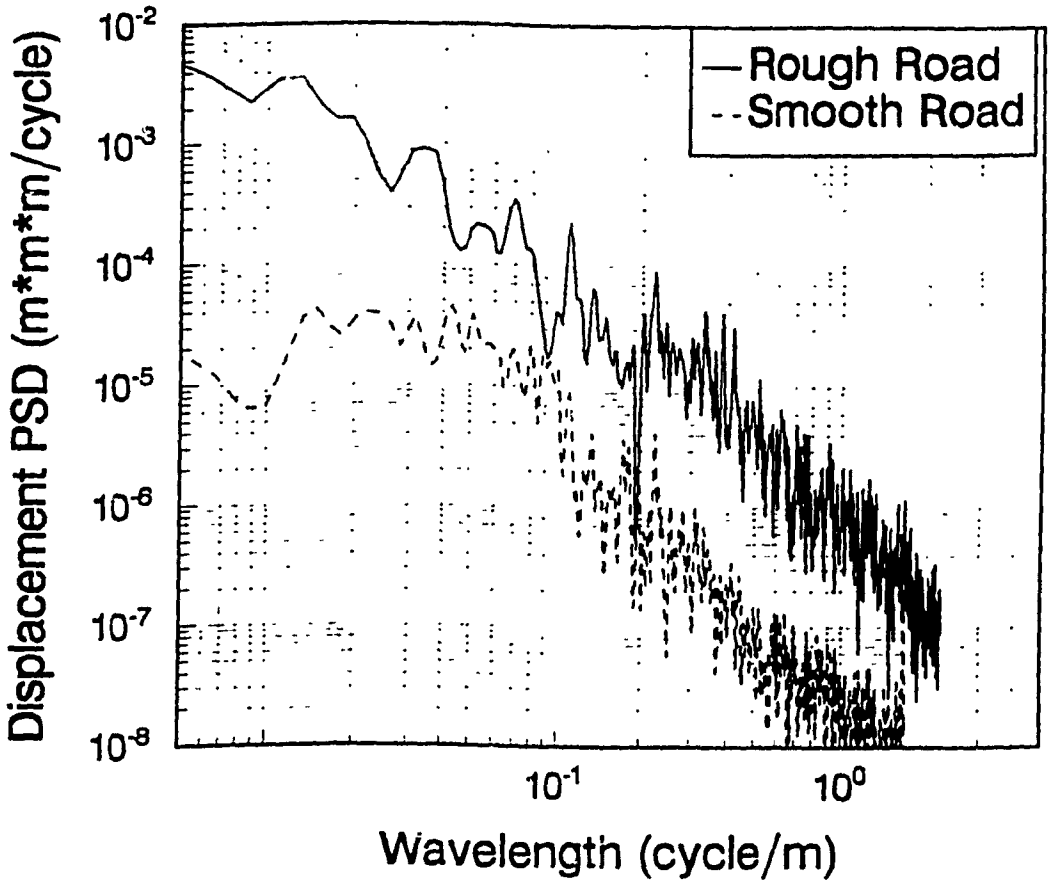


Figure 6.4: Spatial displacement power spectral density (PSD) of the two road profiles.

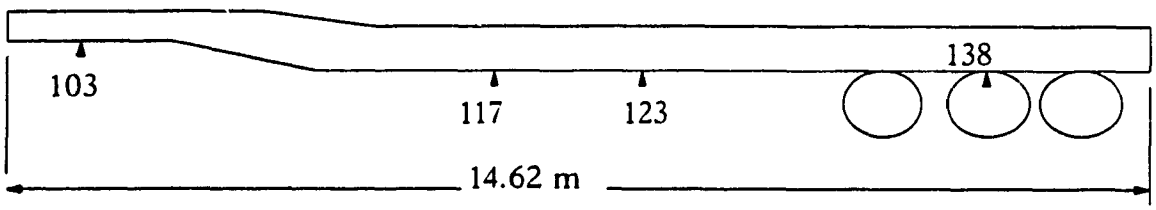


Figure 6.5: Location of selected nodes on the main-beam.

longitudinal axis, the nodes (103,117,123,138) are selected to illustrate the dynamic response of one of the main-beams only (left main-beam). The selected node 103 is located at a distance of 0.813m from the leading edge of the trailer, and corresponds to the king-pin location. Node 117, located at a distance of 6.0 m from the leading edge of the trailer corresponds to the point of maximum static deflection location. Node 123 is located between node 117 and the first wheel suspension support, as shown in Figure 6.5. Node 138 is mid-point of the tridem axle assembly, located at a distance of 12.21m from the leading edge of the trailer.

**Table 6.1 Operating Conditions for Dynamic Response studies**

| | Road Profile | Rough (IRI ≈ 4.7) (R1) | Smooth (IRI ≈ 1.0) (R2) |
|---|---|---|---|
| | Trailer Speed | 120 km/h (S1) | 100 km/h (S2) |
| Suspension Spring Rate | 1342.2 kN/m (nominal) | 1789.5 kN/m (stiffer) | 805.3 kN/m (softer) |
| Modal Damping | 0.01 (D1) | 0.03 (D2) | 0.05 (D3) |

Figure 6.6 illustrates the time histories of dynamic deflection response at nodes 103, 117, 123, and 138 of the candidate trailer B, subject to dynamic suspension force ($K_s$ =1342.2 kN/m) arising from interactions with the rough road. The deflection response is derived for a vehicle speed of 100 km/h and modal damping ratio of 3%. The response characteristics reveal large magnitudes of dynamic deflections at nodes 117, 123 and 138. The magnitudes of dynamic deflections at nodes 117 and 123 are quite comparable. It should be noted that these two nodes

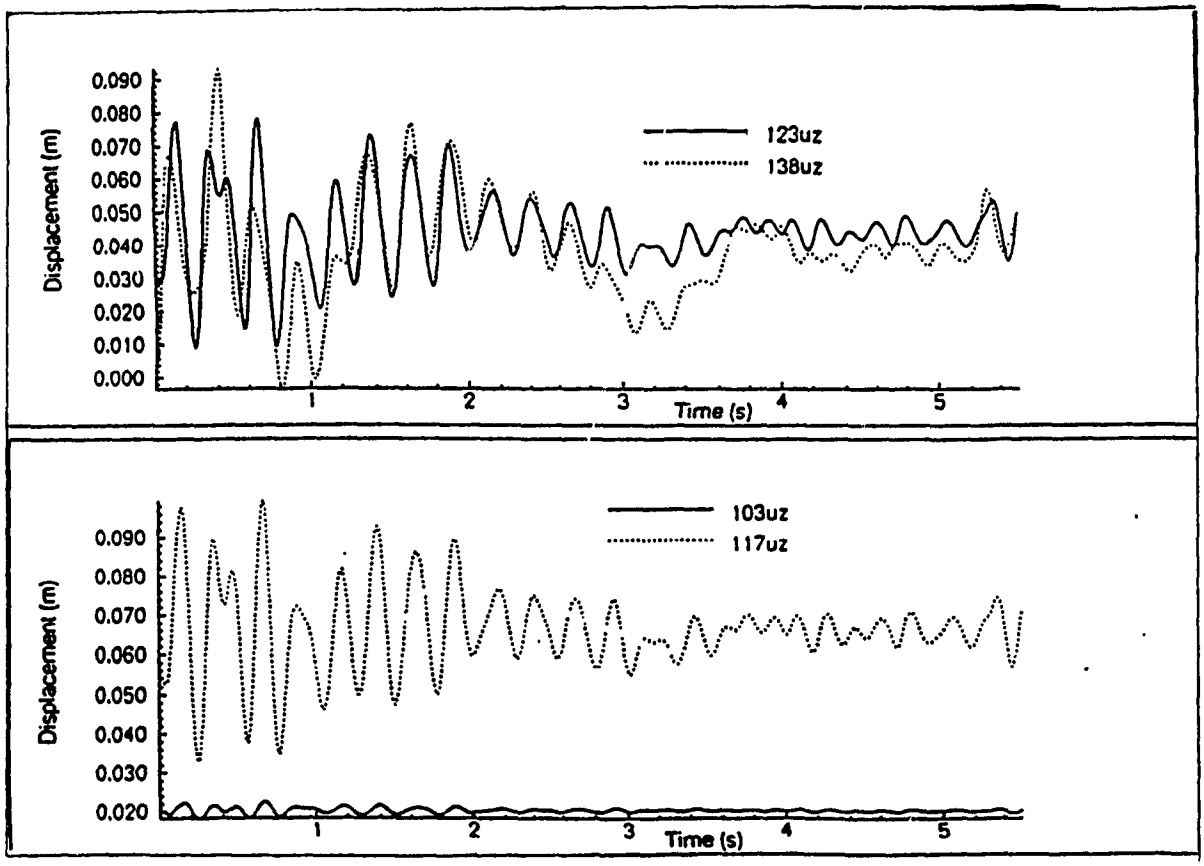


Figure 6.6: Time histories of deflection response of selected nodes (Ks = 1342.2 kN/m; rough road; speed = 100 km/h).

are located near the middle of main-beam span between the king-pin and suspension supports. Furthermore, the node 117 corresponds to the location of maximum deflection under static loading, as discussed earlier in Figure 4.8. Although the static deflection response at node 138 was observed to be relatively small, the magnitudes of its dynamic deflection is considerably large as shown in Figure 6.6. This high magnitude of dynamic deflection is directly attributable to the high suspension forces transmitted to the main-beam in the vicinity of this node. The dynamic deflection response of the main-beam near the lateral axis passing through the king-pin support is observed to be considerably small, due to constraints posed by the articulation model. The dynamic deflection response at the selected nodes further exhibit oscillations near a predominant frequency of 4Hz, which is close to the bounce mode frequency of the trailer structure as discussed earlier in section 4.5.

The frequency characteristics of the dynamic deflections are further evaluated using the FFT algorithm. The rms deflection response of the selected nodes is presented in Figure 6.7. The results exhibit secondary peaks near the excitation frequencies of 14.5 Hz and 28.5 Hz, which are identified as first and second flexural frequencies as discussed in Chapter 4. The magnitudes of dynamic displacement of the trailer structure corresponding to the higher flexural/torsional mode frequencies, however are considerably when compared to that corresponding to the bounce mode frequency.

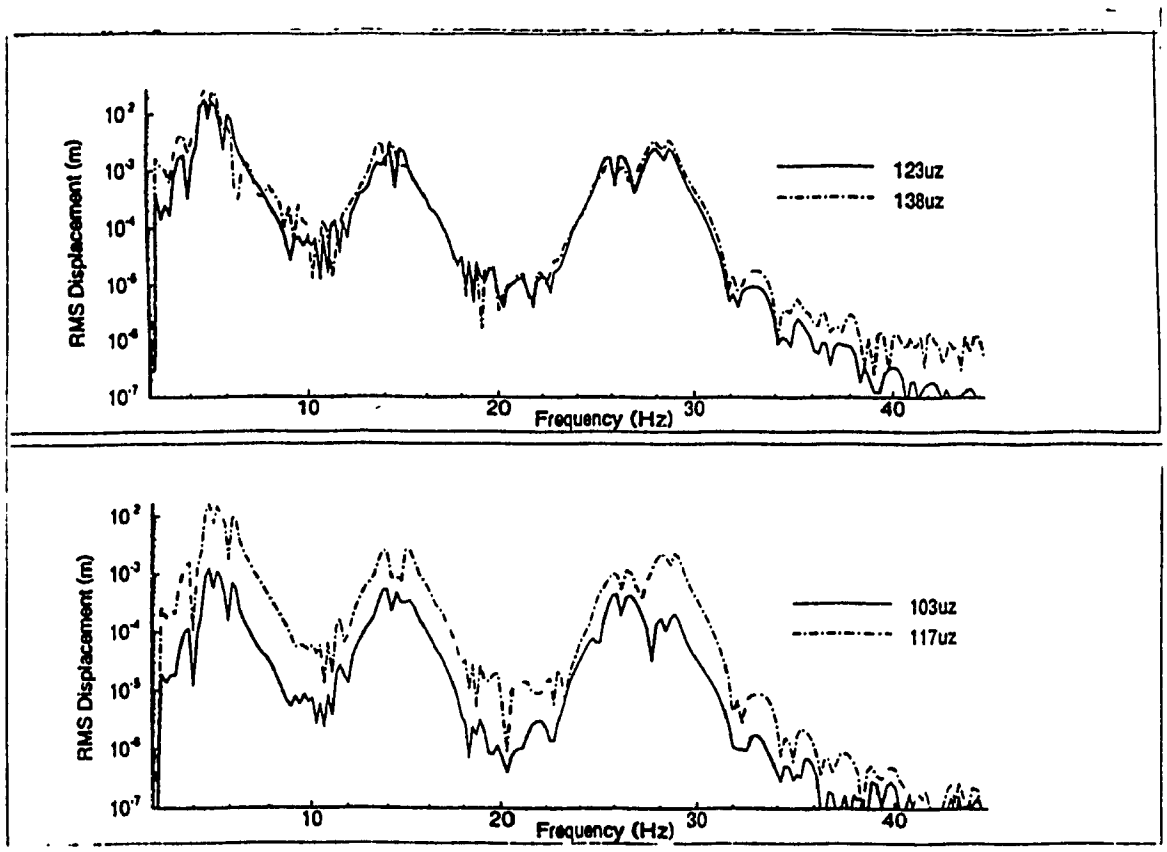


Figure 6.7: RMS deflection response of selected nodes
(Ks = 1342.2 kN/m; rough road; speed = 100 km/h).

### 6.4.1 INFLUENCE OF SUSPENSION SPRING RATE

Figure 6.8 presents the rms displacement response at the nodes 103, 117 and 138, of trailer main-beam in the 2-45 Hz frequency range. The results are derived for suspension forces arising from three different spring rates and the vehicle traversing at a speed of 120 km/h, while the modal damping ratio is selected as 5%. The response characteristics are presented for suspension spring rates of 1342.2 kN/m (nominal), 805.3 kN/m (softer), and 1789.5 kN/m (stiffer). The results show that an increase in suspension spring rate yields increased rms displacement of all the nodes at low frequencies, upto 5 Hz, due to increased suspension forces acting on the structure. The increase in deflection response is primarily attributed to the presence of bounce mode near 4 Hz. The peak displacement of node 138 of the structure with nominal suspension, 84 mm, increases to 90 mm when a stiffer suspension is employed, and decreases to 80 mm with softer suspension. The deflection response of the selected nodes, however, exhibits insignificant influence of the suspension spring rate at higher frequencies.

### 6.4.2 INFLUENCE OF MODAL DAMPING

The influence of modal damping on the dynamic response characteristics of the structure, when the trailer is traversing at 120 km/h on a rough road profile and fitted with the nominal suspension spring is presented in Figure 6.9. The rms displacement of nodes (103, 117 and 138) is illustrated as a function of modal damping and excitation frequency. Three damping values are considered, namely, 1%, 3%, and 5%. An increase in the structural damping tends to suppress the peak rms deflections associated with the bounce mode (near 4 Hz), first flexural

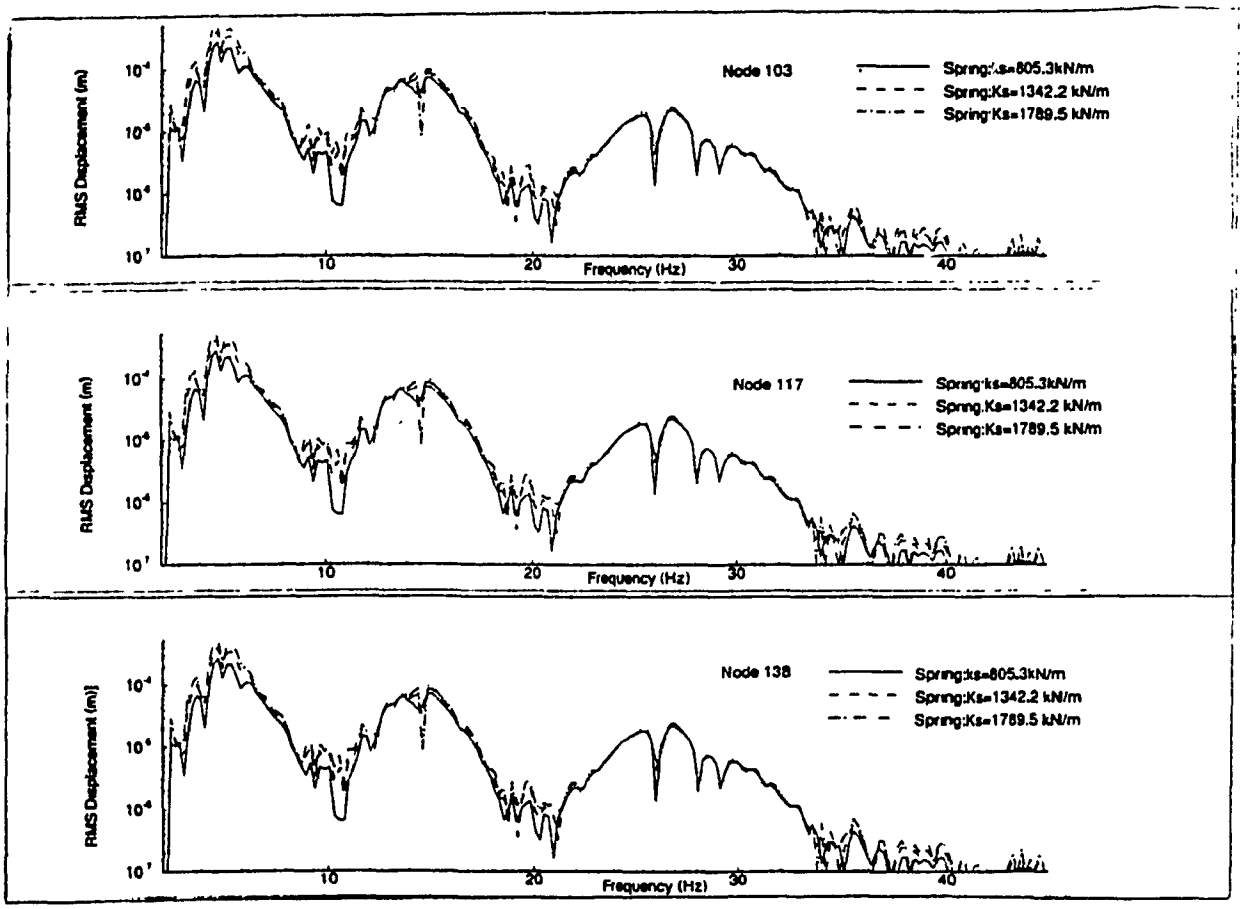


Figure 6.8: Influence of suspension spring on the rms deflection response of selected nodes (rough road; speed = 120 km/h; modal damping = 0.05).

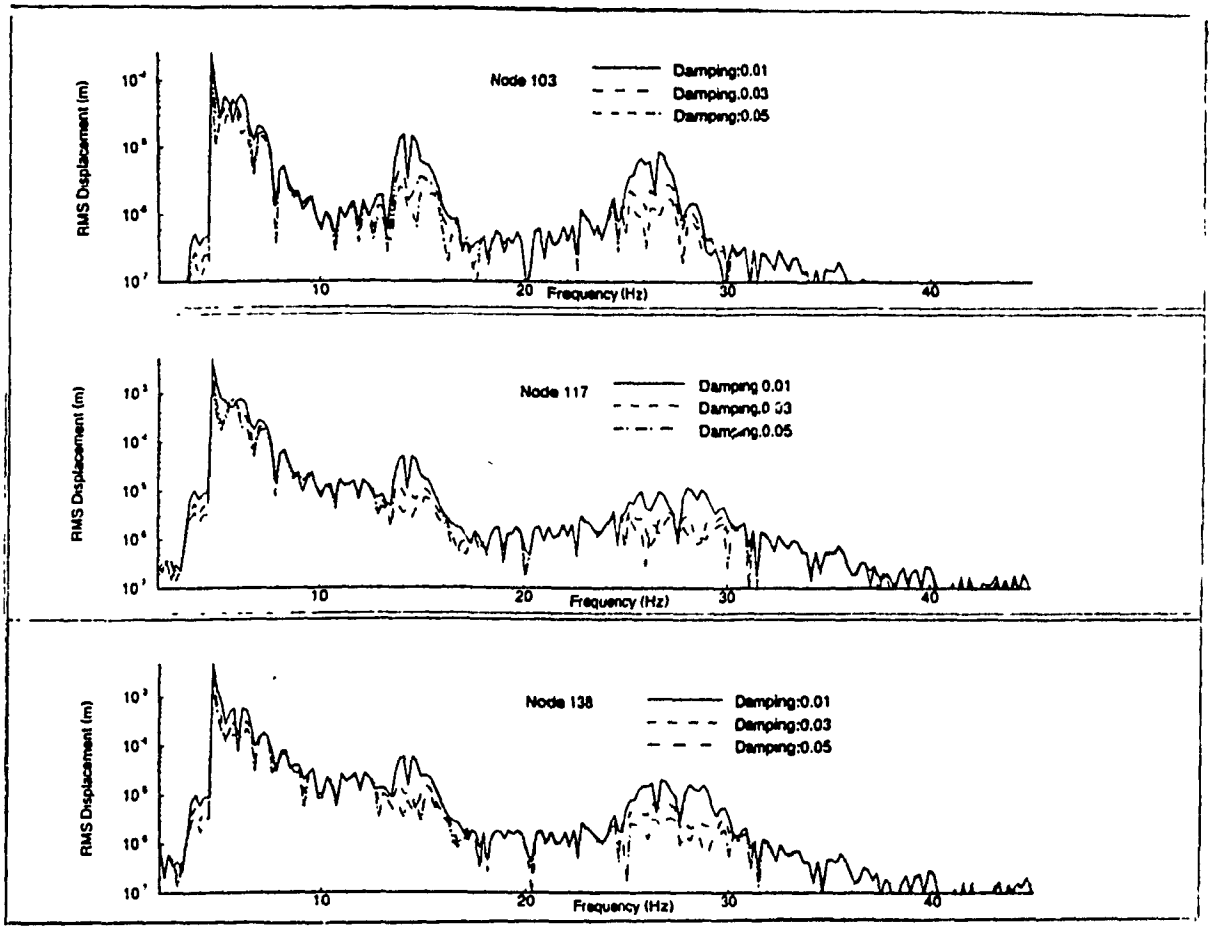


Figure 6.9: Influence of modal damping on the rms deflection response of selected nodes (rough road; speed = 120 km/h; Ks = 1342.2 kN/m).

mode (near 14.5 Hz), and second flexural mode (24 Hz) and second torsion mode (near 28 Hz). The peak deflection response of the selected nodes also decreases with increase in damping. The peak deflections of node 117 attained as 118 mm, 104 mm and 97 mm, respectively, is illustrated as a function of modal damping and excitation frequency. The deflection response of nodes 117 and 138 is most significantly affected by the damping at frequencies greater than 12 Hz. The increase in modal damping can effectively suppress the dynamic deflection of the structure corresponding to flexural and torsional modes.

### 6.4.3 INFLUENCE OF VEHICLE SPEED

Figure 6.10 presents the influence of vehicle speed on the rms deflection of the trailer structure, fitted with the nominal spring and a modal damping ratio of 5%, when traversing on a rough road. The results clearly illustrate an increase in the deflection response with increase in vehicle speed. The peak values of response of all the selected nodes (103, 117, and 138) increase with the vehicle speed in the entire frequency range of 2-45 Hz, as shown in the Figure. This increase in the peak deflection response is primarily attributed to the increase in suspension forces at a higher speed. An increase in vehicle speed also yields slight variations in dominant frequency associated with the bounce mode, due to variations in the frequency components of road profile. The peak deflection response of node 138 predominates near the bounce mode frequency and its magnitudes are attained as 4.6 mm and 8.2 mm, respectively, for excitations encountered at speeds of 100 km/h and 120 km/h. The deflection response of node 138 also varies with the vehicle speed in a similar manner.

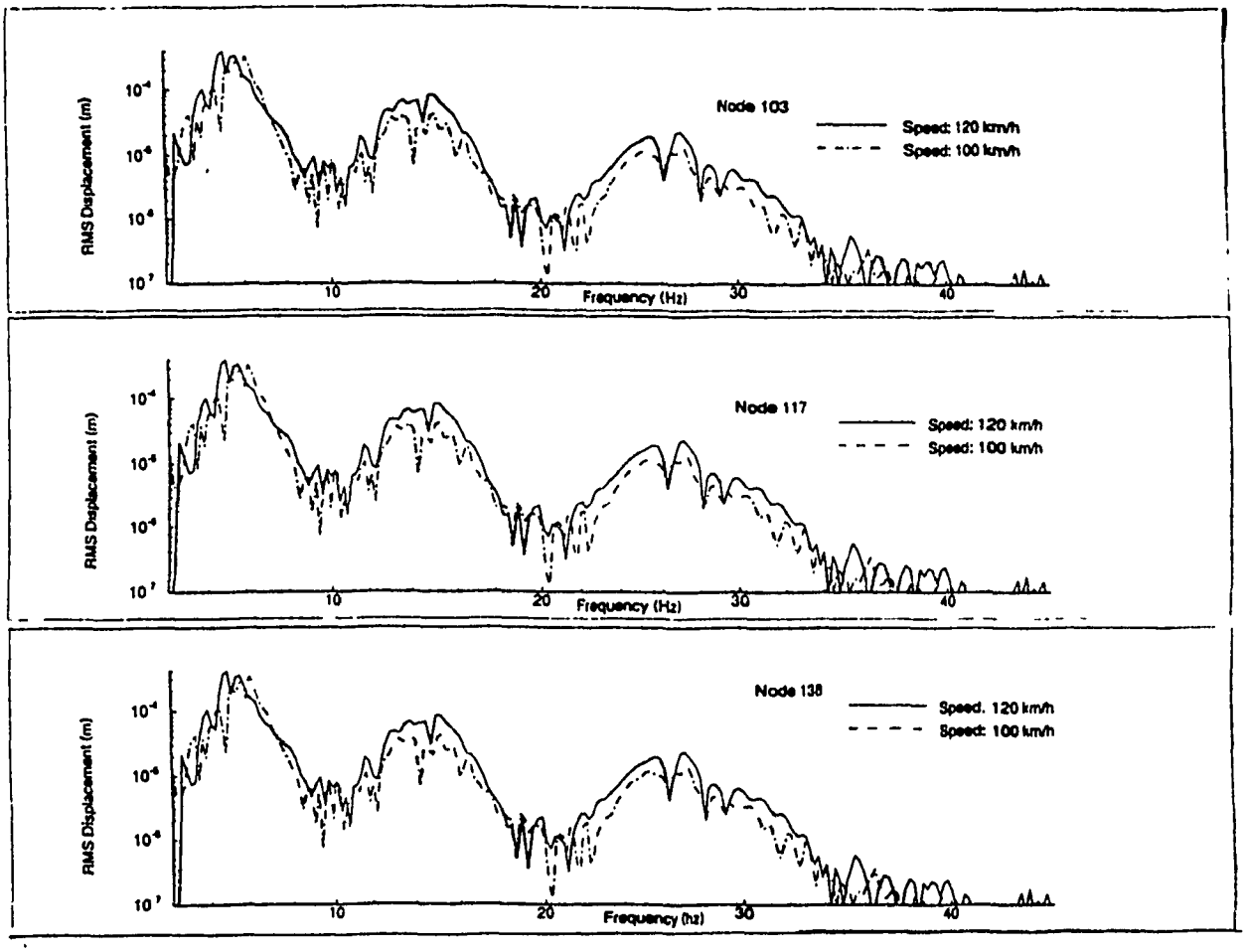


Figure 6.10: Influence of vehicle speed on the rms deflection response of selected nodes (Ks = 1342.2 kN/m; rough road; modal damping = 0.05%).

### 6.4.4 INFLUENCE OF ROAD SURFACE PROFILE

The suspension forces transmitted to the trailer structure are strongly influenced by the road profile. The dynamic deflection response of the trailer structure is thus directly influenced by the road profile. Figure 6.11 illustrates the rms deflection response of the selected nodes (103, 117 and 138) for excitations arising from the two road profiles: rough and smooth. The results are attained for the trailer structure with 5% modal damping, supported on the nominal suspension rates, and traversing the road profile at a speed of 120 km/h. The results clearly illustrate the effect of road profile on the rms deflection response, which increases considerably in the entire frequency range with the increase in road roughness. The influence of above design and operating variables on the peak dynamic deflection and flexural stress response of the structure are summarized in Tables 6.2 and 6.3.

## 6.5 Summary

An analytical method to predict the dynamic displacement response of the candidate trailer B has been developed. Dynamic forces arising from the tire-terrain interactions are estimated from the suspension spring rate and road profile, assuming negligible contributions due to dynamics of the unsprung mass. information from the approximate force computations neglecting the unsprung mass The dynamic response of the structure subject to tire forces are evaluated using the response relation of uncoupled single DOF expressions, in conjunction with mode-superposition analysis. Eigensolutions of the first 15 modes are considered to envelope the effect upto 45 Hz, which is range of the most significant excitation frequencies affecting the structural performance.

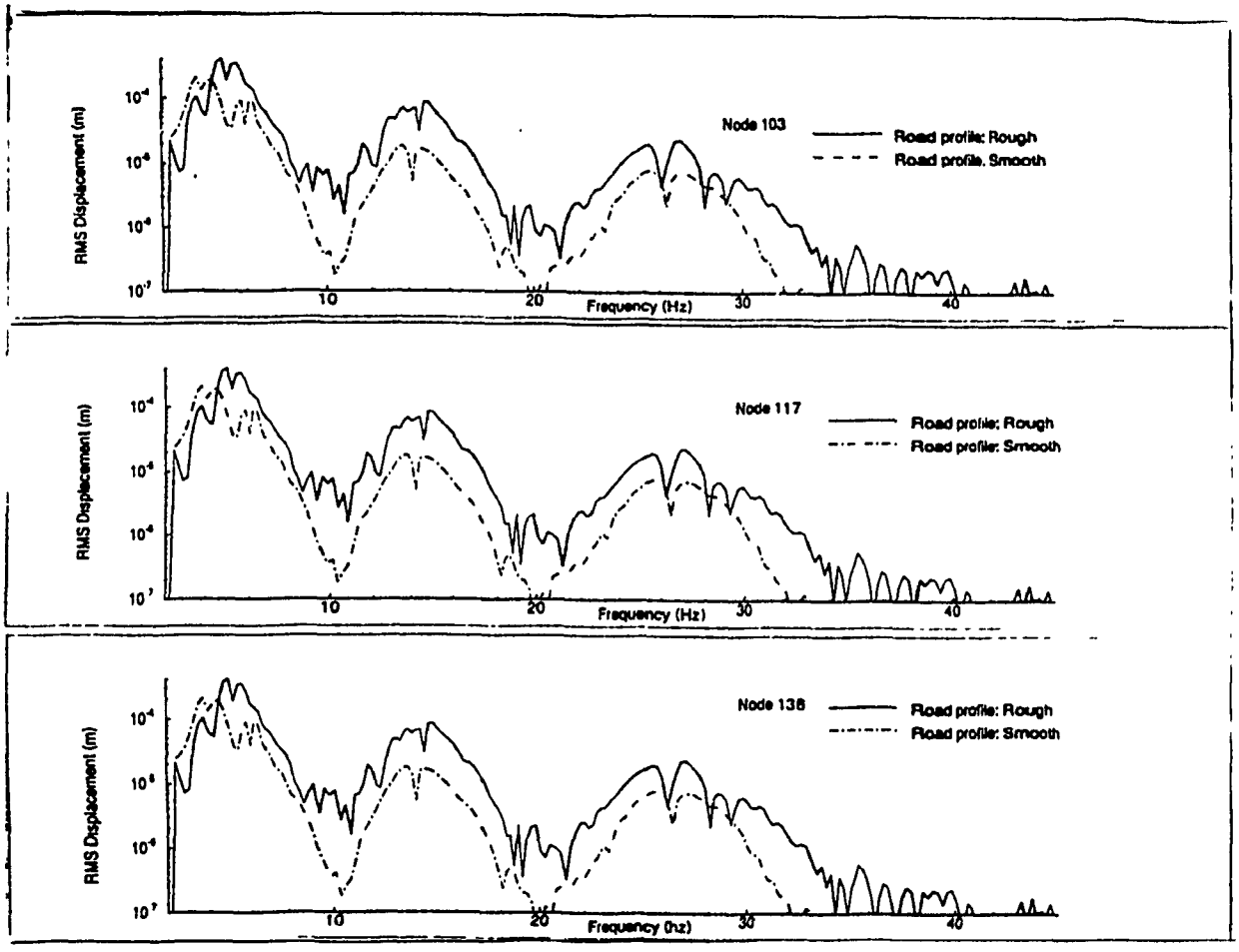


Figure 6.11: Influence of road profile on the rms deflection response of selected nodes (modal damping = 0.05; Ks = 1342.2 kN/m; speed 120 km/h).

## Table 6.2 Dynamic Structural Response of Trailer-B

| SPRING 1342.2 kN/m (nominal) | | Peak dynamic displacement (mm) | | | |
|---|---|---|---|---|---|
| | | 100 km/h | | 120 km/h | |
| Node | ζ | Rough | Smooth | Rough | Smooth |
| 103 | 0.01 | 25 | 21 | 30 | 21 |
| | 0.03 | 21 | 20 | 22 | 21 |
| | 0.05 | 21 | 20 | 21 | 20 |
| 117 | 0.01 | 102 | 75 | 118 | 90 |
| | 0.03 | 100 | 70 | 104 | 85 |
| | 0.05 | 97 | 70 | 97 | 80 |
| 123 | 0.01 | 85 | 53 | 100 | 69 |
| | 0.03 | 70 | 50 | 85 | 60 |
| | 0.05 | 65 | 45 | 76 | 55 |
| 138 | 0.01 | 90 | 47 | 110 | 50 |
| | 0.03 | 80 | 45 | 95 | 45 |
| | 0.05 | 65 | 43 | 84 | 43 |

| SPRING 1789.5 kN/m (stiffer) | | Peak dynamic displacement (mm) | | | |
|---|---|---|---|---|---|
| | | 100 km/h | | 120 km/h | |
| Node | ζ | Rough | Smooth | Rough | Smooth |
| 103 | 0.05 | 22 | 22 | 23 | 22 |
| 117 | 0.05 | 100 | 75 | 105 | 80 |
| 123 | 0.05 | 70 | 50 | 80 | 60 |
| 138 | 0.05 | 70 | 45 | 90 | 45 |

| SPRING 805.3 kN/m (softer) | | Peak dynamic displacement (mm) | | | |
|---|---|---|---|---|---|
| | | 100 km/h | | 120 km/h | |
| Node | ζ | Rough | Smooth | Rough | Smooth |
| 103 | 0.05 | 21 | 20 | 21 | 20 |
| 117 | 0.05 | 90 | 65 | 95 | 75 |
| 123 | 0.05 | 60 | 47 | 75 | 50 |
| 138 | 0.05 | 60 | 43 | 80 | 43 |

## Table 6.3 Dynamic Structural Response of Trailer-B

| SPRING 1342.2 kN/m (nominal) | | Peak dynamic stress (close to respective nodes) (MPa) | | | |
|---|---|---|---|---|---|
| | | 100 km/h | | 120 km/h | |
| Node | $\zeta$ | Rough | Smooth | Rough | Smooth |
| 103 | 0.01 | 42.5 | 35.7 | 51.0 | 35.7 |
| | 0.03 | 35.7 | 34.0 | 35.7 | 34.0 |
| | 0.05 | 35.7 | 34.0 | 35.7 | 34.0 |
| 117 | 0.01 | 173.4 | 127.5 | 200.6 | 153.0 |
| | 0.03 | 169.0 | 119.0 | 174.8 | 142.5 |
| | 0.05 | 163.9 | 119.0 | 163.9 | 135.5 |
| 123 | 0.01 | 144.5 | 90.1 | 169.0 | 117.3 |
| | 0.03 | 119.0 | 84.5 | 142.5 | 101.5 |
| | 0.05 | 110.5 | 76.5 | 128.2 | 93.2 |
| 138 | 0.01 | 85.0 | 31.9 | 109.5 | 37.6 |
| | 0.03 | 68.0 | 28.5 | 76.5 | 35.5 |
| | 0.05 | 42.5 | 25.0 | 74.0 | 20.5 |

| SPRING 1789.5 kN/m (stiffer) | | Peak dynamic stress (close to respective nodes) (MPa) | | | |
|---|---|---|---|---|---|
| | | 100 km/h | | 120 km/h | |
| Node | $\zeta$ | Rough | Smooth | Rough | Smooth |
| 103 | 0.05 | 37.2 | 37.2 | 39.5 | 37.2 |
| 117 | 0.05 | 168.5 | 126.3 | 177.6 | 136.0 |
| 123 | 0.05 | 119.0 | 83.5 | 136.0 | 101.2 |
| 138 | 0.05 | 46.0 | 28.5 | 80.6 | 25.6 |

| SPRING 805.3 kN/m (softer) | | Peak dynamic stress (close to respective nodes) (MPa) | | | |
|---|---|---|---|---|---|
| | | 100 km/h | | 120 km/h | |
| Node | $\zeta$ | Rough | Smooth | Rough | Smooth |
| 103 | 0.05 | 35.6 | 34.0 | 35.60 | 34.0 |
| 117 | 0.05 | 152.6 | 109.7 | 161.0 | 126.8 |
| 123 | 0.05 | 101.5 | 78.9 | 125.5 | 83.6 |
| 138 | 0.05 | 40.5 | 25.0 | 50.6 | 20.5 |

The influence of selected design and operating conditions on the peak dynamic displacement, rms displacement, and peak bending stress are investigated and the results are discussed to highlight the effects of speed, road roughness, and suspension spring rates. The results show that increased modal damping of the trailer structure operating on a smooth road profile yield pronounced effects in attenuating the structural response.

# CHAPTER 7

# CONCLUSIONS AND RECOMMENDATIONS

## 7.1 Highlights of the Investigation

In this investigation, analytical methods are developed for efficient design analysis and reanalysis of large scale structures. The computational efficiency of the methods is specifically emphasized to perform analyses in a personal computer environment. The reanalysis-based methodologies are implemented to study the design of large scale trailer structures. The major highlights of this investigation are summarized in the following subsections:

### 7.1.1 Development of Reanalysis Technique Based Upon Substructure and Potters' Method

A reanalysis solution technique, by seeking solutions through design sensitivity vectors using the first order Taylor series expansion about the present design space has been developed, using the substructure method. The reanalysis method primarily utilizes the decomposed stiffness matrices derived only once for the original design. The modified stiffness matrix of substructures affected by the local design changes also are generated, and incorporated into the overall formulation. The method thus requires minimal computations resulting in highly efficient design reanalysis. The method provides the design sensitivity vector, which are used to evaluate the new solution using the Taylor series approximation.

The validity and effectiveness of the method is demonstrated through analysis of benchmark structures. The candidate trailer structures are modeled using the proposed method. The analytical models are validated by comparing the response characteristics with those derived from experimental model analysis and a commercial finite element software.

### 7.1.2 Development of Reanalysis Technique Using Extended Finite Element Transfer Matrix (EFETM) Method

The compactness of Transfer matrix method and efficiency of FEM are combined to develop the reanalysis methodology based upon EFETM. The EFETM technique involves extended station vectors, comprising the static vector and design sensitivity vector. The design sensitivity vector is conveniently used to derive reanalysis solutions based upon Taylor series approximation. The validity and the numerical efficiency of the method was investigated through analysis of a ten-bar cantilever truss and a complex three-dimensional space truss. Subsequently the technique was implemented to seek reanalysis solutions for a candidate trailer subject to design changes in section modulus of the main-beam.

### 7.1.3 Validation of the Reanalysis Software

The reanalysis methodologies developed in this investigation are validated in a systematic manner. The validations are performed through analysis of benchmark structures, experimental modal analysis and analyses using commercial packages, described below:

a. Validation through analysis of selected benchmark structures and comparison with the published results.

b. Validation through analysis of an example structure and comparison of the results with those derived from other well established tools.

c. Validation through comparison of modal response of a large scale trailer structure with those derived from experimental model analysis.

d. Validation through comparison of static response behavior of a candidate trailer with that derived from a commercial package.

### 7.1.4 Design Performance Indices for Trailer Structures

Cargo trailers employed in highway transportation vary considerably in terms of load capacity, structure design, configuration, suspension and tire properties, etc.. In light of such variation, performance measures to assess the structure design do nor yet exist. In this study, design performance indices are proposed to assess the trailer structure design in terms of the vertical and torsional deformation, and strength margins. Deflection Performance Index (DPI) is defined to carry out relative deflection behavior of different trailer. Maximum flexural and torsional stresses encountered under normal and severe torsional loading conditions are assessed through the strength (SPI) and torsional (TPI) performance indices. A methodology to assess the torsional performance of the structure under twist loads encountered during severe directional maneuvers is proposed.

### 7.1.5 Forced response analysis

The trailer structures are subject to considerable magnitudes of dynamic suspension forces arising from tire-terrain interactions and the deflection behavior

of the vehicle. The analysis methodologies developed in this investigation are applied to determine the dynamic deflections stress response characteristics of the trailer structures subject to dynamic road load. The dynamic response comprising first 15 modes of vibration in the 0-45 Hz frequency range. The method of simultaneous matrix iteration was used to identify the desired number of modes. The dynamic response of the trailer structure is evaluated for different road roughness, vehicle speed, modal damping, and suspension stiffness.

## 7.2 Conclusions

Following conclusions are drawn from the systematic investigation carried out in this dissertation:

a. Reanalysis methods can provide highly efficient solutions of the modified structures involving only local design changes. The large scale structures can be effectively analyzed using substructuring techniques. The typical trailer structures with repetitive ladder-type designs are ideally suited for analysis using substructuring. Substructuring in combination with reanalysis algorithms can considerably reduce the design cycle time in arriving at the acceptable design.

b. The size of global stiffness matrix can be further reduced using Potters' method of solution. The trailer structure modeled with 936 degrees-of-freedom can be represented by a (24 x 24) overall stiffness matrix using the Potters' partitioning technique.

c. The method of EFETM combines the compactness of the transfer-matrix and substructuring, and numerical efficiency of the finite element techniques. While the FETM technique yields only (24 x 24) overall

stiffness matrix for the trailer structure, the EFETM technique results in the matrix size of (48 x 48). The station vectors used in EFETM method, however, includes the design sensitivity vector, which can be effectively used to seek reanalysis and optimization solutions.

d. The design sensitivity vector derived from EFETM and pseudo-force vector derived from Potters' solution provide the basis of reanalysis solutions using the first order Taylor series approximation.

e. Validations of the two methods performed through analysis of benchmark structures demonstrated the effectiveness and efficiency of the proposed methods. The proposed methods provided good correlations with the results obtained from commercial finite-element analysis tools and experimental modal analysis.

f. The reanalysis method based upon EFETM technique required only 40 s execution time using a 486 DX 33 Hz PC for analysis of a three-dimensional space truss in comparison with 70 s required for direct computation using FETM.

g. The EFETM method required only 50 s execution time for reanalysis of a 810 degree-of freedom model of trailer A structure, while the FETM analysis required 170 s execution time using the same personal computer. The Potters' method of analysis and reanalysis required 220 s and 90 s execution time, respectively, for the same structure model. The reanalysis methods has resulted in a reduction in execution time by as much as 70%. Furthermore, intermediate load changes and intermediate constraints can be easily accommodated in the EFETM method.

h. Design sensitivity computation indicate the direction for achieving desired results indicating the modifications from the present design space. The gradient vector can be effectively used to seek the optimal solutions.

i. Reanalysis methods provide an accurate estimate of structural deflection and stress response in a highly efficient manner. The peak error between the direct and reanalysis solutions of the trailer structures was observed to be less than 5%.

j. The relative performance characteristics of trailer designs can be effectively evaluated through deflection, and flexural and torsional stress performance indices. The torsional performance of the trailer structure subject to twist loads encountered under severe directional maneuvers can be assessed by eliminating the suspension supports on one side of the trailer.

k. Reanalysis solution when applied for variations in beam depth H provide an accurate estimate of flexural stresses. The reanalysis solution when applied to variations in flange width provide an accurate torsional response, the flexural stress response exhibits peak error of approximately 10 %.

l. The peak flexural stresses of the structure subject to excitations arising from dynamic tire-terrain interactions increases by approximately 75%. The corresponding peak deflection amplitude increases by approximately 65%.

m. The magnitudes of dynamic deflections and stresses can be considerably reduced by selecting soft suspension springs and materials with higher damping properties.

## 7.3 Suggestions for Further Work

The dissertation research has proposed efficient analysis and reanalysis tools for large scale trailer structures. The tools, however, need to be further explored for their applications to optimization and design of energy efficient light-weight trailers. Specifically, following further studies are recommended:

1. The reanalysis tools may be further developed to achieve reanalysis solutions under realistic dynamic excitations. The sensitivity vectors comprising the sensitivity of eigenvalues and eigenvectors may be derived to attain dynamic reanalyses solutions.
2. The gradient information provided by the design sensitivity vectors in the reanalysis methods in conjunction with the reanalysis algorithm should be further explored to develop efficient structural optimization techniques.
3. A systematic design methodology involving variations in design variables identified through the knowledge base on the trailer designs should be formulated to derive optimal designs.
4. A total trailer design tool can be developed by integrating proposed reanalysis tools together with the fatigue analysis and forcing vectors comprising axial and lateral loads.
5. The reanalysis methods should be implemented to determine optimal number and locations of cross-beams in order to derive light-weight designs.

# REFERENCES


1. Williams, W. and Nader.J. ,"Managing Trucking to Cut Costs " CPPA Annual Meeting. Monteral, March 1993. pp. 5.
2. NASTRAN: User Reference Manual, The MacNeal-Schwendler Corporation, USA.
3. ANSYS: User Reference Manual, Swanson Analysis Inc., Houston, Pa, 15342, USA.
4. ALGOR: User Reference Manual, 150 Beta Drive, Pittsburgh, Pa, 15238, USA.
5. I-DEAS: Structural Dynamics Research Corporation, Milford, Ohio 45150-2789, USA.
6. AUTOCAD: Reference Manual, Autodesk Inc. USA.
7. CADKEY: SOLID User Reference Guide, Manchester, CT, USA.
8. Kirsch, U.,"*Optimum Structural Design, Concepts, Methods, and Application,* " McGraw-Hill Book company, 1987.
9. Tesar A. and Fillo, L., " *Transfer Matrix Method,*" Kluwer Academic Publishers, Dordrecht, 1988.
10. Dokainish, M.A. ," A New Approach for Plate Vibration, Combination of Transfer Matrix and Finite Elemement Technique, " Transactions ASME, J. Engineering for Industry, 1972, pp.526-530.
11. Sankar, S. and Hoa, S.V , " An Extended Transfer Matrix-Finite Element Method for Free Vibration of Plates, " J. Sound and vibration, pp 205-211, 1980.
12. Arora, J.S. , "Survey of Structural Reanalysis Techniques, " Journal of Struct. Divn., ASCE., vol. 102, no. ST4, Proc. paper12056, April 1976, pp.783-802.

13. Pilkey, W.D. and Wang, B.P. , " Structural Analysis Revisited ," SAE Paper No. 880955 , 1988.

14. Argyris, O.E. , Bronlund and Roy, J.R. ," A Direct Modification for the Displacement Method, " AIAA Journal, Vol. 9, No. 9, 1971, pp. 782-802.

15. Jalon, J.G. and Viadero, F. , " A New Direct Method for the Simple and Efficient Reanalysis of Structures, " Computers and Structures, Vol.21, No. 5, 1985, pp. 1059-1066.

16. Phansalkar, S.R. , " Matrix Iterative Methods for Structural Reanalysis, " Computers and Structures, Vol. 4, 1972, pp. 779-800.

17. Kirsch, U. and Rubinstein, F. , " Structural Reanalysis by Iteration, "Computers and Structures, Vol.2, 1972, pp. 497-510.

18. Noor, A.K. and Lowder, H.E. ," Approximate Techniques of Structural analysis, " Computers and Structures, Vol.4, 1974, pp. 801-812

19. Noor, A.K. and Lowder, H. E. ," Approximate Reanalysis with Substructuring, "Journal of the Structural Division, ASCE, ST8, August 1975.

20. Noor, A.K. and Lowder, H.E. ," Structural Reanalysis via a Mixed Method, " Computers and Structures, Vol. 5, 1975, pp. 9-12.

21. Arora, J.S. and Govil, A..K. ," Design Sensitivity Analysis with Substructuring, " Journal of the Engineering Mechanics Division, ASCE. EM4, August 1977.

22. Exler, R.L ., " Frame Rigidity- How Much and Where, " SAE Paper No. 769 B, presented at the National Transportation Meeting , October 1963.

23. Shomberger, S.J. and Wingerson, E.A. , " Truck Frame Siderail Design " SAE Paper No. 769 C, presented at the Natonal Powerplant Meeting, Chicago, Illinois, October 1963.

24. Carver, G.C. , "Application of Variable Depth Siderail to Heavy Truck Frames, " SAE Paper No. 69174 , 1969.

25. McNitt, L.F. , " Truck Frame Side Rail Buckling Stresses," SAE Paper No. 690176, International Automotive Engineering Congress, Detroit, Mich. Jan. 1969.

26. Beermann, H.J. , "Joint Deformations and Stresses of Commercial Vehicle Frame under Torsion, " International Conference on Vehicle Structures. Paper No. C178/84, I. Mech E Publications 1984.

27. Rusinski, E. and Teisseyre, J.H. , "Torsional Stiffness of Chassis Frames with Point-Welded Nodes, " International Conference on vehicle Structures. Paper No. C162/84, I. Mech. E Publications 1984.

28. Nitto, H. , Herai, T. and Mizui, M. , " The State and Concept of Fatigue Evaluation of Steel Sheets for Automotive use at Automakers and steelmakers in Japan, " Nippon Steel Corporation Rept. 1982.

29. Lawrence, F.V. , Wang, P.C. and Corten, H.T. , " An Empirical Method for Estimating the Fatigue Resistance of Tensile-Shear Spot Welds, " SAE Paper No. 830035, International Congress and Exposition, Detroit, Mich. Feb. 28- Mar. 4, 1983.

30. Monasa, F. and Chipman, T., " Evaluation of Structural Strength Capacity of Bus Body Structures " SAE Paper No. 811305, 1981.

31. Beermann, H.J. , " Static Analysis of Commercial Vehicle Frame : A Hybrid - Finite element and Analytical Method, " International J. of Vehicle Design, Vol. 5, Nos. 1/2, 1984.

32. Yoshikawa, H. , Yamauchi, T. , Takeda, N. and Sakai, T. , " Analysis of Bending Stress of Heavy Duty Truck Frame by FEM , " SAE Paper No. 922472, 1992.

33. Ramamurti, V. and Sujatha, C. , " Bus Vibration Study - Finite Element Modelling and Determination of the Eigenpairs, " International J. of Vehicle Design, Vol. 11, Nos. 4/5, 1990.

34. Kim, S.S. , Shabana, A.A. and Haug, E.J. , " Automated Vehicle Dynamic Analysis with Flexible Components, " J. of Mechanisms, Transmissions, and Automation in Design, Trans. of ASME, Vol.106, March 1984.

35. Tidbury, G. H. , " The Design of Bus and Truck Structures for Passenger and Crew safety, " International J. of Vehicle Design , Vol. 5, Nos. 1/2, 1984.

36. Winter, R. , Mantus , M. and Pifco, A..B. , " Finite Element Crash Analysis of a Rear-Engine Automobile, " SAE Paper No. 811306, Fourth International Conference on Vehicle Structural Mechanics, 1981.

37. Matyas, M. and Sheth, N.J., " Determination of Extreme Structural Loads in Service, " SAE Paper No. 78010, Congress and Exposition, Cobo Hall, Detroit, Feb.27- Mar. 3, 1978.

38. Sharmann, P.W. , " The Use of Dynamic Strain Records to Estimate the Fatigue Life of a Semi-Trailer Chassis, " Inst. of Phys, Stress anaysis Group, Annual Conf. Stress, Vibration and Noise analysis in Vehicle, University of Aston, Birmingham, 1975.

39. Arora, J.S. and Govil, A.K. , " Design Sensitivity Analysis with Substructuring, " Journal of the Engineering Mechanics Division, ASCE. EM4, August 1977.

40. Haug, E.J. , Arora, J.S. and Feng, T.T. , " Sensitivity Analysis and Optimization of Structures for Dynamic Response, " presented at the Design Engineering Technical Conference, Chicago, Ill. ASME, Sept.26-30, 1977.

41. Gangadharan, S.N. , Haftka, R.T. and Nikolaidis, E. , " An Alternate Static Codensation Method For Sensitivity Analysis of Structures," CSME Mechanical Engineering Forum 1990.

42. Gupta, V. , " A Submodel Component Reanalysis Technique for Liquid Tanker Body Design Using the Finite Element Method," M.Eng. Thesis, Department of Mechanical Engineering, Concordia University, Montreal, Quebec, Canada, March 1988.

43. Arora, J.S. and Haug, E.J. ," Methods of Design Sensitivity Analysis in Structural Optimization" AIAA Journal, Vol. 17, No. 9, 179, pp. 970-974.

44. Ervin, R.D. , Guy, Y. , " The influence of Weights asnd Dimensions on the Stability and Control of Heavy-duty Trucks in Canada", UMTRI Report No. 86-35, July 1986.

45 Noor, A..K. , and Lowder, H.E. , "Approximate Reanalysis With Substructuring," Computers and Structures, Vol. 5, 1975, pp. 9-12.

46. Noor, A.K. , and Peters, J. M. , "A New Partitioning Strategy for Efficient Reanalysis of Large Structural Systems, "Computers in Engineering, 1989, Vol. 6, Dec. 1989, pp. 303-315.

47. Haftka, R.T. and Kamat, M. , "*Elements of Structural Optimization*, " Martnus Niijhoff Publishers, Dordrecht, 1985.

48. Fox, R.L. , " Approximate Analysis Techniques for Design Calculations", AIAA Journal, vol. 9 , No.. 1, 1971..

49. Ramamurti, V. ,"*Computer Aided Design In Mechanical Engineering*, " Tata- McGraw Hill Publishing Co. Newdelhi, 1987.

50. Rakheja, S., and Sankar, S. , " Analysis of Off-road Vehicle Structures Using Integrated Computer-aided Analysis and Testing", International Conference on Modal Analysis, 1988.

51. Ahmed, A.K.W. and Piche, A. , " Experimental Modal Analysis of a Log-Hauling Semitrailer, CONCAVE Report, Concordia University, Montral, Canada, 1994.

52. Storaasli, O. , and Sobiezczanski, J. , " On the Accuracy of the Taylor Approximation for Structural Resizing, " AIAA journal, vol.12, Jan. 1974, pp. 231-233

53. Austin, M.D. , and Moore, G. , "Finite Element Modeling of Vehicle Bodies Using Substructure Methods, I. Mech. E. Conference Publication 1984-7, Paper No, C160/84, pp. 83-90.

54. Coppolino, R.N. , " Employment of Hybrid Experimentally Analytical Modeling in Component Mode Synthesis of Structures. Colloquium on Combined Experimental/Analytical; Modeling of Dynamic Structure Synthesis, Joint ASME/ASCE App. Mech. Conf. New Mexico, 1985.

55. Barek, P. and Sachs, H. , "On the Optimal Ride Control of a Dynamic Model for an Automotive Vehicle System" , Proc. 9th IVAD Symposium held at Linkping, Sweden, June 24-28, pp. 15-29, 1985.

56. Cebon. D. , "Heavy Vehicle Vibrations - A Case Study", Proc. 9th IAVSD Symposium held at Linkoping, Sweden, June 24-28, pp. 30-43, 1985.

57 Ruf. G. , " The Calculation of the Vibrations of a Four-Wheeled Vehicle Induced by Random Road Roughness of the Left and Right Track", Vehicle System Dynamics, 7, pp. 1-23, 1978.

58 Healey, A.J. , Nathman, E. and Smith, C.C. , " An Analytical and Experimental Study of Automobile Dynamics, with Random Roadway Inputs", Trans. ASME, pp. 284-292, 1977.

59. Gillespie, T.D. and Karamihas, S.M. , " Characterizing the Road-Damaging Dynamics of Truck Tandem Suspensions", SAE series , Paper No. 932994, pp. 137-144, 1993.

60. Rakheja and Woodroofe, " Role of Suspension Damping in Enhancement of Road Friendliness of Heavy Vehicles, " International J. of Vehicle Design, Heavy Vehicle Systems, 1995 (in-press).

61. Damien, T.M. et al. , " Pavement Profiling Various Pavements: Ottawa/Smith Falls", John Emery Geotechnical Engineering Report, 1992.

63. Whitesell, J.E. , "Rational Approximants in Structural Design Reanalysis," Journal of Mechanisms, Transmissions, and Automated Design, Tran. ASME, 83-DET-70, 1983.

64. Leckie, A. and Pestel, E.C. , "*Matrix methods in Elastomechanics,* " McGraw Hill Book Co. New York, 1962.

65 Ohga, M. Shigmatsu, T. and Hara, T. , "Structural analysis by a Combined Finite Element-Transfer Matrix Method," Computers and Structures, Vol. 17, No. 3, pp. 321-326, 1983.

66 Bhatti, M. , Stoner, J.W. and Hington, J. , "Simulation of Dynamic Loads from Different Vehicle Configurations," International J. of Vehicle Design, Heavy Vehicle Systems, Vol. 1, No. 4, 1994.